Insights into the role of the flagellar glycosylation system in *Campylobacter jejuni* phage-host interactions

by

Jessica Christiane Sacher

A thesis submitted in partial fulfillment of the requirements for the degree of

Doctor of Philosophy

in

Microbiology and Biotechnology

Department of Biological Sciences

University of Alberta

Abstract

Bacteriophages (phages) are the viruses that infect bacteria. Studying how phages interact with their hosts can inspire new ways of controlling bacterial pathogens and can highlight important facets of the biology of both organisms. Furthermore, phage-host characterization can inform exploitation of phages for therapeutics, diagnostics and research tools.

Campylobacter jejuni is a deadly foodborne pathogen of humans, and its extensive surface structure glycosylation plays an important role in its virulence. In particular, *C. jejuni* flagella are required for colonization of its niche in the gastrointestinal tract of birds, and are also required for virulence in humans. *C. jejuni* devotes a substantial proportion of its genetic repertoire to flagellar biogenesis, which requires glycosylation with sialic acid-like sugars for assembly. *Campylobacter* phages tend to target either capsular polysaccharides or flagella, but little more than this is known about the factors governing *Campylobacter* phage-host interactions.

My thesis describes the study of *C. jejuni* interactions with phages in the context of flagellar glycobiology. I found that *C. jejuni* phage NCTC 12673 interacts with host flagella and flagellar glycans in ways not previously described for other phage-host systems. Furthermore, this phage encodes a protein of unknown function (Gp047) with specific binding affinity for host flagellar glycans. I sought to determine how the *C. jejuni* flagellar glycosylation system and the NCTC 12673 phage each impact the biology of the other.

I found that Gp047 inhibits growth of *C. jejuni* expressing flagellar acetamidino-modified pseudaminic acid glycans, that probing with Gp047 reveals previously unexplored diversity in

C. jejuni flagellar glycans, and that Gp047 binding to motile, glycosylated flagella induces downregulation of pathways for cellular energy metabolism. I also found that *C. jejuni* pseudaminic acid biosynthesis (flagellar glycosylation) genes are required for bacteriophage NCTC 12673 infection, that a requirement for motility likely explains this dependence, and that oxidative stress sensitivity may explain the reduced ability of phage NCTC 12673 to plaque on non-motile *C. jejuni* mutants. Finally, I found that expression of the flagellar glycan binding protein Gp047 correlates with a lack of plaquing by phage NCTC 12673 on non-motile *C. jejuni* cells, providing an interesting foundation for future research.

Overall, my work points toward flagellar glycosylation as an important factor affecting *C. jejuni* phage-host dynamics, and provides insight into the role of a flagellar glycan-binding phage protein in these interactions. These findings contribute to the fields of phage biology and bacterial glycobiology by providing insight into how a *Campylobacter* phage interacts with its heavily glycosylated host.

Preface

Chapter 2 was published as Sacher, J. C.; Flint, A.; Butcher, J.; Blasdel, B.; Reynolds, H. M.; Lavigne, R.; Stintzi, A.; Szymanski, C. M. Transcriptomic analysis of the *Campylobacter jejuni* response to T4-like phage NCTC 12673 infection. *Viruses* **2018,** *10*, 332. I designed and performed the experiments, analyzed the data, and wrote the paper. Annika Flint and Hayley Reynolds performed experiments, James Butcher, Bob Blasdel and Rob Lavigne provided guidance, analyzed the data and edited the manuscript, Alain Stintzi contributed materials, guided the experiments, and analyzed the data, and Christine Szymanski supervised and funded the project, analyzed the data and edited the manuscript.

Chapter 3 was published as Javed, M. A.; Sacher, J. C.; van Alphen, L. B.; Patry, R. T.; Szymanski, C. M. A flagellar glycan-specific protein encoded by *Campylobacter* phages inhibits host cell growth. *Viruses* **2015,** *7*, 6661-6674. I contributed the data for 4/6 figures, contributed 1/3 tables, helped analyze the data, edited the manuscript, and wrote part of the discussion. Afzal Javed designed and performed experiments, provided training, analyzed the data and wrote the original version of the manuscript. Lieke van Alphen and Robert Patry performed experiments. Christine Szymanski supervised and funded the project, analyzed the data and edited the manuscript.

A version of Chapter 4 will be submitted for publication as Sacher, J. C.; Shajahan, A.; Patry, R. T.; Butcher, J.; Flint, A.; Stintzi, A.; Azadi, P.; Szymanski, C. M. Novel insights into *Campylobacter jejuni* flagellar glycan diversity revealed by probing with a conserved glycan-specific bacteriophage binding protein. I designed the experiments, analyzed the data and wrote the chapter. Asif Shajahan performed the MS experiments and analyzed the data. Rob

Patry and Annika Flint performed experiments, James Butcher provided guidance and analyzed the data, Alain Stintzi and Parastoo Azadi contributed materials, guided the experiments, and analyzed the data, and Christine Szymanski supervised and funded the project, analyzed the data and edited the manuscript.

A version of Chapter 5 will be submitted for publication as Sacher, J. C.; Javed, M. A.; Reynolds, H. M.; Butcher, J.; Flint, A.; Stintzi, A.; Szymanski, C. M. *Campylobacter jejuni* phage NCTC 12673 dependence on flagellar glycosylation and flagellar motor genes is overcome by a single escape mutant. I designed the experiments, analyzed the data and wrote the manuscript. Hayley Reynolds and Annika Flint performed experiments, James Butcher provided guidance and analyzed the data, Alain Stintzi contributed materials, guided the experiments, and analyzed the data, and Christine Szymanski supervised and funded the project, analyzed the data and edited the manuscript.

A version of Appendix I was published as Sacher, J. C.; Yee, E.; Szymanski, C. M.; Miller, W. G. Complete genome sequences of three *Campylobacter jejuni* phage-propagating strains. *Genome Announc.* ***2018,*** *6,* e00514-18. A version of Appendix II of this thesis was published as Sacher, J. C., Yee, E., Szymanski, C. M., & Miller, W. G. Complete genome sequence of *Campylobacter jejuni* strain 12567, a livestock-associated clade representative. *Genome Announc.* **2018,** *6*, e00513-18. I grew the strains, extracted and submitted gDNA for Illumina sequencing, assembled strain information, initiated the submission of the genomes to NCBI, and wrote the first draft of the Genome Announcement. Emma Yee prepared gDNA for PacBio sequencing. William Miller annotated the genomes, contributed reagents, analyzed the data, and aided in preparing the genomes for submission and the Genome Announcement for

publication. Christine Szymanski supported and guided the projects, analyzed the data and edited the Genome Announcements.

Acknowledgements

I would like to thank my supervisor, Christine Szymanski, for her incredible mentorship over the last 9 years. From my first day meeting you back in 2009, when I was a 3rd year undergraduate student eager to take your Microbial Glycobiology class, I was inspired by your enthusiasm and passion for science. Since then, your excitement for science has never seemed to waver, no matter how close we got to deadlines or how far into the wee hours of the morning it was. I have learned more than I can describe from your mentorship – about working with people, speaking in public, prioritizing, finding motivation, thinking through complex sets of data, and coming up with exciting new plans no matter what the experimental outcome. I don't think there's a person on Earth who could find the silver lining in a situation faster or more consistently than you. I am so thankful for all you have done to help me become the scientist I am today. I would also like to thank my committee members, Lisa Stein and Stefan Pukatzki, for their kindness, enthusiasm, support and guidance. I always looked forward to meeting with you about my projects, and always came out of those meetings with a list full of excellent experimental suggestions and the feeling that the possibilities for my project were endless. I am so grateful for the colleagues I was lucky enough to go through this experience with, both at the University of Alberta and during my time spent at the Universities of Ottawa and Georgia. I am particularly thankful for the mentorship, unwavering patience and friendship of David Simpson, Afzal Javed, Denis Arutyunov, Harald Nothaft, Ritika Dwivedi, Cory Wenzel and Bernadette Beadle. I will always take joy in talking science or life with any one of you, and have countless memories that I will treasure. Jolene, Rob, Justin, Cody and Clay, you have been incredible people to have by my side in the lab, and it will take me a very long time to get used to life without you each day. Thank you all for putting up with my tendencies to hoard lab supplies, and for being willing to laugh about it each time. I adore

you all, and I'll treasure your friendship for life. Thank you also to the undergraduate students I was fortunate enough to mentor: Lily Li, Stephanie Guerra, and Hayley Reynolds. Your enthusiasm in the lab made coming to work such a joy! Somehow each of you were able to convert my sporadic and sometimes conflicting instructions into amazing progress in the lab, and your help with moving our projects along will not be forgotten. (Also, Hayley, I'm pretty sure I wouldn't be graduating if it weren't for you). I would also like to thank Alain Stintzi, James Butcher and Annika Flint for their amazing mentorship during my research exchange in their lab in Ottawa. I learned so much from all of you, and so appreciate your generosity with your time and your kind, welcoming natures. I enjoyed my time in your lab immensely, and almost every single one of my thesis chapters is influenced by the work I did in just five weeks with your lab. I would also like to thank all the people who helped with administration, teaching assistantship coordination, and lab safety over the years; particularly Chesceri Mason, Tom Hantos, Kirstin Veugelers, Mark Wolansky, Dean Wilson and Lori Dammann - I secretly adored coming to visit each of you whenever I could, and your help and encouragement always went far beyond your job descriptions. Thank you. To my family, thank you for not saying anything when I decided to stop pursuing dental school and instead enrolled in grad school. I love you all so much, and your support in everything I do continues to be unparalleled. Finally, I am extremely grateful to the Natural Sciences and Engineering Research Council of Canada (NSERC), which funded me throughout my graduate studies.

Table of Contents

LIST OF TABLES

LIST OF FIGURES

Chapter 1: General Introduction

1.1. Introduction

In this chapter, I begin by introducing the reasons for studying phage-bacterial interactions in general. I then introduce *C. jejuni* biology and pathogenesis, with a particular focus on the importance of flagella and flagellar glycans in *C. jejuni* virulence. I then describe known *Campylobacter*-phage interaction mechanisms, with a particular focus on phage NCTC 12673 and what is known about its interactions with *C. jejuni* glycans. The goal of my thesis work has been to learn about the possible ways phages might influence *C. jejuni* glycobiology and about the ways glycobiology might influence phage infectivity.

1.2. Importance of studying phage-host interactions

1.2.1. Essential insights into host biology

Bacteriophages (phages), the viruses that infect bacteria, represent the most abundant biological entity on Earth, with an estimated total number of 10^{31} virions on the planet [1]. These bacterial viruses are found everywhere, outnumbering bacteria approximately 10:1 in most environments [2]. Phages, the natural 'predators' of bacteria, have been evolving alongside their bacterial hosts for billions of years, which makes their study an attractive source of information about the way bacteria adapt to their external world. For instance, some bacterial virulence factors are thought to have evolved to protect cells from phages, as exemplified by the attenuation of phage-resistant *Vibrio cholerae* isolates observed by Seed *et al.* (2014) [3]. Overall, studying phage interactions with bacteria remains an unexplored but promising avenue of research.

A key reason to study phages lies in their ability to selectively infect their bacterial hosts. Phages rely on specific recognition factors (known as receptor binding proteins or RBPs) to accurately identify their target prior to infection, frequently discriminating between different strains of the same species. This selectivity and the mechanisms that support it have become the subject of substantial research over the past few decades, especially in light of the emergence of multi-drug resistant pathogens as a result of nearly 75 years of widespread antibiotic use [4].

The exploitation of phage selectivity provides a new avenue toward the goal of eradicating bacterial disease [5]. By elucidating which bacterial surface structures are targeted by phages, we can glean information regarding the identity of important, conserved structures that a given organism requires for survival. These bacterial structures could be targeted through vaccines or through targeted antimicrobials [6,7].

1.2.2. Improved safety and efficacy of phage therapy

In addition to the information that can be learned about bacterial pathogens by studying their interactions with phages, a second benefit of studying phage-host interactions is that this information can improve the safety and efficacy of phage therapy. As antibiotic resistance now threatens to kill more people per year than cancer by 2050, there is a great need to explore alternative therapies, and phages represent a viable strategy. Today, human phage therapy is done routinely in some parts of the world, such as in the Republic of Georgia and in Poland, but it remains an experimental treatment option in most countries. However, other countries are beginning to consider phage therapy in light of the current global antibiotic resistance crisis, and popular media outlets are increasingly covering phage therapy [8–10].

Acceptance of phage therapy depends on the demonstration of its safety and efficacy. Historical use of phages to treat human infections led to low efficacy compared to antibiotics, though this is to be expected based on the host specificity of phages compared to the broad-spectrum activity of antibiotics. Although there have been very few documented negative side effects of phage therapy, the risk of administering any poorly characterized entity to humans poses safety risks. In particular, the risk of phage-induced horizontal gene transfer of antibiotic resistance and virulence genes must be considered. Phages may transfer virulence traits to infected organisms, which could increase their pathogenicity [11-12]. A well-known example of this is represented by *Vibrio cholerae* and its historical acquisition of cholera toxin genes from a phage [13-14]. Unfortunately, uncharacterized phage genes, which make up a substantial proportion of most sequenced phage genomes to date, cannot easily be flagged as potentially harmful [15-16]. Other risks involve the possibilities that bacteria could evolve to be more virulent upon evolving to evade phage predation, that phages could lead to release of toxic bacterial products upon cell lysis, and that phages could induce an immune response in patients.

Outside of the above-mentioned safety risks, because of the strain-specificity of phages, the identity of the bacterial pathogen to be treated must be known before phage preparations can be generated [17]. Phage treatment must either be tailored to each patient isolate, or diverse sets of phages must be combined into cocktails to make broad-spectrum phage preparations. Importantly, bacterial resistance to phages does occur, so regardless of the strategy, many phages are generally required to treat a given infection. Therefore, large libraries of well-characterized phages targeting human bacterial pathogens are in high demand, and detailed

information regarding the interactions between phages and pathogens is important for the success of phage therapy.

1.2.3. Exploitation of phage proteins for biotechnology applications

1.2.3.1. Bacterial biocontrol and diagnostics

In addition to being used for direct human therapy, phages can also be applied as agents of controlling bacterial contamination in food preparation and agricultural settings [18-19]. One example involves the spraying of phage preparations onto fresh produce and meat, which are being used successfully to control contamination of several pathogens and has led to several products currently on the market [20]. Phages are also being used in bacterial diagnostic applications; certain phages have been exploited as sensitive methods of detecting live bacteria in infection-dependent luminescent assays [21], and others have been immobilized on solid surfaces in order to take advantage of their host-specific binding properties [22]. Importantly, the efficacy of these technologies also requires extensive phage characterization.

Alternatively, phage-encoded host-recognition proteins can be exploited in bacterial biocontrol and diagnostic technologies [23]. Phage receptor binding proteins (RBPs), such as tailspikes and tail fiber proteins, have been shown to agglutinate specific bacterial cells, providing a rapid visible indicator of bacterial presence [24], and have even been shown to reduce bacterial colonization *in vivo* as a result of this activity [25]. Some phage RBPs have been fused with bactericidal agents such as pyocins, which allow for customizable and targeted killing of bacteria [26-27].

1.2.3.2. Phage proteins as reagents for glycobiology research

Bacteria make a diversity of surface glycans, many of which are distinct from known eukaryotic glycans, and are thus not specifically recognized by most currently available antibodies or lectins. Phage glycan-binding proteins (GBPs) can be exploited as useful tools, both for bacterial detection and for bacterial study [28]. Therefore, phages represent an important reservoir of bacteria-specific glycan-binding proteins that can be used to understand more about the structures and diversity of bacterial glycans as well as effects of targeting these structures on bacterial biology and evolution. This knowledge is essential for the development of effective vaccines and other antibacterial strategies; it is appreciated that many pathogens are extensively surface-glycosylated, and thus exploiting novel methods to examine the glycobiology of their target pathogens provides valuable resources for their study.

1.3. *Campylobacter jejuni*

1.3.1. Incidence, pathology and treatment

Campylobacter jejuni is a microaerophilic Gram-negative epsilon-proteobacterium that causes diarrheal disease in humans worldwide [29,30]. Campylobacteriosis is considered one of the most widespread infectious diseases of the last century, and evidence suggests its prevalence is rising in both high and low resource countries [30]. In fact, 85% of children in 8 low-resource countries were infected with *Campylobacter* in the first year of life, many of them asymptomatically [31,32].

Many *Campylobacter species* cause disease by adhering to and invading gastrointestinal epithelial cells following ingestion of contaminated food or water, which results in an inflammatory response that can result in moderate to severe diarrhea [33,34]. Although frequently self-limiting in healthy individuals, particularly in high-resource settings, campylobacteriosis can lead to Guillain-Barré syndrome, septicaemia, arthritis, and has also been associated with irritable bowel syndrome [30,33]. In low-resource settings, campylobacteriosis has been shown to be associated with growth stunting in children. Most human campylobacteriosis cases are caused by *C. jejuni* and *Campylobacter coli* [33]. In high-resource settings, *Campylobacter* infections tend to arise from mishandling or consuming contaminated poultry or dairy products, whereas in low-resource settings, *Campylobacter* infections commonly arise upon consumption of contaminated water [30].

The natural reservoir for *C. jejuni* is the chicken lower gastrointestinal (GI) tract, where it resides as part of the chicken commensal microbiota [33]. In fact, it is normal for chickens to be colonized with up to 10^9 CFU per gram of cecal contents [35]. *C. jejuni* also asymptomatically colonizes other domestic and wild birds, as well as mammals, including ruminants and even companion animals [33]. In general, and for as yet unknown reasons, *C. jejuni* only causes disease in humans and non-human primates.

One of the primary strategies to reduce *C. jejuni* incidence in humans is to reduce its incidence in the avian reservoirs where it is most prevalent, namely, on poultry farms [33,35,36]. It has been predicted that a reduction by even 2 $\log_{10}$ units would lead to a 30-fold decrease in human infections [37]. Antibiotic resistance, particularly to macrolides (e.g. erythromycin) and

fluoroquinolones (e.g. ciprofloxacin), is becoming a growing problem in *Campylobacter* species, and antibiotic use is generally contraindicated for treating *C. jejuni* due to its generally self-limiting nature [38–40]. To date, progress has been made toward testing several alternative strategies to reduce *Campylobacter* incidence in poultry, including poultry vaccination and treatment of flocks with probiotics, bacteriocins and bacteriophages [33,41–43]. However, difficulties associated with administering these treatments or prophylactics to poultry flocks, paired with high strain-strain variability and rapid adaptation by *C. jejuni*, mechanisms behind which are poorly understood (as discussed below), complicates the use of these biocontrol strategies [33]. Strategies for treating human *C. jejuni* infections are hampered by similar hurdles, and improved understanding of the biology of *C. jejuni* will contribute greatly to the design of rational and specific anti-*Campylobacter* strategies.

1.3.2. Biology and pathogenesis

C. jejuni virulence mechanisms are poorly understood, and many common virulence factors encoded by other pathogens are missing from *C. jejuni* [44]. However, some of the most important factors known to contribute to *C. jejuni* pathogenesis are the features that allow it to colonize the human GI tract, and strategies aimed at preventing this colonization could lead to effective control of this pathogen. Prominent examples of colonization factors in *C. jejuni* include its expression of glycoconjugate structures and its highly motile flagella. In addition, *C. jejuni* displays a high degree of variation in the presentation of many of these surface structures.

1.3.2.1 Flagellar motility

C. jejuni forms spiral shaped rods with bipolar flagella, and flagellar motility is required for efficient colonization of the mucous lining of the GI tract of its hosts [45]. Flagella mediate adherence, invasion and biofilm formation in *C. jejuni*, and the importance of this organelle is further underscored by the fact that two out of the three sigma factors encoded by *C. jejuni* are mainly dedicated to regulation of flagella and motility [46]. The flagellar filament in bacteria is driven by the proton motive force (PMF) via a mechanical motor made up of a multi-subunit stator system (MotA and MotB proteins) [47]. In *Campylobacter,* the flagellar motor is larger than that made by other proteobacteria, which has been shown to provide more torque and allow *Campylobacter* cells to swim more efficiently through viscous substances, such as the mucous lining of the GI tract [47]. As well, the *Campylobacter* flagellar filament is also made differently from that of other proteobacteria; 11 protofilaments, instead of 7 for *E. coli* and *Salmonella,* make up the *Campylobacter* filament [48]. Notably, *Campylobacter* flagella are not detected by mammalian TLR5 receptors, which recognize *E. coli* and *Salmonella* flagella due to an internal region that is missing in *Campylobacter* flagellin [49]. Another important difference between *Campylobacter* flagella and that of *E. coli* and *Salmonella* is that only *Campylobacter* flagella require glycosylation for proper filament formation [50]. It is hypothesized that the requirement for *Campylobacter* flagellar glycosylation evolved as a way of compensating for the lack of the TLR5-recognized internal portion of flagellar filament proteins in other bacteria [51]. As well, it has been hypothesized that glycans allow the filament to move through aqueous environments due to the charges contributed by glycan residues [52].

1.3.2.2. Expression of surface glycoconjugates

Another factor that contributes to *C. jejuni* pathogenesis is its unusually high capacity to synthesize surface glycoconjugates, and the fact that different *C. jejuni* strains tend to express different glycan structures [53–56]. This diversity results in part from different strains possessing different sets of glycoconjugate biosynthetic enzymes. As well, many of these genes harbour phase-variable poly-G tracts, leading to layers of variability mechanisms driving *C. jejuni* glycoconjugate presentation [53,56,57]. The next sections will describe the current understanding of *C. jejuni* glycobiology in general, with a focus on flagellar glycosylation in particular.

1.3.2.2.1. Overview

Glycobiology, the study of carbohydrates in biological systems, is a rapidly advancing field in the natural sciences. It has been long known that bacteria make uniquely glycosylated structures, in particular surface-exposed structures, such lipopolysaccharides (LPS), lipoteichoic acids (LTA), teichoic acids (TA), capsules (CPS) and glycoproteins [54,56,58,59].

Four main classes of surface glycans are synthesized by *C. jejuni*, and all four classes are important for *C. jejuni* gut colonization and virulence [56]. Two are lipid-anchored, namely lipooligosaccharides (LOS) and CPS, and two are protein-linked, namely N-linked and O-linked glycoproteins. With the exception of N-linked protein glycosylation, all classes of *C. jejuni* glycoconjugate structures display high inter- and intra-strain variation [56]. Therefore, in *C. jejuni,* gene content at the biosynthetic loci does not necessarily dictate the structure of glycoconjugates displayed.

1.3.2.2.2. Lipid-anchored glycan expression

Lipid-anchored glycans are commonly displayed on bacterial cell surfaces. These include CPS and LOS synthesized by *C. jejuni* [56]. These sugars form thick matrices surrounding bacterial cells that help avoid complement and protect from other forms of immune responses [56]. They are synthesized in the cytoplasm and transported through the membranes by ATP-driven pumps [56].

C. jejuni CPS are lipid-linked polysaccharides composed of a repeating set of core glycans; these glycans are highly variable among *C. jejuni* strains in terms of gene content [60]. As well, phase-variable poly-G tracts are contained within the open reading frames of CPS-associated glycosyltransferases [61]. CPS is required for virulence and serum resistance, is important for adherence and invasion, plays a role in phage susceptibility and resistance, and may play a role in environmental survival [56,62]. As a result of these strain-strain differences, differences in CPS form the main basis for the heat-stable Penner serotyping scheme in *Campylobacter* [63,64].

C. jejuni LOS glycans are lipid A-substituted oligosaccharides that extend from the outer leaflet of the outer membrane. They are distinct from LPS, as they do not contain the repeating O-antigen that is characteristic of many other Gram-negative bacteria. LOS has been shown to be highly variable among strains, which results from both slipped strand mispairing and by differences in gene content [56]. LOS has been shown to facilitate adherence and invasion, and certain LOS glycans lead to reduced immunoreactivity and increased serum resistance [65,66].

C. jejuni LOS is responsible for causing the autoimmune response that causes Guillain-Barré syndrome [67,68]. As certain *C. jejuni* strains display human ganglioside-mimicking glycans on their LOS, antibodies can be generated against these glycans that cross-react with human neuronal gangliosides and cause neurodegeneration [68].

1.3.2.2.3. Protein glycosylation

1.3.2.2.3.1. Overview

Protein glycosylation, the conjugation of glycans to protein carriers, is being increasingly well-studied due to the abundance and importance in cells across all domains of life [54,69,70]. Protein glycosylation was first described as early as the 1930s, and was thought to be a strictly eukaryotic process until the 1970s, when an archaeon and a hyperthermophilic bacterium were found to glycosylate their surface (S-) layers [71–73]. Protein glycosylation can be separated into two main types: N-linked glycosylation, where proteins are glycosylated at asparagine residues, and O-linked glycosylation, where proteins are typically glycosylated at serine or threonine residues [54]. As well, S-layer glycoproteins have been shown to comprise tyrosine-linked glycans [74,75]. Although bacteria were thought to use only O-glycosylation for many years, evidence for an N-linked glycosylation pathway in the Gram-negative epsilon-proteobacterium *C. jejuni* was obtained in 1999 [76]. It is now appreciated that both *N*- and *O*-linked glycosylation pathways are present across all three domains of life, but understanding the breadth of their roles within cellular lifecycles, particularly in bacteria, has just begun.

1.3.2.2.3.2. General (*N*-linked) protein glycosylation

More than 60 cell envelope proteins are glycosylated by the *C. jejuni N*-linked protein glycosylation system [77]. The role of *N*-linked protein glycosylation is still unclear, and appears to vary according to the protein [78]. For example, some proteins appear to require *N*-glycosylation for proper folding, others for protease resistance, and others for enzymatic function. As well, N-glycosylation mutants cannot properly colonize chickens or mice [79]. N-linked protein glycosylation is unique in *C. jejuni* as it is the only glycoconjugate pathway that is conserved among strains and which does not exhibit phase-variation [56].

1.3.2.2.3.3. Flagellar (*O*-linked) protein glycosylation

The *C. jejuni O*-linked protein glycosylation system is only known to target the flagellar filament proteins FlaA and FlaB [51]. In certain strains, namely *C. jejuni* 11168, *C. jejuni* 81-176 and *C. coli* VC167, flagellar glycosylation genetics and biology have been well characterized over the past two decades. This has resulted from the use of mass spectrometric (MS) and nuclear magnetic resonance (NMR) technologies to analyze both flagellar glycopeptides and cytoplasmically accumulated nucleotide-activated precursors to these glycans [80–86]. In *Campylobacter,* each flagellin subunit can be glycosylated at up to 19 serine or threonine sites, which corresponds to ~400,000 glycans per flagellar filament [51,87]. Importantly, without flagellar glycosylation, *Campylobacter* flagellar filaments are not assembled and motility is abolished, leading to defective host colonization and reduced virulence [88]. To further illustrate the importance of this system, *C. jejuni* uses its flagella to coordinate symmetrical cell division [89], and of its three sigma factors, it devotes two almost exclusively to controlling flagellar biosynthesis, assembly and glycosylation [46].

C. jejuni glycosylates its flagella with nonulosonic (9-carbon) sialic acid-like sugars including pseudaminic acid (Pse5Ac7Ac), legionaminic acid (Leg5Ac7Ac) and modified derivatives of these [90,91]. Strikingly, the genome sequence of *C. jejuni* 11168 revealed 50 genes involved in flagellar glycosylation alone, seven of which are required for Pse5Ac7Ac biosynthesis (*pseB, pseC, pseH, pseG, pseI, pseF,* and *pseE)* and are known to be required for flagellar filament assembly [53,90]. Leg5Ac7Ac is synthesized through the action of *ptm* and *leg* genes in *C. jejuni* NCTC 11168 and *C. coli* VC167, but notably not in *C. jejuni* 81-176, which lacks these genes [83].

In the *C. jejuni* cytoplasm, PseB through PseF successively convert UDP-N-acetylglucosamine (UDP-GlcNAc) into CMP-pseudaminic acid (CMP- Pse5Ac7Ac) through a six-step mechanism [90]. CMP- Pse5Ac7Ac can then either be transferred to individual flagellin monomers by the action of PseE, or can be converted to acetamidino-modified pseudaminic acid (Pse5Ac7Am) by the action of PseA, a putative aminotransferase [90,92]. PseAm is then transferred by its own glycosyltransferase, PseD*,* onto flagellin proteins [82]. Some *C. jejuni* strains, which cluster together in a clade known as the livestock-associated clade, encode genes for synthesis and transfer of the Leg variants Leg5Am7Ac and Leg5NMeAm7Ac [93,94]. Many of the genes in the flagellar glycosylation locus in *C. jejuni* (10 in *C. jejuni* 11168) are phase-variable, and the roles of some of these genes in flagellar glycosylation have been determined [95]. For instance, Hitchen *et al.* (2010) showed that Cj1295 is involved in di-*O*-methyl-glyceric acid (DMGA) modification of Pse5Ac7Ac sugars in *C. jejuni* 11168 [95]. Following glycosylation, flagellin

monomers are presumed to be secreted in unfolded form through the flagellar type III secretion system (T3SS) and assembled at the apical tip of the growing filament [90].

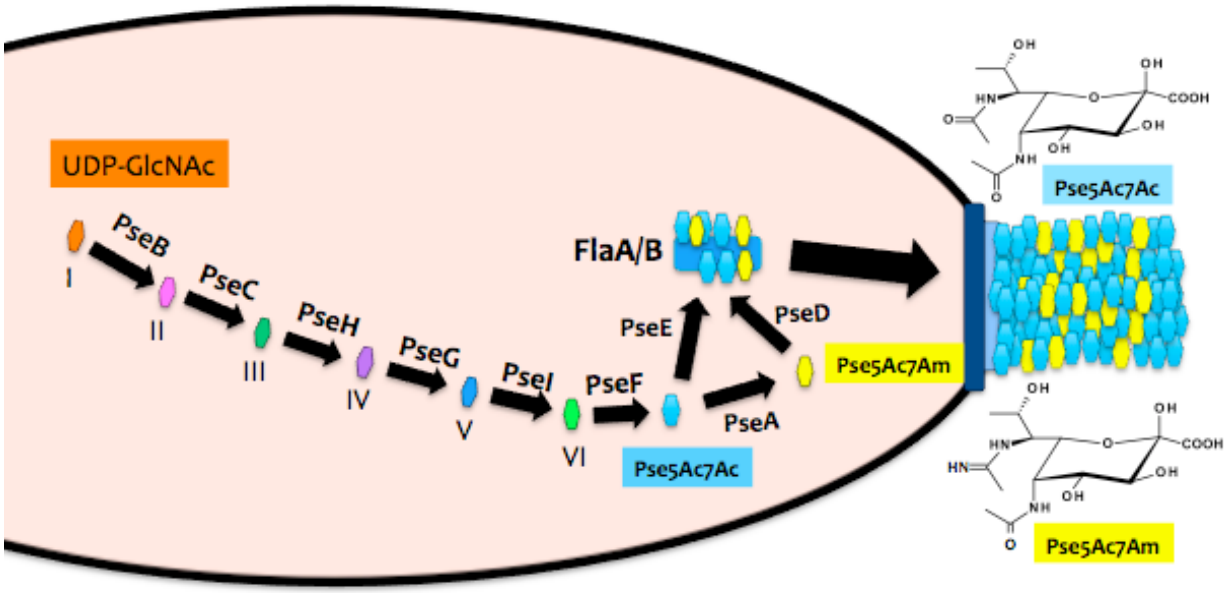

Figure 1-1. A schematic of the pseudaminic acid and acetamidino-pseudaminic acid biosynthetic pathway in *C. jejuni*.

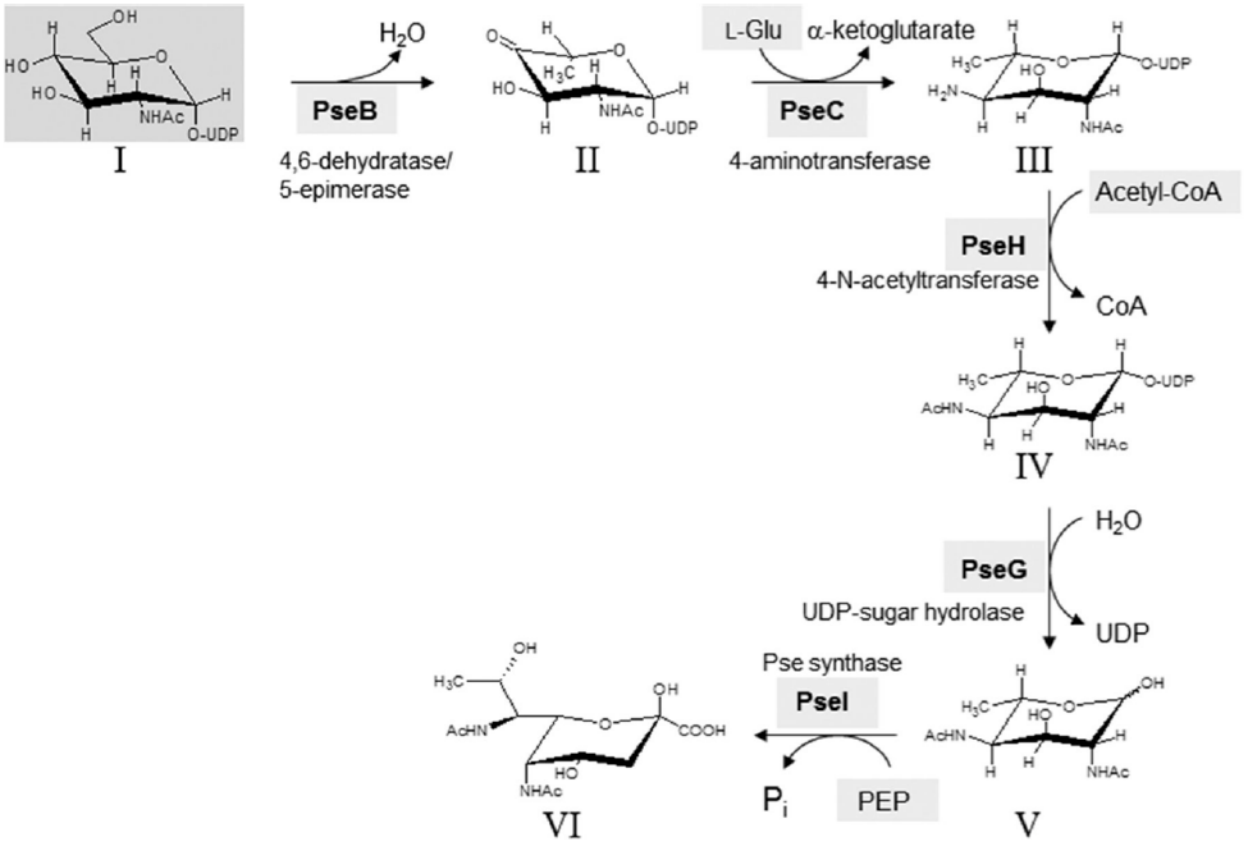

Figure 1-2. The pseudaminic acid biosynthetic pathway in *C. jejuni.* Figure reproduced from Ménard *et al.* (2014) with permission [96].

Although the glycosyltransferases involved in transfer of other *C. jejuni* glycoconjugates have been identified and characterized, there has been a notable absence of homologues of glycosyltransferases in *Campylobacter* flagellar glycosylation loci [56]. However, the observation that *pseD* and *pseE* mutants lead to cytoplasmic accumulation of Pse5Ac7Am and Pse5Ac7Ac, respectively, suggests that PseD and PseE transfer these glycans to FlaA and FlaB [82]. Interestingly, most *C. jejuni* strains analyzed to date each encode several other homologues of *pseD* and *pseE,* which are known as "motility-associated factor" (*maf*) genes [97,98]. Although roles for most *maf* genes are unknown, it is possible that these genes may function in

transferring the diverse array of glycans destined for flagellar presentation in *Campylobacter* [56] or are gene duplications used for recombination.

Data collected over the past two decades suggest that flagellar glycans play important roles in various aspects of *C. jejuni* biology and pathogenesis, and that diversity in glycan presentation may be particularly important. For example, Guerry *et al.* (2006) showed that whereas Pse5Ac7Ac is the only sugar required for flagellar assembly, the presence of Pse5Ac7Am is important for autoagglutination (AAG) of *Campylobacter* cells [92], which has been shown to be important for *C. jejuni* biofilm formation [99]. As well, a lack of Pse5Ac7Am on *C. jejuni* flagella led to reduced epithelial cell adherence and invasion, and also led to reduced virulence in a ferret model [92]. Howard *et al.* (2009) have shown that Leg5Am7Ac and Leg5NMeAm7Ac, which are acetamidino- and N-methyl-acetamidino-modified derivatives of Leg5Ac7Ac, are important for cell charge and for chicken colonization [94]. Interestingly, the related organism *Helicobacter pylori*, which also glycosylates its flagella with Pse5Ac7Ac, does not display the heterogeneity of sugar structures observed for *C. jejuni* [100]. This is presumably because *H. pylori* flagella are sheathed by an extension of the outer membrane, and thus flagellar glycans would not be expected to interact with the extracellular environment like those of *C. jejuni*.

Although flagellar glycosylation with Pse5Ac7Ac, Leg5Ac7Ac and their derivatives is clearly important to *Campylobacter* biology, much remains to be understood about the diversity of glycans displayed, the mechanisms governing their biosynthesis, transfer, distribution, and regulation, and the biological effects of displaying different glycans and combinations of

glycans. As well, little is known about how these glycans impact human infection outcomes. However, a recent study by Crofts *et al.* (2018) documented the experimental infection of humans with *C. jejuni,* and identified *C. jejuni* flagellar glycosylation gene variants associated with both acute and persistent human infection [101]. In this study, human subjects were infected with *C. jejuni,* and *C. jejuni* isolates colonizing subjects experiencing acute and recurrent gastrointestinal symptoms were sequenced. This revealed that *pseD*, which is thought to be responsible for Pse5Ac7Am transfer to flagellin, was expressed in every primary infection sample, but nonsense mutations in this gene were detected in one third of relapse infection samples. Sequence variations in other flagellar glycosylation genes were also observed among isolates causing both acute and relapsed infections. These results suggest that flagellar glycan variation plays a role in *C. jejuni* pathogenesis in humans.

1.3.2.3. Mechanisms of genetic variability

C. jejuni has a small genome of only ~1.6 Mb, with a very high density of protein-coding sequences [53]. *C. jejuni* is thought to make up for this small genome by encoding many mechanisms of variability in its gene and surface factor expression that likely contribute to its ability to rapidly adapt to a range of conditions. For instance, *C. jejuni* encodes many phase-variable homopolymeric tracts in its genes, which allow on/off switching of gene expression via slipped-strand mispairing during DNA replication [102]. The best characterized *C. jejuni* strain*, C. jejuni* 11168, has been shown to encode 28 homopolymeric tracts, and these tracts are predicted to switch on and off approximately 1 in 1000 cell divisions [53,57].

C. jejuni can also vary its gene expression in other ways. For instance, non-phase variable frameshift mutations have been shown to alter specificity of glycosyltransferases important for sialic acid display on *C. jejuni* LOS [103]. Another variability mechanism encoded by *C. jejuni* is through homologous recombination; *C. jejuni* is naturally competent, and readily takes up DNA from the environment [104].

Overall, the factors driving the extensive variability in *C. jejuni* gene expression, particularly in the context of surface structure glycosylation, are not well understood, but this variability is presumed to help *C. jejuni* colonize a range of dynamic environments and to allow it to evade phage predation and immune recognition [56,105,106].

1.4. *Campylobacter* interactions with phages

Although the natural selective pressures driving *C. jejuni* flagella and glycoconjugate expression are largely unknown, their presence and variability mechanisms are likely to be intricately linked with phage biology, as *Campylobacter* phages frequently target glycan receptors and flagella. The next section will describe the general features of *Campylobacter* phages and what is known about phage-host interactions in *C. jejuni,* particularly within the context of host glycobiology.

1.4.1. General features of *Campylobacter* phages

1.4.1.1. Phylogeny

Tailed phages of the order *Caudovirales* represent 95% of phages targeting bacterial pathogens [107]. Phages of the *Caudovirales* have historically been classified according to their virion structure. The family *Myoviridae*, which includes the well-characterized *E. coli* phage T4, is characterized by the presence of long contractile tails [108]. *Siphoviridae*, which make up the largest proportion of the *Caudovirales*, are characterized by long non-contractile tails, and include the lambda phage [109]. *Podoviridae* are characterized by their short non-contractile tails, of which the *Salmonella* phage P22 is an example [110].

Most characterized *Campylobacter* phages (over 200 isolated to date) belong to the *Myoviridae* family, although some have been found to belong to the *Siphoviridae* family [111,112]. Within the *Myoviridae*, most well characterized *Campylobacter* phages are classified within the subfamily *Eucampyvirinae*. Within the *Eucampyvirinae*, *Campylobacter* phages make up three separate groups according to morphology, genome size and sequence homology. Group I comprises phages with genomes of approximately 320 kbp and capsids approximately 143 nm in diameter, but these phages are highly unstable and refractory to analysis, and as a result have not been well studied [111]. Group II (known as Cp220viruses) comprises phages with genomes of approximately 175-195 kbp and capsids of approximately 99 nm in diameter, whereas Group III (known as Cp8viruses) comprises phages with genomes of approximately 130-140 kbp and capsids of approximately 100 nm in diameter. Several phages of the latter two groups have been sequenced, annotated and used in anti-*Campylobacter* treatment in chickens and on farms [33,42].

Campylobacter phage genomes of the *Eucampyvirinae* are considered part of the T4-like superfamily of phages based on presence of several core T4-like genes (most of which are involved in virion structure). However, *Eucampyvirinae* phage genomes are more similar overall to T4-like cyanophages, which infect ocean bacteria such as *Prochlorococcus* and *Synechococcus*, than they are to T4 itself [111].

1.4.1.2. Lifestyles

Most *Campylobacter* phages are lytic, though work has been done to characterize *Campylobacter* prophages as well, demonstrating that lysogeny in *Campylobacter* phages also occurs in nature [113]. Prophage sequences suggest that these phages have genomes of approximately 40 kbp, suggesting that these phages are taxonomically distinct from the *Eucampyvirinae* described above. Of note, no prophage sequences were identified in the most well-characterized *C. jejuni* strain, NCTC 11168 [53]. Overall, little is known about the effect of prophages on *Campylobacter* biology and evolution.

Two lytic Cp8virus phages (CP30a and CP8) of *Campylobacter* have been shown to undergo a pseudolysogenic "carrier state" life cycle (CSLC), which involves long-term association of phage with host without integration of the phage genome into the host chromosome [114–116]. This type of phage life cycle has been observed for phages targeting other bacteria, such as *Salmonella*, and appears to constitute a mechanism by which phages hedge their bets under conditions when it might be unfavourable to lyse their hosts [114,117,118]. These conditions may include low surrounding host concentration, high surrounding phage concentration, poor host growth conditions, or a variety of other factors. It has been observed that CSLC phages in

association with *C. jejuni* strain PT14 correlates with a loss of flagellar filaments and an increase in aerotolerance, suggesting that CSLC phages may induce motility reduction to reduce GI colonization of their hosts and promote their excretion into the environment [114]. These authors also showed that feeding CSLC phage-infected *C. jejuni* to chickens colonized with phage-free *C. jejuni* led to propagation of the CSLC phages on the previously phage-free population, supporting their model that CSLC phages use *C. jejuni* as a vehicle to transport themselves into new environments, presumably to increase the probability of finding uninfected cells [114].

Although intriguing as a model, it is not yet understood what molecular mechanisms lead to the decision between lytic infection and CSLC association, and whether these mechanisms are phage- or host-induced. It is also unknown whether this phenomenon is limited to certain phages of *Campylobacter,* or whether CSLC association might be more widespread. Of note, CSLC association was initially observed upon long-term phage-host association in an *in vitro* biofilm setting, suggesting that *Campylobacter* biofilms may be a prerequisite for this association and supporting the notion that CSLC association may be driven by such conditions.

1.4.1.3. Host tropism

Several phages used in historical phage typing schemes for tracking *C. jejuni* and *C. coli* strains were subsequently characterized for their receptor binding requirements, and found to target either CPS or flagella [106,119]. It has been determined that phase-variable modifications on *C. jejuni* CPS, such as *O*-methylphosphoramidate (MeOPN) affects infectivity of several *Campylobacter* phages [105,120,121]. Most of these phages are classified as Cp8viruses (ie.

group III *Campylobacter* phages). Cp220viruses have been shown to require motile flagella to infect their hosts, as evidenced by testing these phages on *C. jejuni* with paralyzed flagella (e.g. *pflA*, *motA, motB* mutants) [122,123]. Although flagella-specific *Campylobacter* phages have been identified, none have thus far been shown to require or to be blocked by particular flagellar glycans [122]. A study that identified several new *C. jejuni* phages found that phages isolated on one strain were CPS-dependent, whereas all those isolated on a second strain were flagella-dependent [123]. *Campylobacter* phages that require both CPS and flagella, or which require neither, have not yet been well-characterized.

Notably, no *Campylobacter* phages targeting N-glycosylated proteins or LOS have been identified. Others have suggested that sialylated LOS may contribute to phage defense based on the inverse correlation they observed between sialylated LOS expression and the presence of CRISPR-Cas genes [124]. However, CRISPR-Cas has not been shown to function in *C. jejuni* phage defense, weakening the hypothesis that LOS sialylation plays a role in phage defense [125].

1.4.2. Phage defense and counter-defense

1.4.2.1. Host-encoded phage defense systems

Representatives of all four known restriction/methylation classes have been identified in *C. jejuni,* suggesting a role for these enzymes in phage defense [126]. However, little work has been done to examine the effects of these systems, or other phage defense systems, on *Campylobacter* phage infection. One study showed that the minor flagellar filament gene *flaB* may play a role in *C. jejuni* phage defense, as mutagenesis of this gene led to increased phage

infectivity [127]. However, the mechanism by which FlaB exerts this effect is unknown. As mentioned above, though the *C. jejuni* CRISPR-Cas system can selectively degrade endogenous RNA, and can degrade DNA as well, it has not yet been shown to restrict *Campylobacter* phage infection [125]. Interestingly, carrier state association with phages showed increased endogenous spacer acquisition in *C. jejuni* PT14, suggesting that much remains to be learned about the interactions between phages and *C. jejuni* CRISPR-Cas action [128].

1.4.2.2. Phage avoidance of host defense mechanisms

Several phages, including T4 phage, have been shown to express hypermodified DNA, which may have evolved as a means of protecting their DNA from nucleases [129–135]. It has been suggested that *Campylobacter* phage DNA is similarly modified, as DNA from both group II and group III phages has been found to be refractory to PCR-amplification and restriction enzyme cleavage [136–138]. The nature of *Campylobacter* DNA modification has been suggested to be protein-mediated, in part based on the propensity of phage DNA to partition into the interphase upon phenol-chloroform extraction [137–139]. Alternatively, *Campylobacter* phage DNA could be modified by non-canonical nucleotides, as has been observed for other phages, including the related T4 [134,135].

1.4.3. Uses of *Campylobacter* phages in industry and biotechnology

Prior to the general availability and economic feasibility of whole-genome sequencing for epidemiological purposes, *Campylobacter* phages were used in phage typing schemes, including as recently as 2000, when they were used during the Walkerton, Ontario outbreak [119,140–142].

As even moderate reduction in *Campylobacter* levels in chickens is predicted to substantially reduce numbers of human campylobacteriosis cases, the use of *Campylobacter* phages to treat chickens in agricultural settings has garnered interest [42,43,143,144]. In fact, significant progress has been made toward showing that *Campylobacter* phages can be effective at reducing *C. jejuni* and *C. coli* in chicken flocks [33,42,43,145–149]. However, to date, the phage titers so far shown to be necessary to significantly reduce *Campylobacter* on farms are extremely high [33,143]. This indicates poor feasibility of this treatment strategy. However, increased understanding of *Campylobacter* phage infection dynamics that could lead to optimization of burst size, adsorption rate, and inoculation timing could help improve feasibility of this approach [42].

To date, no studies have tested the efficacy of phage therapy as a treatment of *Campylobacter* infections in humans. However, as the levels of *Campylobacter* in humans are substantially lower than those in chickens, the numbers of phages required to treat these infections would likely be much lower compared to the numbers required to eliminate *Campylobacter* from chickens [33]. As antibiotic resistance in *C. jejuni* continues to rise, and based on the known ill effects of antibiotic use, it is becoming recognized that the use of phages to treat human infections is worth pursuing.

1.4.4. *Campylobacter* phage NCTC 12673

NCTC 12673 is a *C. jejuni*-specific lytic phage of the *Myoviridae* family of tailed phages. This phage has a long, contractile tail and its 135-kbp plinear dsDNA chromosome is contained by an

icosahedral protein capsid [137]. This phage was originally used as a *Campylobacter* typing phage and has been shown to require *C. jejuni* CPS for infection [106,141]. Although NCTC 12673 phage falls within the Cp8virus group, which is typically considered to be CPS-specific [106,123], we recently found that this phage can no longer successfully infect *C. jejuni* when certain early genes of this phage's flagellar glycosylation pathway (*pseC* or *pseH*) are disrupted. This suggests a dependence on host *O*-glycosylation, which has not previously been described for any *Campylobacter* phage.

1.4.5. Gp047, a flagellar glycan-specific *Campylobacter* phage protein

Interestingly, we found that in addition to its dependency on the *C. jejuni* Pse pathway, NCTC 12673 phage also encodes a protein, Gp047, that binds specifically to Pse5Ac7Am sugars displayed on *C. jejuni* flagellin. In fact, we have shown that this protein recognizes flagellin from nearly all *C. jejuni* and *C. coli* strains tested to date, even strains resistant to infection by NCTC 12673 phage itself [24]. Interestingly, all members of the Eucampyvirinae, across both Cp220virus and Cp8virus genera, encode homologues of Gp047 [111,150,151]. Homologues are also found in some sequenced *C. jejuni* strains, but no known function exists for this protein in either context. The prevalence of *gp047* across *Campylobacter* phage genera suggests a conserved role for this protein in the phage lifecycle. Gp047 was not identified during proteomic analysis of the phage virion, and α-Gp047 polyclonal antibodies do not recognize the mature virion, suggesting that Gp047 is not a structural component of the virion but rather has an accessory role in the phage lifecycle [137,152,153].

The unknown yet presumably important role of Gp047 paired with its specificity for a prominent and virulence-associated *C. jejuni* flagellar glycan led us to explore its function in *C. jejuni*-phage dynamics. We surmised that understanding the role and function of this protein might provide the key to understanding the reason the CPS-specific phage NCTC 12673 requires flagellar glycan biosynthesis to infect its host.

1.5. Research objectives

Aim 1: Characterize phage-host interactions between NCTC 12673 and *C. jejuni*

Little is known about *C. jejuni* phage-host interactions. To understand the factors governing phage NCTC 12673 infection of *C. jejuni*, I analyzed total phage and host transcription during phage infection. Notably, phage infection induced host upregulation of genes associated with oxidative stress defense, multidrug efflux, and a putative, yet uncharacterized, phage defense operon. I subsequently determined that NCTC 12673 plaquing efficiency is reduced in the absence of antioxidant-encoding genes *katA, ahpC* and *sodB*, and is increased in the absence of the predominant *C. jejuni* multidrug efflux pump CmeABC. This work provides exciting new insights into possible *C. jejuni* phage defense mechanisms, and is described in Chapter 2.

Aim 2: Understand the function of Gp047, a flagellar glycan-binding phage protein

Early on in my program, I helped determine that *Campylobacter* phage-encoded flagellar glycan-binding protein Gp047 inhibits growth of *C. jejuni* cells, which was published as [153] and makes up Chapter 3 of my thesis. I then sought to determine the mechanism for this

inhibition. I found that Gp047-induced growth inhibition requires the presence of a functional flagellar motor, and that Gp047 causes downregulation of energy metabolism pathways. To explore how *C. jejuni* cells might alter their flagellar glycans and avoid this fate, I characterized *C. jejuni* strains exhibiting reduced Gp047 binding using flagellar mass spectrometry and genome sequence analysis. I identified a phase-variable switch on the gene encoding Pse5Ac7Am, the Gp047 receptor, in one strain that appears to be variably able to bind the protein. This work led to new insights into Gp047 interactions with *C. jejuni* cells that also illuminated possible new mechanisms of flagellar glycan variation in *C. jejuni*, and is described in Chapter 4.

Aim 3: Determine the role of *C. jejuni* flagellar glycan biosynthesis in phage infection

To understand why NCTC 12673 is unable to infect flagellar glycosylation (*pse*) pathway mutants, I analyzed the transcriptomes of two *pse* mutants and characterized a phage escape mutant. I found that *pse* mutants substantially down-regulate their flagellar genes, which led me to test NCTC 12673 for plaquing on the paralyzed flagellar mutants *motA* and *motB*. Phage infection was abolished, suggesting that NCTC 12673 phage inability to plaque on *pse* mutants may result from their lack of motility. I also found that a *pseC* escape mutant phage, MutC, could plaque efficiently on *pseCFGH* and *motAB* mutants. Interestingly, MutC could also plaque better than NCTC 12673 on oxidative stress mutants *katA* and *ahpC.* This suggested that phage plaquing defects on non-motile strains may be linked to oxidative stress, as non-motile *C. jejuni* mutants are known to be hypersensitive to oxidants [154]. Finally, genome sequence comparison showed a MutC-encoded frameshift mutation in a poly-T tract of *gp047,* which is

predicted to result in a severely truncated protein. Overall, these data suggest new insights into NCTC 12673 phage-host interactions and the role of Gp047, and is described in Chapter 5.

1.6. Final statement

The main goal of my doctoral work has been to study *C. jejuni*-phage interactions, with a special focus on how *C. jejuni* glycobiology influences this two-way interaction. Specifically, I have sought to characterize how a phage glycan-binding protein influences *C. jejuni* biology, and how flagellar glycosylation impacts phage infection. My work has uncovered new aspects of *Campylobacter*-phage interactions, including new ways *C. jejuni* might defend itself against phages, the effects of a conserved *Campylobacter* phage protein on host biology, insights into how *C. jejuni* might vary its flagellar glycans, and new information about the possible role of oxidative stress in *C. jejuni* phage-host interactions.

1.7. References

1. Suttle, C. A. Viruses in the sea. *Nature* **2005**, *437*, 356–361, doi:10.1038/nature04160.
2. Stern, A.; Sorek, R. The phage–host arms race: shaping the evolution of microbes. *Bioessays* **2011**, *33*, 43-51.
3. Seed, K. D.; Yen, M.; Shapiro, B. J.; Hilaire, I. J.; Charles, R. C.; Teng, J. E.; Ivers, L. C.; Boncy, J.; Harris, J. B.; Camilli, A. Evolutionary consequences of intra-patient phage predation on microbial populations. *Elife* **2014,** *3*, e03497.
4. Alanis, A. J. Resistance to Antibiotics: Are We in the Post-Antibiotic Era? *Arch. Med.*

Res. **2005**, *36*, 697–705, doi:10.1016/j.arcmed.2005.06.009.

5. Campbell, A. The future of bacteriophage biology. *Nat. Rev. Genet.* **2003**, *4*, 471–477, doi:10.1038/nrg1089.
6. Drulis-Kawa, Z.; Majkowska-Skrobek, G.; Maciejewska, B.; Delattre, A.-S.; Lavigne, R. Learning from Bacteriophages - Advantages and Limitations of Phage and Phage-Encoded Protein Applications. *Curr. Protein Pept. Sci.* **2012**, doi:10.2174/138920312804871193.
7. Drulis-Kawa, Z.; Majkowska-Skrobek, G.; Maciejewska, B. Bacteriophages and Phage-Derived Proteins – Application Approaches. *Curr. Med. Chem.* **2015**, *22*, 1757–1773, doi:10.2174/0929867322666150209152851.
8. Huys, I.; Pirnay, J. P.; Lavigne, R.; Jennes, S.; De Vos, D.; Casteels, M.; Verbeken, G. Paving a regulatory pathway for phage therapy. Europe should muster the resources to financially, technically and legally support the introduction of phage therapy. *EMBO Rep.* **2013**, doi:10.1038/embor.2013.163.
9. Pirnay, J. P.; Verbeken, G.; Ceyssens, P. J.; Huys, I.; de Vos, D.; Ameloot, C.; Fauconnier, A. The magistral phage. *Viruses* **2018**, *10*, doi:10.3390/v10020064.
10. Chan, B. K.; Sistrom, M.; Wertz, J. E.; Kortright, K. E.; Narayan, D.; Turner, P. E. Phage selection restores antibiotic sensitivity in MDR *Pseudomonas aeruginosa*. *Sci. Rep.* **2016**, *6*, doi:10.1038/srep26717.
11. Krylov, V. N. Role of horizontal gene transfer by bacteriophages in the origin of pathogenic bacteria. *Genetika* **2003**, *39*, 595–620.
12. Boyd, E. F. Bacteriophage-encoded bacterial virulence factors and phage-pathogenicity island interactions. *Adv. Virus Res.* **2012**, *82*, 91–118, doi:10.1016/B978-0-12-394621-

8.00014-5; 10.1016/B978-0-12-394621-8.00014-5.

13. Faruque, S. M.; Mekalanos, J. J. Phage-bacterial interactions in the evolution of toxigenic Vibrio cholerae. *Virulence* **2012**, *3*.

14. Das, B.; Bischerour, J.; Barre, F. X. Molecular mechanism of acquisition of the cholera toxin genes. *Indian J. Med. Res.* **2011**, *133*, 195–200.

15. Hatfull, G. F.; Hendrix, R. W. Bacteriophages and their genomes. *Curr. Opin. Virol.* **2011**, *1*, 298–303, doi:10.1016/j.coviro.2011.06.009; 10.1016/j.coviro.2011.06.009.

16. Klumpp, J.; Fouts, D. E.; Sozhamannan, S. Next generation sequencing technologies and the changing landscape of phage genomics. **2012**, 1–10.

17. Hyman, P.; Abedon, S. T. Bacteriophage host range and bacterial resistance. *Adv. Appl. Microbiol.* 2010.

18. Brovko, L. Y.; Anany, H.; Griffiths, M. W. Bacteriophages for detection and control of bacterial pathogens in food and food-processing environment. *Adv. Food Nutr. Res.* **2012**, *67*, 241–288, doi:10.1016/B978-0-12-394598-3.00006-X

19. Singh, A.; Poshtiban, S.; Evoy, S. Recent advances in bacteriophage based biosensors for food-borne pathogen detection. *Sensors (Basel).* **2013**, *13*, 1763–1786, doi:10.3390/s130201763; 10.3390/s130201763.

20. Leverentz, B.; Conway, W. S.; Camp, M. J.; Janisiewicz, W. J.; Abuladze, T.; Yang, M.; Saftner, R.; Sulakvelidze, A. Biocontrol of *Listeria monocytogenes* on fresh-cut produce by treatment with lytic bacteriophages and a bacteriocin. *Appl. Environ. Microbiol.* **2003**, *69*, 4519–4526.

21. Hagens, S.; Loessner, M. J. Application of bacteriophages for detection and control of foodborne pathogens. *Appl. Microbiol. Biotechnol.* **2007**, *76*, 513-519.

22. Singh, A.; Glass, N.; Tolba, M.; Brovko, L.; Griffiths, M.; Evoy, S. Immobilization of bacteriophages on gold surfaces for the specific capture of pathogens. *Biosens. Bioelectron.*, **2009,** *24*, 3645-3651.

23. Singh, A.; Arya, S. K.; Glass, N.; Hanifi-Moghaddam, P.; Naidoo, R.; Szymanski, C. M.; Tanha, J.; Evoy, S. Bacteriophage tailspike proteins as molecular probes for sensitive and selective bacterial detection. *Biosens. Bioelectron.* **2010**, *26*, 131–138, doi:DOI: 10.1016/j.bios.2010.05.024.

24. Javed, M. A.; Poshtiban, S.; Arutyunov, D.; Evoy, S.; Szymanski, C. M. Bacteriophage Receptor Binding Protein Based Assays for the Simultaneous Detection of *Campylobacter jejuni* and *Campylobacter coli*. *PLoS One* **2013**, *8*, doi:10.1371/journal.pone.0069770.

25. Waseh, S.; Hanifi-Moghaddam, P.; Coleman, R.; Masotti, M.; Ryan, S.; Foss, M.; MacKenzie, R.; Henry, M.; Szymanski, C. M.; Tanha, J. Orally administered P22 phage tailspike protein reduces salmonella colonization in chickens: prospects of a novel therapy against bacterial infections. *PLoS One* **2010**, *5*, e13904, doi:10.1371/journal.pone.0013904; 10.1371/journal.pone.0013904.

26. Scholl, D.; Cooley, M.; Williams, S. R.; Gebhart, D.; Martin, D.; Bates, A.; Mandrell, R. An engineered R-type pyocin is a highly specific and sensitive bactericidal agent for the food-borne pathogen *Escherichia coli* O157:H7. *Antimicrob. Agents Chemother.* **2009**, *53*, 3074–3080, doi:10.1128/AAC.01660-08; 10.1128/AAC.01660-08.

27. Williams, S. R.; Gebhart, D.; Martin, D. W.; Scholl, D. Retargeting R-type pyocins to generate novel bactericidal protein complexes. *Appl. Environ. Microbiol.* **2008**, *74*, 3868–3876, doi:10.1128/AEM.00141-08.

28. Simpson, D. J. D. J.; Sacher, J. C. J. C.; Szymanski, C. M. C. M. Exploring the interactions between bacteriophage-encoded glycan binding proteins and carbohydrates. *Curr. Opin. Struct. Biol.* **2015**, *34*, 69–77, doi:10.1016/j.sbi.2015.07.006.

29. Kaakoush, N. O.; Mitchell, H. M.; Man, S. M. *Campylobacter*. In *Molecular Medical Microbiology*; 2015; pp. 1187–1236 ISBN 978-0-12-397169-2.

30. Kaakoush, N. O., Castaño-Rodríguez, N., Mitchell, H. M., & Man, S. M. Global epidemiology of *Campylobacter* infection. *Clin. Microbiol. Rev.* **2015**, *28*, 3, 687-720.

31. Amour, C.; Gratz, J.; Mduma, E.; Svensen, E.; Rogawski, E. T.; McGrath, M.; Seidman, J. C.; McCormick, B. J. J. J.; Shrestha, S.; Samie, A.; Mahfuz, M.; Qureshi, S.; Hotwani, A.; Babji, S.; Trigoso, D. R.; Lima, A. A. M. M.; Bodhidatta, L.; Bessong, P.; Ahmed, T.; Shakoor, S.; Kang, G.; Kosek, M.; Guerrant, R. L.; Lang, D.; Gottlieb, M.; Houpt, E. R.; Platts-Mills, J. A.; Etiology, Risk Factors, and Interactions of Enteric Infections and Malnutrition and the Consequences for Child Health and Development Project (MAL-ED) Network Investigators Epidemiology and Impact of *Campylobacter* Infection in Children in 8 Low-Resource Settings: Results from the MAL-ED Study. *Clin. Infect. Dis.* **2016**, *63*, 1171–1179, doi:10.1093/cid/ciw542.

32. Miller, M.; Acosta, A. M.; Chavez, C. B.; Flores, J. T.; Olotegui, M. P.; Pinedo, S. R.; Trigoso, D. R.; Vasquez, A. O.; Ahmed, I.; Alam, D.; Ali, A.; … and Shrestha, S. K. The MAL-ED study: A multinational and multidisciplinary approach to understand the relationship between enteric pathogens, malnutrition, gut physiology, physical growth, cognitive development, and immune responses in infants and children up to 2 years of . *Clin. Infect. Dis.* **2014**, *59*, S193–S206, doi:10.1093/cid/ciu653.

33. Johnson, T. J.; Shank, J. M.; Johnson, J. G. Current and Potential Treatments for

Reducing *Campylobacter* Colonization in Animal Hosts and Disease in Humans. *Front. Microbiol.* **2017**, *8*, 487, doi:10.3389/fmicb.2017.00487.

34. Backert, S.; Hofreuter, D. Molecular methods to investigate adhesion, transmigration, invasion and intracellular survival of the foodborne pathogen *Campylobacter jejuni*. *J. Microbiol. Methods* **2013**.

35. Meunier, M.; Guyard-Nicodème, M.; Dory, D.; Chemaly, M. Control strategies against *Campylobacter* at the poultry production level: Biosecurity measures, feed additives and vaccination. *J. Appl. Microbiol.* **2016**.

36. Wassenaar, T. M. Following an imaginary *Campylobacter* population from farm to fork and beyond: A bacterial perspective. *Lett. Appl. Microbiol.* 2011, *53*, 253–263.

37. Rosenquist, H.; Nielsen, N. L.; Sommer, H. M.; Nørrung, B.; Christensen, B. B. Quantitative risk assessment of human campylobacteriosis associated with thermophilic *Campylobacter* species in chickens. *Int. J. Food Microbiol.* **2003**, doi:10.1016/S0168-1605(02)00317-3.

38. Kumar, A.; Drozd, M.; Pina-Mimbela, R.; Xu, X.; Helmy, Y. A.; Antwi, J.; Fuchs, J. R.; Nislow, C.; Templeton, J.; Blackall, P. J.; Rajashekara, G. Novel anti-*Campylobacter* compounds identified using high throughput screening of a pre-selected enriched small molecules library. *Front. Microbiol.* **2016**, doi:10.3389/fmicb.2016.00405.

39. Moore, J. E.; Barton, M. D.; Blair, I. S.; Corcoran, D.; Dooley, J. S. G.; Fanning, S.; Kempf, I.; Lastovica, A. J.; Lowery, C. J.; Matsuda, M.; McDowell, D. A.; McMahon, A.; Millar, B. C.; Rao, J. R.; Rooney, P. J.; Seal, B. S.; Snelling, W. J.; Tolba, O. The epidemiology of antibiotic resistance in *Campylobacter*. *Microbes Infect.* 2006.

40. Ternhag, A.; Asikainen, T.; Giesecke, J.; Ekdahl, K. A meta-analysis on the effects of

antibiotic treatment on duration of symptoms caused by infection with *Campylobacter* species. *Clin. Infect. Dis.* **2007**, doi:10.1086/509924.

41. Nothaft, H.; Davis, B.; Lock, Y. Y.; Perez-Munoz, M. E.; Vinogradov, E.; Walter, J.; Coros, C.; Szymanski, C. M. Engineering the *Campylobacter jejuni* N-glycan to create an effective chicken vaccine. *Sci. Rep.* **2016**, doi:10.1038/srep26511.
42. Connerton, P. L.; Timms, A. R.; Connerton, I. F. *Campylobacter* bacteriophages and bacteriophage therapy. *J. Appl. Microbiol.* 2011, *111*, 255–265.
43. Carvalho, C. M.; Gannon, B. W.; Halfhide, D. E.; Santos, S. B.; Hayes, C. M.; Roe, J. M.; Azeredo, J. The in vivo efficacy of two administration routes of a phage cocktail to reduce numbers of *Campylobacter coli* and *Campylobacter jejuni* in chickens. *BMC Microbiol.* **2010**, *10*, 232, doi:10.1186/1471-2180-10-232.
44. Bolton, D. J. *Campylobacter* virulence and survival factors. *Food Microbiol.* 2015, *48*, 99–108.
45. Guerry, P. *Campylobacter* flagella: not just for motility. *Trends Microbiol.* 2007, *15*, 456–461.
46. Hendrixson, D. R. Regulation of flagellar gene expression and assembly. In; Nachamkin, I., Szymanski, C. M., Blaser, M. J., Eds.; *Campylobacter*; American Society for Microbiology: Washington, D.C., 2008; pp. 545–558.
47. Beeby, M.; Ribardo, D. A.; Brennan, C. A.; Ruby, E. G.; Jensen, G. J. Diverse high-torque bacterial flagellar motors assemble wider stator rings using a conserved protein scaffold. **2016**, 1–10, doi:10.1073/pnas.1518952113.
48. Gilbreath, J. J.; Cody, W. L.; Merrell, D. S.; Hendrixson, D. R. Change is good: variations in common biological mechanisms in the epsilonproteobacterial genera

Campylobacter and *Helicobacter*. *Microbiol. Mol. Biol. Rev.* **2011**, *75*, 84–132, doi:10.1128/MMBR.00035-10.

49. Galkin, V. E.; Yu, X.; Bielnicki, J.; Heuser, J.; Ewing, C. P.; Guerry, P.; Egelman, E. H. Divergence of quaternary structures among bacterial flagellar filaments. *Science (80-.).* **2008**, *320*, 382–385, doi:10.1126/science.1155307.

50. Gao, B.; Lara-Tejero, M.; Lefebre, M.; Goodman, A. L.; Galán, J. E. Novel components of the flagellar system in epsilonproteobacteria. *MBio* **2014**, *5*, doi:10.1128/mBio.01349-14.

51. Logan, S. M. Flagellar glycosylation - A new component of the motility repertoire? *Microbiology* 2006, *152*, 1249–1262.

52. Thibault, P.; Logan, S. M.; Kelly, J. F.; Brisson, J. R.; Ewing, C. P.; Trust, T. J.; Guerry, P. Identification of the Carbohydrate Moieties and Glycosylation Motifs in *Campylobacter jejuni* Flagellin. *J. Biol. Chem.* **2001**, *276*, 34862–34870, doi:10.1074/jbc.M104529200.

53. Parkhill, J.; Wren, B. W.; Mungall, K.; Ketley, J. M.; Churcher, C.; Basham, D.; Chillingworth, T.; Davies, R. M.; Feltwell, T.; Holroyd, S.; Jagels, K.; Karlyshev, A. V.; Moule, S.; Pallen, M. J.; Penn, C. W.; Quail, M. A.; Rajandream, M. A.; Rutherford, K. M.; Van Vliet, A. H. M.; Whitehead, S.; Barrell, B. G. The genome sequence of the food-borne pathogen *Campylobacter jejuni* reveals hypervariable sequences. *Nature* **2000**, doi:10.1038/35001088.

54. Nothaft, H.; Szymanski, C. M. Protein glycosylation in bacteria: sweeter than ever. *Nat. Rev. Microbiol.* **2010**, *8*, 765–778, doi:10.1038/nrmicro2383.

55. Guerry, P.; Szymanski, C. M. *Campylobacter* sugars sticking out. *Trends Microbiol.*

2008, 16, 428-435, doi:10.1016/j.tim.2008.07.002.

56. Karlyshev, A. V.; Ketley, J. M.; Wren, B. W. The *Campylobacter jejuni* glycome. *FEMS Microbiol. Rev.* 2005, *29*, 377–390.

57. Lango-Scholey, L.; Aidley, J.; Woodacre, A.; Jones, M. A.; Bayliss, C. D. High throughput method for analysis of repeat number for 28 phase variable loci of *Campylobacter jejuni* strain NCTC11168. *PLoS One* **2016**, *11*, doi:10.1371/journal.pone.0159634.

58. Merino, S.; Tomás, J. M. Gram-negative flagella glycosylation. *Int. J. Mol. Sci.* 2014, *15*, 2840–2857.

59. Eichler, J.; Koomey, M. Sweet New Roles for Protein Glycosylation in Prokaryotes. *Trends Microbiol.* **2017**, doi:10.1016/j.tim.2017.03.001.

60. Karlyshev, A. V.; Champion, O. L.; Churcher, C.; Brisson, J. R.; Jarrell, H. C.; Gilbert, M.; Brochu, D.; St Michael, F.; Li, J.; Wakarchuk, W. W.; Goodhead, I.; Sanders, M.; Stevens, K.; White, B.; Parkhill, J.; Wren, B. W.; Szymanski, C. M. Analysis of *Campylobacter jejuni* capsular loci reveals multiple mechanisms for the generation of structural diversity and the ability to form complex heptoses. *Mol. Microbiol.* **2005**, doi:10.1111/j.1365-2958.2004.04374.x.

61. Karlyshev, A. V.; Champion, O. L.; Churcher, C.; Brisson, J. R.; Jarrell, H. C.; Gilbert, M.; Brochu, D.; St Michael, F.; Li, J.; Wakarchuk, W. W.; Goodhead, I.; Sanders, M.; Stevens, K.; White, B.; Parkhill, J.; Wren, B. W.; Szymanski, C. M. Analysis of *Campylobacter jejuni* capsular loci reveals multiple mechanisms for the generation of structural diversity and the ability to form complex heptoses. *Mol. Microbiol.* **2005**, *55*, 90–103, doi:10.1111/j.1365-2958.2004.04374.x.

62. Bacon, D. J.; Szymanski, C. M.; Burr, D. H.; Silver, R. P.; Alm, R. A.; Guerry, P. A phase-variable capsule is involved in virulence of *Campylobacter jejuni* 81-176. *Mol. Microbiol.* **2001**, *40*, 769–777, doi:10.1046/j.1365-2958.2001.02431.x.

63. Penner, J. L.; Hennessy, J. N.; Congi, R. V. Serotyping of *Campylobacter jejuni* and *Campylobacter coli* on the basis of thermostable antigens. *Eur. J. Clin. Microbiol.* **1983**, doi:10.1007/BF02019474.

64. Karlyshev, A. V; Linton, D.; Gregson, N. A.; Lastovica, A. J.; Wren, B. W. Genetic and biochemical evidence of a *Campylobacter jejuni* capsular polysaccharide that accounts for Penner serotype specificity. *Mol. Microbiol.* **2000**, *35*, 529–541.

65. Guerry, P.; Ewing, C. P.; Hickey, T. E.; Prendergast, M. M.; Moran, A. P. Sialylation of lipooligosaccharide cores affects immunogenicity and serum resistance of *Campylobacter jejuni*. *Infect. Immun.* **2000**, doi:10.1128/IAI.68.12.6656-6662.2000.

66. Guerry, P.; Szymanski, C. M.; Prendergast, M. M.; Hickey, T. E.; Ewing, C. P.; Pattarini, D. L.; Moran, A. P. Phase variation of *Campylobacter jejuni* 81-176 lipooligosaccharide affects ganglioside mimicry and invasiveness in vitro. *Infect. Immun.* **2002**, doi:10.1128/IAI.70.2.787-793.2002.

67. Yuki, N.; Susuki, K.; Koga, M.; Nishimoto, Y.; Odaka, M.; Hirata, K.; Taguchi, K.; Miyatake, T.; Furukawa, K.; Kobata, T.; Yamada, M. Carbohydrate mimicry between human ganglioside GM1 and *Campylobacter jejuni* lipooligosaccharide causes Guillain-Barre syndrome. *Proc. Natl. Acad. Sci.* **2004**, *101*, 11404–11409, doi:10.1073/pnas.0402391101.

68. Yuki, N. Carbohydrate mimicry: a new paradigm of autoimmune diseases. *Curr. Opin. Immunol.* **2005**, *17*, 577–582, doi:10.1016/j.coi.2005.09.004.

69. Iwashkiw, J. A.; Vozza, N. F.; Kinsella, R. L.; Feldman, M. F. Pour some sugar on it: The expanding world of bacterial protein O-linked glycosylation. *Mol. Microbiol.* **2013**, *89*, 14–28.

70. Abu-Qarn, M.; Eichler, J.; Sharon, N. Not just for Eukarya anymore: protein glycosylation in Bacteria and Archaea. *Curr. Opin. Struct. Biol.* 2008, *18*, 544–550.

71. Mescher, M. F.; Strominger, J. L. Purification and characterization of a prokaryotic glucoprotein from the cell envelope of *Halobacterium salinarium*. *J. Biol. Chem.* **1976**, *251*, 2005–2014.

72. Sleytr, U. B. Heterologous reattachment of regular arrays of glycoproteins on bacterial surfaces. *Nature* **1975**, *257*, 400–402.

73. Neuberger, A. Carbohydrates in protein: The carbohydrate component of crystalline egg albumin. *Biochem. J.* **1938**, *32*, 1435–1451.

74. Kandiba, L.; Aitio, O.; Helin, J.; Guan, Z.; Permi, P.; Bamford, D. H.; Eichler, J.; Roine, E. Diversity in prokaryotic glycosylation: An archaeal-derived N-linked glycan contains legionaminic acid. *Mol. Microbiol.* **2012**, *84*, 578–593, doi:10.1111/j.1365-2958.2012.08045.x.

75. Guerry, P. N-linked glycosylation in Archaea: Two paths to the same glycan. *Mol. Microbiol.* **2011**, *81*, 1133–1135.

76. Szymanski, C. M.; Yao, R.; Ewing, C. P.; Trust, T. J.; Guerry, P. Evidence for a system of general protein glycosylation in *Campylobacter jejuni*. *Mol. Microbiol.* **1999**, *32*, 1022–1030, doi:10.1046/j.1365-2958.1999.01415.x.

77. Szymanski, C. M.; Logan, S. M.; Linton, D.; Wren, B. W. *Campylobacter* - A tale of two protein glycosylation systems. *Trends Microbiol.* 2003, *11*, 233–238.

78. Nothaft, H.; Szymanski, C. M. Bacterial protein n-glycosylation: New perspectives and applications. *J. Biol. Chem.* **2013**, *288*, 6912–6920.

79. Alemka, A.; Nothaft, H.; Zheng, J.; Szymanski, C. M. N-glycosylation of *Campylobacter jejuni* surface proteins promotes bacterial fitness. *Infect. Immun.* **2013**, doi:10.1128/IAI.01370-12.

80. Soo, E. C.; Hui, J. P. Metabolomics in glycomics. *Methods Mol. Biol.* **2010**, *600*, 175–186, doi:10.1007/978-1-60761-454-8_12; 10.1007/978-1-60761-454-8_12.

81. Schirm, M.; Schoenhofen, I. C.; Logan, S. M.; Waldron, K. C.; Thibault, P. Identification of unusual bacterial glycosylation by tandem mass spectrometry analyses of intact proteins. *Anal. Chem.* **2005**, *77*, 7774–7782, doi:10.1021/ac051316y.

82. McNally, D. J.; Hui, J. P. M.; Aubry, A. J.; Mui, K. K. K.; Guerry, P.; Brisson, J. R.; Logan, S. M.; Soo, E. C. Functional characterization of the flagellar glycosylation locus in *Campylobacter jejuni* 81-176 using a focused metabolomics approach. *J. Biol. Chem.* **2006**, *281*, 18489–18498, doi:10.1074/jbc.M603777200.

83. McNally, D. J.; Aubry, A. J.; Hui, J. P. M.; Khieu, N. H.; Whitfield, D.; Ewing, C. P.; Guerry, P.; Brisson, J. R.; Logan, S. M.; Soo, E. C. Targeted metabolomics analysis of *Campylobacter coli* VC167 reveals legionaminic acid derivatives as novel flagellar glycans. *J. Biol. Chem.* **2007**, *282*, 14463–14475, doi:10.1074/jbc.M611027200.

84. Ulasi, G. N.; Creese, A. J.; Hui, S. X.; Penn, C. W.; Cooper, H. J. Comprehensive mapping of O-glycosylation in flagellin from *Campylobacter jejuni* 11168: A multienzyme differential ion mobility mass spectrometry approach. *Proteomics* **2015**, *15*, 2733–2745, doi:10.1002/pmic.201400533.

85. Zampronio, C. G.; Blackwell, G.; Penn, C. W.; Cooper, H. J. Novel glycosylation sites

localized in *Campylobacter jejuni* flagellin FlaA by liquid chromatography electron capture dissociation tandem mass spectrometry. *J. Proteome Res.* **2011**, *10*, 1238–1245, doi:10.1021/pr101021c.

86. Zebian, N.; Merkx-Jacques, A.; Pittock, P. P.; Houle, S.; Dozois, C. M.; Lajoie, G. A.; Creuzenet, C. Comprehensive analysis of flagellin glycosylation in *Campylobacter jejuni* NCTC 11168 reveals incorporation of legionaminic acid and its importance for host colonization. *Glycobiology* **2016**, *26*, 386–397, doi:10.1093/glycob/cwv104.

87. Ewing, C. P.; Andreishcheva, E.; Guerry, P. Functional characterization of flagellin glycosylation in *Campylobacter jejuni* 81-176. *J. Bacteriol.* **2009**, *191*, 7086–7093, doi:10.1128/JB.00378-09.

88. Goon, S.; Kelly, J. F.; Logan, S. M.; Ewing, C. P.; Guerry, P. Pseudaminic acid, the major modification on *Campylobacter* flagellin, is synthesized via the Cj1293 gene. *Mol. Microbiol.* **2003**, *50*, 659–671, doi:10.1046/j.1365-2958.2003.03725.x.

89. Kazmierczak, B. I.; Hendrixson, D. R. Spatial and numerical regulation of flagellar biosynthesis in polarly flagellated bacteria. *Mol. Microbiol.* **2013**, *88*, 655–663, doi:10.1111/mmi.12221; 10.1111/mmi.12221.

90. Logan, S. M.; Schoenhofen, I. C.; Guerry, P. O-linked flagellar glycosylation in *Campylobacter*. In; Nachamkin, I., Szymanski, C. M., Blaser, M. J., Eds.; *Campylobacter*; ASM Press: Washington, D.C., 2008; pp. 471–481.

91. Zunk, M.; Kiefel, M. J. The occurrence and biological significance of the α-keto-sugars pseudaminic acid and legionaminic acid within pathogenic bacteria. *RSC Adv.* **2014**, *4*, 3413–3421, doi:10.1039/C3RA44924F.

92. Guerry, P.; Ewing, C. P.; Schirm, M.; Lorenzo, M.; Kelly, J.; Pattarini, D.; Majam, G.;

Thibault, P.; Logan, S. Changes in flagellin glycosylation affect *Campylobacter* autoagglutination and virulence. *Mol. Microbiol.* **2006**, *60*, 299–311, doi:10.1111/j.1365-2958.2006.05100.x.

93. Champion, O. L.; Gaunt, M. W.; Gundogdu, O.; Elmi, A.; Witney, A. A.; Hinds, J.; Dorrell, N.; Wren, B. W. Comparative phylogenomics of the food-borne pathogen *Campylobacter jejuni* reveals genetic markers predictive of infection source. *Proc. Natl. Acad. Sci.* **2005**, *102*, 16043–16048, doi:10.1073/pnas.0503252102.

94. Howard, S. L.; Jagannathan, A.; Soo, E. C.; Hui, J. P. M.; Aubry, A. J.; Ahmed, I.; Karlyshev, A.; Kelly, J. F.; Jones, M. A.; Stevens, M. P.; Logan, S. M.; Wren, B. W. *Campylobacter jejuni* glycosylation island important in cell charge, legionaminic acid biosynthesis, and colonization of chickens. *Infect. Immun.* **2009**, *77*, 2544–2556, doi:10.1128/IAI.01425-08.

95. Hitchen, P.; Brzostek, J.; Panico, M.; Butler, J. A.; Morris, H. R.; Dell, A.; Linton, D. Modification of the *Campylobacter jejuni* flagellin glycan by the product of the Cj1295 homopolymeric-tract-containing gene. *Microbiology* **2010**, *156*, 1953–1962, doi:10.1099/mic.0.038091-0.

96. Ménard, R.; Schoenhofen, I. C.; Tao, L.; Aubry, A.; Bouchard, P.; Reid, C. W.; Lachance, P.; Twine, S. M.; Fulton, K. M.; Cui, Q.; Hogues, H.; Purisima, E. O.; Sulea, T.; Logan, S. M. Small-molecule inhibitors of the pseudaminic acid biosynthetic pathway: Targeting motility as a key bacterial virulence factor. *Antimicrob. Agents Chemother.* **2014**, *58*, 7430–7440, doi:10.1128/AAC.03858-14.

97. Karlyshev, A. V.; Linton, D.; Gregson, N. A.; Wren, B. W. A novel paralogous gene family involved in phase-variable flagella-mediated motility in *Campylobacter jejuni*.

Microbiology **2002**, *148*, 473–480, doi:10.1099/00221287-148-2-473.

98. van Alphen, L. B.; Wuhrer, M.; Bleumink-Pluym, N. M. C.; Hensbergen, P. J.; Deeldere, A. M.; Van Putten, J. P. M. A functional *Campylobacter jejuni maf4* gene results in novel glycoforms on flagellin and altered autoagglutination behaviour. *Microbiology* **2008**, *154*, 3385–3397, doi:10.1099/mic.0.2008/019919-0.

99. Svensson, S. L.; Pryjma, M.; Gaynor, E. C. Flagella-mediated adhesion and extracellular DNA release contribute to biofilm formation and stress tolerance of *Campylobacter* jejuni. *PLoS One* **2014**, *9*, e106063, doi:10.1371/journal.pone.0106063; 10.1371/journal.pone.0106063.

100. Schirm, M.; Soo, E. C.; Aubry, A. J.; Austin, J.; Thibault, P.; Logan, S. M. Structural, genetic and functional characterization of the flagellin glycosylation process in *Helicobacter pylori*. *Mol. Microbiol.* **2003**, *48*, 1579–1592, doi:10.1046/j.1365-2958.2003.03527.x.

101. Crofts, A. A.; Poly, F. M.; Ewing, C. P.; Kuroiwa, J. M.; Rimmer, J. E.; Harro, C.; Sack, D.; Talaat, K. R.; Porter, C. K.; Gutierrez, R. L.; DeNearing, B.; Brubaker, J.; Laird, R. M.; Maue, A. C.; Jaep, K.; Alcala, A.; Tribble, D. R.; Riddle, M. S.; Ramakrishnan, A.; McCoy, A. J.; Davies, B. W.; Guerry, P.; Trent, M. S. *Campylobacter jejuni* transcriptional and genetic adaptation during human infection. *Nat. Microbiol.* **2018**, *3*, 494, doi:10.1038/s41564-018-0133-7.

102. Bayliss, C. D.; Bidmos, F. A.; Anjum, A.; Manchev, V. T.; Richards, R. L.; Grossier, J. P.; Wooldridge, K. G.; Ketley, J. M.; Barrow, P. A.; Jones, M. A.; Tretyakov, M. V. Phase variable genes of *Campylobacter jejuni* exhibit high mutation rates and specific mutational patterns but mutability is not the major determinant of population structure

during host colonization. *Nucleic Acids Res.* **2012**, *40*, 5876–5889, doi:10.1093/nar/gks246.

103. Cheng, J.; Yu, H.; Lau, K.; Huang, S.; Chokhawala, H. A.; Li, Y.; Tiwari, V. K.; Chen, X. Multifunctionality of *Campylobacter jejuni* sialyltransferase CstII: Characterization of GD3/GT3 oligosaccharide synthase, GD3 oligosaccharide sialidase, and trans-sialidase activities. *Glycobiology* **2008**, doi:10.1093/glycob/cwn047.

104. Beauchamp, J. M.; Leveque, R. M.; Dawid, S.; DiRita, V. J. Methylation-dependent DNA discrimination in natural transformation of *Campylobacter jejuni*. *Proc. Natl. Acad. Sci.* **2017**, 201703331, doi:10.1073/pnas.1703331114.

105. Gencay, Y. E.; Sørensen, M. C. H.; Wenzel, C. Q.; Szymanski, C. M.; Brøndsted, L. Phase Variable Expression of a Single Phage Receptor in *Campylobacter jejuni* NCTC12662 Influences Sensitivity Toward Several Diverse CPS-Dependent Phages. *Front. Microbiol.* **2018**, *9*, 82, doi:10.3389/fmicb.2018.00082.

106. Coward, C.; Grant, A. J.; Swift, C.; Philp, J.; Towler, R.; Heydarian, M.; Frost, J. A.; Maskell, D. J. Phase-variable surface structures are required for infection of *Campylobacter jejuni* by bacteriophages. *Appl. Environ. Microbiol.* **2006**, *72*, 4638–4647, doi:10.1128/AEM.00184-06.

107. Casjens, S. R. Comparative genomics and evolution of the tailed-bacteriophages. *Curr. Opin. Microbiol.* **2005**, *8*, 451–458, doi:10.1016/j.mib.2005.06.014.

108. Leiman, P. G.; Shneider, M. M. Contractile tail machines of bacteriophages. *Adv. Exp. Med. Biol.* **2012**, *726*, 93–114, doi:10.1007/978-1-4614-0980-9_5; 10.1007/978-1-4614-0980-9_5.

109. Davidson, A. R.; Cardarelli, L.; Pell, L. G.; Radford, D. R.; Maxwell, K. L. Long

noncontractile tail machines of bacteriophages. *Adv. Exp. Med. Biol.* **2012**, *726*, 115–142, doi:10.1007/978-1-4614-0980-9_6; 10.1007/978-1-4614-0980-9_6.

110. Casjens, S. R.; Molineux, I. J. Short noncontractile tail machines: adsorption and DNA delivery by podoviruses. *Adv. Exp. Med. Biol.* **2012**, *726*, 143–179, doi:10.1007/978-1-4614-0980-9_7; 10.1007/978-1-4614-0980-9_7.

111. Javed, M. A.; Ackermann, H. W.; Azeredo, J.; Carvalho, C. M.; Connerton, I.; Evoy, S.; Hammerl, J. A.; Hertwig, S.; Lavigne, R.; Singh, A.; Szymanski, C. M.; Timms, A.; Kropinski, A. M. A suggested classification for two groups of *Campylobacter* myoviruses. *Arch. Virol.* **2014**, *159*, 181–190, doi:10.1007/s00705-013-1788-2.

112. Johnson, T. J.; Shank, J. M.; Patel, K. M.; Paredes, M. D.; Lee, E. D.; Mitchell, M. K.; Denes, T. G.; Johnson, J. G. Moderate-Throughput Identification and Comparison of *Campylobacter*-Infecting Bacteriophages. *bioRxiv* **2017**, 201822, doi:10.1101/201822.

113. Clark, C. G.; Ng, L.-K. Sequence variability of *Campylobacter* temperate bacteriophages. *BMC Microbiol.* **2008**, *8*, 49, doi:10.1186/1471-2180-8-49.

114. Siringan, P.; Connerton, P. L.; Cummings, N. J.; Connerton, I. F. Alternative bacteriophage life cycles: the carrier state of *Campylobacter jejuni*. *Open Biol.* **2014**, *4*, 130200, doi:10.1098/rsob.130200.

115. Hooton, S. P. T.; Brathwaite, K. J.; Connerton, I. F. The bacteriophage carrier state of *Campylobacter jejuni* features changes in host non-coding RNAs and the acquisition of new host-derived CRISPR spacer sequences. *Front. Microbiol.* 2016, *7*.

116. Brathwaite, K. J.; Siringan, P.; Connerton, P. L.; Connerton, I. F. Host adaption to the bacteriophage carrier state of *Campylobacter jejuni*. *Res. Microbiol.* **2015**, *166*, 504–515, doi:10.1016/j.resmic.2015.05.003.

117. Cenens, W.; Makumi, A.; Govers, S. K.; Lavigne, R.; Aertsen, A. Viral Transmission Dynamics at Single-Cell Resolution Reveal Transiently Immune Subpopulations Caused by a Carrier State Association. *PLoS Genet.* **2015**, 1–19, doi:10.1371/journal.pgen.1005770.

118. Cenens, W.; Makumi, A.; Mebrhatu, M. T.; Lavigne, R.; Aertsen, A. Phage-host interactions during pseudolysogeny: Lessons from the Pid/dgo interaction. *Bacteriophage* **2013**, *3*, e25029, doi:10.4161/bact.25029.

119. Sails, A. D.; Wareing, D. R. A.; Bolton, F. J.; Fox, A. J.; Curry, A. Characterisation of 16 *Campylobacter jejuni* and *C. coli* typing bacteriophages. *J. Med. Microbiol.* **1998**, *47*, 123–128, doi:10.1099/00222615-47-2-123.

120. Sørensen, M. C. H.; van Alphen, L. B.; Fodor, C.; Crowley, S. M.; Christensen, B. B.; Szymanski, C. M.; Brøndsted, L. Phase Variable Expression of Capsular Polysaccharide Modifications Allows *Campylobacter jejuni* to Avoid Bacteriophage Infection in Chickens. *Front. Cell. Infect. Microbiol.* **2012**, *2*, doi:10.3389/fcimb.2012.00011.

121. Sørensen, M. C. H.; van Alphen, L. B.; Harboe, A.; Li, J.; Christensen, B. B.; Szymanski, C. M.; Brøndsted, L. Bacteriophage F336 recognizes the capsular phosphoramidate modification of *Campylobacter jejuni* NCTC11168. *J. Bacteriol.* **2011**, *193*, 6742–6749, doi:10.1128/JB.05276-11.

122. Baldvinsson, S. B.; Holst Sørensen, M. C.; Vegge, C. S.; Clokie, M. R. J.; Brøndsted, L. *Campylobacter jejuni* motility is required for infection of the flagellotropic bacteriophage F341. *Appl. Environ. Microbiol.* **2014**, *80*, 7096–7106, doi:10.1128/AEM.02057-14.

123. Sørensen, M. C. H.; Gencay, Y. E.; Birk, T.; Baldvinsson, S. B.; Jäckel, C.; Hammerl, J. A.; Vegge, C. S.; Neve, H.; Brøndsted, L. Primary isolation strain determines both phage

type and receptors recognised by *Campylobacter jejuni* bacteriophages. *PLoS One* **2015**, *10*, doi:10.1371/journal.pone.0116287.

124. Louwen, R.; van Baarlen, P. Are bacteriophage defence and virulence two sides of the same coin in *Campylobacter jejuni*? *Biochem. Soc. Trans.* **2013**, *41*, 1475–81, doi:10.1042/BST20130127.

125. Dugar, G.; Leenay, R. T.; Eisenbart, S. K.; Bischler, T.; Aul, B. U.; Beisel, C. L.; Sharma, C. M. CRISPR RNA-Dependent Binding and Cleavage of Endogenous RNAs by the *Campylobacter jejuni* Cas9. *Mol. Cell* **2018**, *69*, 893–905.e7, doi:10.1016/j.molcel.2018.01.032.

126. Gardner, S. P.; Olson, J. W. Barriers to Horizontal Gene Transfer in *Campylobacter* jejuni. *Adv. Appl. Microbiol.* **2012**, *79*, 19–42, doi:10.1016/B978-0-12-394318-7.00002-4.

127. Lis, L.; Connerton, I. F. The minor flagellin of *Campylobacter jejuni* (FlaB) confers defensive properties against bacteriophage infection. *Front. Microbiol.* **2016**, *7*, doi:10.3389/fmicb.2016.01908.

128. Hooton, S. P. T.; Connerton, I. F. *Campylobacter jejuni* acquire new host-derived CRISPR spacers when in association with bacteriophages harboring a CRISPR-like Cas4 protein. *Front. Microbiol.* **2015**, *6*, 1–9, doi:10.3389/fmicb.2014.00744.

129. Weigele, P.; Raleigh, E. A. Biosynthesis and Function of Modified Bases in Bacteria and Their Viruses. *Chem. Rev.* **2016**, *116*, 12655–12687, doi:10.1021/acs.chemrev.6b00114.

130. Lee, Y.-J.; Dai, N.; Walsh, S. E.; Müller, S.; Fraser, M. E.; Kauffman, K. M.; Guan, C.; Corrêa, I. R.; Weigele, P. R. Identification and biosynthesis of thymidine hypermodifications in the genomic DNA of widespread bacterial viruses. *Proc. Natl.*

Acad. Sci. **2018**, doi:10.1073/pnas.1714812115.

131. Thiaville, J. J.; Kellner, S. M.; Yuan, Y.; Hutinet, G.; Thiaville, P. C.; Jumpathong, W.; Mohapatra, S.; Brochier-Armanet, C.; Letarov, A. V.; Hillebrand, R.; Malik, C. K.; Rizzo, C. J.; Dedon, P. C.; de Crécy-Lagard, V. Novel genomic island modifies DNA with 7-deazaguanine derivatives. *Proc. Natl. Acad. Sci.* **2016**, doi:10.1073/pnas.1518570113.

132. Hutinet, G.; Swarjo, M. A.; de Crécy-Lagard, V. Deazaguanine derivatives, examples of crosstalk between RNA and DNA modification pathways. *RNA Biol.* 2017.

133. Kropinski, A. M.; Turner, D.; E Nash, J. H.; - Wolfgang Ackermann, H.; Lingohr, E. J.; Warren, R. A.; Ehrlich, K. C.; Ehrlich, M.; Lingohr, E. The Sequence of Two Bacteriophages with Hypermodified Bases Reveals Novel Phage - Host Interactions., *Viruses*, **2018**, doi:10.3390/v10050217.

134. Bryson, A. L.; Hwang, Y.; Sherrill-Mix, S.; Wu, G. D.; Lewis, J. D.; Black, L.; Clark, T. A.; Bushman, F. D. Covalent Modification of Bacteriophage T4 DNA Inhibits CRISPR-Cas9. *MBio* **2015**, *6*, e00648-15, doi:10.1128/mBio.00648-15.

135. Miller, E. S.; Kutter, E.; Mosig, G.; Arisaka, F.; Kunisawa, T.; Rüger, W. Bacteriophage T4 genome. *Microbiol. Mol. Biol. Rev.* **2003**, *67*, 86–156, table of contents, doi:10.1128/MMBR.67.1.86-156.2003.

136. Hammerl, J. A.; Jackel, C.; Reetz, J.; Beck, S.; Alter, T.; Lurz, R.; Barretto, C.; Brussow, H.; Hertwig, S. *Campylobacter jejuni* Group III Phage CP81 Contains Many T4-Like Genes without Belonging to the T4-Type Phage Group: Implications for the Evolution of T4 Phages. *J. Virol.* **2011**, *85*, 8597–8605, doi:10.1128/JVI.00395-11.

137. Kropinski, A. M.; Arutyunov, D.; Foss, M.; Cunningham, A.; Ding, W.; Singh, A.;

Pavlov, A. R.; Henry, M.; Evoy, S.; Kelly, J.; Szymanski, C. M. Genome and proteome of *Campylobacter jejuni* bacteriophage NCTC 12673. *Appl. Environ. Microbiol.* **2011**, *77*, 8265–8271, doi:10.1128/AEM.05562-11.

138. Timms, A. R.; Cambray-Young, J.; Scott, A. E.; Petty, N. K.; Connerton, P. L.; Clarke, L.; Seeger, K.; Quail, M.; Cummings, N.; Maskell, D. J.; Thomson, N. R.; Connerton, I. F. Evidence for a lineage of virulent bacteriophages that target *Campylobacter*. *BMC Genomics* **2010**, *11*, 214, doi:10.1186/1471-2164-11-214.

139. Arutyunov, D.; Szymanski, C. M. A novel DNA-binding protein from *Campylobacter* jejuni bacteriophage NCTC12673. *FEMS Microbiol. Lett.* **2015**, *362*, doi:10.1093/femsle/fnv160.

140. Frost, J. A.; Kramer, J. M.; Gillanders, S. A. Phage typing of *Campylobacter jejuni* and *Campylobacter coli* and its use as an adjunct to serotyping. *Epidemiol. Infect.* **1999**, *123*, S095026889900254X, doi:10.1017/S095026889900254X.

141. Grajewski, B. A.; Kusek, J. W.; Gelfand, H. M. Development of bacteriophage typing system for *Campylobacter jejuni* and *Campylobacter coli*. *J. Clin. Microbiol.* **1985**, *22*, 13–18.

142. Clark, C. G.; Price, L.; Ahmed, R.; Woodward, D. L.; Melito, P. L.; Rodgers, F. G.; Jamieson, F.; Ciebin, B.; Li, A.; Ellis, A. Characterization of waterborne outbreak-associated *Campylobacter jejuni*, Walkerton, Ontario. *Emerg. Infect. Dis.* **2003**, *9*, 1232–1241, doi:10.3201/eid0910.020584.

143. El-Shibiny, A.; Scott, A.; Timms, A.; Metawea, Y.; Connerton, P.; Connerton, I. Application of a group II *Campylobacter* bacteriophage to reduce strains of *Campylobacter jejuni* and *Campylobacter coli* colonizing broiler chickens. *J. Food Prot.*

2009, *72*, 733–740.

144. Atterbury, R. J.; Dillon, E.; Swift, C.; Connerton, P. L.; Frost, J. A.; Dodd, C. E. R.; Rees, C. E. D.; Connerton, I. F. Correlation of *Campylobacter* bacteriophage with reduced presence of hosts in broiler chicken ceca. *Appl. Environ. Microbiol.* **2005**, *71*, 4885–4887, doi:10.1128/AEM.71.8.4885-4887.2005.

145. Janež, N.; Loc-Carrillo, C. Use of phages to control campylobacter spp. *J. Microbiol. Methods* **2013**, *95*, 68–75, doi:10.1016/j.mimet.2013.06.024.

146. Loc Carrillo, C.; Atterbury, R. J.; El-Shibiny, A.; Connerton, P. L.; Dillon, E.; Scott, A.; Connerton, I. F. Bacteriophage therapy to reduce *Campylobacter jejuni* colonization of broiler chickens. *Appl. Environ. Microbiol.* **2005**, *71*, 6554–6563, doi:71/11/6554 [pii] 10.1128/AEM.71.11.6554-6563.2005.

147. Kittler, S.; Fischer, S.; Abdulmawjood, A.; Glünder, G.; Kleina, G. Effect of bacteriophage application on *Campylobacter jejuni* loads in commercial broiler flocks. *Appl. Environ. Microbiol.* **2013**, *79*, 7525–7533, doi:10.1128/AEM.02703-13.

148. Fischer, S.; Kittler, S.; Klein, G.; Glünder, G. Impact of a Single Phage and a Phage Cocktail Application in Broilers on Reduction of *Campylobacter jejuni* and Development of Resistance. *PLoS One* **2013**, *8*, doi:10.1371/journal.pone.0078543.

149. Wagenaar, J. A.; Bergen, M. A. P. V; Mueller, M. A.; Wassenaar, T. M.; Carlton, R. M. Phage therapy reduces *Campylobacter jejuni* colonization in broilers. *Vet. Microbiol.* **2005**, *109*, 275–283, doi:10.1016/j.vetmic.2005.06.002.

150. O'Sullivan, L.; Lucid, A.; Neve, H.; Franz, C. M. A. P.; Bolton, D.; McAuliffe, O.; Paul Ross, R.; Coffey, A. Comparative genomics of Cp8viruses with special reference to *Campylobacter* phage vB_CjeM_los1, isolated from a slaughterhouse in Ireland. *Arch.*

Virol. **2018**, 1–16, doi:10.1007/s00705-018-3845-3.

151. Janež, N.; Kokošin, A.; Zaletel, E.; Vranac, T.; Kovač, J.; Vučković, D.; Možina, S. S.; Serbec, V. C.; Zhang, Q.; Accetto, T.; Podgornik, A.; Peterka, M. Identification and characterisation of new *Campylobacter* group III phages of animal origin. *FEMS Microbiol. Lett.* **2014**, *359*, 64–71.

152. Javed, M. A.; van Alphen, L. B.; Sacher, J.; Ding, W.; Kelly, J.; Nargang, C.; Smith, D. F.; Cummings, R. D.; Szymanski, C. M. A receptor-binding protein of *Campylobacter jejuni* bacteriophage NCTC 12673 recognizes flagellin glycosylated with acetamidino-modified pseudaminic acid. *Mol. Microbiol.* **2015**, *95*, 101–115, doi:10.1111/mmi.12849.

153. Javed, M. A. M. A.; Sacher, J. C. J. C.; van Alphen, L. B. L. B.; Patry, R. T. R. T.; Szymanski, C. M. C. M. A flagellar glycan-specific protein encoded by *Campylobacter* phages inhibits host cell growth. *Viruses* **2015**, *7*, 6661–6674, doi:10.3390/v7122964.

154. Palyada, K.; Sun, Y. Q.; Flint, A.; Butcher, J.; Naikare, H.; Stintzi, A. Characterization of the oxidative stress stimulon and PerR regulon of *Campylobacter jejuni*. *BMC Genomics* **2009**, *10*, 481, doi:10.1186/1471-2164-10-481.

Chapter 2: Transcriptomic Analysis of *Campylobacter jejuni* Response to T4-Like Phage NCTC 12673 Infection

A version of this paper was published as:

Sacher, J. C.; Flint, A.; Butcher, J.; Blasdel, B.; Reynolds, H. M.; Lavigne, R.; Stintzi, A.; Szymanski, C. M. Transcriptomic analysis of the *Campylobacter jejuni* response to T4-like phage NCTC 12673 infection. *Viruses* **2018,** *10*, 332.

Abstract

Campylobacter jejuni is a frequent foodborne pathogen of humans. As *C. jejuni* infections commonly arise from contaminated poultry, phage treatments have been proposed to reduce *C. jejuni* load on farms to prevent human infections. Whereas a prior report documented the transcriptome of *C. jejuni* phages during the carrier state life cycle, transcriptomic analysis of a lytic *C. jejuni* phage infection has not been reported. We used RNA-sequencing to profile the infection of *C. jejuni* NCTC 11168 by the lytic T4-like myovirus NCTC 12673. Interestingly, we found that the most highly up-regulated host genes upon infection make up an uncharacterized operon (*cj0423-cj0425*), which includes genes with similarity to T4 superinfection exclusion and antitoxin genes. Other significantly up-regulated genes include those involved in oxidative stress defense and the multidrug efflux pump CmeABC. We found that phage infectivity is altered by mutagenesis of the oxidative stress defense genes catalase (*katA*), alkyl-hydroxyperoxidase (*ahpC*), and superoxide dismutase (*sodB*), and by mutagenesis of the efflux pump genes *cmeA* and *cmeB*. This suggests a role for these gene products in phage infection. Together, our results shed light on the phage-host dynamics of an important foodborne pathogen during lytic infection by a T4-like phage.

2.1. Introduction

Bacteriophages (phages), the viruses that infect bacteria, represent a diverse class of natural bacterial 'predators' that have shaped bacterial evolution for an estimated three billion years. Studying how phages interact with their hosts can highlight important facets of bacterial biology and inspire new ways of controlling bacterial pathogens. As antibiotic resistant infections now

threaten to cause more deaths per year than cancer by 2050 [1], there is a great need to explore alternative antimicrobial therapies. Phages represent a viable antibiotic alternative, both in human healthcare settings and in agriculture [2–4]. To ensure the safety and efficacy of employing phages in these settings, only well-characterized phages should be used.

Since the discovery of phages more than a century ago, phage-host characterization has progressed through many stages, from examining plaque morphology, to molecular genetics using model phage-host systems, to classifying phages by transmission electron microscopy, to genome sequencing and annotation. Each of these techniques is useful, and the information gained from each strategy continues to feed information into the still-accelerating collective understanding of phage biology. However, these techniques provide limited information about the host response to infection or the extent to which a phage manipulates host metabolism during infection. As a result, many questions regarding phage infection mechanisms and the host factors that help or hinder these processes remain to be answered for most phages. However, recent advances in whole-genome and whole-transcriptome sequencing now accommodate a much more detailed analysis of both phage and host gene expression profiles during an infection [5]. Within the last few years, whole-transcriptome sequencing methods such as RNA-sequencing (RNA-seq) have been applied to several phage-host pairs, and are rapidly providing a wealth of information on phage infection and assembly programs, host responses to phages, and the mechanisms these phages use to counter these responses [6–16].

C. jejuni is a frequent foodborne pathogen of humans. Strain NCTC 11168 was the first to be genome-sequenced [17,18], and remains one of the best characterized of the species. As *C.*

jejuni infections tend to arise from handling and consuming contaminated poultry [19,20], phages have been considered as a method of reducing *C. jejuni* load on farms to prevent human infections [4,21–23]. Whereas a prior report described the transcriptomes of two *C. jejuni* phages, CP30A and CP8, during carrier-state association with their host, *C. jejuni* PT14 [11], transcriptomic analysis of a lytic *C. jejuni* phage infection has not yet been reported.

NCTC 12673 phage is a 135-kbp T4-like myovirus that was isolated from poultry [24]. Previously, we sequenced the NCTC 12673 genome and identified 172 ORFs and 3 tRNA genes [25]. Interestingly, NCTC 12673 is more similar to T4-related cyanobacteria specific myoviruses than to other phages targeting proteobacteria [25]. NCTC 12673 is a group III *Campylobacter* phage, which is a member of the *Cp8virus* genus of the *Eucampyvirinae* subfamily of the *Myoviridae* [26]. Members of this group tend to require capsular polysaccharide (CPS) for infection [27,28], and indeed, host range analysis revealed that NCTC 12673 is CPS-dependent [28]. No CPS-specific receptor binding protein (RBP) has yet been identified for this phage, although it was previously thought that Gp047 (formerly Gp48) served this function. However, extensive characterization of Gp047 has shown this protein is a flagellar glycan-specific protein [29,30]. NCTC 12673 encodes its own DNA polymerase, but no RNA polymerase has so far been annotated [25].

In this report, we used RNA-seq to profile phage-host interactions between phage NCTC 12673 and *C. jejuni* NCTC 11168 during infection. To better understand the impact of host gene expression changes upon phage infection, we used targeted mutagenesis to confirm the role of selected up-regulated host pathways on phage infectivity. We identified possible roles for

oxidative stress defense proteins and for the CmeABC multi-drug efflux pump in phage infectivity. We also found that the uncharacterized *C. jejuni* operon *cj0423-cj0425* made up the most highly up-regulated genes upon infection. Together our results highlight new aspects of *C. jejuni* phage-host interactions and contribute to the understanding of phage infection dynamics among the T4-like phages.

2.2. Materials and Methods

2.2.1. Bacterial growth conditions

C. jejuni NCTC 11168 (MP21) [31] and its isogenic deletion mutants were grown on 1.5% NZCYM agar plates, supplemented with 50 μg/mL kanamycin or 12-25 μg/mL chloramphenicol where needed, at 37°C under microaerobic conditions (85% N_2, 10% CO_2, 5% O_2). *Escherichia coli* strains were grown on LB agar, supplemented with 50 μg/mL kanamycin or 25 μg/mL chloramphenicol where needed. The list of bacterial strains and phages used in this study is given in Table 2-1.

2.2.2. Phage propagation, titration and concentration

Phage NCTC 12673 and its propagating strain, *C. jejuni* 12661 [32], were obtained from the National Collection of Type Cultures (NCTC; Salisbury, United Kingdom). Phage propagation and titration were performed following the methods described in [33], except that 4-h pre-growth of cultures was done with NZCYM broth instead of CBHI broth. To increase phage titres prior to RNA-sequencing experiments, 0.22-mm-filtered phage lysates were ultracentrifuged at 207,870 x *g* in an SW-28 swinging bucket rotor for 1.5 h at 4°C. Pellets from

25-mL volumes of lysate were resuspended in 1 mL SM buffer containing gelatin [33], pooled and titred on *C. jejuni* NCTC 11168 cells.

2.2.3. Total RNA extraction

Cells were harvested from overnight NZCYM plate cultures, pelleted and washed once in NZCYM broth and set to an OD_{600} of 0.05 (2 x 10^8 CFU/mL) in 20 mL NZCYM broth in 125-mL Erlenmeyer flasks, each containing a 1-inch sterile magnetic stir-bar. Cells were grown under microaerobic conditions and magnetically stirred at 200 rpm. After 4.5 h incubation (mid-log phase, cells had achieved approximately 5.65 +/- 0.79 x 10^8 CFU/mL), 6.5 mL NCTC 12673 phage (2.33 x 10^9 PFU/mL in SM buffer) was added to each of 3 flasks, giving a multiplicity of infection (MOI) of approximately 1.37 +/- 0.25. As negative controls, 6.5 mL SM buffer was added to each of 3 other flasks. At t= 30 min, 1 h and 2 h, one phage-containing and one buffer-containing flask was removed from the incubator, and the entire contents of each flask was transferred to a pre-prepared tube containing 2.6 mL (0.1 volume) ice cold 10% buffered phenol in 100% ethanol to stabilize RNA followed by immediate mixing and storage on ice until all samples were collected [34]. RNA was extracted from each sample using a hot phenol method [34]. RNA samples were sequentially DNAse-treated (37°C for 30 min) using RNAse-free DNAse I (Epicentre) and cleaned using the Zymo RNA Clean & Concentrator. PCR was used to confirm the absence of residual DNA. Total RNA quality was assessed using an Agilent Bioanalyzer and RNA was stored at -80°C until further use. Samples were extracted in biological triplicate.

2.2.4. RNA sequencing

Total mRNA libraries from all replicates were generated. Samples were depleted of rRNA using the RiboZero Bacterial kit according to the manufacturer's instructions. Successful rRNA depletion was confirmed using the Agilent Bioanalyzer RNA 6000 Pico Kit. Strand-specific barcoded sequencing libraries were constructed using the Ion Total RNA-seq kit. Libraries were quality-checked and quantified using the Bioanalyzer High Sensitivity DNA kit and pooled together in equimolar amounts. Template preparation from pooled libraries was done using the Ion PI Hi-Q kit and sequenced on an Ion Torrent Proton using the Ion PI Hi-Q sequencing 200 kit on a single Proton V2 chip.

The raw sequencing reads were de-multiplexed by the Ion Torrent suite software and sequentially mapped to the host (NCTC 11168) and phage (NCTC 12673) genomes using STAR [35] (Table 2-S1). Reads aligning to coding regions were counted using HT-seq using the default settings [36]. The raw, de-multiplexed sequencing reads have been deposited at the NCBI SRA archive under accession number PRJNA454099. DESeq2 was used to identify differentially expressed transcripts over time and between different time points. Genes with a fold change +/- 1.5 and false discovery rate (FDR)-corrected *p*-value <0.05 were considered differentially expressed. Host and phage gene expression was analyzed separately. We also conducted gene set enrichment analysis (GSEA) on *C. jejuni* Kyoto Encyclopedia of Genes and Genomes (KEGG) pathways using the generally applicable gene set enrichment (GAGE) method [37] with a minimum FDR cutoff of <0.1 [35].

Figure 2-1 was assembled by summarizing phage reads from all infected samples into count tables of total gene reads that align to each 250-bp section of the genome independently for each strand. These counts were then graphed independently for each strand. Putative promoters were predicted by systematically identifying clear transcription start sites indicated by RNA-Seq data, and searching for motifs on the relevant strand in the region 50 bp upstream and 150 bp downstream using Multiple Em for Motif Elicitation (MEME v4.12.0, [38]). The phage genome was then scanned for these motifs using Find Individual Motif Occurrences and additional examples were annotated (FIMO v4.12.0, [39]).

2.2.5. Efficiency of plating (EOP) assays

Efficiency of plating (EOP) assays were done by spotting serial dilutions of NCTC 12673 phage onto different strains and determining the proportion of plaque forming units formed on mutant strains compared to the corresponding wild type strain. Briefly, overnight bacterial cultures were harvested in NZCYM broth and set to an OD_{600} of 0.35. A 5-mL aliquot of this suspension was transferred to a standard sized empty Petri dish and incubated at 37 °C without shaking for 4 h under microaerobic conditions. The suspension was then set to an OD_{600} of 0.5, and 200 μL of this was mixed with 5 mL sterile 0.6% molten NZCYM agar at 45 °C. This suspension was poured onto the surface of a pre-warmed NZCYM plate containing 1.5% agar. Plates were allowed to solidify for 15 min and then 10 μL of serial dilutions of a phage suspension (starting at 10^7 PFU/mL) was spotted onto the agar surface and allowed to completely soak into the agar (15 min) before inverting the plate and incubating at 37°C under microaerobic conditions. Plaques were counted after 18–24 h and converted to PFU/mL by multiplying countable

numbers by the total dilution factor. This method is stored on Protocols.io (DOI: dx.doi.org/10.17504/protocols.io.mahc2b6).

Table 2-1. List of bacterial strains and phages used in this study.

Name	Source	Reference
C. jejuni NCTC 11168 MP21	Chicken	[17,18,31]
Phage NCTC 12673	Chicken	[24,25]
C. jejuni NCTC 11168 Δ*katA*	*C. jejuni* NCTC 11168	[38]
C. jejuni NCTC 11168 Δ*ahpC*	*C. jejuni* NCTC 11168	[38]
C. jejuni NCTC 11168 Δ*sodB*	*C. jejuni* NCTC 11168	[38]
C. jejuni NCTC 11168 Δ*cmeA*	*C. jejuni* NCTC 11168	Patry *et al.* submitted [41]
C. jejuni NCTC 11168 Δ*cmeB*	*C. jejuni* NCTC 11168	[39]

2.3. Results

2.3.1. NCTC 12673 phage infection resulted in clear differences in overall *C. jejuni* gene transcription

To better understand *Campylobacter* phage-host dynamics during lytic infection, we performed RNA-seq on *C. jejuni* NCTC 11168 cells at three time points (30, 60 and 120 min) post NCTC 12673 phage infection. These time points were selected to capture cellular responses to phages prior to lysis of the cultures [43]. We grew 20-mL *C. jejuni* cultures in NZCYM broth until mid-log phase before infecting with phages at a multiplicity of infection (MOI) of approximately 1. We then sequenced total mRNA from infected and mock-infected samples to identify differentially-expressed host genes at each time point. Importantly, the use of a relatively low

MOI allows changes in gene expression of both phage-infected and uninfected *C. jejuni* cells to be examined concurrently as RNA from both populations is sequenced. As others have observed that signals transmitted from phage-infected cells to uninfected sister cells can have important impacts on their physiology [14,44,45], we were also interested in the responses of the uninfected population during infection. Of note, this type of analysis does not allow attribution of gene expression differences to one population or the other, but instead surveys the pooled responses of both infected and uninfected cells. Infection with NCTC 12673 phage resulted in clear differences in overall gene transcription between the groups. Notably, the infected and uninfected controls showed clear separation using principal component analysis, however we did not note any clear trends for the transcriptomes to separate by sampling time (Figure 2-S1).

2.3.2. Phage transcriptional analysis validates *in silico* predictions and suggests two new promoter motifs

Although information about temporal phage gene regulation can only be determined for synchronously infected cells, considerable information about the genetic structure underlying phage gene expression, including identification of transcription start and stop sites, promoter sequences and non-coding RNA species, can be gleaned from a study of this design. We analyzed whether read counts across the phage genome mapped according to predicted transcription start and stop sites. We found that the host promoters and Rho-independent terminators predicted by Kropinski *et al.* (2011) [25] could be validated by RNA-Seq data, though most transcription appears to be driven by one of two novel A/T rich predicted promoter motifs (Figure 2-1).

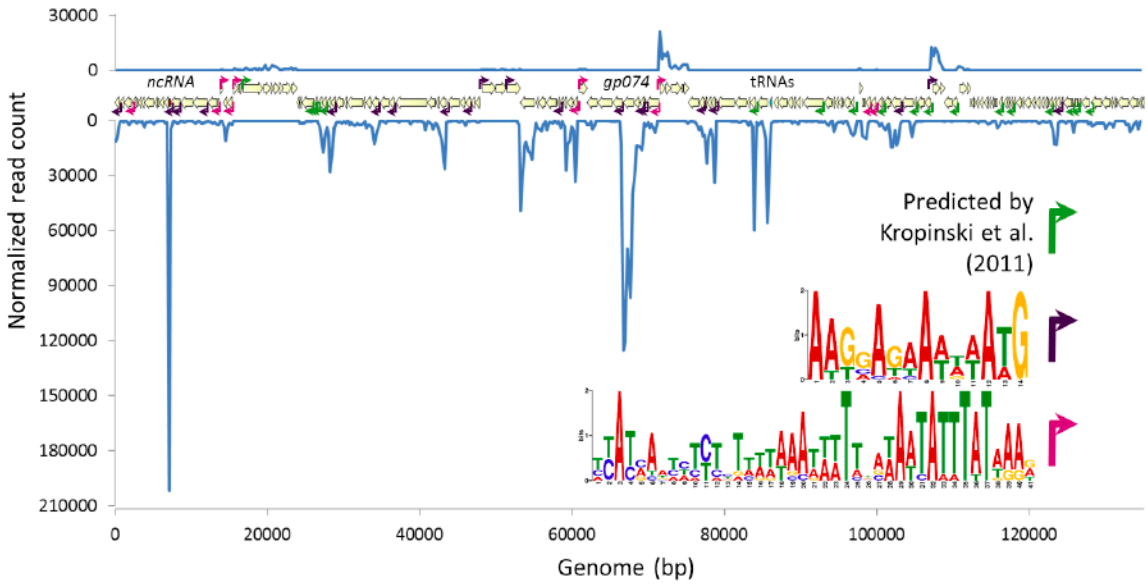

Figure 2-1. RNA read counts across the NCTC 12673 phage genome aligning to the Watson (top) and Crick (bottom) strands. Previously predicted promoters [25] are indicated by green arrows, whereas two newly predicted promoter motifs are indicated with fuchsia and purple arrows. Coding sequences are indicated with beige arrows, whereas the tRNA region is indicated with a blue arrow and a newly identified ncRNA is highlighted with a red bar.

NCTC 12673 phage is predicted to encode 171 ORFs, and we detected transcripts from 166 ORFs [25]. The five ORFs without any assigned reads correspond to *gp013*, *gp054, gp071, gp081* and *gp124,* which are predicted to encode pseudogenes. Of the 166 transcribed genes detected, only 62 (37%) have predicted functions. No statistically significant differences in phage gene expression were identified among different time points post infection. The most densely transcribed feature in the phage genome was a previously unannotated 158-bp non-coding RNA between *gp012* and *gp013* (Figure 2-S2). However, the major capsid protein-encoding gene, *gp074,* was the most highly expressed phage coding sequence (Table 2-S3). Average RPKM values for genes encoding products detected in the structural proteome for this

phage [25] were greater than those corresponding to genes not detected in the proteome ($p < 10^{-9}$ by Student's T-test). However, although NCTC 12673 phage encodes several homologues to structural protein-encoding genes commonly shared among T4-like phages, seven of the top ten most highly expressed NCTC 12673 protein-encoding genes lack predicted functions.

2.3.3. Phage infection induces widespread induction of host genes and downregulation of energy metabolism pathways

To identify cellular processes important for the infection program of phage NCTC 12673 and to identify host responses to phage infection, we analyzed differentially expressed host genes and pathways during infection at an MOI of about 1. We observed an increasing number of differentially expressed host genes over time in response to phage infection, with many more genes up-regulated than down-regulated at all time points (Table 2-S2). At 30 min p.i., we observed upregulation of 3.7 % and downregulation of 0.06% of host genes, at 60 min we observed upregulation of 1.9 % and downregulation of 0.5 % of host genes, and at 120 min we observed upregulation of 12.7 % and downregulation of 4.7 % of host genes. However, as the number of infected cells at any given time under our experimental conditions may be very low, these proportions are not necessarily representative of the changes in host transcription occurring on a single-cell level upon infection.

To gain a broad view of which host metabolic pathways were differentially expressed upon phage infection, we analyzed for enrichment of KEGG categories among up-regulated and down-regulated genes. Among up-regulated genes, only the the KEGG ribosome pathway (cje03010) was statistically enriched during infection (FDR-adjusted $p = 0.003$, 120 min).

However, among down-regulated genes, we observed statistically significant enrichment of many KEGG pathways pertaining to energy metabolism, such as pyruvate, propanoate and butanoate metabolism pathways and the TCA cycle (Table 2-S4). This suggests that energy metabolism is decreased upon NCTC 12673 phage infection, but that translation may increase upon infection.

2.3.4. Genes involved in DNA, RNA, amino acid and protein synthesis are up-regulated in infected cultures

As would be expected to be important for phage replication based on studies of T4 and other T4-like phages [9,46–48], we identified several genes involved in DNA synthesis, replication and repair, as well as transcription and translation, to be differentially expressed upon NCTC 12673 phage infection of *C. jejuni* cultures (Table 2-S5). When genes in these categories were differentially expressed, they were nearly always up-regulated, and statistically significant differences were predominantly only observed at the last time point.

Although the phage itself encodes its own ribonucleotide reductases (*gp162* and *gp163*), the two host ribonucleotide reductase subunits *nrdA* (+1.9-fold) and *nrdB* (+1.6-fold) were up-regulated at 120 min p.i. The phage also encodes its own DNA polymerase (*gp101*), but we also observed that the host DNA polymerase III delta prime subunit (*cj0584)* was up-regulated by 1.9-fold at 120 min p.i. Purine biosynthesis genes *purBHLE* (+2-fold each at 120 min p.i.), were also up-regulated at 120 min p.i. Of note, *purE* was down-regulated twofold at 60 min p.i., yet was still up-regulated similarly to the other *pur* genes at 120 min. In terms of genes associated with DNA modification and repair, the EcoRI-like adenine-specific methylase *cj0208*, the G:T/U mismatch

glycosylase *cj1254*, and the exoDNAse VII *xseA* were up-regulated 2.9-, 2.6- and 1.9-fold, respectively, at 120 min. As the NCTC 12673 phage does not encode its own RNA polymerase, similar to T4 phage, we expected to observe upregulation of host RNA polymerase genes upon phage infection, and indeed the RNA polymerase subunits *rpoABC* were up-regulated 1.9-, 2.0- and 1.6-fold, respectively, at 120 min. As anticipated during a lytic phage infection, and in line with our KEGG pathway analysis results, we also observed upregulation of many ribosomal protein-encoding genes. We also observed several tRNA modification genes to be up-regulated, as well as one, seryl-tRNA synthetase (-1.6-fold at 120 min p.i.)., which was down-regulated.

Several genes involved in amino acid metabolism were up-regulated by 120 min p.i., including arginine biosynthesis genes *argBCD*, which were all up-regulated by 2.7-3.3 fold. As well, the branched chain amino acid transport genes *livFHJ* were up-regulated 1.4-1.8 fold, and the leucine biosynthesis genes *leuACD* were each up-regulated by 2 fold. Not all differentially expressed genes involved in amino acid biosynthesis were up-regulated. The aspartate aminotransferase gene *aspB,* which is essential for growth on glutamate [49], and the aspartate/glutamate transport genes *cj0919c*, *cj0920c* and *peb1A*, were all down-regulated 1.6- to 2.5-fold by 120 min p.i., as were the proline and serine biosynthesis/transport genes *proA*, *putP* and *sdaAC*, which were down-regulated approximately twofold at 120 min p.i.

2.3.5. Canonical phage defense systems are not differentially expressed upon phage infection

We have previously observed that phage NCTC 12673 infects *C. jejuni* NCTC 11168 to a lesser extent (1-2 orders of magnitude less efficiently) than it infects its propagating host, *C. jejuni*

NCTC 12661 (Sacher *et al.,* unpublished data). Therefore, we hypothesized that phage defense systems expressed by NCTC 11168 cells might act to reduce NCTC 12673 phage infection efficiency. NCTC 11168 is known to encode a type II-C CRISPR-Cas system and type I and type II restriction modification systems [50–53]. However, the only gene belonging to either category that was up-regulated upon infection was *cj0140,* which is predicted to encode the McrC component of an McrBC 5-methylcytosine restriction system (+1.75-fold, 120 min p.i.) (Table 2-S5). The McrBC system is known to play a role in *E. coli*-mediated degradation of modified cytosine-containing DNA, and is thought to have led to T4 phage evolution of glycosylated hydroxymethylcytosine in its DNA [46]. Whether this system plays a role in *C. jejuni* phage defense remains to be determined, but the fact that McrC is up-regulated upon NCTC 12673 infection is intriguing. No other restriction endonuclease system genes and no CRISPR-Cas genes were up-regulated, suggesting that these systems are not induced by NCTC 12673 infection.

Another common method of phage defense is through alteration of surface receptors. NCTC 12673 phage is CPS-specific [28]. Of note, two genes annotated as glycosyltransferases, *cj1434c* and *cj1442c,* which are both found in the *C. jejuni* NCTC 11168 CPS locus, were up-regulated 2- to 3-fold at 60 and 120 min post infection (Table 2-S5). We also noticed that two other CPS-associated genes, *cj1420c* and *cj1422c,* which encode a putative methyltransferase and putative *O*-methylphosphoramidate (MeOPN) transferase, respectively [54], were each up-regulated approximately 2-fold at 120 min upon NCTC 12673 infection, though *cj1420* was also down-regulated 1.7-fold at 60 min.

2.3.6. Host operons *cmeABC*, *chuABCD* and *cj0423-cj0425* are among the most highly up-regulated upon phage infection

We sought to determine whether any up-regulated host pathways affected phage infection, either as stress or defense mechanisms up-regulated by infected or surrounding cells, or as phage-induced pathways that might facilitate a cellular environment more favourable to infection. To identify the most highly phage-responsive genes with the strongest associated statistical significance, we plotted significance versus fold change for all host genes (Figure 2-2). We identified three operons that were highly expressed during host infection: *cmeABC*, *chuABCD* (plus *chuZ*, which is expressed from a different promoter but located adjacently to *chuABCD*), and the uncharacterized operon *cj0423-cj0425* (Figure 2-2, Table 2-2). In all cases, all genes making up the operon displayed high fold change and high significance values at two or more time points.

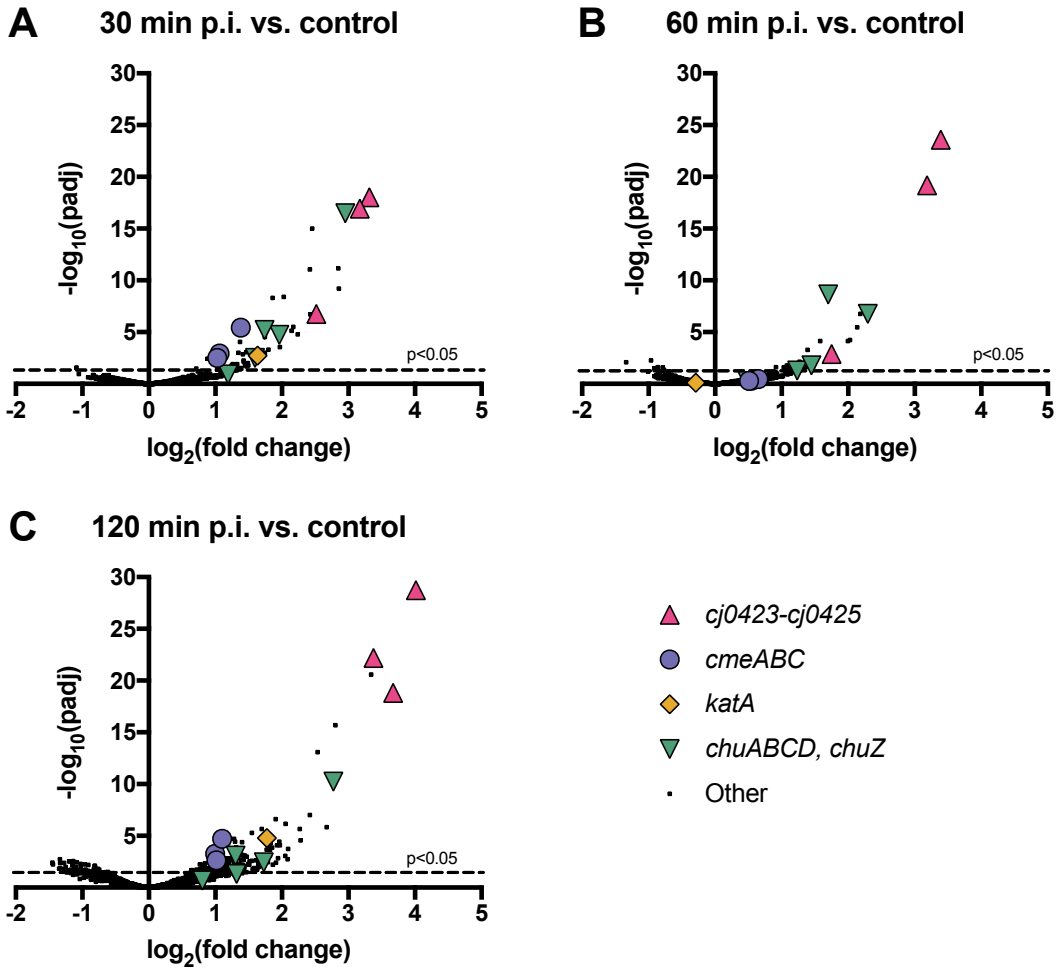

Figure 2-2. Many *C. jejuni* NCTC 11168 genes are up-regulated in response to NCTC 12673 phage infection, whereas relatively few are down-regulated. Volcano plots show all transcribed *C. jejuni* NCTC 11168 genes at (**A**) 30, (**B**) 60 and (**C**) 120 min post infection by NCTC 12673 phage compared to mock-infected controls at each time point. The negative log of the false discovery rate-adjusted *P*-value vs. the $\log_2$ fold change between the conditions indicated is plotted for each gene. Selected highly significantly differentially expressed genes are represented by different colours and symbols according to their predicted or known function.

Table 2-2. Fold changes in gene expression for selected *C. jejuni* NCTC 11168 genes at 30, 60 and 120 min post NCTC 12673 phage addition compared to mock-infected controls at each time point.

		Fold Change (*P*-value)[a]		
Gene	**Annotation**	**30 min (*P*)**	**60 min (*P*)**	**120 min (*P*)**
Multi-drug efflux pump CmeABC				
cmeA	Periplasmic fusion protein CmeA (multidrug efflux system CmeABC)	2.6 (<0.01)	NS	1.99 (<0.01)
cmeB	Inner membrane efflux transporter CmeB (multidrug efflux system CmeABC)	2.09 (<0.01)	NS	2.14 (<0.01)
cmeC	Outer membrane channel protein CmeC (multidrug efflux system CmeABC)	2.04 (<0.01)	NS	2.02 (<0.01)
Oxidative stress and iron metabolism				
katA	Catalase	3.1 (<0.01)	NS	3.42 (<0.01)
chuA	Haemin uptake system outer membrane receptor	7.73 (<0.01)	4.9 (<0.01)	6.84 (<0.01)
chuB	Putative haemin uptake system permease protein	3.02 (<0.01)	NS	1.8 (0.02)
chuC	Putative haemin uptake system ATP-binding protein	NS	NS	2.49 (0.05)
chuD	Putative haemin uptake system periplasmic haemin-binding protein	3.9 (<0.01)	2.73 (0.02)	3.31 (<0.01)
chuZ[b]	Iron-responsive cellular heme oxygenase	3.34 (<0.01)	3.25 (<0.01)	2.47 (<0.01)
Uncharacterized operon *cj0423-cj0425*				
cj0423	Putative integral membrane protein	5.73 (<0.01)	3.36 (<0.01)	16.14 (<0.01)
cj0424	Putative acidic periplasmic protein	9.95 (<0.01)	10.51 (<0.01)	12.75 (<0.01)
cj0425	Putative periplasmic protein	9.01 (<0.01)	9.1 (<0.01)	10.39 (<0.01)

[a]Genes were considered differentially expressed when false discovery rate-corrected *P*-value < 0.05. NS = not statistically significant, cells were left blank.

[b]Annotation updated according to [52].

2.3.6.1. The *C. jejuni* CmeABC multi-drug efflux pump may function in phage defense

Interestingly, we observed approximately 2-fold upregulation of the entire *cmeABC* multidrug efflux pump at 30 and 120 min p.i. (Table 2-2), which has previously been shown to mediate *C. jejuni* resistance to antibiotics, ethidium bromide and bile [56,57]. Whereas multidrug efflux pumps serve as receptors for some phages [58], no previous link between multidrug efflux and phage infectivity has been established for *Campylobacter.* To test the hypothesis that the CmeABC system reduces phage infectivity in *C. jejuni* NCTC 11168*,* we assessed phage EOP on insertional mutants of *cmeA* and *cmeB.* Interestingly, we saw that the phage was able to infect *cmeA* (EOP = 2.00, $P = 0.02$) and *cmeB*-mutant cells (EOP = 2.26, $P = 0.008$) at higher levels than wild type cells (EOP = 1.00) (Figure 2-3). In addition to a reduction in EOP, plaques on *cmeA* and *cmeB* mutants were larger and clearer compared to those on the wild type strain.

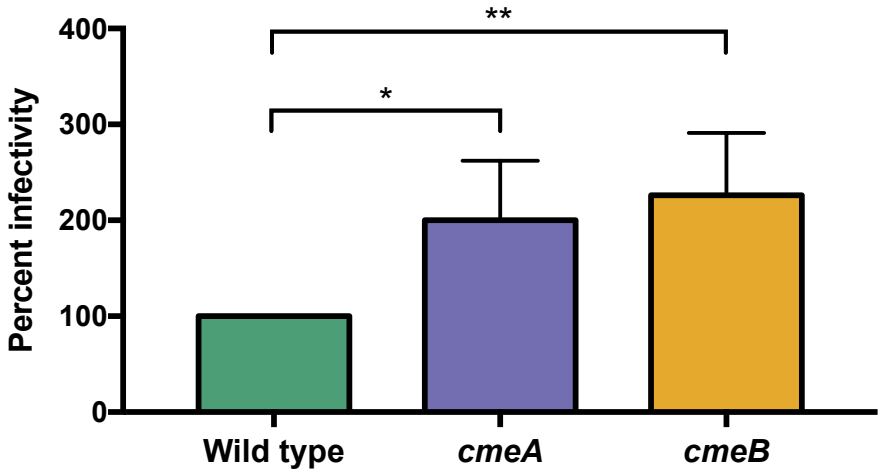

Figure 2-3. NCTC 12673 phage efficiency of plating is greater on a *cmeA* and on a *cmeB* mutant compared to wild type *C. jejuni* NCTC 11168. Bars represent the average of four

biological replicates, and error bars represent standard deviation. Statistical significance as determined by unpaired t-test is indicated by asterisks as follows: $P < 0.05$ (*), $P < 0.01$ (**).

2.3.6.2. Oxidative stress defense may affect *C. jejuni* interactions with phage NCTC 12673

We observed that the genes encoding the *chuABCD* heme transporter, along with the heme oxygenase *chuZ,* were among the most highly up-regulated genes upon *C. jejuni* phage infection (+2-7-fold at most time points, Figure 2-2, Table 2-2). Additionally, several other iron uptake pathways were similarly up-regulated (Table 2-S5). These include genes involved in transport of several siderophores, such as rhodotorulic acid (*cj1658, p19, cj1660-1662*), enterobactin (*cfrA, ceuB*) and lactoferrin/transferrin (*ctuA*) (Table 2-2) [59]. All of these genes are iron-repressed in *C. jejuni* NCTC 11168 [59]. In *C. jejuni,* iron homeostasis is closely linked to oxidative stress defense, as the main ferric uptake regulator in *C. jejuni*, Fur, also regulates many oxidative stress defense genes (Figure 2-S4) [40]. Interestingly, we also observed upregulation of the oxidative stress defense gene *katA* (+3-fold at 30 and 120 min p.i.). *katA* codes for the enzyme catalase, which catalyzes the dismutation of hydrogen peroxide to water and oxygen in *C. jejuni* and in most aerobic organisms [60]. *C. jejuni katA* mutants are known to be more sensitive to oxidative stresses [61]. It is noteworthy that *katA* along with the *chuABCD* heme transporter were all up-regulated during infection, as KatA activity depends on heme [62].

To determine whether oxidative stress impacted NCTC 12673 infectivity, we determined the EOP of NCTC 12673 phage on a *katA* mutant. Interestingly, we found that NCTC 12673 phage had an EOP of 0.15 ($P = 0.009$) on a *katA* mutant (Figure 2-4). To explore the effect of other types of oxidative stress on phage infection, we also tested EOP on two more mutants defective

in oxidative stress defense, *ahpC*, which encodes alkyl-hydroxyperoxidase, and *sodB*, which encodes superoxide dismutase (Figure 2-S4). We observed that both mutants showed lower EOP, with *ahpC* mutation leading to an EOP of 0.01 ($P < 0.0001$) and *sodB* mutation resulting in an EOP of 0.30 ($P = 0.02$). Together these results suggest that NCTC 12673 infectivity may be altered by multiple types of oxidative stresses (Figure 2-4).

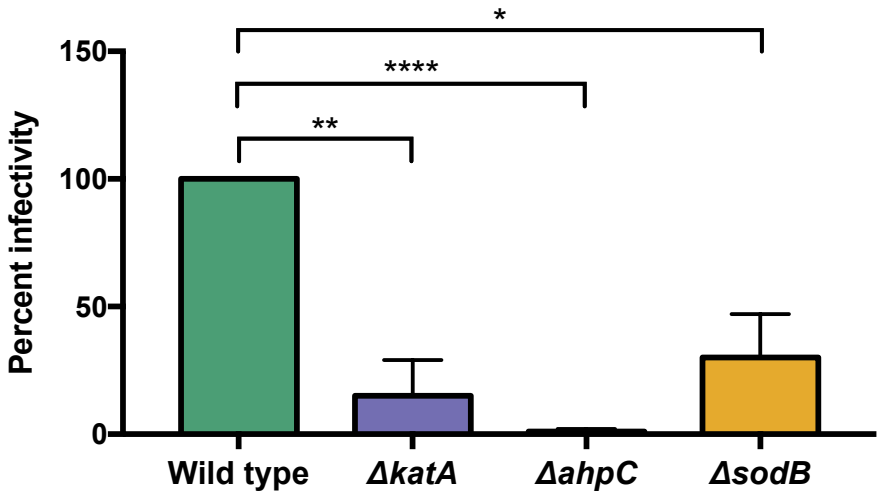

Figure 2-4. NCTC 12673 phage infection efficiency is reduced on a *katA* mutant, a *sodB* mutant and an *ahpC* mutant compared to wild type *C. jejuni* NCTC 11168. Bars represent the average of three biological replicates, and error bars represent standard deviation. Statistical significance as determined by unpaired t-test is indicated by asterisks as follows: $P < 0.05$ (*), $P < 0.01$ (**), $P < 0.0001$ (****).

2.3.6.3. *cj0423-cj0425* is the most highly up-regulated host operon upon phage infection

Interestingly, the host operon with the highest differential expression in response to phage infection across all time points was an uncharacterized operon comprised of *cj0423, cj0424* and *cj0425.* These genes were up-regulated between 3- and 16-fold across all time points p.i. (Table

2-2). Although their functions have not been elucidated to date, *cj0423, cj0424* and *cj0425* are predicted to encode a putative integral membrane protein, a putative acidic periplasmic protein and a putative periplasmic protein, respectively [17,18].

It has been previously reported that highly expressed gene clusters upon phage infection can be indicative of resident prophage expression [14,15]. As well, BLAST analysis showed that *cj0423-cj0425* is not universally conserved among *C. jejuni* strains. These features could indicate that *cj0423-cj0425* are prophage or cryptic prophage elements, but this is unlikely as previous work had suggested that *C. jejuni* NCTC 11168 genome does not contain these features [17,18].

Instead, BLASTp analysis showed that the amino acid sequence of Cj0423 displays 40% identity (97% coverage, E value = 3e-14,) to the T4 superinfection immunity (Imm) protein (P08986) (Figure 2-S3A), and both constitute members of the PFAM14373 Imm_superinfect family. Similar analysis of *cj0424* showed 36% identity (87% coverage, E value = 6e-8) to the *ywqK* antitoxin component of the putative YwqJK toxin-antitoxin system in *Bacillus subtilis* strain 168 (Figure 2-S3B) [63]. In contrast, BLASTp analysis did not reveal information about possible functions for *cj0425.*

2.4. Discussion

We used whole-transcriptome sequencing to better understand the gene expression program of phage NCTC 12673, a lytic T4-like myovirus with a 135-kbp dsDNA genome most similar to

T4-like cyanophages, and to characterize the response of *C. jejuni* NCTC 11168 to infection. Previous *C. jejuni* phage transcriptome experiments examined infection of the highly phage-susceptible strain *C. jejuni* PT14 (NCTC 12662) during carrier state association with the host [11]. We report the study of NCTC 12673 infection of *C. jejuni* NCTC 11168 as a host, which is notably not the propagating strain for this phage. The propagating strain, *C. jejuni* NCTC 12661, propagates NCTC 12673 to higher titres compared to NCTC 11168, for as-yet unknown reasons. However, NCTC 11168, being the first genome-sequenced strain of the species, has been much more extensively characterized. Thus, we chose to study the transcriptional profile of NCTC 12673 infection of 11168 cells.

We performed our RNA-seq analysis on cells infected at a relatively low MOI (MOI = 1) compared to other phage-host RNA-seq studies, which have reported MOIs in the range of 10-25 [15]. However, the study of low-MOI infections, which are likely to be more representative of phage infections in nature, has lagged behind [64]. A high MOI allows for insights into phage transcriptional regulation to be gained, since nearly all cells in a culture are infected at once. In contrast, low MOI studies can lead to interesting insights into population-level host adaptation to phages, as phage-induced perturbations of both infected and uninfected neighbouring cells in a culture can be analyzed simultaneously. For instance, a recent study reported RNA-seq analysis of a *Staphylococcus aureus* phage infection at an MOI of 10^{-5}, which uncovered phage-induced gene expression changes that led to increased biofilm production [65]. Phage-infected cells have been shown to delay lysis in response to the presence of infected sister cells nearby [44,45], and quorum sensing molecules have been shown to alter factors affecting phage susceptibility [14,47,66]. It is expected that other examples of phage-induced warning systems

will be uncovered as more phage-host interactions are examined in detail [64]. It is thus becoming clear that studies examining phage infections at both high and low-MOIs are independently useful for obtaining a comprehensive picture of phage-host dynamics.

Upon infection of *C. jejuni* NCTC 11168 with NCTC 12673 phage, we did not observe the rapid reduction in relative host transcript abundance shortly after infection that has been observed for other phages [13,46]. However, since our infections were done at low MOI, our data do not preclude the possibility that NCTC 12673 degrades host transcripts on an individual cell level. Of note, NCTC 12673 does not appear to encode a homologue of the T4 phage *alc* gene, which is responsible for the near-immediate cessation of host transcription observed upon infection [46]. Therefore, if phage NCTC 12673 does inhibit host transcription, it likely does so by another mechanism. This study also allowed us to gain insight into the host genes that might be involved in phage DNA, RNA and protein synthesis during *C. jejuni* infection. In line with expectations for this phage, which does not encode its own RNA polymerase, we observed that host RNA polymerase genes were up-regulated upon infection. Unexpectedly, genes like host DNA polymerase III and ribonucleotide reductases, versions of which are also encoded by the phage, were also up-regulated. It remains to be determined to what extent the phage- vs. host-derived versions of these genes function in phage replication, but it is interesting to speculate that both versions might play roles in phage replication.

By analyzing phage transcripts, we were able to validate previously predicted transcriptional start sites, termination sites, and promoters, as well as identify two putative promoter motifs. We observed expression of most NCTC 12673 coding sequences predicted by Kropinski *et al.*

(2011), and our analysis revealed that many of the proteins detected in the NCTC 12673 structural proteome tended to be more highly expressed relative to other phage genes [25]. The majority of predicted NCTC 12673 ORFs lack assigned functions and our validation of previous genomic and proteomic studies of this phage should assist in guiding further studies toward elucidating these functions.

As transcriptional analysis of phage-host interactions has become more common, many phages have now been shown to induce differential gene expression in their hosts. For instance, cyanophages have been shown to alter expression of host metabolic genes and stress responses [9] and the *Pseudomonas* phage PAK_P4 has been suggested to alter expression of host iron-scavenging genes in *P. aeruginosa* [15]. We observed differential expression of many genes involved in other metabolic functions in the host cell, such as genes involved in amino acid metabolism, oxidative stress defense, iron homeostasis, multi-drug efflux pump production, as well as several uncharacterized genes.

We observed differential expression of several amino acid pathways upon phage infection, including upregulation of genes involved in asparagine, leucine, isoleucine and valine metabolism, and downregulation of components involved in aspartate, glutamate, serine and proline metabolism. *C. jejuni* is known to tightly regulate its amino acid metabolism, and has been shown to metabolize amino acids sequentially in order of preference, beginning with serine, followed by aspartate, asparagine and glutamate [67]. It is possible that NCTC 12673 phage infection may have different amino acid requirements compared to the uninfected cell, perhaps leading it to induce changes in gene expression to procure the amino acids it requires. It

is particularly interesting that three of the four amino acids most preferentially utilized by *C. jejuni* are down-regulated upon phage NCTC 12673 infection.

Phage nutritional requirements have not yet been well studied, though recent metabolomics studies have documented phage-specific changes in amino acid metabolism for several *Pseudomonas* phages and a *Roseobacter* phage [47,48]. As well, an earlier study showed that lambda phage requires the branched chain amino acids leucine, isoleucine, valine and threonine [68]. Amino acid availability was shown to affect T4 lytic infection of stationary phase *E. coli,* although specific amino acids important for phage propagation were not identified [69]. Whereas changes in amino acid metabolism could represent a phage-directed response, it has also been suggested that phage-infected cells may alter amino acid metabolism as a way of limiting phage infection [14,47]. Further work should seek to understand whether NCTC 12673 phage requires specific amino acids for infection, and whether phage and/or host manipulates these stores to their own advantage.

Interestingly, several host genes involved in inorganic ion transport and metabolism were up-regulated upon NCTC 12673 phage infection. In particular, the heme-related genes *chuABCD* and *chuZ,* as well as the heme-dependent oxidative stress defense enzyme *katA,* were among the most highly up-regulated. Upregulation of iron acquisition genes has been observed in other phage-host systems, such as PAK_P4 infection of *P. aeruginosa*, but this phenomenon is not well understood [15]. Of note, phage PAK_P3, a different but related *P. aeruginosa* phage, does not induce iron uptake gene expression in the same host strain, suggesting that PAK_P4 iron uptake may be phage directed as opposed to host-directed [15].

The presence of iron leads to increased oxidative stress sensitivity in *C. jejuni,* and the regulation of responses to oxidative stress and iron levels are highly intertwined in this organism [40]. We therefore hypothesized that phage infection-induced upregulation of iron uptake systems might lead to oxidative stress sensitivity in the cells, and that this might alter NCTC 12673 phage infection efficiency. To test the effect of oxidative stress sensitivity on phage infection efficiency, we examined whether the phage could efficiently infect mutants defective in three oxidative stress defense genes: *katA*, *ahpC* and *sodB*. *ahpC* encodes alkyl-hydroxyperoxidase, and although catalase is the primary detoxifier of H_2O_2 in *C. jejuni*, AhpC is also capable of converting H_2O_2 and organic hydroperoxides (ROOH) to their corresponding alcohols. *sodB* encodes a superoxide dismutase, which converts superoxide to hydrogen peroxide. Interestingly, we observed a reduction in phage infectivity on all three mutants, suggesting that oxidative stress negatively affects NCTC 12673 phage infection.

Neither *ahpC* nor *sodB* were up-regulated upon phage infection, which may be related to the fact that *katA* is co-regulated by the *C. jejuni* ferric uptake regulator (Fur), whereas *ahpC* and *sodB* are not [40]. Given the observed importance of oxidative stress defense genes for NCTC 12673 phage infection and the fact that many classical members of the Fur regulon are up-regulated during infection, our data suggests that iron homeostasis may be the initial perturbation upon phage infection, and that oxidative stress may follow later. It is unknown why iron uptake pathways would be up-regulated upon phage infection, particularly as our infections were done in iron-replete media. Interestingly, Bartual *et al.* (2010) have shown that T4 phage expresses iron-coordinating tail fibre proteins that allow the phage to bind to and infect

siderophore receptor-expressing cells [70]. In addition to T4, other *E. coli* phages have since been found to coordinate iron in their tail proteins [71]. These findings have led to the "Ferrojan Horse Hypothesis", whereby phages provide a "gift" of iron prior to lysing their target cell [71]. These findings, together with the observation by Blasdel *et al.* (2018) that phage PAK_P4 induces iron uptake genes upon *P. aeruginosa* infection [15], and with our observed up-regulation of iron uptake upon phage NCTC 12673 infection of *C. jejuni*, suggest that iron uptake may play important roles in the lifecycles of many diverse phages.

With the exception of the *mcrC* component of an McrBC 5-methylcytosine restriction system at one time point p.i., we did not observe host upregulation of restriction enzymes or CRISPR-Cas genes in response to NCTC 12673 phage infection. *C. jejuni* encodes a Type II-C CRISPR-Cas system, and Dugar *et al.* found that CRISPR regions were found to be among the most highly transcribed loci in *C. jejuni* NCTC 11168 [72]. Although carrier state-associated *C. jejuni* phages were shown to induce host-directed spacer acquisition, however, *C. jejuni* CRISPR-Cas has not yet been shown to function in phage defense [51]. Others have identified an inverse correlation between *C. jejuni* strains that encode plasmids, prophages or other phage defense mechanisms and those that encode CRISPR-Cas systems, suggesting a possible role for CRISPR-Cas in phage defense [72,73]. It has also been suggested that *Campylobacter* CRISPR-Cas evolved a function unrelated to phage defense, perhaps to regulate its own genes, as has been shown for other organisms [73–75]. Very recently, *Campylobacter* CRISPR-Cas systems were shown to specifically target endogenous mRNA and ssRNA, supporting this possibility [74,76].

We also observed upregulation of genes involved in MeOPN addition to CPS upon phage infection. Notably, we and others have previously shown that changes in MeOPN on *C. jejuni* CPS affects susceptibility to several other *Campylobacter* phages, and that phage pressure can lead to changes in expression of these structures through slipped strand mispairing in phase-variable genes [31,77–79]. Our observation that NCTC 12673 phage pressure induces changes in transcription of CPS biosynthesis genes suggests another possible mechanism by which *C. jejuni* might alter its CPS in response to phage infection, but further work is required to determine whether changes in CPS gene transcription might affect susceptibility to phages. Although canonical phage defense systems were not up-regulated in response to NCTC 12673 infection, we observed upregulation of the multidrug efflux pump genes *cmeABC* and found that *cmeA* and *cmeB* efflux pump deletion mutants were more efficiently infected by NCTC 12673. This suggests a possible role of this efflux pump in phage defense. It could be hypothesized that an efflux pump might function to pump out metabolites that a phage requires for efficient infection (ie. similar to a 'scorched earth' strategy, whereby an infected cell depletes phages of necessary resources to reduce infection efficiency) [14,80]. Alternatively, an efflux pump could function in phage resistance by pumping out factors that might alert sister cells of an imminent phage threat. Others have observed upregulation of *P. aeruginosa* multidrug efflux pump genes in response to phage infection [14], but to our knowledge, efflux pumps have not been shown to function in phage defense. Some phages have been shown to require efflux pumps to bind host cells [81], and increased resistance to antibiotics has also been described in response to phage infection [64,82,83]. It is intriguing to speculate that phage-induced expression of efflux pumps might increase antibiotic resistance under some conditions. Further work into understanding the influence of efflux pumps like *cmeABC* on phage infection and antibiotic susceptibility is thus

required, as knowledge in this area is particularly relevant for safe administration of therapeutic phages.

Interestingly, we observed significant upregulation of the uncharacterized operon *cj0423-cj0425* in response to phage infection, which comprises one gene (*cj0423)* encoding a protein homologous to the T4 superinfection immunity protein Imm, and another (*cj0424*) encoding a protein homologous to an antitoxin component of the RNAse-mediated toxin-antitoxin system YwqJK [63]. Imm is a component of one of two T4 superinfection exclusion (Sie) systems, and has been shown to block T-even phage DNA injection into *Escherichia coli* cells [46,84,85]. As well, it should be noted that toxin-antitoxin systems have been shown to function in anti-phage abortive infection systems [86]. The last gene of this operon, *cj0425*, displays no homology to phage defense genes. However, others have speculated that *cj0425* may contribute to oxidative stress tolerance based on its identification as one of two *C. jejuni* NCTC 11168 genes with a CXXC redox motif not present in the more oxygen-susceptible strain *C. jejuni* RM1221 [87]. Others have shown that *cj0425* is down-regulated upon low-oxygen in vitro growth and chick colonization of *C. jejuni* [87–89], supporting a possible role in oxygen tolerance. It is intriguing that this last gene appears to be involved in oxidative stress, considering the importance of oxidative stress for NCTC 12673 infectivity that we have described here.

It is possible that this operon represents a phage exclusion system that may help explain the reduced phage EOP on *C. jejuni* NCTC 11168 compared to other strains. In support of this hypothesis, this operon is not encoded by the propagating strain for this phage, *C. jejuni* NCTC 12661, which is more efficiently infected by NCTC 12673. Further work is required to

determine whether *cj0423-0425* expression prevents or reduces phage infection in *C. jejuni.* It is also of interest to identify whether this operon is induced by phage-infected cells and/or by uninfected cells in the vicinity of phage infection. If this operon does function in phage defense, it is perhaps more likely that uninfected cells rather than infected cells would express this operon. However, not all phage defense systems serve to completely abolish phage infection, and certain defense mechanisms are proposed to reduce infection vigour without necessarily abolishing it [14,90]. Notably, our results do not rule out either possibility.

The changes in host gene expression upon infection that we have observed can suggest either a host response to the phage, phage modulation of host genes, or a combination of both. To distinguish between whether changes in gene expression are phage- or host-induced, analysis of the same phage on multiple hosts, and/or analysis of multiple phages on the same host, should be done [14,15,91]. To determine whether observed changes in gene expression occur in infected and/or uninfected hosts, RNA-seq using a higher MOI could be done to effectively eliminate detection of RNA from uninfected cells. Overall, whether the observed phage infection-induced transcriptional responses are driven by phages, by infected hosts, or by uninfected hosts, RNA-seq analysis of this complex interplay by is a useful first step toward generating important new data about phage-host interactions.

2.5. Conclusions

This work represents the first reported whole-transcriptome sequencing analysis of *C. jejuni* during lytic phage infection. Little is known about the determinants of phage susceptibility

among different *C. jejuni* strains, and yet understanding these determinants is essential to the success of phage-mediated biocontrol of *C. jejuni.* Furthermore, understanding the factors governing phage-host dynamics of any bacterial species can lead to important insights into its evolution. Finally, this analysis represents one of the first RNA-seq-based analyses of a low MOI phage infection, and has highlighted several genes that may play roles in population-wide *C. jejuni* responses to phage infection.

2.6. Supplementary data

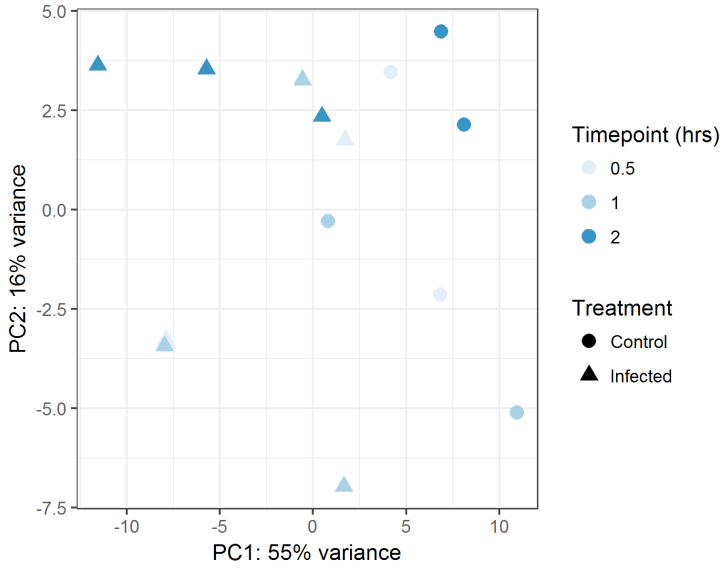

Figure 2-S1. Principal component analysis plot for infected vs. uninfected controls at each time point post NCTC 12673 phage infection of *C. jejuni* NCTC 11168 cells. Plots were generated using the data from the 500 genes with the greatest variation in expression across samples.

Table 2-S1. RNA-seq read statistics.

Sample Barcode	Replicate Number	Group	Sampling Timepoint (h)	Total Reads	Reads Aligning to NCTC 11168	Reads aligning to NCTC 12673
BC01	1	Infected	0.5	4675121	3624270	497744
BC02	1	Infected	1	4158337	3481256	254092
BC03	1	Infected	2	6029137	5401531	369292
BC04	2	Infected	0.5	7329874	6525606	465763
BC05	2	Infected	1	6627184	5896267	403863
BC06	2	Infected	2	6446221	5803434	361905
BC07	2	Control	0.5	8711385	8649245	41
BC08	2	Control	1	6454979	6405427	330
BC09	2	Control	2	7161982	7111778	6
BC10	3	Infected	0.5	7173169	6580235	360334
BC11	3	Infected	1	6510986	6113184	236263
BC12	3	Infected	2	5850072	5354073	320383
BC13	3	Control	0.5	7241333	7183906	65
BC14	3	Control	1	8448990	8381159	27
BC15	3	Control	2	6872600	6819512	28

Table 2-S2. Number and percentage of *C. jejuni* NCTC 11168 genes differentially expressed (DE) at each time point post NCTC 12673 phage infection.

	30 min p.i.		60 min p.i.		120 min p.i.	
Differentially expressed host genes[a]	**Number**	**% of total**	**Number**	**% of total**	**Number**	**% of total**
Up-regulated	61	3.7 %	32	1.9 %	212	12.7 %
Down-regulated	1	0.06 %	8	0.5 %	78	4.7 %
Total DE	62	3.7 %	40	2.4 %	290	17.4 %

[a]Genes were considered DE if they underwent a fold change of >1.5 or <-1.5 with a false discovery rate (FDR)-adjusted p-value of <0.05.

Table 2-S3. Relative transcription of NCTC 12673 phage genes during *C. jejuni* NCTC 11168 infection.

Locus Tag	Annotation	% AA coverage[a] (Kropinski *et al.* 2011)	Relative transcription (log_{10}(RPKM))[b]
nc001[d]	Novel non-coding RNA	N/A	5.81
gp074	Gp23 major capsid protein	43	5.23

gp089	Hypothetical protein	21.3	4.89
gp060	Gp18 tail sheath protein	0	4.66
gp068	Conserved hypothetical protein	7.6	4.40
gp075	Hypothetical protein	0	4.66
gp087	Conserved hypothetical protein	0	4.45
gp069	Hypothetical protein	7.3	4.65
gp112	Conserved hypothetical protein	0	4.40
gp153	Hypothetical protein	13.2	4.38
gp051	Gp32 ssDNA binding protein	0	4.41
gp079	Conserved hypothetical protein	4.7	4.49
gp036	Gp19 tail tube protein	6.9	4.36
gp038	Conserved hypothetical protein	0	4.48
gp076	Gp21 prohead core scaffold and protease	0	4.35
gp119	Hypothetical protein	16.8	4.12
gp117	Conserved hypothetical protein	2.5	4.37
gp111	Conserved hypothetical protein	0	3.94
gp001	Hypothetical protein	7.3	4.18
gp122	Gp23 major head protein II	25.3	4.24
gp080	Gp13 neck protein	6.6	4.18
gp088	Hypothetical protein	8.5	4.08
gp085	Phosphatidylserine decarboxylase	5.1	4.13
gp086	Co-chaperonin GroES	0	4.16
gp019	Hypothetical protein	22.7	4.13
gp037	Gp19 tail tube protein II	0	4.07
gp044	Amidinotransferase	20.8	4.14
gp108	Conserved hypothetical protein	18.3	4.08
gp123	Gp14 head completion protein	0	3.98
gp160	Hypothetical protein	0	3.19
gp138	Putative exonuclease	9.5	3.87
gp163	Ribonucleotide reductase, small subunit	0	3.57
gp116	Conserved hypothetical protein	2.7	3.78
gp043	Gp45 sliding clamp protein	0	3.88
gp115	Hypothetical protein	0	3.59
gp062	Conserved hypothetical protein	0	3.88
gp170	Hypothetical protein	0	3.70
gp077	Phage hypothetical protein	0	3.44
gp168	RecA	0	3.79
gp094	Conserved hypothetical protein	2.4	3.54
gp083	Gp19 tail tube protein III	7.8	3.81
gp171	Hypothetical protein	0	3.20
gp152	Gp4 head completion protein	0	3.68
gp035	Hypothetical protein	0	3.78
gp104	Conserved hypothetical protein	0	3.76
gp017	Hypothetical protein	0	3.79

gp078	Gp20 portal vertex protein	16.9	3.76
gp110	Conserved hypothetical protein	0	3.26
gp066	Conserved hypothetical protein	0	3.80
gp082	Hypothetical protein	0	3.25
gp026	Hypothetical protein	0	3.68
gp158	Hypothetical protein	0	3.80
gp048	Putative RNAse H	0	3.55
gp020	Conserved hypothetical protein	0	3.62
gp166	Hypothetical protein	0	3.63
gp041	Gp6 baseplate wedge subunit	0	3.55
gp098	Hypothetical protein	0	3.47
gp050	Gp62 clamp loader subunit	0	3.46
gp064	Hypothetical protein	0	3.71
gp154	Hypothetical protein	0	3.13
gp126	Gp15 tail sheath stabilizer and completion protein	0	3.57
gp049	Hypothetical protein	0	3.32
gp030	Gp5 baseplate hub subunit and tail lysozyme	0	3.43
gp061	Hypothetical protein	0	3.30
gp093	Hypothetical protein	16.2	3.44
gp159	Hypothetical protein	0	3.16
gp162	Ribonucleotide reductase, large subunit	0	3.54
gp099	Hypothetical protein	0	3.39
gp067	Hypothetical protein	0	3.58
gp155	RnlA; RNA ligase	0	3.15
gp165	Conserved hypothetical protein	0	3.41
gp063	Gp30 DNA ligase	0	3.49
gp102	Putative methyltransferase	0	3.45
gp148	Conserved hypothetical protein	0	3.35
gp105	Thymidine kinase	0	3.22
gp140	Hypothetical protein	0	3.46
gp006	Potential dUTP pyrophosphatase	0	3.11
gp149	Hypothetical protein	10.1	2.86
gp012	Conserved hypothetical protein	0	3.33
gp025	Hypothetical protein	0	3.36
gp142	Conserved hypothetical protein	0	3.32
gp109	Gp3 tail completion and sheath stabilizer protein	0	3.33
gp032	Probable Gp5.4 conserved hypothetical protein	0	3.46
gp007	Hypothetical protein	0	3.39
gp151	Hypothetical protein	0	3.22
gp016	Conserved hypothetical protein	0	3.32
gp156	Conserved hypothetical protein	0	2.94
gp114	Conserved hypothetical protein	0	3.42

gp027	Hypothetical protein	0	3.44
gp132	Hypothetical protein	0	3.18
gp169	Hypothetical protein	0	3.40
gp005	Hypothetical protein	0	3.33
gp003	Gp44 sliding clamp loader subunit (DNA polymerase accessory protein)	0	3.28
gp065	Hypothetical protein	0	3.31
gp107	Gp61 DNA primase subunit	0	3.08
gp084	Hef85 homing endonuclease	0	3.32
gp092	Putative repair and recombination protein	0	2.97
gp015	Gp39; topoisomerase II large subunit	0	3.27
gp042	Gp25 baseplate wedge subunit	0	3.27
gp028	Hypothetical protein	0	2.91
gp008	Potential NAD(FAD)-utilizing dehydrogenase	0	3.29
gp164	Hypothetical protein	0	3.26
gp141	Conserved hypothetical protein	0	3.05
gp103	Hypothetical protein	0	3.02
gp039	Hypothetical protein	0	3.34
gp029	Conserved hypothetical protein	0	3.20
gp118	Gp46 recombination endonuclease	0	3.05
gp139	Conserved hypothetical protein	0	3.11
gp045	Gp41 DNA primase-helicase subunit	0	3.20
gp033	Hef34 homing endonuclease	0	3.11
gp021	Hypothetical protein	0	3.13
gp127	Conserved hypothetical protein	0	3.06
gp135	Hypothetical protein	0	3.30
gp128	Hypothetical protein	0	2.95
gp134	Hypothetical protein	0	3.37
gp009	Hypothetical protein	0	3.19
gp024	Putative peptidase	0	3.14
gp040	Conserved hypothetical protein	0	3.14
gp056	Thymidylate synthetase	0	3.19
gp002	Hypothetical protein	17.9	3.08
gp047	Conserved hypothetical protein; flagellar glycan binding protein[c]	0	3.11
gp091	DNA helicase UvsW	0	3.08
gp146	Conserved hypothetical protein	0	2.70
gp143	Hypothetical protein	0	2.82
gp053	Gp2 DNA end protector protein	0	2.96
gp147	Conserved hypothetical protein	0	3.03
gp034	Hypothetical protein	0	2.63
gp133	Conserved hypothetical protein	0	2.75

gp144	Conserved hypothetical protein	0	2.75
gp070	Hef71 homing endonuclease	0	2.98
gp101	Gp43 DNA polymerase	0	2.95
gp096	Possible methylase	0	2.80
gp121	Gp55 Sigma factor for T4 late transcription	0	2.76
gp095	Conserved hypothetical protein	6.5	2.79
gp120	Gp47 recombination endonuclease	0	2.93
gp161	Putative poly A polymerase	0	2.93
gp018	Hypothetical protein	0	2.55
gp023	Hypothetical protein	0	2.57
gp136	Conserved hypothetical protein	0	2.92
gp145	Hypothetical protein	0	2.75
gp052	Hef53 homing endonuclease	0	2.84
gp097	Putative recB family exonuclease	0	2.62
gp073	Hef74 homing endonuclease	0	2.94
gp022	Hypothetical protein	0	2.73
gp129	Hypothetical protein	0	2.33
gp150	Hypothetical protein	0	2.52
gp004	Hypothetical protein	0	2.83
gp055	Conserved hypothetical protein	0	2.58
gp157	Hypothetical protein	0	2.70
gp014	Hef15 homing endonuclease	0	2.88
gp137	Hypothetical protein	0	2.64
gp100	Hypothetical protein	0	2.89
gp167	Hef168 homing endonuclease	0	2.64
gp010	Hypothetical protein	0	2.66
gp113	Conserved hypothetical protein	0	2.64
gp106	Hypothetical protein	0	2.67
gp011	Hypothetical protein	0	2.54
gp057	Hef58 homing endonuclease	0	2.70
gp131	Conserved hypothetical protein	0	2.54
gp046	Hypothetical protein	0	2.09
gp090	Putative DEAD/DEAH box helicase	0	2.45
gp072	Hef73 homing endonuclease	0	2.48
gp059	Hef60 homing endonuclease	0	2.59
gp031	Hypothetical protein	0	2.04
gp058	Hef59 homing endonuclease	0	2.33
gp130	Hypothetical protein	0	1.04

[a]Percent amino acid (AA) coverage following mass spectrometry of purified virions as determined by Kropinski *et al.* (2011); "0" indicates no peptides mapping to predicted AA sequence were detected

[b]RPKM (reads per kilobase million) values for each gene

[c]Annotation updated according to Javed *et al.* (2015)

[d]Non-coding RNA

5'-CAAGGTTATGGTAAGCTTATTATGTTAATTTTCTCTTTACTTCTAAAGAGACC ATAGCCTGAGTAATAAAATAGAACACATAAGGTTAATACGCAGACCTAAAATA AGGTCCCTCCTTTCAATCTTCAGATACTCTTAACCTGGTGTTCTCTAAACAT-3'

Figure 2-S2. Nucleotide sequence of the novel 158-bp non-coding RNA (ncRNA) identified between *gp012* and *gp013* (nucleotides 7110-7267) on the phage genome.

Table 2-S4. KEGG pathways for *C. jejuni* NCTC 11168 genes statistically significantly down-regulated at 30, 60 and 120 min post NCTC 12673 phage infection.

Significantly down-regulated pathways[a]	**Significance value (*p*-value)[b]**		
KEGG pathway	**30 min**	**60 min**	**120 min**
cje00010 Glycolysis / Gluconeogenesis	0.02	<0.01	0.01
cje00020 Citrate cycle (TCA cycle)	0.00	<0.01	<0.01
cje00190 Oxidative phosphorylation			0.02
cje00250 Alanine, aspartate and glutamate metabolism	0.03	0.01	
cje00520 Amino sugar and nucleotide sugar metabolism	0.03		0.03
cje00620 Pyruvate metabolism	0.03	<0.01	0.01
cje00640 Propanoate metabolism	0.04	<0.01	0.01
cje00650 Butanoate metabolism	0.04	0.03	0.01
cje00680 Methane metabolism	0.04		
cje00970 Aminoacyl-tRNA biosynthesis		0.02	
cje01100 Metabolic pathways	<0.01	<0.01	<0.01

cje01110 Biosynthesis of secondary metabolites	0.02	<0.01	
cje01120 Microbial metabolism in diverse environments	<0.01	<0.01	<0.01
cje01130 Biosynthesis of antibiotics	<0.01	<0.01	0.01
cje01200 Carbon metabolism	<0.01	<0.01	<0.01
cje01230 Biosynthesis of amino acids		<0.01	
cje02020 Two-component system		0.02	0.03
cje02030 Bacterial chemotaxis		0.03	0.03
cje02040 Flagellar assembly		0.03	

[a]Differentially expressed host genes for each condition were subjected to gene set enrichment analysis (GSEA) on annotated Kyoto Encyclopedia of Genes and Genomes (KEGG) pathways using GAGE with an FDR cutoff of <0.1. KEGG pathways along with their significance values at each time point are listed in Table 2-5.

[b]Numerical values correspond to FDR-adjusted p-values (<0.05 was considered to be significant). A blank space indicates that the corresponding category was not statistically significantly down-regulated.

Table 2-S5. Differentially expressed *C. jejuni* NCTC 11168 genes upon NCTC 12673 phage infection according to COG categories.

Gene and annotation according to COG category[a]		**Fold change (p-value)[b]**		
Gene	**Annotation**	**30 min (*P*)**	**60 min (*P*)**	**120 min (*P*)**
Amino acid transport and metabolism				
argB	acetylglutamate kinase			3.3 (<0.01)
argC	N-acetyl-gamma-glutamyl-phosphate reductase			2.72 (<0.01)
argD	putative acetylornithine/succinyldiaminopimelate aminotransferase			3.18 (<0.01)
aroQ	3-dehydroquinate dehydratase			-1.72 (0.04)
aspB	aspartate aminotransferase			-2.04 (0.01)

cj0731	putative ABC transport system permease			3.08 (0.02)
cj0732	ABC transport system ATP-binding protein			3.29 (<0.01)
cj0919c	putative ABC-type amino-acid transporter permease protein			-1.63 (0.03)
cj0920c	putative ABC-type amino-acid transporter permease protein			-2.3 (<0.01)
cj0980	putative peptidase			-1.72 (0.03)
cj1111c	putative MarC family integral membrane protein			-1.97 (0.04)
cj1581c	putative peptide ABC-transport system ATP-binding protein	5.38 (<0.01)	4.4 (<0.01)	4.82 (<0.01)
cj1583c	putative peptide ABC-transport system permease protein	2.13 (<0.01)		4.82 (<0.01)
ilvD	dihydroxy-acid dehydratase		-1.82 (0.02)	4.82 (<0.01)
leuA	2-isopropylmalate synthase			2.62 (<0.01)
leuC	3-isopropylmalate dehydratase large subunit			2.37 (<0.01)
leuD	3-isopropylmalate dehydratase small subunit			2.43 (<0.01)
livF	branched-chain amino-acid ABC transport system ATP binding protein			1.89 (0.02)
livH	branched-chain amino-acid ABC transport system permease protein			1.69 (0.04)
livJ	branched-chain amino-acid ABC transport system periplasmic binding protein			1.47 (0.05)
metE	5-methyltetrahydropteroyltriglutamate--homocysteine methyltransferase			1.8 (0.01)
peb1A	aspartate/glutamate-binding ABC transporter protein			-2.51 (0.01)
proA	gamma-glutamyl phosphate reductase			-1.88 (0.02)
putP	putative sodium/proline symporter			-1.96 (0.02)
sdaA	L-serine dehydratase			-1.82 (0.03)
sdaC	amino acid transporter			-1.76 (<0.01)
thrB	putative homoserine kinase			1.92 (<0.01)
trpD	anthranilate synthase component II			1.86 (0.02)
Carbohydrate transport and metabolism				
Gene	**Annotation**	**30 min (P)**	**60 min (P)**	**120 min (P)**
cj0035c	putative efflux protein	2.08 (0.04)		3.05 (<0.01)
cj1241	putative MFS (Major Facilitator Superfamily) transporter protein			2.64 (0.02)
cj1548c	putative NADP-dependent alcohol dehydrogenase		-1.7 (0.04)	2.64 (0.02)

dcuA	anaerobic C4-dicarboxylate transporter			2.64 (0.02)
kgtP	alpha-ketoglutarate permease			-2.26 (0.04)
pyk	pyruvate kinase			-1.81 (0.03)
Cell cycle control, cell division, chromosome partitioning				
Gene	**Annotation**	**30 min (P)**	**60 min (P)**	**120 min (P)**
pbpC	penicillin-binding protein			1.68 (0.04)
Cell motility				
Gene	**Annotation**	**30 min (P)**	**60 min (P)**	**120 min (P)**
cj1506c	putative MCP-type signal transduction protein			-1.53 (0.03)
fliR	flagellar biosynthetic protein			2.7 (<0.01)
Cell wall/membrane/envelope biogenesis				
Gene	**Annotation**	**30 min (P)**	**60 min (P)**	**120 min (P)**
cadF	outer membrane fibronectin-binding protein			-1.52 (0.04)
cj0313	putative integral membrane protein			2.12 (0.02)
cj0505c	putative aminotransferase (degT family)			2.11 (<0.01)
cj0646	putative lipoprotein			1.74 (<0.01)
cj0826	putative integral membrane protein	3.07 (<0.01)		3.46 (<0.01)
cj0958c	putative membrane protein			1.79 (<0.01)
Int	putative apolipoprotein N-acyltransferase	2.37 (0.02)		2.71 (0.01)
cj1180c	putative ABC transporter ATP-binding protein			3.41 (<0.01)
cj1434c	putative sugar transferase		1.89 (0.02)	3.41 (<0.01)
cj1442c	putative sugar transferase		2.04 (0.03)	3.41 (<0.01)
cj1661	possible ABC transport system permease	2.54 (<0.01)		2.27 (0.03)
cj1662	putative integral membrane protein			2.82 (<0.01)
iamB	putative ABC transport system permease			1.7 (0.03)
lpxC	UDP-3-O-[3-hydroxymyristoyl] N-acetylglucosamine deacetylase			-1.76 (<0.01)
murD	UDP-N-acetylmuramoylalanine-D-glutamate ligase			1.69 (0.03)
tonB1	TonB transport protein	2.53 (0.03)		3 (0.01)
tonB2	putative TonB transport protein1	3.92 (<0.01)	2.67 (0.02)	3.13 (0.01)
Coenzyme transport and metabolism				
Gene	**Annotation**	**30 min (P)**	**60 min (P)**	**120 min (P)**
bioB	putative biotin synthase			1.73 (0.04)

birA	putative biotin--[acetyl-CoA-carboxylase] synthetase			2.19 (0.03)
chuC	putative haemin uptake system ATP-binding protein			2.49 (0.05)
cj0230c	putative transferase protein			1.68 (0.03)
hemN	putative oxygen-independent coproporphyrinogen III oxidase	1.84 (<0.01)		2.43 (<0.01)
cj0541	polyprenyl synthetase		2.11 (0.02)	1.8 (0.02)
cj1420c	putative methyltransferase		-1.73 (0.03)	1.8 (0.02)
hemA	glutamyl-tRNA reductase			1.65 (0.02)
hemC	porphobilinogen deaminase			1.63 (0.03)
hemH	putative ferrochelatase			2.27 (<0.01)
cj0725c	molybdopterin biosynthesis protein			-1.87 (0.04)
ribD	riboflavin-specific deaminase/reductase			3.24 (<0.01)

Defense mechanisms				
Gene	**Annotation**	**30 min (P)**	**60 min (P)**	**120 min (P)**
cj0140	hypothetical protein Cj0140			1.75 (0.03)
cj0424	putative acidic periplasmic protein	9.95 (<0.01)	10.51 (<0.01)	12.75 (<0.01)
cj1174	putative efflux protein (multidrug resistance protein)			2.45 (0.03)
cj1298	putative N-acetyltransferase		2.5 (0.02)	2.45 (0.03)

Energy production and conversion				
Gene	**Annotation**	**30 min (P)**	**60 min (P)**	**120 min (P)**
ackA	acetate kinase			-2.42 (<0.01)
acnB	aconitate hydratase			-2.16 (0.03)
cj0037c	putative cytochrome C	2.51 (0.01)		-2.16 (0.03)
cj0073c	conserved hypothetical protein Cj0073c			-2.38 (0.01)
cj0074c	putative iron-sulfur protein			-2.32 (0.02)
cj0604	putative polyphosphate kinase			-2.72 (<0.01)
cj0833c	putative oxidoreductase			-1.86 (0.03)
cydA	cytochrome bd oxidase subunit I			2.33 (0.01)
cydB	cytochrome bd oxidase subunit II			2.54 (<0.01)
gltA	citrate synthase			-2.55 (0.01)
hydB	Ni/Fe-hydrogenase large subunit			-1.77 (0.05)
hydC	Ni/Fe-hydrogenase B-type cytochrome subunit			-1.95 (<0.01)
icd	isocitrate dehydrogenase		-1.87 (0.04)	-2.03 (0.04)

lctP	L-lactate permease			-2.28 (<0.01)
oorB	OORB subunit of 2-oxoglutarate:acceptor oxidoreductase			-1.87 (0.03)
pta	putative phosphate acetyltransferase			-2.25 (0.02)
putA	putative proline dehydrogenase/delta-1-pyrroline-5-carboxylate dehydrogenase			-2.22 (<0.01)
sucC	succinyl-coA synthetase beta chain			-2.09 (0.03)
sucD	succinyl-coA synthetase alpha chain			-1.9 (0.05)
icd	isocitrate dehydrogenase		-1.87 (0.04)	-1.9 (0.05)

Function unknown				
Gene	**Annotation**	**30 min (P)**	**60 min (P)**	**120 min (P)**
cj0014c	putative integral membrane protein			-1.69 (0.04)
cj0177	putative iron transport protein			3.84 (<0.01)
cj0189c	conserved hypothetical protein Cj0189c			1.7 (0.03)
cj0341c	putative integral membrane protein			2.18 (0.04)
cj0449c	conserved hypothetical protein Cj0449c			-2.43 (0.02)
cj0602c	MOSC-domain containing protein			-2.2 (0.03)
cj0728	putative periplasmic protein			3.37 (<0.01)
cj1384c	hypothetical protein Cj1384c			3.64 (<0.01)
cj1660	putative integral membrane protein			2.85 (<0.01)

General function prediction only				
Gene	**Annotation**	**30 min (P)**	**60 min (P)**	**120 min (P)**
cj0145	putative TAT (Twin-Arginine Translocation) pathway signal sequence domain protein	2.5 (0.02)		3.55 (<0.01)
cj0184c	putative serine/threonine protein phosphatase			2.37 (<0.01)
cj0504c	putative oxidoreductase			2.31 (0.01)
cj0605	putative amidohydrolase			-2.2 (<0.01)
cj0620	conserved hypothetical protein Cj0620		2.71 (0.02)	-2.2 (<0.01)
cj0711	hypothetical protein Cj0711		2.41 (0.02)	2.45 (0.03)
cj0730	putative ABC transport system permease			2.76 (0.03)
cj0937	putative integral membrane protein	7.19 (<0.01)	4.54 (<0.01)	10.14 (<0.01)
cj1028c	putative purine/pyrimidine phosphoribosyltransferase	2.36 (0.02)		2.7 (<0.01)
cj1225	conserved hypothetical protein Cj1225			-1.88 (<0.01)
cj1373	putative integral membrane protein			1.89 (0.02)

cj1500	putative integral membrane protein			4.26 (<0.01)
cj1164c	hypothetical protein Cj1164c	-2.13 (0.03)		4.26 (<0.01)

Inorganic ion transport and metabolism				
Gene	**Annotation**	**30 min (P)**	**60 min (P)**	**120 min (P)**
arsB	arsenical pump membrane protein			2.14 (0.03)
ceuB	enterochelin uptake permease			3.36 (<0.01)
cfrA	ferric enterobactin uptake receptor			2.33 (0.03)
cft	ferritin			-2.05 (0.02)
chuA	haemin uptake system outer membrane receptor	7.73 (<0.01)	4.9 (<0.01)	6.84 (<0.01)
chuD	putative haemin uptake system periplasmic haemin-binding protein	3.9 (<0.01)	2.73 (0.02)	3.31 (<0.01)
cj0167c	putative integral membrane protein	3.35 (<0.01)	2.71 (0.01)	5.35 (<0.01)
cj0178	putative TonB-denpendent outer membrane receptor	4.5 (<0.01)		4.86 (<0.01)
cj0186c	putative TerC family integral membrane protein			2.27 (<0.01)
cj0727	putative periplasmic solute-binding protein			2.5 (0.02)
cj0909	putative periplasmic protein			-2.73 (<0.01)
cj1609	putative sulfate adenylyltransferase			-1.7 (0.02)
cj1613c	putative pyridoxamine 5'-phosphate oxidase	3.34 (<0.01)	3.25 (<0.01)	2.47 (<0.01)
cj1658	putative iron permease	2.4 (0.01)		2.93 (<0.01)
feoB	ferrous iron transport protein			-1.64 (0.04)
katA	catalase	3.1 (<0.01)		3.42 (<0.01)
kdpB	potassium-transporting ATPase B chain			3.61 (<0.01)
ktrA	putative K+ uptake protein	4.08 (<0.01)	2.78 (<0.01)	6.99 (<0.01)
ktrB	putative K+ uptake protein	3.63 (<0.01)	2.4 (0.01)	5.8 (<0.01)
ppk	polyphosphate kinase			-1.9 (0.03)
pstS	putative periplasmic phosphate binding protein			1.8 (0.02)
chuB	putative haemin uptake system permease protein	3.02 (<0.01)		1.8 (0.02)

Intracellular trafficking, secretion, and vesicular transport				
Gene	**Annotation**	**30 min (P)**	**60 min (P)**	**120 min (P)**
cj0975	putative outer-membrane protein	2.77 (0.01)	2.43 (0.05)	3.13 (<0.01)
exbB1	biopolymer transport protein			3.76 (<0.01)
exbD3	putative exbD/tolR family transport protein			1.84 (0.04)
ffh	signal recognition particle protein			1.64 (0.05)
secY	preprotein translocase subunit			2.49 (<0.01)

Lipid transport and metabolism

Gene	Annotation	30 min (P)	60 min (P)	120 min (P)
acs	acetyl-coenzyme A synthetase		-2.53 (<0.01)	-2.03 (0.02)
cj0807	putative oxidoreductase			-1.69 (0.03)
fabH	3-oxoacyl-[acyl-carrier-protein] synthase			1.56 (0.02)
p19	periplasmic protein p19			2.23 (0.01)
plsC	putative 1-acyl-SN-glycerol-3-phosphate acyltransferase			1.77 (0.02)
pycA	pyruvate carboxylase A subunit			-2.04 (<0.01)

Nucleotide transport and metabolism

Gene	Annotation	30 min (P)	60 min (P)	120 min (P)
nrdA	ribonucleoside-diphosphate reductase alpha chain			1.93 (0.01)
oorD	OORD subunit of 2-oxoglutarate:acceptor oxidoreductase			-1.76 (0.04)
purB	adenylosuccinate lyase			2.15 (0.02)
purH	phosphoribosylaminoimidazolecarboxamide formyltransferase / IMP cyclohydrolase			2.64 (<0.01)
purL	phosphoribosylformylglycinamidine synthase			2.2 (<0.01)
purE	phosphoribosylaminoimidazole carboxylase catalytic subunit		-1.95 (<0.01)	2.2 (<0.01)

Posttranslational modification, protein turnover, chaperones

Gene	Annotation	30 min (P)	60 min (P)	120 min (P)
cj0190c	conserved hypothetical protein Cj0190c			1.95 (<0.01)
cj0911	putative periplasmic protein			-2.17 (0.02)
cj0954c	putative DnaJ-like protein			2.31 (0.01)
cj1501	conserved hypothetical protein Cj1501			4.14 (<0.01)
dnaK	heat shock protein DnaK			1.59 (0.05)
dsbD	putative thiol:disulphide interchange protein			-2.1 (0.03)
htpG	hsp90 family heat shock protein			1.58 (0.04)

Replication, recombination and repair

Gene	Annotation	30 min (P)	60 min (P)	120 min (P)
cj0208	putative DNA modification methylase (adenine-specific methyltransferase)			2.93 (<0.01)
cj0777	putative ATP-dependent DNA helicase			1.88 (0.02)
cj1254	hypothetical protein Cj1254			2.63 (<0.01)

ruvC	crossover junction endodeoxyribonuclease			3.51 (<0.01)
ssb	single-strand DNA binding protein			2.5 (0.01)
topA	DNA topoisomerase I			1.53 (0.04)
xseA	exodeoxyribonuclease VII large subunit			1.85 (0.03)
Secondary metabolites biosynthesis, transport and catabolism				
Gene		**30 min (P)**	**60 min (P)**	**120 min (P)**
cj0021c	putative fumarylacetoacetate (FAA) hydrolase family protein			-2.26 (0.02)
cj1199	putative iron/ascorbate-dependent oxidoreductase	2.31 (0.03)		-2.26 (0.02)
Signal transduction mechanisms				
Gene	**Annotation**	**30 min (P)**	**60 min (P)**	**120 min (P)**
cj0241c	putative iron-binding protein	2.69 (<0.01)		3.54 (<0.01)
cj1224	putative iron-binding protein			-1.98 (0.02)
cj1258	putative phosphotyrosine protein phosphatase			-2.53 (<0.01)
cstA	putative integral membrane protein (CstA homolog)		-1.82 (0.03)	-2.53 (<0.01)
typA	GTP-binding protein TypA homolog			-2.53 (<0.01)
Transcription				
Gene	**Annotation**	**30 min (P)**	**60 min (P)**	**120 min (P)**
cj1556	putative transcriptional regulator			1.83 (0.05)
hrcA	putative heat shock regulator			2.01 (<0.01)
rpoA	DNA-directed RNA polymerase alpha chain			1.87 (<0.01)
rpoC	DNA-directed RNA polymerase beta' chain			1.55 (0.05)
Translation, ribosomal structure and biogenesis				
Gene	**Annotation**	**30 min (P)**	**60 min (P)**	**120 min (P)**
cj0123c	putative tRNA-dihydrouridine synthase			2.24 (<0.01)
cj0154c	putative tetrapyrrole methylase family protein			2.18 (0.01)
cj0225	putative acetyltransferase			3.27 (<0.01)
rplY	putative 50S ribosomal protein L25 (general stress protein Ctc)			1.64 (0.04)
cj0495	putative methyltransferase domain protein			2.86 (<0.01)
cj0636	NOL1/NOP2/sun family protein			2.14 (0.02)
cj1172c	conserved hypothetical protein Cj1172c			1.63 (0.05)
cj1709c	putative ribosomal pseudouridine synthase			1.85 (0.03)

cj1713	putative radical SAM domain protein			2.28 (0.02)
fmt	methionyl-tRNA formyltransferase			2.16 (<0.01)
prfA	peptide chain release factor 1			2.65 (<0.01)
pth	peptidyl-tRNA hydrolase			1.77 (0.02)
rimM	putative 16S rRNA processing protein			2.02 (<0.01)
rplD	50S ribosomal protein L4			1.59 (0.03)
rplF	50S ribosomal protein L6			1.91 (<0.01)
rplJ	50S ribosomal protein L10			1.94 (<0.01)
rplK	50S ribosomal protein L11			1.85 (0.03)
rplM	50S ribosomal protein L13			1.8 (0.01)
rplT	50S ribosomal protein L20			1.7 (<0.01)
rplW	50S ribosomal protein L23			2.17 (<0.01)
rpmC	50S ribosomal protein L29			1.77 (0.04)
rpmE	50S ribosomal protein L31			2.51 (<0.01)
rpsB	30S ribosomal protein S2			1.87 (<0.01)
rpsC	30S ribosomal protein S3			1.57 (0.02)
rpsD	30S ribosomal protein S4			1.71 (0.02)
rpsE	30S ribosomal protein S5			1.69 (0.02)
rpsF	30S ribosomal protein S6			1.63 (0.03)
rpsH	30S ribosomal protein S8			1.86 (0.01)
rpsI	30S ribosomal protein S9			2.46 (<0.01)
rpsK	30S ribosomal protein S11			2.31 (<0.01)
rpsM	30S ribosomal protein S13			1.57 (0.05)
rpsQ	30S ribosomal protein S17			2.05 (0.02)
rpsR	30S ribosomal protein S18			2.12 (<0.01)
rpsS	30S ribosomal protein S19			1.73 (0.04)
rpsT	30S ribosomal protein S20			1.74 (0.04)
serS	seryl-tRNA synthetase			-1.64 (0.04)
tlyA	putative haemolysin			2.37 (<0.01)
trmD	tRNA (guanine-N1)-methyltransferase		2.22 (0.03)	2.68 (<0.01)
tsf	elongation factor TS			2.04 (<0.01)
Uncategorized				
Gene	**Annotation**	**30 min (P)**	**60 min (P)**	**120 min (P)**
bioC	putative biotin synthesis protein	2.39 (0.04)		2.95 (0.02)

cca	putative multifunctional Cca protein			2.13 (<0.01)
cdtA	cytolethal distending toxin A			-1.76 (0.03)
cgb	single domain haemoglobin			2.56 (0.02)
cj0011c	putative non-specific DNA binding protein			-2.12 (<0.01)
cj0030	hypothetical protein Cj0030	2.13 (0.04)	2.41 (<0.01)	2.49 (<0.01)
cj0038c	putative poly(A) polymerase family protein			3.33 (<0.01)
cj0069	hypothetical protein Cj0069			-2.03 (0.04)
cj0075c	putative oxidoreductase iron-sulfur subunit			-2.52 (<0.01)
cj0080	putative membrane protein			3.14 (0.01)
cj0093	putative periplasmic protein			1.64 (0.02)
cj0111	putative periplasmic protein			1.98 (<0.01)
cj0120	hypothetical protein Cj0120			2.19 (0.03)
cj0124c	putative membrane protein			2.2 (<0.01)
cj0223	pseudogene (putative IgA protease family protein)			1.72 (0.05)
cj0254	hypothetical protein Cj0254			-1.54 (0.04)
cj0260c	small hydrophobic protein		2.13 (0.02)	2.56 (0.02)
cj0267c	putative integral membrane protein			2.53 (0.02)
cj0295	putative acetyltransferase			2.4 (0.02)
cj0323	hypothetical protein Cj0323			1.82 (0.05)
cj0344	hypothetical protein Cj0344			-2.17 (0.01)
cj0350	hypothetical protein Cj0350			-1.77 (0.02)
cj0391c	hypothetical protein Cj0391c	1.64 (0.03)		-1.77 (0.02)
cj0406c	putative lipoprotein			-1.66 (0.05)
cj0414	putative oxidoreductase subunit			2.15 (0.04)
cj0421c	putative integral membrane protein	2.59 (0.03)		6.38 (<0.01)
cj0423	putative integral membrane protein	5.73 (<0.01)	3.36 (<0.01)	16.14 (<0.01)
cj0425	putative periplasmic protein	9.01 (<0.01)	9.1 (<0.01)	10.39
cj0427	hypothetical protein Cj0427			-2.11 (0.02)
cj0444	pseudogene (putative TonB-denpendent outer membrane receptor)	2.04 (0.04)	2.12 (0.04)	2.29 (<0.01)
cj0448c	putative MCP-type signal transduction protein			-2.17 (0.05)
cj0494	putative exporting protein			2.57 (<0.01)
cj0515	putative periplasmic protein			1.82 (0.02)
cj0520	putative membrane protein			2.2 (<0.01)
cj0522	putative Na+/Pi cotransporter protein			2.68 (<0.01)

cj0544	putative integral memnbrane protein			2.3 (<0.01)
cj0566	hypothetical protein Cj0566	7.23 (<0.01)	3.99 (<0.01)	2.3 (<0.01)
cj0584	hypothetical protein Cj0584			1.94 (0.03)
cj0590	putative SAM-dependent methyltransferase			1.86 (0.03)
cj0648	putative membrane protein			2.22 (0.01)
cj0651	putative integral membrane protein		2.8 (<0.01)	2.22 (0.01)
cj0694	putative periplasmic protein			1.57 (0.03)
cj0700	hypothetical protein Cj0700			-1.82 (0.04)
cj0729	putative type I phosphodiesterase/nucleotide	2.77 (0.02)	2.57 (0.02)	4.25 (<0.01)
cj0735	putative periplasmic protein	2.58 (<0.01)		4.25 (<0.01)
cj0736	hypothetical protein Cj0736	5.35 (<0.01)	2.49 (0.04)	4.25 (<0.01)
cj0742	pseudogene (putative outer membrane protein)	4.71 (<0.01)	4.07 (<0.01)	3.91 (<0.01)
cj0752	pseudogene (IS element transposase)	2.72 (0.02)	2.68 (0.02)	3.54 (<0.01)
cj0794	hypothetical protein Cj0794	3.22 (<0.01)		2.6 (0.02)
cj0834c	ankyrin repeat-containing putative periplasmic protein			-1.82 (0.04)
cj0873c	hypothetical protein Cj0873c			-2.14 (0.01)
cj0910	putative periplasmic protein			-2.21 (<0.01)
cj0944c	putative periplasmic protein		-1.88 (0.03)	-2.21 (<0.01)
cj0951c	putative MCP-domain signal transduction protein			-1.8 (0.04)
cj0967	putative periplasmic protein	4.42 (<0.01)		3.8 (<0.01)
cj1012c	putative membrane protein			2.3 (0.01)
cj1041c	putative periplasmic ATP/GTP-binding protein	2.68 (<0.01)		1.95 (0.04)
cj1078	putative periplasmic protein	2.49 (0.05)		1.95 (0.04)
cj1159c	small hydrophobic protein	2.62 (0.03)		2.65 (0.04)
cj1162c	putative heavy-metal-associated domain protein	3.35 (<0.01)		3.31 (<0.01)
cj1169c	putative periplasmic protein			2.21 (0.02)
cj1307	putative amino acid activating enzyme			-1.67 (0.02)
cj1322	hypothetical protein Cj1322	3.48 (<0.01)		2.42 (0.05)
cj1383c	hypothetical protein Cj1383c	2.39 (0.04)		2.42 (0.05)
cj1389	pseudogene (putative C4-dicarboxylate anaerobic carrier)	2.11 (<0.01)		2.42 (0.05)
cj1395	pseudogene (putative MmgE/PrpD family protein)	2.82 (0.02)		2.42 (0.05)
cj1422c	putative sugar transferase			2.42 (0.05)
cj1459	hypothetical protein Cj1459			2.42 (0.05)
cj1664	putative periplasmic thiredoxin	2.66 (<0.01)		2.42 (0.05)
cj1665	putative lipoprotein thiredoxin			2.42 (0.05)

cj1677	putative lipoprotein	5.48 (<0.01)	2.99 (<0.01)	2.42 (0.05)
cj1712	hypothetical protein Cj1712			2.42 (0.05)
cetB	bipartate energy taxis response protein cetB	2.21 (0.03)		2.42 (0.05)
cmeA	periplasmic fusion protein CmeA (multidrug efflux system CmeABC)	2.6 (<0.01)		1.99 (<0.01)
cmeB	inner membrane efflux transporter CmeB (multidrug efflux system CmeABC)	2.09 (<0.01)		2.14 (<0.01)
cmeC	outer membrane channel protein CmeC (multidrug efflux system CmeABC)	2.04 (<0.01)		2.02 (<0.01)
ctsP	putative ATP/GTP-binding protein	2.8 (<0.01)	2.55 (<0.01)	2.47 (0.01)
dba	disulphide bond formation protein	2.44 (0.04)		3.32 (<0.01)
dccR	two-component regulator			-1.93 (0.02)
dprA	DNA processing protein A			1.91 (0.02)
dsbI	disulphide bond formation protein	2.33 (0.03)		4.15 (<0.01)
exoA	exodeoxyribonuclease			1.97 (0.03)
fdxA	ferredoxin			-1.89 (0.05)
flaC	flagellin			-2.1 (0.03)
glpT	pseudogene (putative glycerol-3-phosphate transporter)			-2.12 (0.05)
hldD	ADP-glyceromanno-heptose 6-epimerase			-1.57 (0.03)
kdpA	pseudogene (potassium-transporting ATPase A chain)	2.76 (<0.01)	2.62 (<0.01)	2.27 (<0.01)
kpsC	capsule polysaccharide modification protein			1.6 (0.04)
lolA	putative outer-membrane lipoprotein carrier protein precursor			-1.89 (0.03)
mreC	homolog of E. coli rod shape-determining protein			1.72 (0.04)
nrdB	ribonucleoside-diphosphate reductase beta chain			1.66 (0.04)
cj0096	GTP-binding protein			2.25 (<0.01)
omp50	50 kda outer membrane protein precursor	2.43 (0.05)		3.89 (<0.01)
pglA	GalNAc transferase			1.99 (0.04)
pseI	Pse synthetase			-1.67 (0.03)
rpmJ	50S ribosomal protein L36			1.73 (0.04)
rpoB	DNA-directed RNA polymerase beta chain			1.96 (0.01)
trmE	putative tRNA modification GTPase			2.16 (<0.01)
ubiD	putative 3-octaprenyl-4-hydroxybenzoate carboxy-lyase			1.61 (0.03)

[a]Host genes found to be differentially expressed between infected and control samples for at least one time point were assigned to one of 25 functional categories based on clusters of orthologous groups (COG) classification. Genes were assigned according to the COG function

list for *C. jejuni jejuni* NCTC 11168 according to the Integrated Microbial Genomes and Microbiomes (IMG/M) database (https://img.jgi.doe.gov). Gene annotations were obtained from NCBI.

[b]For each gene, fold change in expression post NCTC 12673 phage infection is listed followed by the adjusted *P*-value (*P*) in brackets. Fold change values for genes whose transcripts were not significantly differentially expressed are not shown.

A

```
Cj0423     1 MEGASGGSIFVT----ILLFILYMLPAIIGLSRKHSNWLIISLLNLFFGWTIIVWLVCLI
Imm        1 METLVAGSIFVVLVSGVLAIIIYMLPWFIALMRGSKSTVGIFFASLLFNWSIIGWFITFI

Cj0423    57 WSFTGSFK------QTIIIKEKNEK
Imm       61 WSIAGETKKSAQPNQVIIIREKE--
```

B

```
Cj0424     1 MTKFLSICSLIAM-------L-------LSGCGSDFPGQPSDVARVQQNKYPNGNLKKEI
YwqK       1 MENEYDVKSIKEKGVDFEDLWFSSVSDEILDNPEDENGQPFT--GIAYELYPNGQIIYFT

Cj0424    47 PYNKDSRIHGLKRAFYDNGQLRAEENYKNGKKDGISREYSRNGQLLEFVHFKDNRGYGDF
YwqK      59 KY-KNGLAHGLTCEFYENGNKKSEKEYRYGQLHGISIIWFENGRKKSEQQMEHSILI---

Cj0424   107 ASYYENGNMRAKGKLLGYNEDGMPEFEGNYKEYYENGTLMCDYNFDNK-GAFDGVQKRYD
YwqK     115 ----------------------------SEKNWDEEGNLLNKYEIDTDSPHFEILESRRE

Cj0424   166 ENGALEDEENYKNGLKNGVFREYKKGEIVREEEYKNGILVAKPKN
YwqK     147 THINLGRE-----------------------------------
```

Figure 2-S3. BLASTp alignment between *C. jejuni* NCTC 11168 protein Cj0423 and T4 phage protein Imm (**A**) and between *C. jejuni* NCTC 11168 protein Cj0424 and *Bacillus subtilis* strain 168 antitoxin protein YwqK (**B**). Alignments were generated using T-Coffee [86] and Boxshade (http://sourceforge.net/projects/boxshade/). Black shading indicates the consensus sequence, grey shading indicates similar residues.

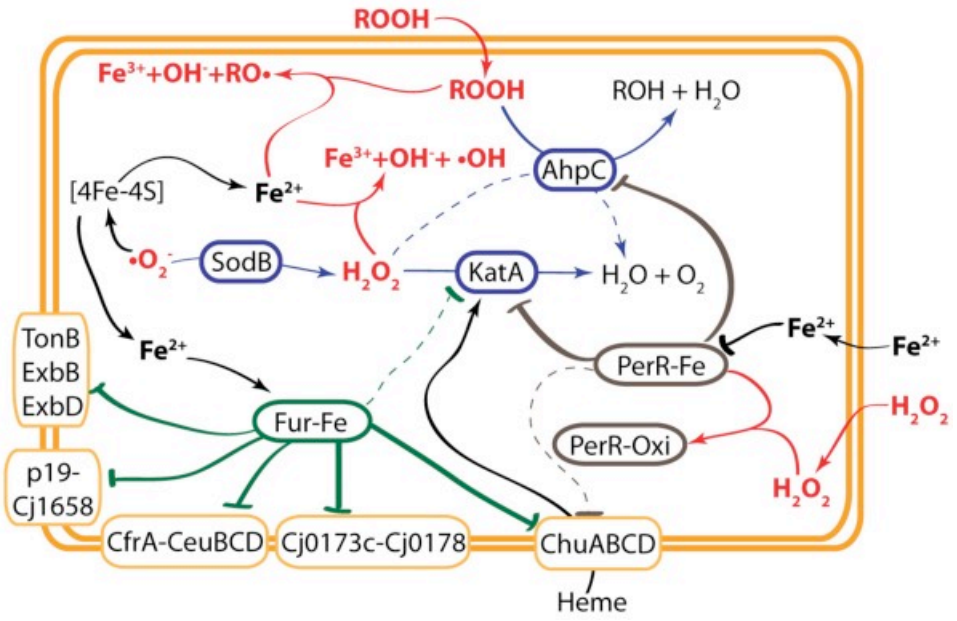

Figure 2-S4. Oxidative stress in *C. jejuni.* Figure reproduced from Palyada *et al.* (2009) with permission [40].

2.7. References

1. O'Neill, J. (2014). Antimicrobial resistance: tackling a crisis for the health and wealth of nations. *The Review on Antimicrobial Resistance* **2014**, *20*. http://amr-review.org/sites/default/files/AMR%20Review%20Paper%20-%20Tackling%20a%20crisis%20for%20the%20health%20and%20wealth%20of%20nations_1.pdf.
2. Huys, I.; Pirnay, J. P.; Lavigne, R.; Jennes, S.; De Vos, D.; Casteels, M.; Verbeken, G. Paving a regulatory pathway for phage therapy. Europe should muster the resources to financially, technically and legally support the introduction of phage therapy. *EMBO Rep.* **2013**, doi:10.1038/embor.2013.163.

3. Roach, D. R.; Debarbieux, L. Phage therapy: awakening a sleeping giant. *Emerg. Top. Life Sci.* **2017**, *1*, 93–103, doi:10.1042/ETLS20170002.
4. Umaraw, P.; Prajapati, A.; Verma, A. K.; Pathak, V.; Singh, V. P. Control of *Campylobacter* in poultry industry from farm to poultry processing unit: A review. *Crit. Rev. Food Sci. Nutr.* **2017**, *57*, 659–665, doi:10.1080/10408398.2014.935847.
5. Blasdel, B.; Ceyssens, P.-J.; Lavigne, R. Preparing cDNA Libraries from Lytic Phage-Infected Cells for Whole Transcriptome Analysis by RNA-Seq. In; 2018; pp. 185–194.
6. Leskinen, K.; Blasdel, B. G.; Lavigne, R.; Skurnik, M. RNA-sequencing reveals the progression of Phage-Host interactions between φR1-37 and *Yersinia enterocolitica*. *Viruses* **2016**, *8*, doi:10.3390/v8040111.
7. Ceyssens, P.-J.; Minakhin, L.; Van den Bossche, A.; Yakunina, M.; Klimuk, E.; Blasdel, B.; De Smet, J.; Noben, J.-P.; Bläsi, U.; Severinov, K.; Lavigne, R. Development of giant bacteriophage ϕKZ is independent of the host transcription apparatus. *J. Virol.* **2014**, *88*, 10501–10, doi:10.1128/JVI.01347-14.
8. Morimoto, D.; Kimura, S.; Sako, Y.; Yoshida, T. Transcriptome Analysis of a Bloom-Forming Cyanobacterium *Microcystis aeruginosa* during Ma-LMM01 Phage Infection. *Front. Microbiol.* **2018**, *9*, 2, doi:10.3389/fmicb.2018.00002.
9. Doron, S.; Fedida, A.; Hernández-Prieto, M. A.; Sabehi, G.; Karunker, I.; Stazic, D.; Feingersch, R.; Steglich, C.; Futschik, M.; Lindell, D.; Sorek, R. Transcriptome dynamics of a broad host-range cyanophage and its hosts. *ISME J.* **2016**, *10*, 1437–55, doi:10.1038/ismej.2015.210.

10. Mojardín, L.; Salas, M. Global transcriptional analysis of virus-host interactions between phage φ29 and *Bacillus subtilis*. *J. Virol.* **2016**, *90*, JVI.01245-16, doi:10.1128/JVI.01245-16.
11. Brathwaite, K. J.; Siringan, P.; Connerton, P. L.; Connerton, I. F. Host adaption to the bacteriophage carrier state of *Campylobacter jejuni*. *Res. Microbiol.* **2015**, *166*, 504–515, doi:10.1016/j.resmic.2015.05.003.
12. Howard-Varona, C.; Roux, S.; Dore, H.; Solonenko, N. E.; Holmfeldt, K.; Markillie, L. M.; Orr, G.; Sullivan, M. B. Regulation of infection efficiency in a globally abundant marine Bacteriodetes virus. *ISME J.* **2017**, *11*, 284–295, doi:10.1038/ismej.2016.81.
13. Chevallereau, A.; Blasdel, B. G.; De Smet, J.; Monot, M.; Zimmermann, M.; Kogadeeva, M.; Sauer, U.; Jorth, P.; Whiteley, M.; Debarbieux, L.; Lavigne, R. Next-Generation "-omics" Approaches Reveal a Massive Alteration of Host RNA Metabolism during Bacteriophage Infection of Pseudomonas aeruginosa. *PLoS Genet.* **2016**, doi:10.1371/journal.pgen.1006134.
14. Blasdel, B. G.; Ceyssens, P.-J.; Chevallereau, A.; Debarbieux, L.; Lavigne, R. Comparative transcriptomics reveals a conserved Bacterial Adaptive Phage Response (BAPR) to viral predation. *bioRxiv* **2018**, doi:10.1101/248849.
15. Blasdel, B. G.; Chevallereau, A.; Monot, M.; Lavigne, R.; Debarbieux, L. Comparative transcriptomics analyses reveal the conservation of an ancestral infectious strategy in two bacteriophage genera. *ISME J.* **2017**, doi:10.1038/ismej.2017.63.
16. Lin, X.; Ding, H.; Zeng, Q. Transcriptomic response during phage infection of a marine cyanobacterium under phosphorus-limited conditions. *Environ. Microbiol.* **2016**, *18*, 450–460, doi:10.1111/1462-2920.13104.

17. Parkhill, J.; Wren, B. W.; Mungall, K.; Ketley, J. M.; Churcher, C.; Basham, D.; Chillingworth, T.; Davies, R. M.; Feltwell, T.; Holroyd, S.; Jagels, K.; Karlyshev, A. V.; Moule, S.; Pallen, M. J.; Penn, C. W.; Quail, M. A.; Rajandream, M. A.; Rutherford, K. M.; Van Vliet, A. H. M.; Whitehead, S.; Barrell, B. G. The genome sequence of the food-borne pathogen *Campylobacter jejuni* reveals hypervariable sequences. *Nature* **2000**, doi:10.1038/35001088.
18. Gundogdu, O.; Bentley, S. D.; Holden, M. T.; Parkhill, J.; Dorrell, N.; Wren, B. W. Re-annotation and re-analysis of the *Campylobacter jejuni* NCTC11168 genome sequence. *BMC Genomics* **2007**, *8*, doi:10.1186/1471-2164-8-162.
19. Kaakoush, N. O.; Mitchell, H. M.; Man, S. M. *Campylobacter*. In *Molecular Medical Microbiology*; 2015; pp. 1187–1236 ISBN 978-0-12-397169-2.
20. Wassenaar, T. M. Following an imaginary *Campylobacter* population from farm to fork and beyond: A bacterial perspective. *Lett. Appl. Microbiol.* 2011, *53*, 253–263.
21. Zampara, A.; Sørensen, M. C. H.; Elsser-Gravesen, A.; Brøndsted, L. Significance of phage-host interactions for biocontrol of *Campylobacter jejuni* in food. *Food Control* **2017**, *73*, 1169–1175, doi:10.1016/j.foodcont.2016.10.033.
22. Fischer, S.; Kittler, S.; Klein, G.; Glünder, G. Impact of a Single Phage and a Phage Cocktail Application in Broilers on Reduction of *Campylobacter jejuni* and Development of Resistance. *PLoS One* **2013**, *8*, doi:10.1371/journal.pone.0078543.
23. Kittler, S.; Fischer, S.; Abdulmawjood, A.; Glünder, G.; Kleina, G. Effect of bacteriophage application on *Campylobacter jejuni* loads in commercial broiler flocks. *Appl. Environ. Microbiol.* **2013**, *79*, 7525–7533, doi:10.1128/AEM.02703-13.

24. Grajewski, B. A.; Kusek, J. W.; Gelfand, H. M. Development of bacteriophage typing system for *Campylobacter jejuni* and *Campylobacter coli*. *J. Clin. Microbiol.* **1985**, *22*, 13–18.

25. Kropinski, A. M.; Arutyunov, D.; Foss, M.; Cunningham, A.; Ding, W.; Singh, A.; Pavlov, A. R.; Henry, M.; Evoy, S.; Kelly, J.; Szymanski, C. M. Genome and proteome of *Campylobacter jejuni* bacteriophage NCTC 12673. *Appl. Environ. Microbiol.* **2011**, *77*, 8265–8271, doi:10.1128/AEM.05562-11.

26. Javed, M. A.; Ackermann, H. W.; Azeredo, J.; Carvalho, C. M.; Connerton, I.; Evoy, S.; Hammerl, J. A.; Hertwig, S.; Lavigne, R.; Singh, A.; Szymanski, C. M.; Timms, A.; Kropinski, A. M. A suggested classification for two groups of *Campylobacter* myoviruses. *Arch. Virol.* **2014**, *159*, 181–190, doi:10.1007/s00705-013-1788-2.

27. Sørensen, M. C. H.; Gencay, Y. E.; Birk, T.; Baldvinsson, S. B.; Jäckel, C.; Hammerl, J. A.; Vegge, C. S.; Neve, H.; Brøndsted, L. Primary isolation strain determines both phage type and receptors recognised by *Campylobacter jejuni* bacteriophages. *PLoS One* **2015**, *10*, doi:10.1371/journal.pone.0116287.

28. Coward, C.; Grant, A. J.; Swift, C.; Philp, J.; Towler, R.; Heydarian, M.; Frost, J. A.; Maskell, D. J. Phase-variable surface structures are required for infection of *Campylobacter jejuni* by bacteriophages. *Appl. Environ. Microbiol.* **2006**, *72*, 4638–4647, doi:10.1128/AEM.00184-06.

29. Javed, M. A.; van Alphen, L. B.; Sacher, J.; Ding, W.; Kelly, J.; Nargang, C.; Smith, D. F.; Cummings, R. D.; Szymanski, C. M. A receptor-binding protein of *Campylobacter jejuni* bacteriophage NCTC 12673 recognizes flagellin glycosylated with acetamidino-

modified pseudaminic acid. *Mol. Microbiol.* **2015**, *95*, 101–115, doi:10.1111/mmi.12849.

30. Javed, M. A.; Sacher, J. C.; van Alphen, L. B.; Patry, R. T.; Szymanski, C. M. A flagellar glycan-specific protein encoded by *Campylobacter* phages inhibits host cell growth. *Viruses* **2015**, *7*, 6661–6674, doi:10.3390/v7122964.
31. Sørensen, M. C. H.; van Alphen, L. B.; Harboe, A.; Li, J.; Christensen, B. B.; Szymanski, C. M.; Brøndsted, L. Bacteriophage F336 recognizes the capsular phosphoramidate modification of *Campylobacter jejuni* NCTC11168. *J. Bacteriol.* **2011**, *193*, 6742–6749, doi:10.1128/JB.05276-11.
32. Frost, J. A.; Kramer, J. M.; Gillanders, S. A. Phage typing of *Campylobacter jejuni* and *Campylobacter coli* and its use as an adjunct to serotyping. *Epidemiol. Infect.* **1999**, *123*, S095026889900254X, doi:10.1017/S095026889900254X.
33. Sørensen, M. C. H.; Gencay, Y. E.; Brøndsted, L. Methods for initial characterization of *Campylobacter jejuni* bacteriophages. In *Methods in Molecular Biology*; 2017; Vol. 1512, pp. 91–105 ISBN 978-1-4939-6536-6.
34. Palyada, K.; Threadgill, D.; Stintzi, A. Iron acquisition and regulation in *Campylobacter jejuni*. *J. Bacteriol.* **2004**, *186*, 4714–4729, doi:10.1128/JB.186.14.4714-4729.2004.
35. Love, M. I.; Huber, W.; Anders, S. Moderated estimation of fold change and dispersion for RNA-seq data with DESeq2. *Genome Biol.* **2014**, *15*, doi:10.1186/s13059-014-0550-8.
36. Dobin, A.; Davis, C. A.; Schlesinger, F.; Drenkow, J.; Zaleski, C.; Jha, S.; Batut, P.; Chaisson, M.; Gingeras, T. R. STAR: Ultrafast universal RNA-seq aligner. *Bioinformatics* **2013**, *29*, 15–21, doi:10.1093/bioinformatics/bts635.

37. Luo, W.; Friedman, M. S.; Shedden, K.; Hankenson, K. D.; Woolf, P. J. GAGE: Generally applicable gene set enrichment for pathway analysis. *BMC Bioinformatics* **2009**, *10*, doi:10.1186/1471-2105-10-161.

38. Bailey, T. L.; Elkan, C. Fitting a mixture model by expectation maximization to discover motifs in biopolymers. *Proceedings. Int. Conf. Intell. Syst. Mol. Biol.* **1994**, *2*, 28–36.

39. Grant, C. E.; Bailey, T. L.; Noble, W. S. FIMO: scanning for occurrences of a given motif. *Bioinformatics* **2011**, *27*, 1017–8, doi:10.1093/bioinformatics/btr064.

40. Palyada, K.; Sun, Y. Q.; Flint, A.; Butcher, J.; Naikare, H.; Stintzi, A. Characterization of the oxidative stress stimulon and PerR regulon of *Campylobacter jejuni*. *BMC Genomics* **2009**, *10*, 481, doi:10.1186/1471-2164-10-481.

41. Patry, R. T.; Stahl, M.; Perez-Munoz, M. E.; Wenzel, C. Q.; Sacher, J. C.; Coros, C.; Walter, J.; Vallance, B. A.; Szymanski, C. M. Bacterial warfare: growth inhibition of ganglioside-mimicking gut bacteria by AB5 toxins. Submitted to *Nat. Microbiol.*

42. Akiba, M.; Lin, J.; Barton, Y.-W.; Zhang, Q. Interaction of CmeABC and CmeDEF in conferring antimicrobial resistance and maintaining cell viability in *Campylobacter jejun*i. *J. Antimicrob. Chemother.* **2006**, *57*, 52–60, doi:10.1093/jac/dki419.

43. Loc Carrillo, C.; Atterbury, R. J.; El-Shibiny, A.; Connerton, P. L.; Dillon, E.; Scott, A.; Connerton, I. F. Bacteriophage therapy to reduce *Campylobacter jejuni* colonization of broiler chickens. *Appl. Environ. Microbiol.* **2005**, *71*, 6554–6563, doi:71/11/6554 [pii] 10.1128/AEM.71.11.6554-6563.2005.

44. Erez, Z.; Steinberger-Levy, I.; Shamir, M.; Doron, S.; Stokar-Avihail, A.; Peleg, Y.; Melamed, S.; Leavitt, A.; Savidor, A.; Albeck, S.; Amitai, G.; Sorek, R. Communication

between viruses guides lysis-lysogeny decisions. *Nature* **2017**, *541*, 488–493, doi:10.1038/nature21049.

45. Abedon, S. T. Commentary: Communication between Viruses Guides Lysis-Lysogeny Decisions. *Front. Microbiol.* **2017**, *8*, 983, doi:10.3389/fmicb.2017.00983.
46. Miller, E. S.; Kutter, E.; Mosig, G.; Arisaka, F.; Kunisawa, T.; Rüger, W. Bacteriophage T4 genome. *Microbiol. Mol. Biol. Rev.* **2003**, *67*, 86–156, table of contents, doi:10.1128/MMBR.67.1.86-156.2003.
47. De Smet, J.; Zimmermann, M.; Kogadeeva, M.; Ceyssens, P. J.; Vermaelen, W.; Blasdel, B.; Bin Jang, H.; Sauer, U.; Lavigne, R. High coverage metabolomics analysis reveals phage-specific alterations to *Pseudomonas aeruginosa* physiology during infection. *ISME J.* **2016**, doi:10.1038/ismej.2016.3.
48. Ankrah, N. Y. D.; May, A. L.; Middleton, J. L.; Jones, D. R.; Hadden, M. K.; Gooding, J. R.; LeCleir, G. R.; Wilhelm, S. W.; Campagna, S. R.; Buchan, A. Phage infection of an environmentally relevant marine bacterium alters host metabolism and lysate composition. *ISME J.* **2014**, *8*, 1089–100, doi:10.1038/ismej.2013.216.
49. Guccione, E.; del Rocio Leon-Kempis, M.; Pearson, B. M.; Hitchin, E.; Mulholland, F.; van Diemen, P. M.; Stevens, M. P.; Kelly, D. J. Amino acid-dependent growth of *Campylobacter jejuni* : key roles for aspartase (AspA) under microaerobic and oxygen-limited conditions and identification of AspB (Cj0762), essential for growth on glutamate. *Mol. Microbiol.* **2008**, *69*, 77–93, doi:10.1111/j.1365-2958.2008.06263.x.
50. Anjum, A.; Brathwaite, K. J.; Aidley, J.; Connerton, P. L.; Cummings, N. J.; Parkhill, J.; Connerton, I.; Bayliss, C. D. Phase variation of a Type IIG restriction-modification enzyme alters site-specific methylation patterns and gene expression in *Campylobacter*

jejuni strain NCTC11168. *Nucleic Acids Res.* **2016**, *44*, 4581–4594, doi:10.1093/nar/gkw019.

51. Hooton, S. P. T.; Connerton, I. F. *Campylobacter jejuni* acquire new host-derived CRISPR spacers when in association with bacteriophages harboring a CRISPR-like Cas4 protein. *Front. Microbiol.* **2015**, *6*, 1–9, doi:10.3389/fmicb.2014.00744.
52. Gardner, S. P.; Olson, J. W. Barriers to Horizontal Gene Transfer in *Campylobacter jejuni*. *Adv. Appl. Microbiol.* **2012**, *79*, 19–42, doi:10.1016/B978-0-12-394318-7.00002-4.
53. Louwen, R.; van Baarlen, P. Are bacteriophage defence and virulence two sides of the same coin in *Campylobacter jejuni*? *Biochem. Soc. Trans.* **2013**, *41*, 1475–81, doi:10.1042/BST20130127.
54. McNally, D. J.; Lamoureux, M. P.; Karlyshev, A. V.; Fiori, L. M.; Li, J.; Thacker, G.; Coleman, R. A.; Khieu, N. H.; Wren, B. W.; Brisson, J. R.; Jarrell, H. C.; Szymanski, C. M. Commonality and biosynthesis of the O-methyl phosphoramidate capsule modification in *Campylobacter jejuni*. *J. Biol. Chem.* **2007**, *282*, 28566–28576, doi:10.1074/jbc.M704413200.
55. Ridley, K. A.; Rock, J. D.; Li, Y.; Ketley, J. M. Heme utilization in *Campylobacter jejuni*. *J. Bacteriol.* **2006**, *188*, 7862–75, doi:10.1128/JB.00994-06.
56. Lin, J.; Michel, L. O.; Zhang, Q. CmeABC functions as a multidrug efflux system in *Campylobacter jejuni*. *Antimicrob. Agents Chemother.* **2002**, *46*, 2124–31, doi:10.1128/AAC.46.7.2124-2131.2002.

57. Pumbwe, L.; Piddock, L. J. V. Identification and molecular characterisation of CmeB, a *Campylobacter jejuni* multidrug efflux pump. *FEMS Microbiol. Lett.* **2002**, *206*, 185–189, doi:10.1111/j.1574-6968.2002.tb11007.x.

58. De Smet, J.; Hendrix, H.; Blasdel, B. G.; Danis-Wlodarczyk, K.; Lavigne, R. *Pseudomonas* predators: Understanding and exploiting phage-host interactions. *Nat. Rev. Microbiol.* 2017.

59. Butcher, J.; Stintzi, A. The Transcriptional Landscape of *Campylobacter jejuni* under Iron Replete and Iron Limited Growth Conditions. *PLoS One* **2013**, *8*, e79475, doi:10.1371/journal.pone.0079475.

60. Grant, K. A.; Park, S. F. Molecular characterization of *katA* from *Campylobacter jejuni* and generation of a catalase-deficient mutant of *Campylobacter coli* by interspecific allelic exchange. *Microbiology* **1995**, *141*, 1369–1376, doi:10.1099/13500872-141-6-1369.

61. Day, W. A.; Sajecki, J. L.; Pitts, T. M.; Joens, L. A.; Joens, L. A. Role of catalase in *Campylobacter jejuni* intracellular survival. *Infect. Immun.* **2000**, *68*, 6337–45.

62. Flint, A.; Sun, Y. Q.; Stintzi, A. Cj1386 is an ankyrin-containing protein involved in heme trafficking to catalase in *Campylobacter jejuni*. *J. Bacteriol.* **2012**, *194*, 334–345, doi:10.1128/JB.05740-11.

63. Holberger, L. E.; Garza-Sánchez, F.; Lamoureux, J.; Low, D. A.; Hayes, C. S. A novel family of toxin/antitoxin proteins in *Bacillus* species. *FEBS Lett.* **2012**, *586*, 132–6, doi:10.1016/j.febslet.2011.12.020.

64. Fernández, L.; Rodríguez, A.; García, P. Phage or foe: an insight into the impact of viral predation on microbial communities. *ISME J.* **2018**, doi:10.1038/s41396-018-0049-5.

65. Fernández, L.; González, S.; Campelo, A. B.; Martínez, B.; Rodríguez, A.; García, P. Low-level predation by lytic phage phiIPLA-RODI promotes biofilm formation and triggers the stringent response in *Staphylococcus aureus*. *Sci. Rep.* **2017**, *7*, 40965, doi:10.1038/srep40965.

66. Moreau, P.; Diggle, S. P.; Friman, V.-P. Bacterial cell-to-cell signaling promotes the evolution of resistance to parasitic bacteriophages. *Ecol. Evol.* **2017**, *7*, 1936–1941, doi:10.1002/ece3.2818.

67. Stahl, M.; Butcher, J.; Stintzi, A. Nutrient acquisition and metabolism by *Campylobacter jejuni*. *Front. Cell. Infect. Microbiol.* **2012**, *2*, 5, doi:10.3389/fcimb.2012.00005.

68. Gots, J. S.; Hunt, G. R. Amino acid requirements for the maturation of bacteriophage in lysogenic *Escherichia coli. J. Bacteriol.* **1953**, *66*, 3, 353-361.

69. Bryan, D.; El-Shibiny, A.; Hobbs, Z.; Porter, J.; Kutter, E. M. Bacteriophage T4 infection of stationary phase *E. coli*: Life after log from a phage perspective. *Front. Microbiol.* **2016**, *7*, doi:10.3389/fmicb.2016.01391.

70. Bartual, S. G.; Otero, J. M.; Garcia-Doval, C.; Llamas-Saiz, A. L.; Kahn, R.; Fox, G. C.; van Raaij, M. J. Structure of the bacteriophage T4 long tail fiber receptor-binding tip. *Proc. Nat. Acad. Sci.* **2010,** *107*, 20287-20292.

71. Bonnain, C.; Breitbart, M.; Buck, K. N. The Ferrojan horse hypothesis: iron-virus interactions in the ocean. *Front. Marine Sci.* **2016,** *3*, 82.

72. Dugar, G.; Herbig, A.; Förstner, K. U.; Heidrich, N.; Reinhardt, R.; Nieselt, K.; Sharma, C. M. High-Resolution Transcriptome Maps Reveal Strain-Specific Regulatory Features of Multiple *Campylobacter jejuni* Isolates. *PLoS Genet.* **2013**, *9*, e1003495, doi:10.1371/journal.pgen.1003495.

73. Louwen, R.; Horst-Kreft, D.; De Boer, A. G.; Van Der Graaf, L.; De Knegt, G.; Hamersma, M.; Heikema, A. P.; Timms, A. R.; Jacobs, B. C.; Wagenaar, J. A.; Endtz, H. P.; Van Der Oost, J.; Wells, J. M.; Nieuwenhuis, E. E. S.; Van Vliet, A. H. M.; Willemsen, P. T. J.; Van Baarlen, P.; Van Belkum, A. A novel link between *Campylobacter jejuni* bacteriophage defence, virulence and Guillain-Barre syndrome. *Eur. J. Clin. Microbiol. Infect. Dis.* **2013**, *32*, 207–226, doi:10.1007/s10096-012-1733-4.

74. Dugar, G.; Leenay, R. T.; Eisenbart, S. K.; Bischler, T.; Aul, B. U.; Beisel, C. L.; Sharma, C. M. CRISPR RNA-Dependent Binding and Cleavage of Endogenous RNAs by the *Campylobacter jejuni* Cas9. *Mol. Cell* **2018**, *69*, 893–905.e7, doi:10.1016/j.molcel.2018.01.032.

75. Li, R.; Fang, L.; Tan, S.; Yu, M.; Li, X.; He, S.; Wei, Y.; Li, G.; Jiang, J.; Wu, M. Type I CRISPR-Cas targets endogenous genes and regulates virulence to evade mammalian host immunity. *Cell Res.* **2016**, *26*, 1273–1287, doi:10.1038/cr.2016.135.

76. Strutt, S. C.; Torrez, R. M.; Kaya, E.; Negrete, O. A.; Doudna, J. A. RNA-dependent RNA targeting by CRISPR-Cas9. *Elife* **2018**, *7*, doi:10.7554/eLife.32724.

77. Sørensen, M. C. H.; van Alphen, L. B.; Fodor, C.; Crowley, S. M.; Christensen, B. B.; Szymanski, C. M.; Brøndsted, L. Phase Variable Expression of Capsular Polysaccharide Modifications Allows *Campylobacter jejuni* to Avoid Bacteriophage Infection in Chickens. *Front. Cell. Infect. Microbiol.* **2012**, *2*, doi:10.3389/fcimb.2012.00011.

78. Aidley, J.; Holst Sørensen, M. C.; Bayliss, C. D.; Brøndsted, L. Phage exposure causes dynamic shifts in the expression states of specific phase-variable genes of *Campylobacter jejuni*. *Microbiol. (United Kingdom)* **2017**, *163*, 911–919, doi:10.1099/mic.0.000470.

79. Gencay, Y. E.; Sørensen, M. C. H.; Wenzel, C. Q.; Szymanski, C. M.; Brøndsted, L. Phase Variable Expression of a Single Phage Receptor in *Campylobacter jejuni* NCTC12662 Influences Sensitivity Toward Several Diverse CPS-Dependent Phages. *Front. Microbiol.* **2018**, *9*, 82, doi:10.3389/fmicb.2018.00082.

80. Hyman, P.; Abedon, S. T. Bacteriophage host range and bacterial resistance. *Adv. Appl. Microbiol.* 2010, *70*, 217–248.

81. Chan, B. K.; Sistrom, M.; Wertz, J. E.; Kortright, K. E.; Narayan, D.; Turner, P. E. Phage selection restores antibiotic sensitivity in MDR *Pseudomonas aeruginosa*. *Sci. Rep.* **2016**, *6*, doi:10.1038/srep26717.

82. Wang, X.; Kim, Y.; Ma, Q.; Hong, S. H.; Pokusaeva, K.; Sturino, J. M.; Wood, T. K. Cryptic prophages help bacteria cope with adverse environments. *Nat. Commun.* **2010**, *1*, 147, doi:10.1038/ncomms1146.

83. Schuch, R.; Fischetti, V. A. Detailed genomic analysis of the Wbeta and gamma phages infecting *Bacillus anthracis*: implications for evolution of environmental fitness and antibiotic resistance. *J. Bacteriol.* **2006**, doi:10.1128/JB.188.8.3037-3051.2006.

84. Lu, M. J.; Henning, U. The immunity (imm) gene of *Escherichia coli* bacteriophage T4. *J. Virol.* **1989**, *63*, 3472–8.

85. Labrie, S. J.; Samson, J. E.; Moineau, S. Bacteriophage resistance mechanisms. *Nat. Rev. Microbiol.* 2010.

86. Fineran, P. C.; Blower, T. R.; Foulds, I. J.; Humphreys, D. P.; Lilley, K. S.; Salmond, G. P. C. The phage abortive infection system, ToxIN, functions as a protein-RNA toxin-antitoxin pair. *Proc. Natl. Acad. Sci. U. S. A.* **2009**, *106*, 894–9, doi:10.1073/pnas.0808832106.

87. Kaakoush, N. O.; Miller, W. G.; De Reuse, H.; Mendz, G. L. Oxygen requirement and tolerance of *Campylobacter jejuni. Res. Microbiol.* **2007**, *158*, 644–650, doi:10.1016/J.RESMIC.2007.07.009.

88. Woodall, C. A.; Jones, M. A.; Barrow, P. A.; Hinds, J.; Marsden, G. L.; Kelly, D. J.; Dorrell, N.; Wren, B. W.; Maskell, D. J. *Campylobacter jejuni* gene expression in the chick cecum: evidence for adaptation to a low-oxygen environment. *Infect. Immun.* **2005**, *73*, 5278–85, doi:10.1128/IAI.73.8.5278-5285.2005.

89. Gaynor, E. C.; Cawthraw, S.; Manning, G.; MacKichan, J. K.; Falkow, S.; Newell, D. G. The genome-sequenced variant of *Campylobacter jejuni* NCTC 11168 and the original clonal clinical isolate differ markedly in colonization, gene expression, and virulence-associated phenotypes. *J. Bacteriol.* **2004**, *186*, 503–17, doi:10.1128/JB.186.2.503-517.2004.

90. Ofir, G.; Melamed, S.; Sberro, H.; Mukamel, Z.; Silverman, S.; Yaakov, G.; Doron, S.; Sorek, R. DISARM is a widespread bacterial defence system with broad anti-phage activities. *Nat. Microbiol.* **2018**, *3*, 90–98, doi:10.1038/s41564-017-0051-0.

91. Howard-Varona, C.; Roux, S.; Dore, H.; Solonenko, N. E.; Holmfeldt, K.; Markillie, L. M.; Orr, G.; Sullivan, M. B. Regulation of infection efficiency in a globally abundant marine *Bacteriodetes* virus. *ISME J.* **2017**, doi:10.1038/ismej.2016.81.

Chapter 3: Gp047, a Flagellar Glycan-Specific Protein Encoded by *Campylobacter* Phages, Inhibits Host Cell Growth

A version of this chapter was published as:

Javed, M. A.; Sacher, J. C.; van Alphen, L. B.; Patry, R. T.; Szymanski, C. M. A Flagellar glycan-specific protein encoded by *Campylobacter* phages inhibits host cell growth. *Viruses* **2015,** *7*, 6661–6674, doi:10.3390/v7122964.

Abstract

We previously characterized a carbohydrate binding protein, Gp047, derived from lytic *Campylobacter* phage NCTC 12673, as a promising diagnostic tool for the identification of *Campylobacter jejuni* and *Campylobacter coli*. We also demonstrated that this protein binds specifically to acetamidino-modified pseudaminic acid residues on host flagella, but the role of this protein in the phage lifecycle remains unknown. Here, we report that Gp047 is capable of inhibiting *C. jejuni* growth both on solid and liquid media, an activity which we found to be bacteriostatic. The Gp047 domain responsible for bacterial growth inhibition is localized to the C-terminal quarter of the protein, and this activity is both contact- and dose-dependent. Gp047 gene homologues are present in all *Campylobacter* phages sequenced to date, and the resulting protein is not part of the phage particle. Therefore, these results suggest that either phages of this pathogen have evolved an effector protein capable of host-specific growth inhibition, or that *Campylobacter* cells have developed a mechanism of regulating their growth upon sensing an impending phage threat.

3.1. Introduction

Bacteriophages (phages) are specific for their hosts, and this specificity is largely directed by their receptor binding proteins (RBPs). Infection of bacteria by lytic phages results in the lysis of host cells, providing an effective means to control bacterial pathogens in the environment and to treat bacterial infections. With the rise in antibiotic resistance among bacterial pathogens, possibilities of exploiting phages for pathogen control are being explored in many research laboratories worldwide. For instance, phages have been shown to reduce *Campylobacter* load

from chicken flocks [1,2], and to effectively treat *Mycobacterium ulcerans* infection in a mouse footpad model [3]. Although phage therapy continues to show promise, the use of whole phage particles to treat infections has been hampered due to the possible spread of virulence-associated genes among bacterial pathogens through phage transduction. For this reason and others, the use of phage-derived proteins offers a suitable alternative to whole phage with no risk of genetic exchange between pathogens.

A commonly studied example of a phage-derived RBP that has been tested for its therapeutic potential is the *Salmonella enterica* serovar Typhimurium P22 phage RBP, Gp9, which binds and cleaves the repeating α-D-mannose-(1,4)-α-L-rhamnose-(1,3)-α-D-galactose *O*-antigen of *Salmonella* lipopolysaccharide (LPS) [4,5,6]. We have previously shown that the phage P22 RBP reduces bacterial motility and can be used to effectively reduce *Salmonella* load in chickens [7]. It has also been reported that the phage AF can degrade *Pseudomonas putida* biofilms, an ability conferred by the RBP of the phage [8]. In addition, phage RBPs have been used to effectively target bacterial killing molecules to specific bacterial cells, such as *Escherichia coli* O157:H7 [9] and *Clostridium difficile* [10]. In addition to phage RBPs, other phage proteins such as endolysins, which break down the peptidoglycan of specific hosts, are also being successfully exploited as therapeutics [11,12]. Overall, phage proteins represent a vast reservoir of exploitable proteins for therapeutic and diagnostic applications [13], particularly as they tend to display high affinities for glycan-specific targets. This property makes them excellent candidates for targeting bacteria, which tend to be extensively adorned with carbohydrates (for a recent review on the diversity of glycan-binding proteins encoded by phages, please see Simpson *et al.* [14]).

Previously, in order to explore diagnostic and therapeutic applications against *Campylobacter jejuni* and *Campylobacter coli*, which are major causative agents of foodborne illness worldwide, our group sequenced the genome of a lytic *Campylobacter* phage, NCTC 12673. We identified a putative RBP in its genome, Gp047, based on similarities in size and synteny to RBPs of other characterized phages in the family *Myoviridae* [15]. Recombinant glutathione-*S*-transferase (GST)-fused Gp047 expressed in *E. coli* was found to form sodium dodecyl sulfate (SDS)-resistant multimers, similarly to the P22 phage tailspike protein (TSP), and anti-Gp047 antibodies raised in rabbits were found to cross-react with *Salmonella* phage P22 TSP trimers [15]. However, these antibodies did not bind to the NCTC 12673 phage particle [16], and Gp047 was not detected upon proteomic analysis by mass spectrometry of purified phage virions [15]. Together, these results indicate that Gp047 is not a structural component of the phage particle. Furthermore, although the NCTC 12673 phage has been shown to recognize capsular polysaccharides (CPS) on its target host cells [17], we found that Gp047 recognizes acetamidino-modified pseudaminic acid on host flagella, agglutinating cells and reducing their motility upon binding [16]. Interestingly, Gp047 also shows a broader host recognition range compared to the phage from which it was derived [18]. For these reasons, we have hypothesized that Gp047 is unlikely to be an RBP of this phage, and may instead function as an effector protein in the phage lifecycle (Table 3-1).

Regardless of its identity, we have shown that Gp047 can be immobilized onto solid surfaces and will specifically capture *C. jejuni* and *C. coli*, two pathogens routinely associated with campylobacteriosis [19]. The Gp047 binding activity is localized in the C-terminal quarter of the

protein (CC-Gp047) [18], and this domain can be exploited in assays for the simultaneous detection of these two pathogens [13,18,19] and for the separation/enrichment of campylobacters from complex food samples [20].

Due to the unusual nature of this protein's glycan binding properties paired with the fact that all *Campylobacter* phages sequenced to date express a homologue of this protein, we speculated that the conserved nature of this protein indicates an important role in the phage lifecycle. We hypothesized that Gp047 may function as an extracellular effector that is released upon phage-induced cell lysis where it binds and reduces the motility of nearby cells, thus providing an advantage to newly released phages attempting to attach to their characteristically highly motile hosts. An alternative hypothesis is that Gp047 acts intracellularly during phage infection by binding to flagellar glycans preventing filament assembly, perhaps as a means of diverting resources from energetically costly flagella toward phage replication.

Table 3-1. Summary of Gp047 properties characterized to date.

Property	**Reference**
Binds to *C. jejuni* and *C. coli* flagella	[16]
Recognizes acetamidino-modified pseudaminic acid residues	[16]
Binding activity localized to C-terminal quarter of the protein	[16]
Agglutinates host bacterial cells	[16,18]
Forms multimers	[15]
Reduces host bacterial motility	[16]
Not identified as a component of the structural phage proteome	[15]
C-terminal homologues encoded by all sequenced *Campylobacter* phages	[21,22]

Effectively captures *C. jejuni* and *C. coli* from complex samples	[20]
Inhibits host bacterial growth	This study
Growth inhibition domain localized to C-terminal quarter	This study
Expression of Gp047 in *C. jejuni* 11168 cells does not affect flagellar phenotype, cell morphology or growth	This study

Here, we report the observation that Gp047 causes bacterial clearance when spotted onto a growing lawn of host cells suspended in agar, and inhibits cell proliferation when added to cells in broth culture. Our observations suggest that zones of observed growth clearance following spotting of phage protein are not necessarily linked to enzymatic degradation of cell surface polysaccharides, as previously reported for other phage proteins, but may instead be the result of bacterial growth inhibition in response to Gp047 binding to their flagella. We also present data suggesting that Gp047 does not affect flagellar assembly when expressed in *C. jejuni* cells. Overall, we have observed that the effect of Gp047 on *C. jejuni* cells appears to involve an extracellular interaction with host cells.

3.3. Materials and methods

3.3.1. Bacterial Growth Conditions

C. jejuni and *C. coli* strains were grown on Mueller Hinton (MH) agar (Difco, Franklin Lakes, NJ, USA) at 37 °C under microaerobic conditions (85% N_2, 10% CO_2, and 5% O_2). E. coli strains were grown on LB agar supplemented with ampicillin, kanamycin or chloramphenicol at a final concentration of 100, 50 or 20 μg/mL, respectively, where needed. The list and sources

of bacterial strains used in this study are given in Table 3-2, whereas plasmids are listed in Table 3-3.

Table 3-2. List of bacterial strains and mutants used in this study.

Strain	Description	Reference
C. jejuni 11168	Human isolate	[23]
C. jejuni 81-176	Clinical isolate	[24]
11168Δ*kpsM*	Acapsular, *kpsM* mutant in *C. jejuni* 11168	[25]
11168Δ*pseG*	Aflagellate, *pseG* (*cj1312*) mutant in *C. jejuni* NCTC 11168	This study
81-176Δ*pseA*	*pseA* (*cj1316c*) mutant in *C. jejuni* 81-176 (flagellate, no acetamidino modification)	[26]
11168Δ*pseA*	*pseA* mutant in *C. jejuni* NCTC 11168	[16]
11168Δ*pseA*:*pseA*	11168Δ*pseA* mutant chromosomally complemented with wild type *pseA*	[16]
111-28 (pCE111-28/*gp047*)	11168 expressing *gp047* on the pCE 111-28 plasmid	This study
11168 (pCE111-28)	11168 expressing empty pCE 111-28 plasmid	This study

Table 3-3. List of plasmids used in this study.

Plasmid	Description	Source or Reference
pGEX 6P-2	Glutathione-S-transferase (GST) fused protein expression vector, ampicillin resistance marker, *tac* promoter	GE Healthcare
pCE 111-28	*Campylobacter-E. coli* shuttle vector for protein expression, chloramphenicol resistance marker, plasmid pRY111 with σ28 promoter of *flaA*	[27]
pGEX_*gp047*	*gp047* cloned in-frame into multiple cloning site of pGEX 6P-2 for expression of GST-fused Gp047	[15]
pGEX_*ntgp047*	Expression construct of GST-fused N-Gp047 in pGEX 6P-2	[18]
pGEX_*ctgp047*	Expression construct of GST-fused C-Gp047 in pGEX 6P-2	[18]
pGEX_*ccgp047*	Expression construct of GST-fused CC-Gp047 in pGEX 6P-2	[18]
pGEX_*ncgp047*	Expression construct of GST-fused NC-Gp047 in pGEX 6P-2	[18]
pCE_*gp047*	Expression construct of untagged Gp047 for expression in pCE 111-28 in *C. jejuni*	This study

3.3.2. Construction of a *pseG* Mutant in *C. jejuni* 11168

A *pseG* mutation in 11168 was generated by transferring this mutation from *C. jejuni* 81-176, where the *pseG* gene was inactivated by transposon insertion [28]. The DNA fragment carrying the *pseG* mutation was amplified from 81-176Δ*pseG* by PCR with primers CS1031 (5′-CTACAACATCAAAATTTTTAGCAATATATTC-3′) and CS1032 (5′-CTTTAACTATAGGTGGCGGGATAA-3′) using Platinum® Taq high fidelity DNA polymerase (Invitrogen, Carlsbad, CA, USA). PCR products were purified using the MinElute® PCR purification kit (Qiagen, Hilden, Germany) according to the manufacturer's protocol. *C. jejuni* 11168 cells were transformed with the PCR product by natural transformation and colonies were selected on MH agar supplemented with chloramphenicol (15 μg per mL). Mutant colonies were confirmed by PCR.

3.3.3. Expression of Gp047 and Its Derivatives

DNA fragments encoding for Gp047 and its truncated versions were cloned into the pGEX 6P-2 vector, expressed in *E. coli* BL21 as GST-fused proteins, and purified as described previously [15,16,18], with the exception that where indicated, Gp047 was used in the GST-column's elution buffer (10 mM reduced L-glutathione, 50 mM Tris, 1 mM DTT at pH 9.0) without first dialyzing into PBS.

For expression in *C. jejuni* cells, the *gp047* gene was amplified from the phage NCTC 12673 genome using Vent polymerase (New England Biolabs, Ipswich, MA, USA) with primers (5′-ATCTCGAGAAGAAGGAGTGTTATGATAGAACCAAAAAGAGAACCTACACAAG-3′)

and (5′-
ATGGTACCTTAATTTATATTGAACGCATATATATAAGAACTATCGTTTGTTTC-3′)
containing a *Xho*I or a *Kpn*I restriction site (underlined), respectively. The PCR product was purified and ligated into *Xho*I/*Kpn*I-digested pCE 111-28. *C. jejuni* 11168 cells were transformed with the resultant construct by natural transformation, and colonies were selected on MH agar supplemented with chloramphenicol (15 μg per mL). Colonies containing the pCE 111-28/*gp047* construct were confirmed by restriction digest of purified plasmid DNA and by sequencing.

3.3.4. Agar Plate Growth Clearance Assay

Clearance of bacterial growth was tested by spotting phage protein onto a freshly inoculated bacterial suspension using a standard overlay agar method as described for phage plaque assays. Overnight bacterial growth was harvested in brain heart infusion broth supplemented with 1 mM $CaCl_2$ and 10 mM $MgSO_4$ (final concentration) and set to an OD_{600} of 0.35. A 3-mL aliquot of this suspension was transferred to a 35 × 10 mm polystyrene dish (Corning Inc., Corning, New York, NY, USA) and incubated at 37 °C for 4 h under microaerobic conditions. Then, 100 μL of this suspension was mixed with 5 mL sterile 0.6% molten NZCYM agar (Difco, Franklin Lakes, NJ, USA) cooled to 45 °C. This suspension was poured onto the surface of a previously solidified, pre-warmed NZCYM or MH agar plate containing 1.5% agar. Plates were allowed to solidify for 15 min and then 5–10 μL phage suspension (10^8 PFU/mL) or sterile protein solution (0.91–1.3 mg/mL) of Gp047, its derivatives or Gp069, a hypothetical protein from phage NCTC 12673 (dissolved in PBS or 10 mM reduced L-glutathione, 50 mM Tris, 1 mM DTT, pH 9.0) was spotted onto the agar surface and allowed to completely soak into the agar. Culture plates

were incubated at 37 °C under microaerobic conditions and zones of growth clearance were observed after 18–24 h.

3.3.5. Scanning Electron Microscopy

Spot assays were performed as described above by spotting 5 µL fresh full-length Gp047 in PBS at 0.91 mg/mL. Following overnight growth of lawns, agar squares were excised using a sterile scalpel from either inside, outside or at the interface of the clearance zone. Slabs were then trimmed to leave the top layer (approximately 2 mm) intact and incubated in scanning electron microscopy (SEM) fixative (2.5% glutaraldehyde; 2% paraformaldehyde in 0.1 M phosphate buffer) overnight at 4 °C. Slabs were then prepared for microscopy using methods described by Bozzola and Russell [29]. Briefly, slabs were washed three times in 0.1 M phosphate buffer for 10 min each and then dehydrated by incubating 15 min each in a series of alternating ethanol and hexamethyldisialazane (HMDS) washes. The washes were done as follows: 50% ethanol, 70% ethanol, 90% ethanol, 100% ethanol, ethanol:HMDS 75:25, ethanol:HMDS 50:50, ethanol:HMDS 25:75 and 100% HMDS. Slabs were incubated in just enough HMDS to cover the slab surface, which was left to evaporate overnight. Once fully dried, slabs were mounted onto SEM stubs, sputter-coated with gold using the Hummer sputtering system (Anatech Ltd., Battle Creek, MI, USA) and imaged using the Philips/FEI (XL30) scanning electron microscope (Philips/FEI, Hillsboro, OR, USA) with an electron beam energy of 20 kV.

3.3.6. Liquid Growth Assays

Cells were harvested from overnight MH plate cultures and set to an OD_{600} of 0.03 (approximately 10^8 colony forming units (CFU)/mL) in MH broth. To each well of a 96-well

Nunclon flat bottom plate, 275 µL of this suspension and 25 µL of either Gp047 (0.91 mg/mL) or buffer (10 mM reduced L-glutathione, 50 mM Tris-HCl, 1 mM DTT, pH 9.0) was added. Cultures were set up in triplicate, and OD_{600} measurements were taken using a plate reader at 0, 0.75, 4, 9, 13, 24 and 30 h. Colony counts were done by serially diluting 10 µL aliquots of cell suspension into MH, plating onto pre-dried MH plates and incubating 48 h until single colonies were observed.

3.3.7. Western Blotting

In order to detect Gp047 protein expression in *C. jejuni* 11168, cells transformed with pCE 111-28/*gp047* were grown on MH agar containing 15 µg/mL chloramphenicol. Whole cell lysates were then examined by Western blotting using Gp047-specific polyclonal antisera. Growth from 1 plate per strain was harvested in PBS, frozen, thawed in the presence of 1x Protease Inhibitor Cocktail (Roche, Basel, Switzerland), and sonicated 4 × 30 s. Supernatants were collected, boiled 10 min in the presence of SDS loading buffer and run on a 12% SDS-polyacrylamide gel electrophoresis (PAGE) gel (120 V, 1.5 h). Gels were transferred to polyvinylidene fluoride (PVDF) (30 V, room temperature, 14 h), blocked with 5% skim milk/PBST 1 h, probed with polyclonal anti-Gp047 antibodies (1:4000) 1 h, washed 3 × 5 min in PBST, probed with goat anti-rabbit-AP antibodies (1:10,000) for 1 h, and developed with nitro-blue tetrazolium chloride (NBT)/ 5-bromo-4-chloro-3'-indolylphosphate (BCIP) until bands were visible.

3.3.8. Immunogold Labeling and Transmission Electron Microscopy

C. jejuni cells were harvested from a plate of overnight growth in MH broth and set to an OD_{600} of 0.5. Immunogold labeling and transmission electron microscopy was done as described

previously [16] with some exceptions. Briefly, Formvar-coated copper grids were floated on drops of the bacterial cell suspensions for 1 h. The grids were washed 3 × 5 min each with blocking solution (PBS containing 5% bovine serum albumin and 0.05% Tween), then blocked with the same solution for 1 h at room temperature (RT) or overnight at 4 °C. The grids were then floated on drops of freshly purified full-length Gp047 (0.91 mg/mL diluted 1:10 in blocking solution) for 1 h at RT or overnight at 4 °C. The grids were washed as above, then floated on rabbit anti-Gp047 antibody solution [15] (diluted 1:200 in blocking solution) for 1 h at RT. After washing again as above, the grids were then floated on goat anti-rabbit IgG (whole molecule) conjugated to 10-nm gold particles (BB International), diluted 1:200 in blocking solution, for 1 h at RT. The grids were then washed 3 × 5 min with blocking solution, 5× with PBS, 5× with distilled water and then air-dried on Whatman filter paper. The grids were examined using a transmission electron microscope (Philips Morgagni 268; FEI Company, Hillsboro, OR, USA). Images were captured with a charge-coupled device camera and controller (Gatan, Pleasanton, CA, USA) and processed using DigitalMicrograph (Gatan, Pleasanton, CA, USA).

3.4. Results

3.4.1. Gp047 Causes Capsular Polysaccharide-Independent Clearance of *C. jejuni* Growth

When spotted on a growing lawn of *C. jejuni* 11168 in semi-solid medium, recombinant Gp047 caused a hazy zone of growth clearance similar to, yet less complete than, clearing caused by the whole phage NCTC 12673 from which Gp047 was derived (Figure 3-1). Another protein of

unknown function (Gp069) originating from the same phage and purified in the same manner using a GST-tag does not cause a zone of clearance, suggesting that Gp047 is the causative agent of *C. jejuni* growth clearance (Figure 3-1A). To further confirm this Gp047-related phenotype, the protein was treated with proteinase K before spotting onto the lawn of growth, which resulted in the absence of a zone of clearance (Figure 3-1B). Previous reports have suggested that incomplete or hazy bacterial growth clearance observed as a halo around some phage plaques is caused by polysaccharide hydrolysis by phage proteins [8]. It has been shown that NCTC 12673 phage recognizes *C. jejuni* CPS [17], so we tested a CPS mutant, 11168Δ*kpsM,* for susceptibility to Gp047-induced growth clearance. As expected, whole NCTC 12673 phage did not form plaques, however, Gp047 was able to cause a zone of clearance on 11168Δ*kpsM* (Figure 3-1C). These results demonstrate that the growth clearing activity by Gp047 is not a result of CPS hydrolysis as it occurs independently of the presence of CPS.

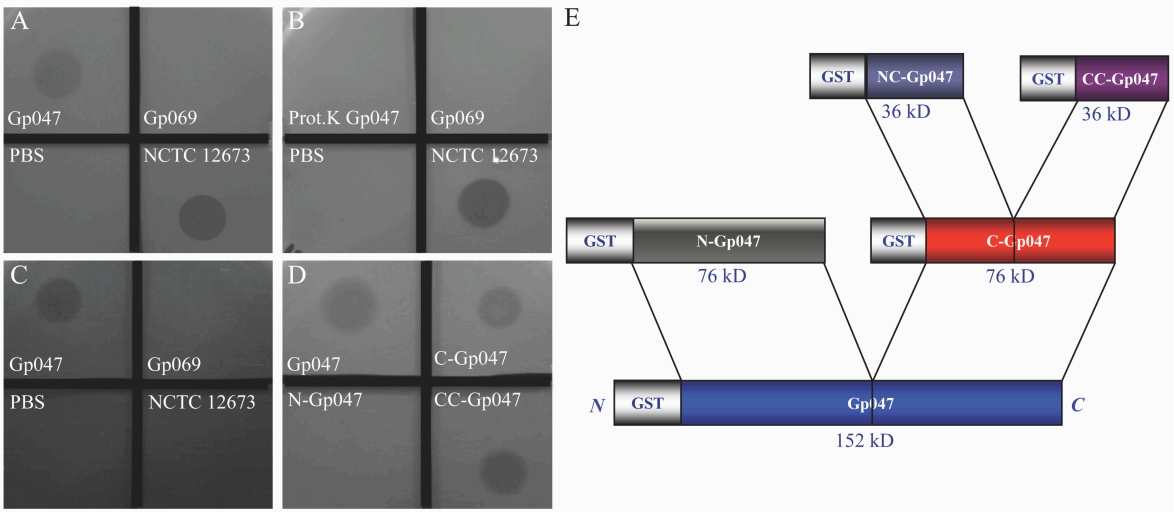

Figure 3-1. *C. jejuni* growth clearance assays. GST-Gp047 and phage NCTC 12673 showed growth clearance of *C. jejuni* 11168 wild type when spotted on the lawn of growth, whereas PBS and GST-Gp069 did not show this phenotype (A); Growth clearance activity of Gp047 was

abolished when the protein was pre-treated with proteinase K before spotting onto a lawn of wild type 11168 growth (B); Gp047 was able to cause growth clearance of the CPS mutant 11168Δ*kpsM*, whereas phage NCTC 12673 was not able to cause lysis of the mutant (C); Similar to the full-length Gp047, truncated derivatives C-Gp047 and CC-Gp047 also caused growth clearance of wild type 11168 cells, whereas N-Gp047 did not (D); A schematic of Gp047 derivatives expressed as GST-fused proteins in pGEX-6P2 as described previously [18] is shown for reference (E).

3.4.2. Growth Clearance-Associated Domain is Localized in the C-Terminal Quarter of Gp047

We previously expressed different lengths of recombinant Gp047 fused with GST (schematic diagram shown in Figure 3-1E), and found that the binding domain of Gp047 is localized in the C-terminal quarter of the protein (CC-Gp047) [18]. Here, we tested these different truncations of Gp047 for their ability to cause *C. jejuni* growth clearance, and found that the growth clearance-associated domain is also localized in the C-terminal quarter, CC-Gp047 (Figure 3-1D).

3.4.3. Clearance Phenotype of Gp047 Is Contact- and Dose-Dependent

We previously performed protein affinity chromatography and different binding assays on several *C. jejuni* mutants and found that Gp047 binds to bacterial host flagella through recognition of acetamidino-modified pseudaminic acid residues on flagellin subunits [16]. To test whether binding of Gp047 to bacterial flagella was important for growth clearance activity of this protein, we tested the clearance activity of CC-Gp047 on a lawn of *C. jejuni*

11168Δ*pseG.* This strain has a mutation in an essential enzyme of the pseudaminic acid biosynthesis pathway, which is required for proper flagellar assembly. This mutation therefore results in aflagellate and non-motile bacterial cells [28]. CC-Gp047 did not show growth clearance of 11168Δ*pseG* (Figure 3-2A).

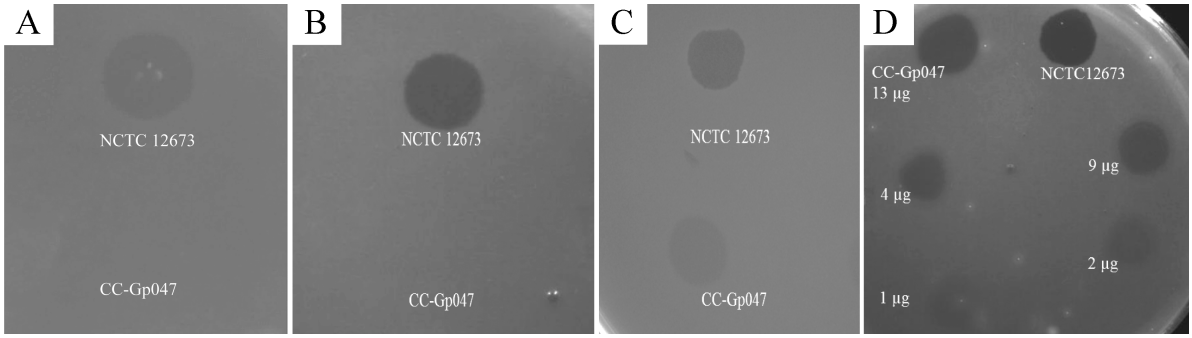

Figure 3-2. CC-Gp047 did not clear growth of the aflagellate mutant 11168Δ*pseG* (A); Growth clearance was also not observed when CC-Gp047 was spotted onto the acetamidino-mutant 11168Δ*pseA* (B); Growth clearance was restored when 11168Δ*pseA* was complemented with a wild type copy of the *pseA* gene (C); (D) CC-Gp047 showed a dose dependent growth clearance when different concentrations (13, 9, 4, 2 and 1 µg) were spotted onto a growing *C. jejuni* lawn.

To verify whether motility or the presence of the flagellar filament was important for the growth clearance activity, we tested 11168Δ*pseA,* a motile strain with flagella displaying pseudaminic acid without the acetamidino modification required for Gp047 binding [16,28]. Here we found that growth of 11168Δ*pseA* was not cleared by CC-Gp047 (Figure 3-2B). Since decoration of *C. jejuni* flagellar filaments with acetamidino-modified pseudaminic acid is required for Gp047 binding, loss of growth clearance by CC-Gp047 in *C. jejuni* 11168Δ*pseA* suggests that growth clearance by Gp047 is contact-dependent. Complementation of 11168Δ*pseA* with a wild type copy of the *pseA* gene [16] restored growth clearance by Gp047 (Figure 3-2C), confirming the

presence of the Gp047 receptor on bacterial flagella to be crucial for the growth clearance activity of the protein.

To find out whether the clearance potential of Gp047 was dose dependent, we spotted varying concentrations of CC-Gp047 onto the *C. jejuni* plates. The zones of clearance showed increasing intensity as the concentration of CC-Gp047 was increased (Figure 3-2D), indicating a dose-dependent response.

3.4.4. Zones of Clearance Observed Using Electron Microscopy Show an Altered Growth Pattern

In order to visualize growth architecture of campylobacters growing within the observed zones of clearance on agar plates, we developed a method to visualize the cells by directly analyzing excised agar slabs by SEM. Agar slabs taken from the interface between clearance zones and outside growth showed a sharp contrast at the interface with a noticeable drop in cell density where protein was spotted (Figure 3-3A,B). We observed a smooth, uniform lawn in the absence of Gp047 (Figure 3-3C), but in the presence of the protein, *C. jejuni* cells were grouped in spherical ultrastructures visible even at low magnification (Figure 3-3E). Individual cell morphology appeared to be unchanged inside and outside the Gp047 zone (Figure 3-3D,F). For consistency, the images in Figures 3B–F were taken from the same agar slab, however this effect was observed in four replicate experiments. These results provide evidence that Gp047 is bacteriostatic, not lytic, since the cells remaining following treatment were normal in morphology, and no presence of lysed cells or debris was observed.

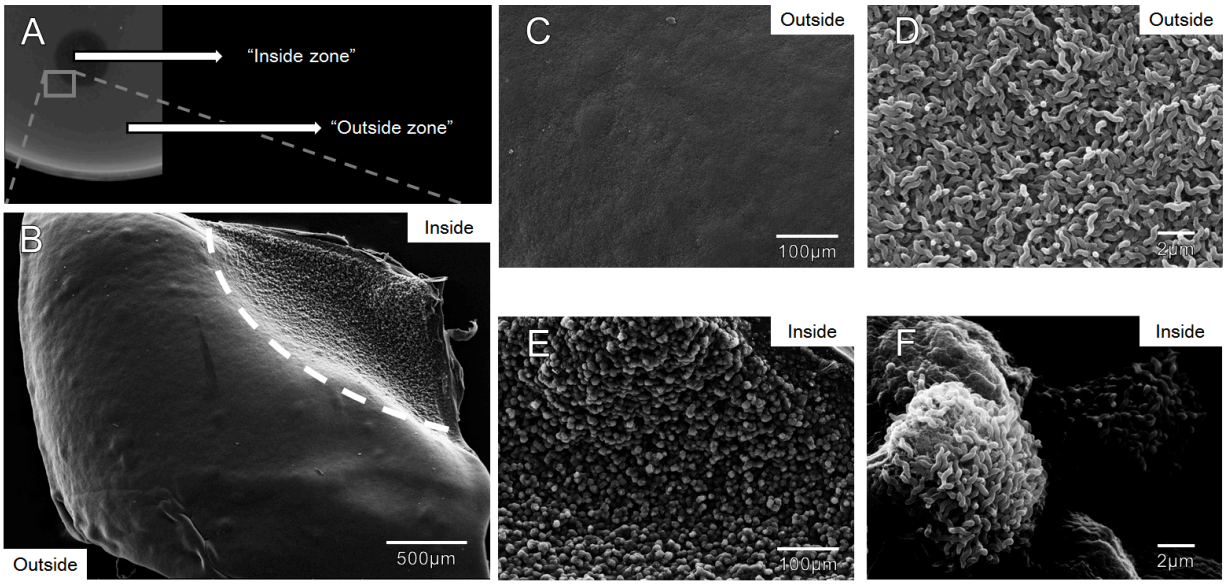

Figure 3-3. Scanning electron micrographs depicting *C. jejuni* 11168 growth in molten NZCYM agar at the interface where purified full-length Gp047 (0.9 mg/mL) was spotted. (A) An image of an excised agar slab where Gp047 was spotted on *C. jejuni* 11168 and the resulting clearance effect observed after 24 h (the grey box shows where the agar slab was excised); (B) A low magnification image highlighting the difference in topology between areas exposed to Gp047 (upper right corner) and those that were not exposed (remainder of the square), separated by a dotted white line; (C and D) Increasingly magnified images of bacterial growth outside the Gp047 spot showing a uniform lawn of *C. jejuni*; (E and F) Increasingly magnified images of the Gp047-exposed region of the agar plate showing spherical ultrastructures of *C. jejuni*. Images are representative of four replicate experiments.

3.4.5. Gp047 Addition to Broth Cultures Inhibits Cell Growth

To verify whether the observed Gp047-induced clearing of *C. jejuni* lawns on agar plates was a result of growth inhibition, we added GST-purified full-length (FL)-Gp047 to MH broth inoculated with approximately 10^8 CFU/mL of *C. jejuni* and proceeded to measure growth by

OD_{600} and by plate counting over the course of 26 h. We found that in comparison to the buffer control, the presence of Gp047 resulted in cell growth inhibition as indicated by OD_{600} measurements and plate counts (Figure 3-4). At $t = 23$ h, control cultures (glutathione elution buffer added in place of Gp047) had grown from an initial concentration of $(3.71 \pm 0.03) \times 10^8$ CFU/mL to $(1.96 \pm 0.42) \times 10^9$ CFU/mL. In contrast, the cell concentration in Gp047-containing cultures remained nearly constant over this time frame, going from $(1.22 \pm 0.03) \times 10^8$ CFU/mL at $t = 0$ to $(1.50 \pm 0.23) \times 10^8$ CFU/mL at $t = 23$ h. These results suggest that cells are not being killed or lysed by the presence of Gp047, but that the protein inhibits their growth resulting in a bacteriostatic effect.

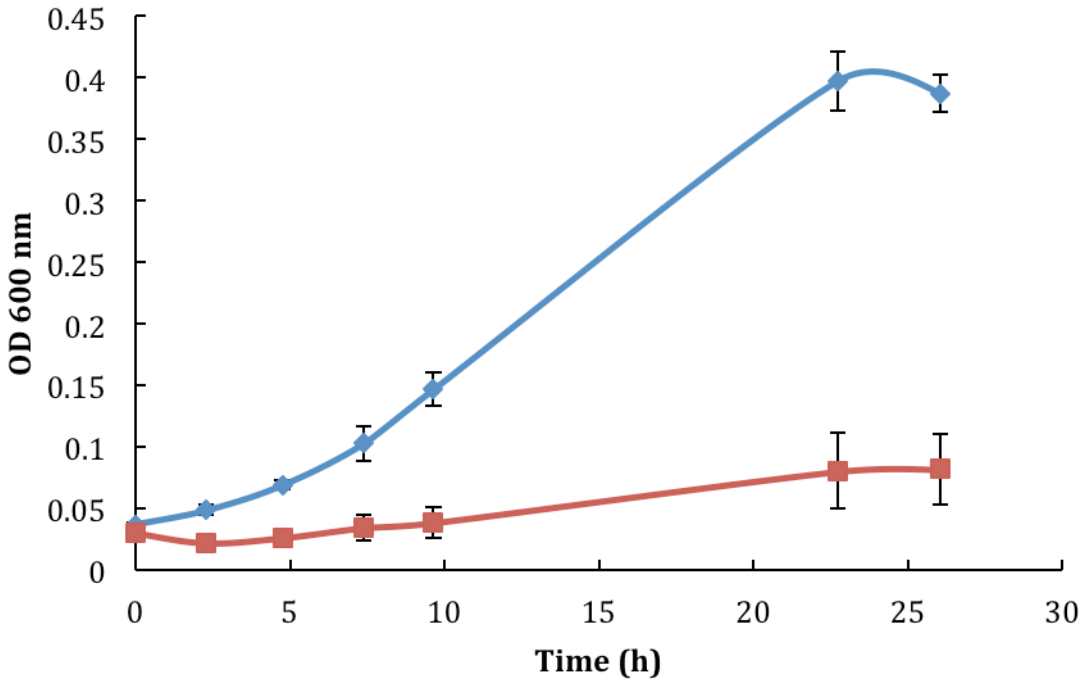

Figure 3-4. Full-length Gp047 added exogenously to *C. jejuni* 11168 broth cultures inhibits cell growth. GST-Gp047 (75 µg/mL final concentration) was added to cells suspended in MH broth and grown at 37 °C under microaerobic conditions. The blue line represents *C. jejuni* growth

with glutathione elution buffer added in place of Gp047, whereas the red line represents *C. jejuni* growth in the presence of Gp047. Error bars represent the standard error calculated from three technical replicates.

3.4.6. Gp047 Expressed in *C. jejuni* Cells Does Not Affect the Flagellar Phenotype

To test the hypothesis that the role of Gp047 in the phage lifecycle is to disrupt the *C. jejuni* flagellar assembly process through sequestration of flagellar glycans within the cytoplasm, we cloned full-length *gp047* and transformed it into *C. jejuni* 11168 cells. Western blotting confirmed that Gp047 was expressed in the resultant cells (Figure 3-5). However, upon analysis by immunogold labeling of Gp047 binding to its flagellar glycan receptor, we found no difference between flagellar labeling of Gp047-expressing cells and the corresponding empty vector control (Figure 3-6). We also did not observe any change in flagellar or cell morphology as a result of endogenous expression of Gp047 (Figure 3-6), nor did the Gp047-expressing strain grow differently than the empty vector control (results not shown).

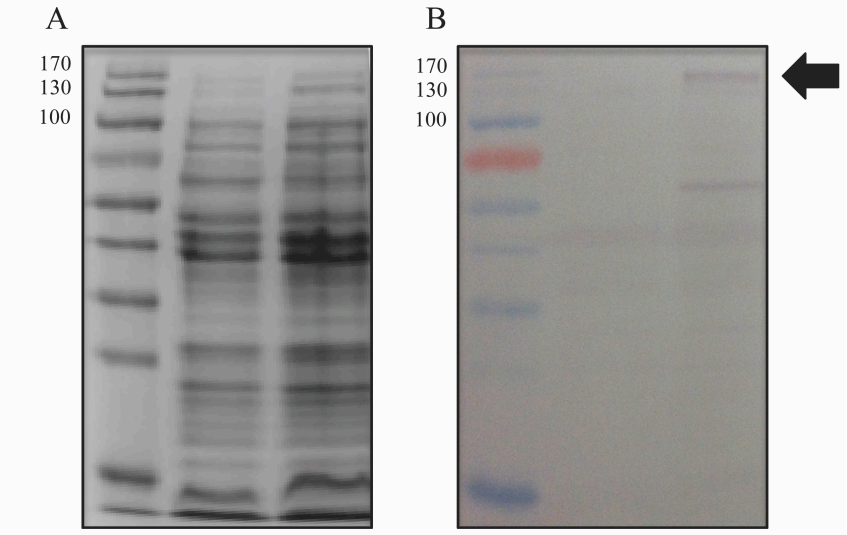

Figure 3-5. Gp047 can be expressed in *C. jejuni* 11168 cells. Gp047 was expressed in 11168 cells on the pCE 111-28 plasmid and cell lysates of wild type 11168 cells (lanes 1, 3) and 11168/pCE_*gp047* (lanes 2, 4) were subjected to SDS-PAGE stained with Coomassie; (A) or transferred to a Western blot and detected with anti-Gp047 antibodies; (B) The arrow indicates the expected size for full-length Gp047 (152 kDa).

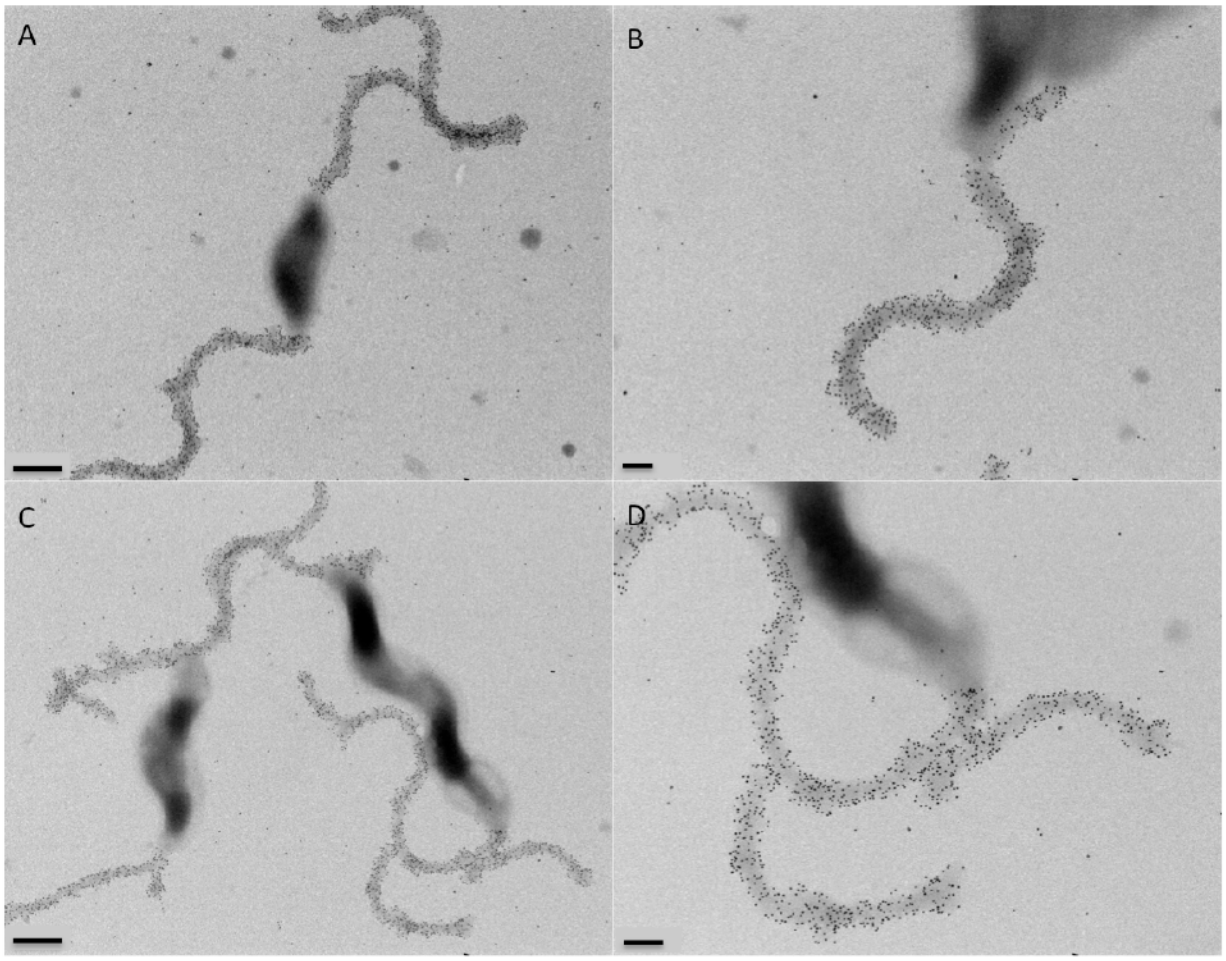

Figure 3-6. Internal Gp047 expression did not influence binding of externally added Gp047 to *C. jejuni* cells. Gp047-expressing (C,D) and empty pCE 111-28-expressing (A,B) *C. jejuni* cells display comparable levels of binding by exogenous Gp047, as shown by anti-Gp047 immunogold labeling. Scale bars represent 500 nm in (A,C) and 200 nm in (B,D).

3.5. Discussion

We recently demonstrated that the *C. jejuni* phage NCTC 12673 binds specifically to acetamidino-modified pseudaminic acid residues displayed on the flagella of most *C. jejuni* and *C. coli* isolates [16]. Furthermore, we have shown that homologues of this protein exist in all sequenced campylobacter phages and that homologues that we tested are also capable of binding to the same sugar residues [16]. These observations were notable considering that many *C. jejuni* phages, including NCTC 12673, recognize the phase-variable capsular polysaccharides and exhibit limited host ranges with high rates of resistance development [17,30]. In addition, it is well known that the 9-carbon sugar known as pseudaminic acid is essential for flagellar filament assembly and thus for bacterial motility and virulence. These observations led us to believe that Gp047 plays an important auxiliary role in the phage lifecycle as opposed to representing an RBP, as was previously thought [15,16].

Interestingly, we found that this protein caused a zone of clearance on agar plates containing *C. jejuni*, which at first glance appeared similar to published reports of surface polysaccharide depolymerization observed previously for other phage proteins. This type of clearing, which can present as a "halo" around phage plaques or as a zone of incomplete clearing on susceptible cell lawns, was directly demonstrated in one case to be caused by Gp19, an exopolysaccharide-degrading RBP from *P. putida* phage AF [8]. However, whereas we have shown here that Gp047-mediated growth clearance is contact- and dose-dependent, depending on the same C-terminal quarter that is essential for flagellar binding, the fact that the receptor for Gp047 is a

sugar monosaccharide on a glycoprotein, paired with our observation that Gp047 clears acapsular mutant cells, suggests a polysaccharide depolymerization-independent mechanism of action.

We tested the possibility that Gp047 could have an intracellular role in *C. jejuni* during phage infection. However, *C. jejuni* cells constitutively expressing Gp047 did not display an altered flagellar morphology or show an obvious difference in the levels of acetamidino-modified pseudaminic acid displayed on their filaments, suggesting that this protein solely has an extracellular role during the phage lifecycle.

We therefore employed a novel SEM-based method to directly observe *C. jejuni* cells on agar at the interface between the Gp047-induced zones of clearance in order to better analyze the effect of this protein on bacterial growth architecture. By excising agar slabs containing cells exposed to Gp047, we were able to see that cells were still present in the clearance zone, but that the smooth, thick layers of cells observed in the absence of treatment appeared disrupted in the presence of the protein. Instead, the remaining cells displayed an altered topology, composed of large, spherical groups of cells surrounded by deep gouges of space in between. We speculate that the first cells to come into direct contact with Gp047 would likely adsorb (and sequester) the protein upon its binding to the flagella (see Figure 3-6 for an illustration of the abundant binding capacity of Gp047 to a single flagellum, as evidenced by the presence of numerous black dots along the length of each filament). From this, we hypothesize that Gp047 might be inhibiting the growth of cells it is able to access as it descends into the bacterial layers, but that many cells would be protected from this activity and may still be able to grow and divide within discrete Gp047-free microenvironments. Whereas this is one possible explanation for the altered

phenotype observed by SEM as a result of Gp047 application, further research is required to unambiguously determine how Gp047 is causing this phenotype.

We have also observed that Gp047 is capable of inhibiting *C. jejuni* growth in broth culture and that cell counts do not decrease as a result of Gp047 addition to cultures but rather remain constant over a 26-h period. These data suggest that Gp047 is not a bactericidal protein but instead may prevent cell division. Although it seems counterintuitive that a phage would encode a protein with the capacity to inhibit the growth of its own host population, we speculate that by keeping the local population of susceptible targets low, the phage population would benefit by being able to diffuse further from the site of cell lysis before attaching to a susceptible host [31,32]. Since only one phage can productively infect and lyse a given cell, extra phage genomes are wasted when multiple phages irreversibly bind one cell [33]. Therefore, reducing host growth in the local environment could allow a greater number of new hosts to be productively infected per phage released from a lysed cell.

Motility of *C. jejuni* 11168 is reduced in semisolid media supplemented with Gp047 [16]. It is possible that binding of Gp047 to the bacterial flagellum interferes with flagellar rotation, consequently reducing motility. Unlike the bacterial host, phages are not motile and must reach their hosts by diffusion. Thus, phages could take advantage of the reduced motility of their host to enhance infectivity. Alternatively, Gp047 binding to bacterial flagella might be triggering a mechanism to reduce bacterial metabolic activity and cell division to conserve energy for phage replication.

From another perspective—the growth reduction effect—we observe could result from *Campylobacter*-induced growth suppression in response to sensing bound proteins. This type of response could have evolved as a phage defense mechanism [16]. Since some *Campylobacter* phages are flagellotropic [30], campylobacters with this activity might benefit from down-regulating their metabolism in response to their flagella being bound by phages and/or their proteins. In this model, which would be reminiscent of phage restriction or abortive infection [33], cells would reduce their own growth and would reduce the efficiency of phage infection in these cells, giving rise to fewer infectious virions and thus tempering the effect of phages on the overall population. Alternatively, if grown in biofilm or semisolid conditions, exemplified by our agar plates, these sacrificed cells might physically protect other cells lying deeper within the matrix.

Other reports have documented cases of proteinaceous compounds causing cellular growth inhibition, killing or signaling, lending support for this model. Firstly, antibodies represent a well-known class of proteins with bacterial-binding activities that have been shown to affect cell growth by mechanisms other than opsonization and complement-mediated killing, such as through inducing oxidative stress in bound pathogens [34,35]. Additionally, antibodies against *Cryptococcus neoformans* polysaccharides were reported to mediate protection against this pathogen by altering expression of genes associated with fatty acid metabolism and protein translation upon binding [36]. Another study showed that monoclonal antibodies raised against the capsule of this pathogen were able to bind and cause stiffness in the fungal capsule, which, in turn, inhibited cell division by means of impaired budding of the yeast cells [37]. *Streptococcus pneumoniae* viability has also been shown to be impaired as a result of binding by

non-opsonic antibodies raised against its CPS. These antibodies were shown to agglutinate bacterial cells, which eventually resulted in increased competence and genetic exchange among the cells, which lead to impaired cell viability [38]. Complement-mediated killing was ruled out in this system.

Interestingly, a recent study has shown that biosynthesis of *C. jejuni* polar flagella in association with the FlhG protein helps regulate cell division in *C. jejuni* [39]. These authors suggest that biosynthesis of polar flagella is involved in symmetric cell division, and thus in production of viable daughter cells. We have previously shown that binding of Gp047 causes thickening of bacterial flagella [16] (also shown in Figure 3-6), and therefore the binding of Gp047 along the length of *Campylobacter* flagella may impair cell division through cellular sensing of altered, perhaps stiffened flagella resulting in a transmission of signals to the cell division machinery. At this point, it is not clear whether *C. jejuni* cells are able to slow their own growth and/or cell division in response to detecting the presence of proteins bound to their flagella, or whether this interaction between Gp047 and *C. jejuni* exists outside the laboratory environment. We are actively pursuing these questions. Overall, these results point toward novel interactions between *Campylobacter* cells and their phages and may identify a new class of phage effector proteins influencing phage propagation.

3.6. References

1. Kittler, S.; Fischer, S.; Abdulmawjood, A.; Glunder, G.; Klein, G. Effect of bacteriophage application on *Campylobacter jejuni* loads in commercial broiler flocks. *Appl. Environ. Microbiol.* 2013, *79*, 7525–7533.

2. Loc Carrillo, C.; Atterbury, R.J.; El-Shibiny, A.; Connerton, P.L.; Dillon, E.; Scott, A.; Connerton, I.F. Bacteriophage therapy to reduce *Campylobacter jejuni* colonization of broiler chickens. *Appl. Environ. Microbiol.* 2005, *71*, 6554–6563.
3. Trigo, G.; Martins, T.G.; Fraga, A.G.; Longatto-Filho, A.; Castro, A.G.; Azeredo, J.; Pedrosa, J. Phage therapy is effective against infection by *Mycobacterium ulcerans* in a murine footpad model. *PLoS Negl. Trop. Dis.* 2013, *7*, e2183.
4. Steinbacher, S.; Seckler, R.; Miller, S.; Steipe, B.; Huber, R.; Reinemer, P. Crystal structure of P22 tailspike protein: Interdigitated subunits in a thermostable trimer. *Science* 1994, *265*, 383–386.
5. Baxa, U.; Steinbacher, S.; Miller, S.; Weintraub, A.; Huber, R.; Seckler, R. Interactions of phage P22 tails with their cellular receptor, Salmonella O-antigen polysaccharide. *Biophys. J.* 1996, *71*, 2040–2048.
6. Iwashita, S.; Kanegasaki, S. Enzymic and molecular properties of base-plate parts of bacteriophage P22.
   Eur. J. Biochem. 1976, *65*, 87–94.
7. Waseh, S.; Hanifi-Moghaddam, P.; Coleman, R.; Masotti, M.; Ryan, S.; Foss, M.; MacKenzie, R.; Henry, M.; Szymanski, C.; Tanha, J. Orally administered P22 phage tailspike protein reduces salmonella colonization in chickens: Prospects of a novel therapy against bacterial infections. *PLoS ONE* 2010, *5*, e13904.
8. Cornelissen, A.; Ceyssens, P.J.; Krylov, V.N.; Noben, J.P.; Volckaert, G.; Lavigne, R. Identification of EPS-degrading activity within the tail spikes of the novel *Pseudomonas putida* phage AF. *Virology* 2012, *434*, 251–256.

9. Scholl, D.; Cooley, M.; Williams, S.R.; Gebhart, D.; Martin, D.; Bates, A.; Mandrell, R. An engineered R-type pyocin is a highly specific and sensitive bactericidal agent for the food-borne pathogen *Escherichia coli* O157:H7. *Antimicrob. Agents Chemother.* 2009, *53*, 3074–3080.
10. Gebhart, D.; Lok, S.; Clare, S.; Tomas, M.; Stares, M.; Scholl, D.; Donskey, C.J.; Lawley, T.D.; Govoni, G.R. A modified R-type bacteriocin specifically targeting *Clostridium difficile* prevents colonization of mice without affecting gut microbiota diversity. *mBio* 2015, *6*, doi:10.1128/mBio.02368-14.
11. Schmelcher, M.; Donovan, D.M.; Loessner, M.J. Bacteriophage endolysins as novel antimicrobials. *Future Microbiol.* 2012, *7*, 1147–1171.
12. Briers, Y.; Walmagh, M.; van Puyenbroeck, V.; Cornelissen, A.; Cenens, W.; Aertsen, A.; Oliveira, H.; Azeredo, J.; Verween, G.; Pirnay, J.P.; *et al*. Engineered endolysin-based "Artilysins" to combat multidrug-resistant gram-negative pathogens. *mBio* 2014, *5*, e01379-14.
13. Singh, A.; Arutyunov, D.; Szymanski, C.M.; Evoy, S. Bacteriophage based probes for pathogen detection. *Analyst* 2012, *137*, 3405–3421.
14. Simpson, D.J.; Sacher, J.C.; Szymanski, C.M. Exploring the interactions between bacteriophage-encoded glycan binding proteins and carbohydrates. *Curr. Opin. Struct. Biol.* 2015, *34*, 69–77.
15. Kropinski, A.M.; Arutyunov, D.; Foss, M.; Cunningham, A.; Ding, W.; Singh, A.; Pavlov, A.R.; Henry, M.; Evoy, S.; Kelly, J.; Szymanski, C.M. Genome and proteome of *Campylobacter jejuni* bacteriophage NCTC 12673. *Appl. Environ. Microbiol.* 2011, *77*, 8265–8271.

16. Javed, M.A.; van Alphen, L.B.; Sacher, J.; Ding, W.; Kelly, J.; Nargang, C.; Smith, D.F.; Cummings, R.D.; Szymanski, C.M. A receptor-binding protein of *Campylobacter jejuni* bacteriophage NCTC 12673 recognizes flagellin glycosylated with acetamidino-modified pseudaminic acid. *Mol. Microbiol.* 2015, *95*, 101–115.
17. Coward, C.; Grant, A.J.; Swift, C.; Philp, J.; Towler, R.; Heydarian, M.; Frost, J.A.; Maskell, D.J. Phase-variable surface structures are required for infection of *Campylobacter jejuni* by bacteriophages. *Appl. Environ. Microbiol.* 2006, *72*, 4638–4647.
18. Javed, M.A.; Poshtiban, S.; Arutyunov, D.; Evoy, S.; Szymanski, C.M. Bacteriophage receptor binding protein based assays for the simultaneous detection of *Campylobacter jejuni* and *Campylobacter coli*. *PLoS ONE* 2013, *8*, e69770.
19. Singh, A.; Arutyunov, D.; McDermott, M.T.; Szymanski, C.M.; Evoy, S. Specific detection of *Campylobacter jejuni* using the bacteriophage NCTC 12673 receptor binding protein as a probe. *Analyst* 2011, *136*, 4780–4786.
20. Poshtiban, S.; Javed, M.A.; Arutyunov, D.; Singh, A.; Banting, G.; Szymanski, C.M.; Evoy, S. Phage receptor binding protein-based magnetic enrichment method as an aid for real time PCR detection of foodborne bacteria. *Analyst* 2013, *138*, 5619–5626.
21. Javed, M.A.; Ackermann, H.-W.; Azeredo, J.; Carvalho, C.M.; Connerton, I.F.; Evoy, S.; Hammerl, J.A.; Hertwig, S.; Lavigne, R.; Singh, A.; *et al*. A suggested classification for two groups of *Campylobacter* Myoviruses. *Arch. Virol.* 2014, *159*, 181–190.
22. Janež, N.; Kokošin, A.; Zaletel, E.; Vranac, T.; Kovač, J.; Vučković, D.; Smole Možina, S.; Čurin Šerbec, V.; Zhang, Q.; Accetto, T.; *et al*. Identification and Characterisation of new *Campylobacter* group III phages of animal origin. *FEMS Microbiol. Lett.* 2014, 359, 64–71.

23. Parkhill, J.; Wren, B.W.; Mungall, K.; Ketley, J.M.; Churcher, C.; Basham, D.; Chillingworth, T.; Davies, R.M.; Feltwell, T.; Holroyd, S.; *et al*. The genome sequence of the food-borne pathogen *Campylobacter jejuni* reveals hypervariable sequences. *Nature* 2000, *403*, 665–668.

24. Black, R.E.; Levine, M.M.; Clements, M.L.; Hughes, T.P.; Blaser, M.J. Experimental *Campylobacter jejuni* infection in humans. *J. Infect. Dis.* 1988, *157*, 472–479.

25. St Michael, F.; Szymanski, C.M.; Li, J.; Chan, K.H.; Khieu, N.H.; Larocque, S.; Wakarchuk, W.W.; Brisson, J.R.; Monteiro, M.A. The structures of the lipooligosaccharide and capsule polysaccharide of *Campylobacter jejuni* genome sequenced strain NCTC 11168. *Eur. J. Biochem.* 2002, *269*, 5119–5136.

26. Thibault, P.; Logan, S.M.; Kelly, J.F.; Brisson, J.R.; Ewing, C.P.; Trust, T.J.; Guerry, P. Identification of the carbohydrate moieties and glycosylation motifs in *Campylobacter jejuni* flagellin. *J. Biol. Chem.* 2001, *276*, 34862–34870.

27. Larsen, J.C.; Szymanski, C.; Guerry, P. *N*-linked protein glycosylation is required for full competence in *Campylobacter jejuni* 81–176. *J. Bacteriol.* 2004, *186*, 6508–6514.

28. Guerry, P.; Ewing, C.P.; Schirm, M.; Lorenzo, M.; Kelly, J.; Pattarini, D.; Majam, G.; Thibault, P.; Logan, S. Changes in flagellin glycosylation affect *Campylobacter* autoagglutination and virulence. *Mol. Microbiol.* 2006, *60*, 299–311.

29. Bozzola, J.J.; Russell, L.D. *Electron Microscopy: Principles and Techniques for Biologists*; Jones and Bartlett Publishers: Sudbury, USA, 1992; pp. 40–62.

30. Sorensen, M.C.; Gencay, Y.E.; Birk, T.; Baldvinsson, S.B.; Jackel, C.; Hammerl, J.A.; Vegge, C.S.; Neve, H.; Brondsted, L. Primary isolation strain determines both phage type

and receptors recognised by *Campylobacter jejuni* bacteriophages. *PLoS ONE* 2015, *10*, e0116287.

31. Gallet, R.; Shao, Y.; Wang, I.N. High adsorption rate is detrimental to bacteriophage fitness in a biofilm-like environment. *BMC Evolut. Biol.* 2009, *9*, 241.
32. Abedon, S.T. *Bacteriophage Ecology: Population Growth, Evolution, and Impact of Bacterial Viruses*; Cambridge University Press: Cambridge, UK, 2008; Volume 15.
33. Gadagkar, R.; Gopinathan, K.P. Bacteriophage burst size during multiple infections. *J. Biosci.* 1980, *2*, 253–259.
34. Wang, P.X.; Sanders, P.W. Immunoglobulin light chains generate hydrogen peroxide. *J. Am. Soc. Nephrol. JASN* 2007, *18*, 1239–1245.
35. Nieva, J.; Wentworth, P., Jr. The antibody-catalyzed water oxidation pathway—A new chemical arm to immune defense? *Trends Biochem. Sci.* 2004, *29*, 274–278.
36. McClelland, E.E.; Nicola, A.M.; Prados-Rosales, R.; Casadevall, A. Ab binding alters gene expression in *Cryptococcus neoformans* and directly modulates fungal metabolism. *J. Clin. Invest.* 2010, *120*, 1355–1361.
37. Cordero, R.J.; Pontes, B.; Frases, S.; Nakouzi, A.S.; Nimrichter, L.; Rodrigues, M.L.; Viana, N.B.; Casadevall, A. Antibody binding to *Cryptococcus neoformans* impairs budding by altering capsular mechanical properties. *J. Immunol.* 2013, *190*, 317–323.
38. Yano, M.; Gohil, S.; Coleman, J.R.; Manix, C.; Pirofski, L.A. Antibodies to *Streptococcus pneumoniae* capsular polysaccharide enhance pneumococcal quorum sensing. *mBio* 2011, *2*, doi:10.1128/mBio.00176-11.

39. Balaban, M.; Hendrixson, D.R. Polar flagellar biosynthesis and a regulator of flagellar number influence spatial parameters of cell division in *Campylobacter jejuni*. *PLoS Pathog.* 2011, *7*, e1002420.

Chapter 4: Novel insights into *Campylobacter jejuni* flagellar glycan diversity revealed by probing with a conserved glycan-specific bacteriophage binding protein

Abstract

Many bacteria display glycosylated surface structures that promote virulence in human and animal hosts, and understanding the diversity of these glycans can lead to important insights into pathogen control. In all environments, viruses known as bacteriophages (phages) infect bacteria by first recognizing subtle differences in bacterial surface structures, many of which are glycosylated. Phage-induced pressures are thus likely to have led bacteria to evolve much of the complexity and variability associated with these structures. Along with the utility of studying phage interactions with bacterial glycans, the glycan-recognizing properties of phages provide valuable glycan-recognizing tools.

In the prominent foodborne pathogen *Campylobacter jejuni,* flagellar glycosylation is essential for virulence, and campylobacters display a variety of sialic acid-like nonulosonic acids on their flagella. Previously, we observed that a protein commonly encoded by *Campylobacter* phages, Gp047, binds specifically to *C. jejuni* flagella decorated with 7-acetamidino-pseudaminic acid (Pse5Ac7Am). Furthermore, we previously showed that Gp047 binding inhibits cell growth and reduces bacterial motility, suggesting that cells may have evolved mechanisms of evading this pressure in nature. However, the mechanism of this growth inhibition has remained unknown, and no mechanisms of varying Pse5Ac7Am presentation have previously been identified.

To examine the mechanism of Gp047-induced growth inhibition, we performed RNA-seq on *C. jejuni* 11168 cells exposed to Gp047, and demonstrated that expression of cellular metabolic pathways were altered. We also discovered a requirement for motile flagella for the altered growth phenotype. To uncover mechanisms by which *C. jejuni* might alter its flagellar glycan

expression to avoid this activity, we examined the genetic content and flagellar glycans of *C. jejuni* strains displaying reduced susceptibility to Gp047. Strain-strain variation in Gp047 binding levels were detected even among strains encoding all known genes for synthesis of its receptor, Pse5Ac7Am. We found that one strain, 12661, uniquely expresses a phase-variable version of the Pse5Ac7Am transferase, PseD. Also, two previously uncharacterized flagellar glycan modifications were observed on the flagella of two Gp047-resistant strains. Analysis of the gene content in the flagellar glycosylation loci of these strains points toward differences in copy number, sequence and phase-variable status of *maf* and DUF2920-containing genes as the primary strain-strain differences. Our findings point toward new possible mechanisms responsible for *C. jejuni* flagellar glycan diversity generation.

4.1. Introduction

Bacterial infections kill millions of people every year, but we continue to uncover novel mechanisms that aid bacteria in causing disease. Understanding this process can allow us to target bacterial virulence factors without threatening essential cellular processes, a strategy that can help minimize drug resistance [1]. This is especially important now, as antibiotic-resistant infections kill 700,000 people globally each year, with this number expected to rise by more than tenfold by 2050 [2]. To establish themselves in their niche, many bacteria express factors that allow them to adhere to tissues, invade host cells, swim through mucus, shield themselves from immune responses and evade bacteriophage (phage) predation. Many bacteria accomplish this by displaying glycosylated structures on their surface, such as capsular polysaccharides (CPS), lipooligosaccharides (LOS), and *N*- and *O*-linked glycoproteins.

Campylobacter jejuni causes severe food poisoning around the world [3], and has recently been found to cause growth defects in low-resource settings [4]. *C. jejuni* relies on glycosylated flagella to colonize the gastrointestinal epithelium of humans and animals [5]. Its flagellin proteins (FlaA and FlaB) are among the most heavily glycosylated proteins known [6], with up to 10% of their molecular weight being contributed by glycans [7]. Unlike some other flagellated bacterial pathogens, such as *Pseudomonas aeruginosa,* whose flagella assemble with or without glycosylation [8], flagellar glycosylation is essential to *C. jejuni* flagellar filament biogenesis, and is thus essential for its motility and virulence [6,9]. The importance of glycosylated flagella to *C. jejuni* is further illustrated by the fact that it devotes approximately 3% of its small, 1.6-Mb genome encoding enzymes associated with flagellar glycosylation, and that two of its three sigma factors are devoted to regulating flagellar biosynthesis and glycosylation [6]. Understanding the diversity of *C. jejuni* flagellar glycans and the factors that contribute to this variety allow us to better understand this ubiquitous pathogen.

C. jejuni glycosylates its flagella with a wide array of rare and variable glycans, and the mechanisms dictating which glycans are expressed are poorly understood [6]. *Campylobacter* species glycosylate their flagella with the nonulosonic acids, pseudaminic acid (5,7-diacetamido-3,5,7,9-tetradeoxy-L-*glycero*-α-L-*manno*-nonulosonic acid, or Pse5Ac7Ac, 316 Da) and legionaminic acid (5,7-diamino-3,5,7,9-tetradeoxy-D-*glycero*-D-*galacto*-nonulosonic acid, or Leg5Ac7Ac, 316 Da), along with a growing list of derivatives of each. So far, this list includes acetamidino Pse (5-acetamido-7-acetamidino-3,5,7,9-tetradeoxy-L-*glycero*-α-L-*manno*-nonulosonic acid, or Pse5Ac7Am, 315 Da), *O*-acetyl Pse (Pse5Ac7Ac8OAc, 358 Da), *N*-acetyl glutamic acid-modified Pse (Pse5Ac7Ac8-GlnAc), dihydroxyproprionyl Pse

(Pse5Pr7Pr, 408 Da), a dimethylglyceric acid (DMGA) derivative of Pse5Ac7Ac (DMGA-Pse5Ac7Ac), DMGA-Pse5Ac7Am, Pse5Ac7Am-deoxypentose, and Pse5Ac7Ac8OAc – deoxypentose [10–18]. The genetic and biochemical pathways for biosynthesis of these glycans and some of their derivatives in a few *C. jejuni* strains and in one *Campylobacter coli* strain, have been extensively studied over the past two decades [5,9–13,15,19–26]. This has primarily been done using mass spectrometry (MS) and nuclear magnetic resonance (NMR) spectroscopy to analyze the flagellar glycans or nucleotide-activated precursors of defined mutants. However, these methods are technically demanding, expensive, and time-intensive to use, and thus the already impressive repertoire of flagellar glycans encoded by *Campylobacter* species has come from the analysis of only a few strains. Furthermore, linking genotype with phenotype in this organism, especially in the context of glycosylation pathways, is complicated by the presence of phase-variable polynucleotide tracts (usually poly-G) within many open reading frames (ORFs) in the flagellin biosynthesis gene cluster. This leads to frequent on/off switching of genes (~1/1000 generations) in a given population due to slipped-strand mispairing during DNA replication, making it difficult to analyze the effect of a given mutation [27]. For example, *C. jejuni* 11168, the first genome-sequenced strain of the species, harbours poly-G tracts in at least 28 of its genes [27,28], 10 of which are found within its ~50-gene flagellar glycosylation locus [29]. Given these challenges, much of the flagellar glycan diversity and the mechanisms that drive it remain unknown.

Insight into the factors contributing to the diversity of flagellar glycan presentation by *C. jejuni* can be gained by studying the interaction between *C. jejuni* and its phages, which recognize *C. jejuni* cells by binding to glycosylated structures, including flagella [30]. Phages are

exceptionally host-specific, and have evolved to express proteins capable of distinguishing between subtle differences in bacterial surface structures. This property makes phages valuable sources of highly specific reagents for glycan detection that can be exploited as inexpensive tools for characterizing bacterial glycans [31]. We previously characterized one such protein, Gp047, which is commonly encoded by *Campylobacter* phages and which binds to *C. jejuni* and *C. coli* flagella displaying Pse5Ac7Am [32–34]. Previously, we showed that Gp047 caused agglutination of 38/40 (95%) *C. jejuni* strains and 17/19 (90%) *C. coli* strains, suggesting that many strains may express Pse5Ac7Am [35]. We also found that Gp047 clears growth of *C. jejuni* upon flagellar binding, but the mechanism for this activity has not yet been established [33].

As flagellar rotation is driven by the proton motive force (PMF), we hypothesized that Gp047 binding to flagella would disrupt PMF balance in the cell and lead to the observed growth inhibition. Since *C. jejuni* frequently coexists with phages expressing Gp047 in nature, we hypothesized that *C. jejuni* might have evolved mechanisms of varying the glycan receptors required for Gp047 binding. Here we describe the use of transcriptomic and targeted mutagenesis analysis to develop insights into the mechanism by which the *Campylobacter* phage protein Gp047 inhibits *C. jejuni* growth. Using a combination of genetic analysis and mass spectrometry of flagellar glycans, we also investigate the possible mechanisms by which two strains resist Gp047-induced binding. Our results suggest that Gp047 binding to motile flagella leads *C. jejuni* to decrease expression of energy metabolism genes, and that strain-strain differences in *C. jejuni* flagellar glycans can confer resistance to this protein.

4.2. Materials and Methods

4.2.1. Bacterial growth conditions

C. jejuni strains were grown on NZCYM (Difco) agar, supplemented with 50 μg/mL kanamycin where needed, at 37°C under microaerobic conditions (85% N2, 10% CO2, 5% O2). *E. coli* was grown on LB agar supplemented with 50 μg/mL kanamycin where needed. The list and sources of bacterial strains used in this study are given in Table 4-1.

4.2.2. Expression and purification of Gp047 and its derivatives

Gp047 was expressed as an N-terminal glutathione-S-transferase (GST) fusion protein as described previously [36]. CC-Gp047 and NC-Gp047 were expressed in *E. coli* BL21 as GST-fused proteins and purified as described previously [35], with the exception that proteins were eluted in 10 mM reduced L-glutathione, 50 mM HEPES, 1 mM DTT at pH 9.0. The list of plasmids used in this study are listed in Table 4-1.

4.2.3. Total RNA extraction

Cells were harvested from overnight NZCYM plate cultures, pelleted and washed once in NZCYM broth and set to an OD_{600} of 0.05 (2 x 10^8 CFU/mL) in 20 mL NZCYM broth in 125-mL Erlenmeyer flasks. Cells were grown under microaerobic conditions with agitation at 200 rpm. After 4.5 h incubation, CC-Gp047 was added to a final concentration of 25 μg/mL. As negative controls, 6 mL HEPES buffer or 6 mL NC-Gp047 were used. Flasks were incubated 30 min before the entire contents of each was harvested and the RNA stabilized using 0.1 volumes of ice cold 10% buffered phenol in 100% ethanol [37]. Total RNA was extracted from each

sample using a hot phenol method as previously described [37]. Genomic DNA was removed from the samples using RNAse-free DNAse I (Epicentre) (37°C for 30 min) and cleaned using the Zymo RNA Clean & Concentrator. PCR was used to confirm the absence of residual DNA and the DNase treatment was repeated until the absence of genomic DNA was confirmed. Total RNA quality was assessed using an Agilent Bioanalyzer and RNA was stored at -80°C until further use. This experiment was done in biological triplicate, with the exception of the NC-Gp047 control, which was done only once.

4.2.4. RNA sequencing

Samples were subsequently depleted of rRNA using the RiboZero Bacterial kit according to the manufacturer's instructions and rRNA depletion was confirmed using the Agilent Bioanalyzer RNA 6000 Pico Kit. The Ion Total RNA-seq kit was used to construct strand-specific barcoded sequencing libraries according to the manufacturer's instructions. Following library construction, each library was quality-checked and quantified using the Bioanalyzer High Sensitivity DNA kit. Once all libraries were completed, they were pooled together in equimolar amounts. Template preparation was done using the Ion PI Hi-Q kit. Sequencing was done on an Ion Torrent Proton using the Ion PI Hi-Q sequencing 200 kit on a single Proton V2 chip.

The raw sequencing reads were demultiplexed by the Ion Torrent suite software and mapped to the 11168 genome using STAR [38]. The raw demultiplexed sequencing reads will be deposited at the NCBI SRA archive. Reads aligning to coding regions were counted using HT-seq using the default settings [39]. DESeq2 was used to identify differentially expressed transcripts between the control and CC-Gp047 treated cells. Genes with a false discovery rate (FDR)-

corrected *p*-value <0.05 were considered differentially expressed. We also conducted gene set enrichment analysis (GSEA) on *C. jejuni* Kyoto Encyclopedia of Genes and Genomes (KEGG) pathways using the generally applicable gene set enrichment (GAGE) method [40] with a minimum FDR cutoff of <0.1 [38].

4.2.5. Generation of *motA, motB,* and *cj1295* mutants

To generate *motA* and *motB* mutants, *C. jejuni* 11168 was transformed by natural transformation with the pDRH3330 (*motA*) or pDRH3331 (*motB*) mutation constructs published by [41]. To generate a *cj1295* mutant, *C. jejuni* 11168 was naturally transformed with the *cj1295* mutation construct (p1295) described by Hitchen *et al.* (2010) and generously provided by Dennis Linton [29].

For natural transformation of mutant constructs, an overnight culture of *C. jejuni* cells was streaked onto BHI containing 2% yeast extract (BHIY), grown for 6 hours under the conditions described above, and harvested into PBS. Cells were washed once in PBS, resuspended in 250 μL PBS, spotted (20-30 x 10-μL spots) onto pre-warmed BHIY plates and allowed to absorb into agar ~5 min. p1295 DNA (20 μg/mL in water) was spotted (~10-μL spots) atop each spot of cell suspension and allowed to dry ~5 min. Plates were incubated for 12-16 hours, then the contents of the plates was harvested and spread or streaked across 4-6 BHI plates containing 50 μg/mL kanamycin. Plates were incubated until colonies appeared (3-5 days). Isolated colonies were patched onto kanamycin-containing BHI plates and grown overnight prior to confirmation of successful mutagenesis by colony PCR (OneTaq, NEB) using gene-specific primers [29]

[41]. This protocol has been deposited into Protocols.io (dx.doi.org/10.17504/protocols.io.magc2bw).

4.2.6. Immunogold labeling and transmission electron microscopy

Immunogold labeling and transmission electron microscopy was done as described previously [42], with some exceptions. Briefly, *C. jejuni* cells (OD_{600} = 3.0) were harvested from a plate of overnight growth in NZCYM broth, incubated with Formvar-coated copper grids for 45 min, washed 1 x 3 min with PBS, then fixed by incubating in 2.5% paraformaldehyde in PBS for 20 min. Grids were then washed 3 x 3 min with PBS, incubated in blocking solution (PBS containing 5% bovine serum albumin and 0.05% Tween) for 35 min, then in freshly purified GST-tagged Gp047 (0.2 mg/mL diluted 1:25 in blocking solution) for 45 min. Grids were then washed 3 x 3 min in blocking solution, incubated in a rabbit anti-Gp047 antibody solution (diluted 1:50 in blocking solution) for 45 min, washed 3 x 3 min as above, and incubated in a solution of goat anti-rabbit IgG (whole molecule) conjugated to 10-nm gold particles (Sigma, diluted 1:50 in blocking solution) for 45 min. Finally, grids were sequentially washed (3 x 3 min each) with blocking solution, PBS, and distilled water, then air-dried on Whatman filter paper overnight. All steps were done at room temperature. Grids were examined using a transmission electron microscope (JEOL JEM1011; JEOL, Inc., Peabody, MA, USA). Images were captured using a high contrast 2k × 2k mid-mount digital camera (Advanced Microscopy Techniques, Corp., Woburn, MA, USA). This protocol has been deposited into Protocols.io (dx.doi.org/10.17504/protocols.io.mv5c686).

4.2.7. Gp047 growth clearance assay

Bacterial growth clearance was tested by spotting phage protein onto a freshly inoculated bacterial suspension using the overlay agar method described previously, with some modifications [33]. Briefly, overnight bacterial cultures were harvested in NZCYM broth and set to an OD_{600} of 0.35. A 5-mL aliquot of this suspension was transferred to a standard sized empty Petri dish and incubated at 37 °C without shaking for 4 h under microaerobic conditions. The suspension was then set to an OD_{600} of 0.5, and 200 µL of this was mixed with 5 mL sterile 0.6% molten NZCYM agar at 45°C. This suspension was poured onto the surface of a pre-warmed NZCYM plate containing 1.5% agar. Plates were allowed to solidify for 15 min and then 10 µL UV-sterilized Gp047 or CC-Gp047 solution (0.91–1.3 mg/mL in 10 mM reduced L-glutathione, 50 mM Tris, 1 mM DTT, pH 9.0) was spotted onto the agar surface and allowed to completely soak into the agar before inverting the plate and incubating at 37°C under microaerobic conditions. Zones of growth clearance were observed after 18–24 h.

4.2.8. Sequence alignments and analysis

Nucleic acid sequence information for *cj1293-cj1342* (the flagellar glycosylation locus in 11168) for strains 11168, 12567, 12660, 12661, and 12664 was obtained from NCBI [43,44]. Nucleotide and amino acid sequence alignments and phylogenetic trees were generated using Geneious version 8 (http://www.geneious.com, [45]). Alignment figures were generated using T-Coffee [46] and Boxshade (http://sourceforge.net/projects/boxshade/). Black shading indicates the consensus sequence, grey shading indicates similar residues.

4.2.9. Preparation of cell-free flagella for MS

Cell-free flagella were prepared for MS as described previously with some modifications [32]. Briefly, bacterial growth was harvested from 20-40 NZCYM agar plates, washed with PBS and resuspended in 100-150 mL PBS and stored up to 7 days at -80°C. Cells were thawed by vortexing and flagella were sheared from cells using a Polytron homogenizer for 6 × 30 sec (allowing 30 sec incubation on ice between rounds) at max rpm on ice. Cells were then removed by centrifugation at 8700 × *g* for 20 min at 4°C. To collect flagellar filaments, the resulting supernatant was ultracentrifuged at 207 870 × *g*, 4°C for 1.5 h using 6 x 30-mL tubes (Beckman). Pellets were washed 3 times by resuspending each pellet in 20 mL distilled water and ultracentrifuging again as above, giving a total of 4 x 1.5 h ultracentrifuge runs. After washing, pellets were resuspended and pooled into a total of 1 ml distilled water and incubated at -20°C until use. Prior to MS analysis, flagella were quantified using a Bradford assay and visualized using SDS-PAGE (the appearance of a prominent ~60-kDa band was taken as an indicator that flagella had been successfully prepared).

4.2.10. Protease digestion of flagella

100 μg of flagella protein sample was dissolved in 25 μL of digestion buffer (50 mM aqueous ammonium bicarbonate (NH_4HCO_3) buffer). 25 μL of dithiothreitol (DTT) solution (25 mM) was added to the samples and incubated at 45 ºC for 45 min. Subsequently, carbamidomethylation was performed by adding 25 μL of iodoacetamide (IAA) solution (90 mM) and incubating at room temperature for 45 min in the dark. The sample was then dialyzed against double distilled water and lyophilized. Flagellin was digested by adding 12.5 μL sequencing-grade trypsin (Promega, 0.4 μg/μL) and incubating at 37 ºC for 12 h. The digest was

desalted by C18 solid phase extraction cartridges and then dried under a speed vacuum. The peptides and glycopeptides were subsequently re-dissolved in 0.1% formic acid in water and stored at - 30 ºC until analysis by nano-LC-MS/MS.

4.2.11. Nano-LC-MS/MS acquisition

Desalted flagellin digests were analyzed on an Orbitrap Fusion Tribrid mass spectrometer (Thermo Scientific) equipped with a nanospray ion source and connected to a Dionex binary solvent system. Pre-packed nano-LC columns (15 cm in length, 75 μm in internal diameter) filled with 3 μm C18 material were used for chromatographic separation of glycoprotein digests. Precursor ion scan was performed at 120,000 resolution in an Orbitrap analyzer, and precursors at a time frame of 3 sec were selected for subsequent fragmentation using higher energy collision dissociation (HCD) at a normalized collision energy of 28 and collision-induced dissociation (CID) at an energy of 35. The threshold for triggering an MS/MS event was set to 500 counts. The fragment ions were analyzed on Orbitrap after HCD and CID fragmentation at a resolution of 30,000. Charge state screening was enabled, and precursors with unknown charge state or a charge state of +1 were excluded (positive ion mode). Dynamic exclusion was enabled with an exclusion duration of 10 sec.

4.2.12. MS data analysis

The LC-MS/MS spectra of the tryptic digest of proteins were searched against the FlaA and FlaB protein sequence of the respective strains in .fasta format using Byonic 2.3 software with trypsin as the digestion enzyme. Carbamidomethylation of cysteine and oxidation of methionine were selected as variable modifications. Glycan modifications such as Pse5Ac7Ac (m/z=

316.12705), Pse5Ac7Am (m/z = 315.14304), DMGA-Pse5Ac7Ac (m/z = 390.16383), and DMGA-Pse5Ac7Am (m/z=389.17981) were used as variable modifications on serines/threonines. The LC-MS/MS spectra were analyzed manually for the glycopeptide fragmentation on HCD and CID with the support of Xcalibur software. To identify glycans, the spectra of the glycopeptides were evaluated for glycan neutral loss patterns, oxonium ions and glycopeptide fragmentations. Unknown derivatives of pseudaminic acid were identified based on the presence of oxonium ions and neutral losses on the spectra of glycopeptides bearing glycosylation sites.

Table 4-1. List of bacterial strains and plasmids used in this study.

Name	**Source**	**Reference**
C. jejuni NCTC 11168 (MP21)	Human enteropathy	[46]
C. jejuni NCTC 12567	Chicken	[24]
C. jejuni NCTC 12660	Chicken	[47]
C. jejuni NCTC 12661	Pigeon	[47]
C. jejuni NCTC 12664	Chicken	[47]
C. jejuni NCTC 11168 Δ*cj1295*	*C. jejuni* NCTC 11168 (MP21)	This work
C. jejuni 11168 Δ*motA*	*C. jejuni* 11168 (MP21)	This work
C. jejuni 11168 Δ*motB*	*C. jejuni* 11168 (MP21)	This work
pGEX_*ccgp047*	Expression construct of GST-fused CC-Gp047 in pGEX 6P-2	[35]
pGEX_*ncgp047*	Expression construct of GST-fused NC-Gp047 in pGEX 6P-2	[35]
pDRH3330 (pUC19::*motA*-cat-*rpsL*)	*motA* mutagenesis construct	[40]
pDRH3331 (pUC19::*motB*-cat-*rpsL*)	*motB* mutagenesis construct	[40]

4.3. Results

4.3.1. Gp047-treated cells up-regulate membrane proteins and down-regulate TCA cycle genes

To determine the mechanism of Gp047 growth inhibition of *C. jejuni* 11168 cells, we sequenced total mRNA (RNA-seq) from cells incubated with CC-Gp047, the C-terminal quarter of Gp047 (previously shown to harbour the growth inhibitory activity, [33]) for 30 min. As negative controls, we extracted RNA from buffer-exposed cells and from cells exposed to NC-Gp047, the N-terminal quarter of Gp047 (previously shown to retain no growth inhibitory activity). PCA plot analysis of all samples showed that the NC-Gp047 clustered with the buffer controls (Figure 4-S2). However, we left this group out of our differential gene expression analysis.

We found that incubation of *C. jejuni* 11168 with CC-Gp047 results in changes in expression of genes encoding energy metabolism enzymes, as well as membrane and periplasmic proteins (Table 4-2). Up-regulated genes include *omp50,* which encodes a major *C. jejuni* porin and phosphotyrosine kinase also known as Cjtk. Cjtk activity has been shown to be important for CPS and N-glycan production in *C. jejuni,* as it positively regulates the UDP-GlcNAc/Glc epimerase Gne, which is required for production of these glycans [49]. Other up-regulated genes include *cj1169c* (a periplasmic protein-encoding gene upstream of *omp50*); *cj0037c*, which encodes cytochrome C; *dsbI*, which encodes a disulfide bond forming protein; *tlp4,* which encodes a chemotaxis receptor; *metB*, which encodes a methionine biosynthesis enzyme; and *cj0761*, which encodes a hypothetical protein. Down-regulated genes include *sdhA* and *sdhB,*

which are misannotated as succinate dehydrogenases but are likely to encode methylmenaquinol:fumarate reductases, which function in the TCA cycle [50,51]. Other down-regulated genes include *cj0426,* which encodes an ABC transporter ATP binding protein, the downstream gene *cj0427, rpmF*, which encodes a 50s ribosomal protein, and *cj0911* and *cj1485c,* which encode hypothetical periplasmic proteins. KEGG pathway analysis showed that several KEGG categories are statistically represented by the down-regulated genes upon CC-Gp047 exposure, including TCA cycle, carbon metabolism, and oxidative phosphorylation pathways (Table 4-3). These results suggest that CC-Gp047 affects cellular energy metabolism, thus presenting a possible mechanism for the growth inhibition phenotype observed.

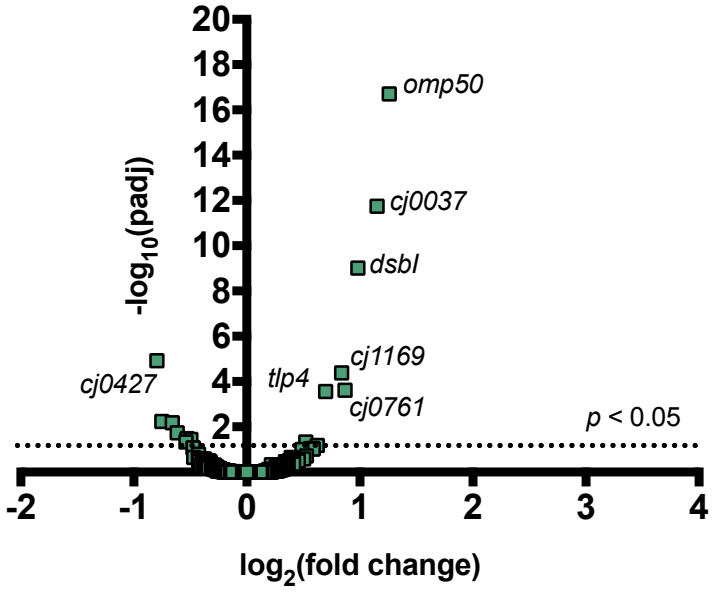

Figure 4-1. Addition of CC-Gp047 to *C. jejuni* 11168 cells leads to changes in gene expression. For all transcribed *C. jejuni* 11168 genes, the negative log of the FDR-adjusted *p*-value is plotted against the $\log_2$ fold change in transcription following CC-Gp047 treatment compared with buffer-treated controls.

Table 4-2. Differentially expressed *C. jejuni* 11168 genes upon CC-Gp047 treatment.

Gene	Annotation	Fold change	*p*-value[a]
omp50	50 kDa outer membrane protein precursor, phosphotyrosine kinase[b]	2.39	< 0.01
cj0037c	Putative cytochrome C	2.22	< 0.01
dsbI	Disulphide bond formation protein	1.98	< 0.01
cj0761	Hypothetical protein Cj0761	1.83	< 0.01
cj1169c	Putative periplasmic protein	1.79	< 0.01
tlp4	Putative methyl-accepting chemotaxis signal transduction protein	1.62	< 0.01
metB	Putative *O*-acetylhomoserine (thiol)-lyase	1.44	0.05
cj0426	Putative ABC transporter ATP-binding protein	-1.41	0.04
cj0911	Putative periplasmic protein	-1.44	0.03
sdhA	Possible methylmenaquinol:fumarate reductase (TCA cycle)[c]	-1.45	0.05
sdhB	Possible methylmenaquinol:fumarate reductase (TCA cycle)[c]	-1.53	0.02
rpmF	50S ribosomal protein L32	-1.58	0.01
cj1485c	Putative periplasmic protein	-1.68	0.01
cj0427	Hypothetical protein Cj0427	-1.74	< 0.01

[a]For each gene, fold change in expression post NCTC 12673 phage infection is listed followed by the FDR-adjusted *p*-value in brackets.

[b]Genbank annotation updated according to Corcionivoschi *et al.* [49]

[c]Genbank annotation updated according to Kassem *et al.* [51]

Table 4-3. Statistically significantly enriched KEGG pathways for down-regulated *C. jejuni* 11168 genes following CC-Gp047 treatment.

Significantly down-regulated KEGG pathways[a]	*p*-value[b]
cje00020 Citrate cycle (TCA cycle)	0.001
cje01200 Carbon metabolism	0.006

cje00190 Oxidative phosphorylation	0.019
cje03010 Ribosome	0.019
cje01130 Biosynthesis of antibiotics	0.019
cje01120 Microbial metabolism in diverse environments	0.019
cje00650 Butanoate metabolism	0.020

[a]Differentially expressed host genes for each condition were subjected to gene set enrichment analysis (GSEA) on annotated Kyoto Encyclopedia of Genes and Genomes (KEGG) pathways using GAGE with an FDR cutoff of <0.1. KEGG pathways along with their significance values at each time point are listed in Table 4-3.

[b]Numerical values correspond to FDR-adjusted *p*-values (<0.05 was considered to be significant).

4.3.2. Gp047 binding to flagellar motor mutants *motA* and *motB* does not cause growth inhibition

We next sought to understand how Gp047 binding to cell flagella might lead to changes in gene expression. Since flagellar motility is reduced upon Gp047 binding [42], we hypothesized that the cell might sense increased Gp047-induced flagellar stiffness and increase proton flow through the flagellar motor channel to compensate for this inhibition of flagellar rotation. This increased proton flow may in turn disrupt proton motive force (PMF) homeostasis, which could prompt cells to respond by altering transcription of energy metabolism pathways. We predicted that flagellar motility mutants, such as *motA* and *motB*, which do not express functional flagellar motors, would thus resist Gp047-induced clearing. To test this, we generated insertional mutants in each of *motA* and *motB* in *C. jejuni* 11168 and tested their binding to Gp047. We found that

binding occurred normally (Figure 4-2), but when we tested growth inhibition of the *motA* and *motB* mutants, we found that Gp047 was unable to clear these mutants (Figure 4-2, inset). This result supported our hypothesis that flagellar function is required for Gp047-mediated growth inhibition.

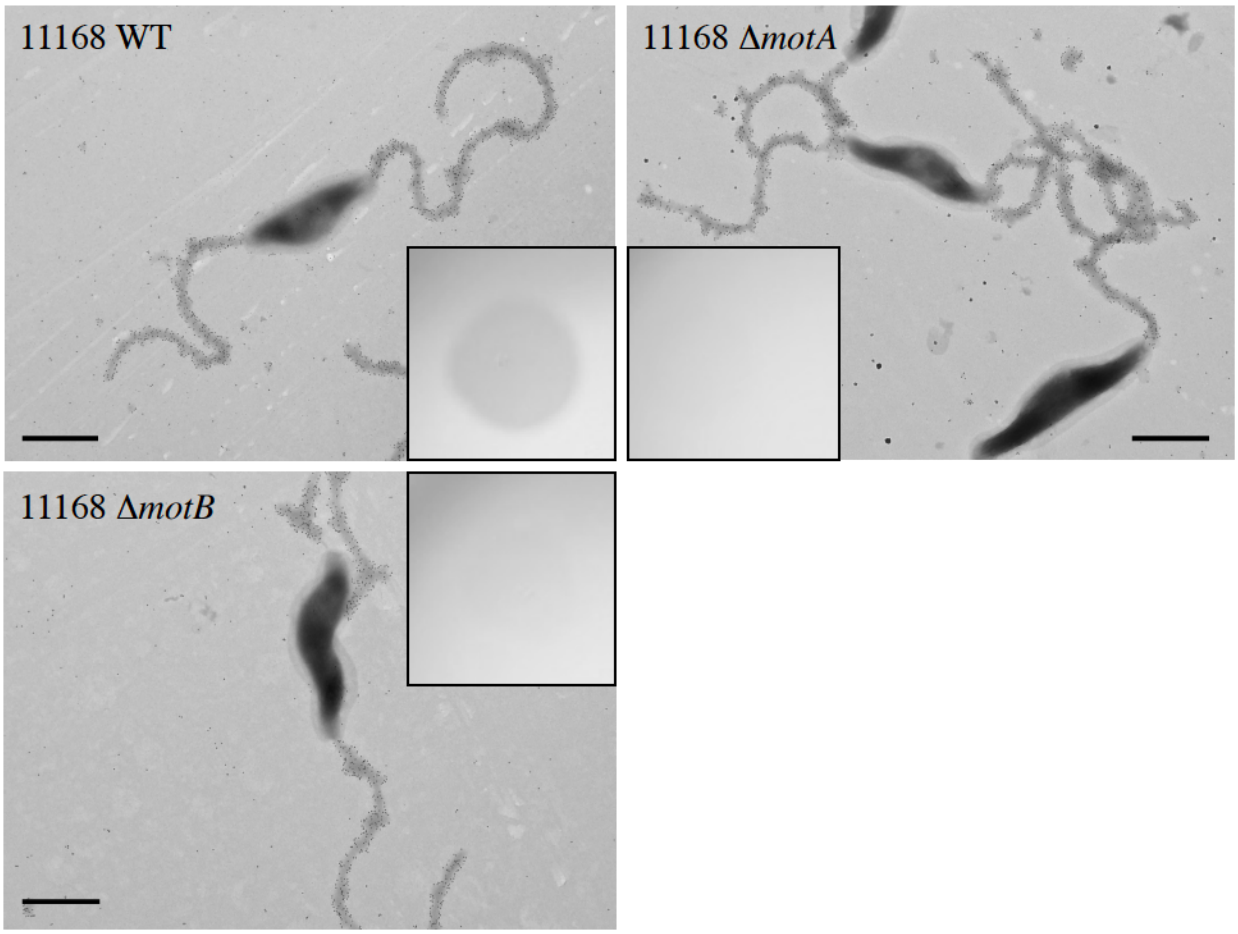

Figure 4-2. *C. jejuni* 11168 wild type, *motA* mutant, and *motB* mutant cells are similarly bound by CC-Gp047, as shown by immunogold labeling with Gp047-specific antibodies and transmission electron microscopy. Inset: only wild type cell growth is cleared by CC-Gp047, as shown by digital images of overnight growth on agar plates following spotting of CC-Gp047. All images are representative of experiments done in duplicate. Scale bars represent 800 nm.

4.3.3. Strain-strain heterogeneity in Gp047 clearing and binding exists among *C. jejuni* strains

We identified four *C. jejuni* strains, 12567, 12660, 12661 and 12664, which were naturally reduced in their ability to be cleared by Gp047 and CC-Gp047 compared to 11168 (Table 4-4). Strain 12567 was cleared to near-11168 levels, whereas strain 12664 was not cleared. Strain 12660 displayed reduced clearing, and strain 12661 was generally not cleared, although one biological replicate of this experiment showed that this strain was cleared well. To better understand the factors mediating Gp047 susceptibility, we sought to determine the mechanism of resistance to Gp047-induced clearing. To test the hypothesis that reduced clearing correlated with reduced Gp047 binding, we first tested whether Gp047 could bind to all strains by probing cells with immunogold-labeled Gp047. We found that 12567 displayed robust Gp047 binding (Figure 4-3), whereas 12660 displayed intermediate levels of binding. Interestingly, we found that biological replicates of 12661 showed either no binding or robust binding to Gp047 (n = 2 each). Finally, we observed a complete lack of Gp047 binding to 12664. Although neither the clearance assay nor the immunogold-labeling assay provides quantitative results, the level of growth clearance observed for these strains appeared to correlate with levels of Gp047 binding to the strains examined. These results show that strain heterogeneity in Gp047 clearing and binding exists, and suggests that reduced Gp047 binding may explain the observed resistance to Gp047 achieved by these strains.

Table 4-4. Growth clearance of *C. jejuni* strains by Gp047 and CC-Gp047.

Strain	Gp047 growth clearance[a]	CC-Gp047 growth clearance[a]

***C. jejuni* NCTC 11168**	+++	+++	++	+
***C. jejuni* 12567**	+	++	+	-
***C. jejuni* NCTC 12660**	+	+	+	-
***C. jejuni* NCTC 12661**	-	-	++	-
***C. jejuni* NCTC 12664**	-	-	-	-

[a]Degree of growth clearance following spotting of full-length Gp047 or CC-Gp047 on growing *C. jejuni* cells and overnight incubation. Clearing was scored visually. (+++) = very clear, (++) = slightly clear, (+) = very faint clearing, (-) = no clearing. Each column represents a separate biological replicate.

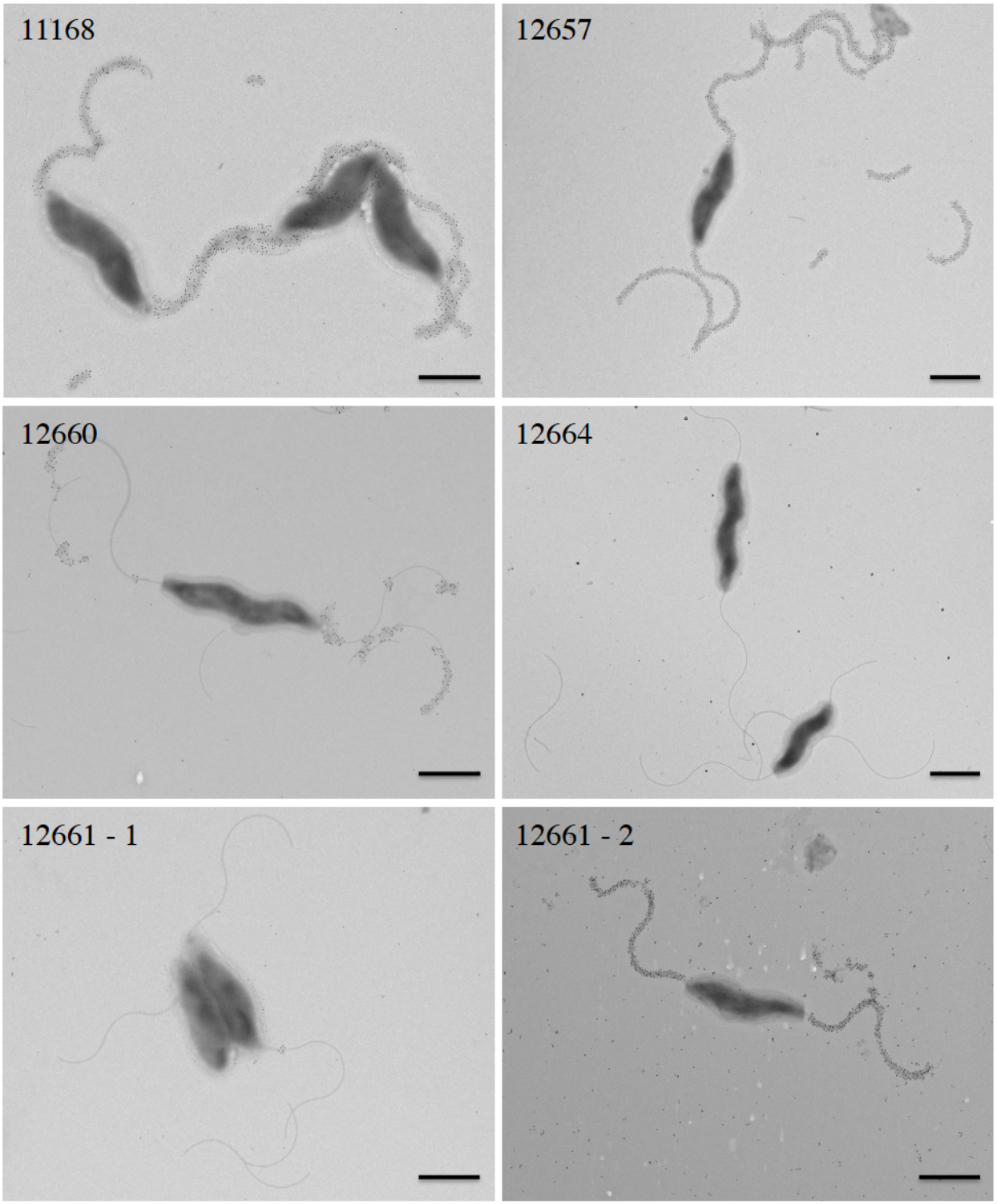

Figure 4-3. Transmission electron microscopy with immunogold labeling using CC-Gp047 followed by anti-Gp047 antibodies and then immunogold-conjugated secondary antibodies to probe *C. jejuni* strains. From top left: strains *C. jejuni* 11168, 12567, 12660, 12664, 12661-1,

12661-2. Strain 12661 is depicted twice to show the two phenotypes that were observed with this strain. Scale bars represent 800 nm.

4.3.4. *C. jejuni* strains resistant to Gp047 binding encode all genes required for biosynthesis and transfer of Pse5Ac7Am

We next sought to understand how cells achieved altered levels of Gp047 binding. As we previously showed that Gp047 binding requires Pse5Ac7Am for binding to *C. jejuni* 11168 flagella [32], we hypothesized that strains displaying reduced levels or differing patterns of Gp047 binding would express different levels of Pse5Ac7Am on their flagella. Pse5Ac7Am is formed by adding the Am group to Pse5Ac7Ac by PseA, an N-acetyl sugar amidotransferase, and is thus dependent on Pse5Ac7Ac synthesis [26]. Pse5Ac7Ac is synthesized by the sequential action of PseB, PseC, PseH, PseG, PseI, and PseF [6]. Pse5Ac7Ac and Pse5Ac7Am are then transferred to flagellin in the cytoplasm by the action of separate transferases: PseE transfers Pse5Ac7Ac, whereas PseD transfers Pse5Ac7Am [26,52,53]. As it has been established that *C. jejuni* and *C. coli* require Pse5Ac7Ac biosynthesis for flagellar biogenesis [9], and all strains examined here are flagellate, we predicted that all strains would encode the genes required for Pse5Ac7Ac synthesis and transfer (ie. *pseBCHGIFE*). However, we hypothesized that 12664, which is unable to bind Gp047, would be missing one or more genes involved in Pse5Ac7Am biosynthesis or presentation, ie. *pseA* and/or *pseD*, and that 12661, which is variably able to bind Gp047, might express phase-variable versions of one or both of these genes. To test these hypotheses, we sequenced the genomes for these strains [43, 44] and examined the region spanning *cj1293-cj1343,* which was previously established to encode the flagellar glycosylation locus in *C. jejuni* 11168 [28].

We found a high degree of similarity at the flagellar glycosylation loci among all five strains (Figure 4-4). Compared to 11168, which encodes 47 genes in this locus, we found that 12567, 12660 and 12664 had between 46-48 genes, whereas 12661 encodes only 40. This is in contrast to *C. jejuni* 81-176, another well-characterized strain, which encodes only 24 of the 47 flagellar glycosylation genes encoded by 11168 [26]. Notably, we found that all strains encode copies of all genes required for Pse5Ac7Ac and Pse5Ac7Am synthesis and transfer.

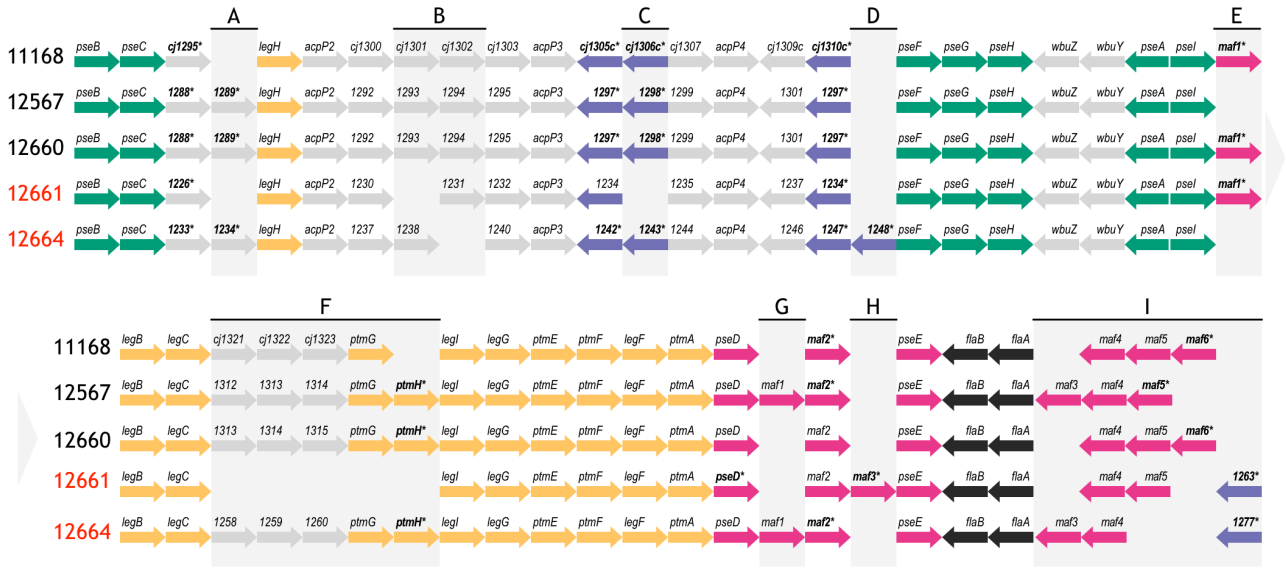

Figure 4-4. Schematic depicting the flagellar glycosylation loci of strains *C. jejuni* 12657, 12660, 12661 and 12664, as compared to *C. jejuni* 11168. Gene lengths are not to scale. Pseudogenes are not depicted. Strain names indicated in red refer to strains that either variably or consistently showed a lack of Gp047 binding by immunogold/TEM. Asterisks/bold text mark genes containing a phase-variable poly-G tract. Colours represent genes involved in the same biological pathway (green: *pse* biosynthesis, yellow: *leg* biosynthesis, black: flagellar filament biosynthesis) or genes within the same family according to predicted function (purple: DUF2920 domain-containing genes, pink: *maf* genes). Other genes are indicated in grey. Letter

codes are used to indicate regions of strain heterogeneity in gene content. Arrow direction indicates direction of transcription.

4.3.5. Strain-level differences in Gp047 binding correlate with differences in PseD sequence

In light of the fact that all strains encoded the genes required for Pse5Ac7Am synthesis and transfer to flagella, we next examined whether sequence differences in PseA or PseD could explain the observed differences in Gp047 binding. We found that PseA was upwards of 98.7% identical among strains, but that PseD diverged among strains (Figure 4-S1). PseD sequences from 11168, 12567 and 12660 were upwards of 96.9% identical to one another, and PseD sequences from 12661 and 12664 were 93.6% identical to one another, but sequences from the 12661/12664 were only 79.6-83.4% identical to PseD from 11168/12567/12660. The most sequence divergence occurred within the third quarter of the PseD amino acid sequence. The fact that the two strains observed to express the most substantial reduction in Gp047 binding grouped apart from the other strains based on their PseD sequence supported the hypothesis that changes in PseD sequence might explain this observation.

4.3.6. C. jejuni 12661 encodes a 25-nucleotide insertion containing a potentially phase-variable poly-G tract in *pseD*

The fact that Gp047 binding to 12661 flagella occurred variably, whereas 12664 displayed a consistent lack of Gp047 binding, pointed to the existence of differences in Pse5Ac7Am expression between these strains. This prompted us to more closely examine the nucleotide

sequence identity of *pseD* from these two strains, which led us to find that 12661 encodes a 25-nt insertion near the 5' end of *pseD* that is not present in any of the other strains (Figure 4-5). Interestingly, this insertion included a 9-G homopolymeric (poly-G) tract. We analyzed the raw Illumina MiSeq reads from our recent whole genome sequence analysis of 12661 and indeed found variability in number of Gs at this locus, indicating that phase variability in *pseD* sequence could occur in this strain (data not shown).

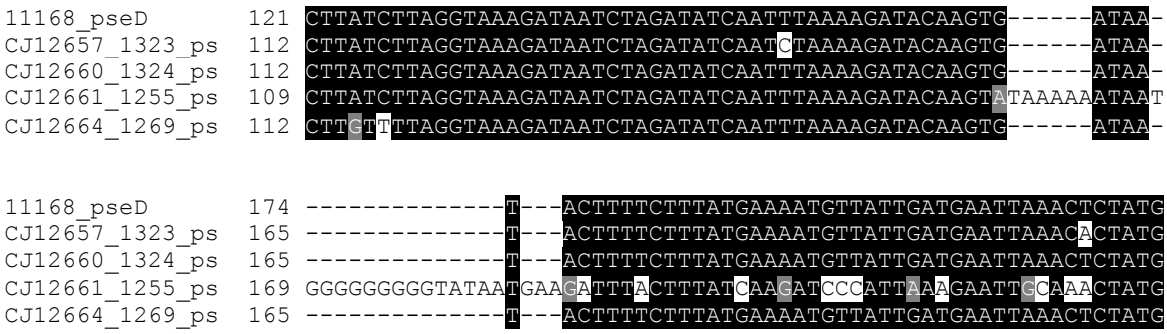

Figure 4-5. Strain 12661 harbours a poly-G tract-containing insertion in *pseD* that is not present in strains 11168, 12567, 12660, or 12664. Nucleotide sequence alignment of an internal region of *pseD* for all strains showing the 25 inserted nucleotides in strain 12661, 9 of which make up a poly-G tract.

4.3.7. Gp047 pressure does not select for *pseD* variants in 12661

To test the hypothesis that slipped strand mispairing in *pseD* at this region drives variation in 12661 binding to Gp047, we amplified the *pseD* region from five single colony isolates, from a mixed population of cells, and from purified genomic DNA, and used Sanger sequencing to determine the length of the poly-G tract in each. To ensure the region we were amplifying was *pseD* and not a homologous sequence, since *C. jejuni* strains tend to encode 6-7 highly similar

maf genes at the flagellar glycosylation locus, we designed our primers to amplify a region anchored within the gene (*ptmA*) upstream of *pseD*. We found that in all cases, the poly-G tract was in the "on" (9 Gs) state, suggesting in-frame expression of PseD.

Although we did not see evidence of poly-G tract phase variation occurring under normal growth conditions, we sought to determine whether the presence of Gp047 would provide a pressure for the strain to phase-vary its *pseD* at a higher frequency. We grew 12661 in the presence of Gp047 and amplified *pseD* from 12661 within and outside the spot of Gp047-induced clearing using colony PCR followed by Sanger sequencing. Sequence analysis of amplicons derived from Gp047-exposed cells (n=2) and Gp047-unexposed cells (n=3) showed that the poly-G tract remained phased-on in each case, with no apparent secondary peaks underneath the primary nucleotide called at each location; however, the small sample size does not rule out the possibility of phase-variation at this locus.

4.3.8. Oxonium ions of 317 and 332 m/z were detected on *C. jejuni* 12661 flagellin

Although phase variation at the poly-G tract within *pseD* may explain the variability in 12661 Gp047 binding, we also sought to test the hypothesis that other flagellar glycans might interfere with Gp047 recognition of the Pse5Ac7Am epitope in 12661. To test this hypothesis, we used high-resolution liquid chromatography with tandem mass spectrometry (LC-MS/MS) to identify and the compare the glycans present on 12661 flagella in its non-Gp047-binding state with those present on 11168 flagella. To do this, we used LC-MS/MS to analyze trypsin-digested flagella from 11168 and 12661.

To verify our methodology, we first examined 11168 flagellar glycans. Ulasi *et al*. (2015) previously reported four locations of O-glycosylation on *C. jejuni* 11168 FlaA: ^{180}IS*SGEVQFTLK^{191}, ^{204}VVISTSVGTGLGAL**EINK^{223}, ^{339}DIL*SG*****AGFG**SF^{357}, and ^{464}TT*FGVK^{470} [16]. In agreement with this prior report, we detected all four of the above peptides and identified several glycoforms for each (Figure 4-6, Figure 4-7). Also in agreement with this report, we detected oxonium ions corresponding to Pse5Ac7Ac (m/z= 317.134), Pse5Ac7Am (m/z = 316.150), DMGA-Pse5Ac7Ac (m/z = 391.164), and DMGA-Pse5Ac7Am (m/z=390.180) [16,18,54]. We also compared the relative glycan abundances at each location by comparing the relative peak intensities between the analyzed glycopeptides. We observed that for all four peptides, 3.81-16.44% of the glycan content corresponded to Pse5Ac7Ac, whereas 56.39-69.89% corresponded to Pse5Ac7Am, 2.64-10.41% corresponded to DMGA-Pse5Ac7Ac, and 12.01-23.65% corresponded to DMGA-Pse5Ac7Am (Figure 4-7).

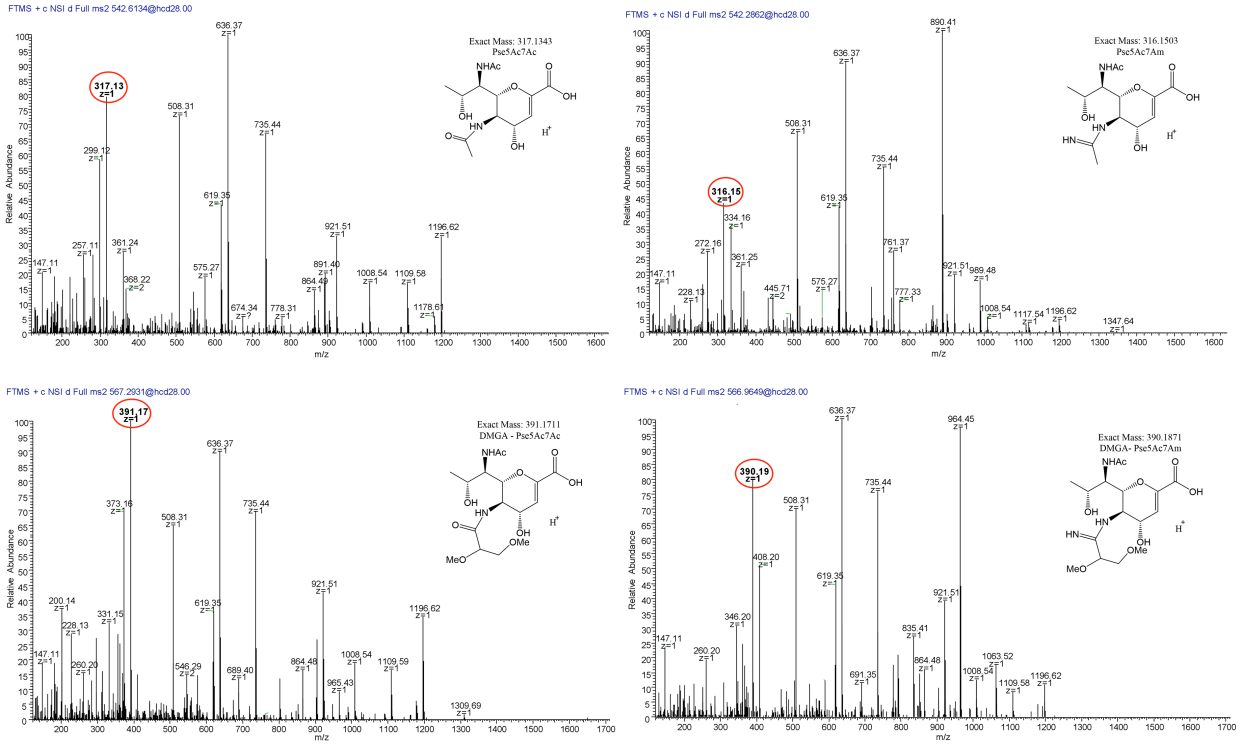

Figure 4-6. LC/MS-MS fragmentation spectra of trypsin-digested *C. jejuni* 11168 flagellar (FlaA) glycopeptide ^{180}ISTSGEVQFTLK^{191}. A) MS^2 spectrum of ^{180}ISTSGEVQFTLK^{191} + Pse5Ac7Ac (oxonium ion m/z = 317.13433) (A), ^{180}ISTSGEVQFTLK^{191} + Pse5Ac7Am (oxonium ion m/z = 316.15031) (B), ^{180}ISTSGEVQFTLK^{191} + DMGA-Pse5Ac7Ac (oxonium ion m/z = 391.17111) (C), ^{180}ISTSGEVQFTLK^{191} + DMGA-Pse5Ac7Am (oxonium ion m/z=390.18709) (D). Oxonium ions are circled, and proposed structures of monosaccharides are shown.

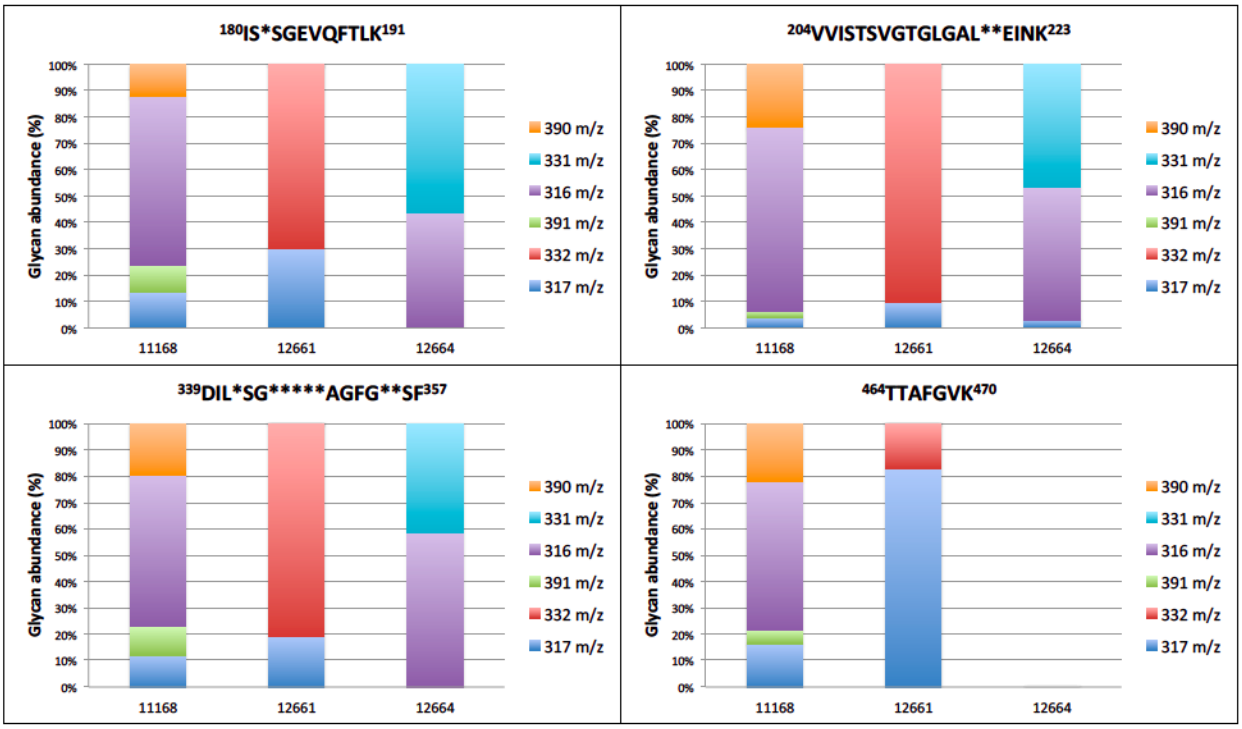

Figure 4-7. Percent relative abundance of flagellar glycans presented by *C. jejuni* 11168, 12661 and 12664 for four detected *C. jejuni* FlaA/FlaB peptides as determined by LC-MS/MS. In 12664, the 464-470 peptide was not detected, and thus no bar is depicted.

We next sought to analyze 12661 flagellar peptides. To confirm the non-Gp047-binding state of the 12661 population used for MS, we used Gp047 immunogold labeling/TEM as described above (data not shown). Our MS analysis of trypsin-digested 12661 flagellin resulted in the detection of the four peptides described for 11168, ^{180}IS*SGEVQFTLK^{191}, ^{204}VVISTSVGTGLGAL**EINK^{223}, ^{339}DIL*SG*****AGFG**SF^{357} and ^{464}TT*FGVK^{470} (Figure 4-8). Interestingly, we detected oxonium ions of m/z= 317.134, which corresponds to either Pse5Ac7Ac or Leg5Ac7Ac, and an oxonium ion of m/z = 332.145, which does not correspond to any known *Campylobacter* flagellar glycans, on all four peptides. Notably, we did not detect oxonium ions corresponding to Pse5Ac7Am, DMGA-Pse5Ac7Ac or DMGA-Pse5Ac7Am. In terms of relative glycan content, we observed that for the first three peptides, glycans corresponding to Pse5Ac7Ac/Leg5Ac7Ac made up 9.78-30.31% of the glycan content, whereas the remaining 69.69-90.22% of the glycan content corresponded to the uncharacterized glycan of m/z = 332.145 (Figure 4-7). However, the ^{464}TT*FGVK^{470} peptide displayed the opposite trend, with 83.00% of the glycan content corresponding to Pse5Ac7Ac/Leg5Ac7Ac and 17.00% corresponding to the glycan of m/z = 332.145.

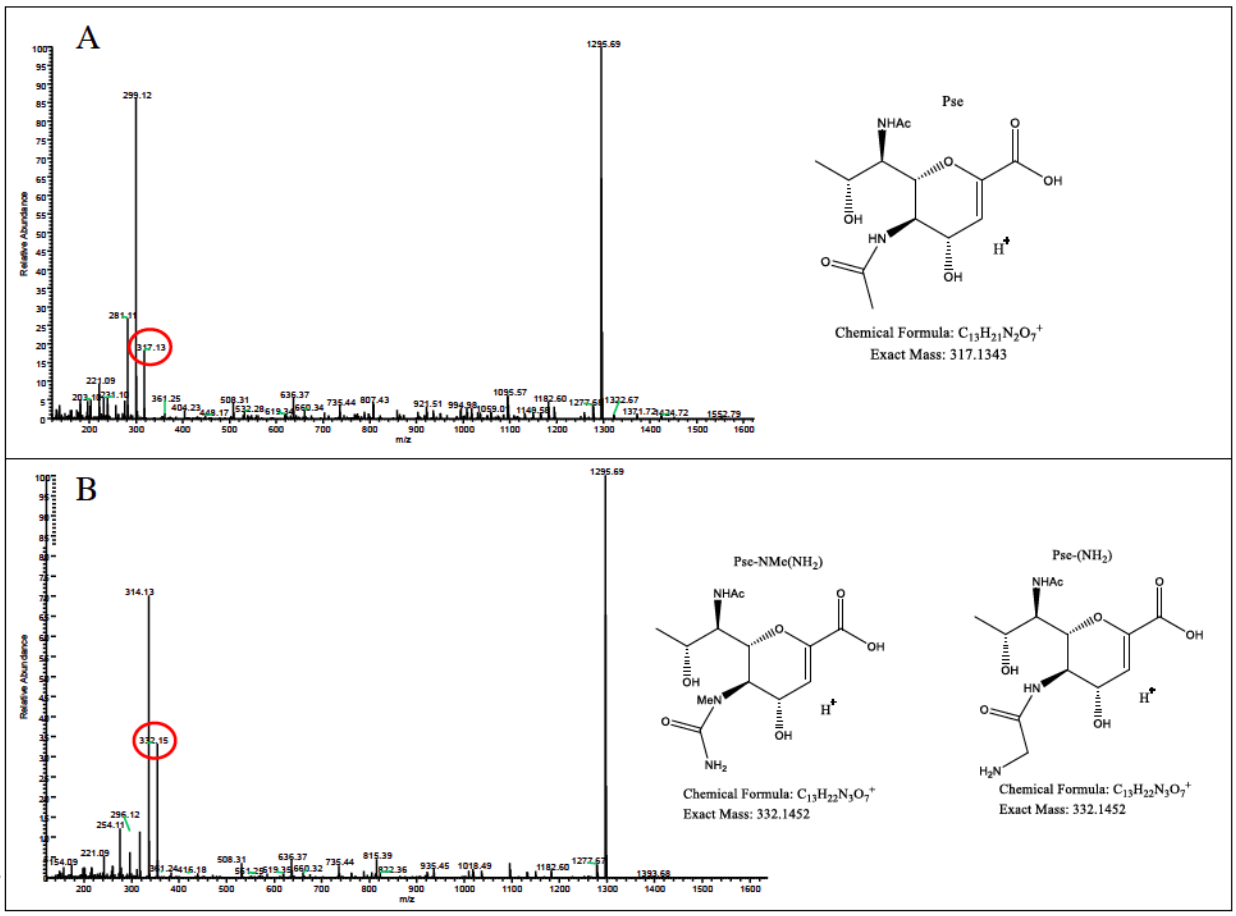

Figure 4-8. LC/MS-MS fragmentation spectra of trypsin-digested *C. jejuni* 12661 flagellar (FlaA) glycopeptide ^{180}ISSSGEVQFTLK^{191}. A) MS^2 spectrum of ^{180}ISSSGEVQFTLK^{191} + a glycan of oxonium ion m/z = 317.1343 ($C_{13}H_{21}O_7N_2^+$), B) MS^2 spectrum of ^{180}ISSSGEVQFTLK^{191} + a glycan of oxonium ion m/z = 332.14529 ($C_{13}H_{22}O_7N_3^+$). Oxonium ions are circled, and proposed structures of monosaccharides are shown.

4.3.9. Oxonium ions of 316 and 331 m/z were detected on *C. jejuni* 12664 flagellin

To test whether 12664 flagellin, which does not bind Gp047, also lacks Pse5Ac7Am, we analyzed 12664 flagella by LC/MS-MS. We detected the first three peptides described above, but not the ^{464}TT*FGVK^{470} peptide, so its glycan profile could not be determined (Figure 4-9,

Figure 4-7). Interestingly, upon analysis of the remaining three peptides, we detected oxonium ions of m/z = 316.15031, which corresponds to either Pse5Ac7Am or Leg5Am7Ac, and m/z = 331.1612, which has not been shown to correspond to a known glycan. However, we did not detect the DMGA derivatives DMGA-Pse5Ac7Ac or DMGA-Pse5Ac7Am. In terms of glycan content, the glycan corresponding to Pse5Ac7Am/Leg5Am7Ac was 43.86-58.60% abundant, whereas the glycan of m/z = 331 was 41.40-56.14% abundant. Also, the glycan corresponding to Pse5Ac7Ac/Leg5Ac7Ac was 3.17% abundant on the ^{204}VVISTSVGTGLGAL**EINK^{223} peptide only, but was not detected on the others.

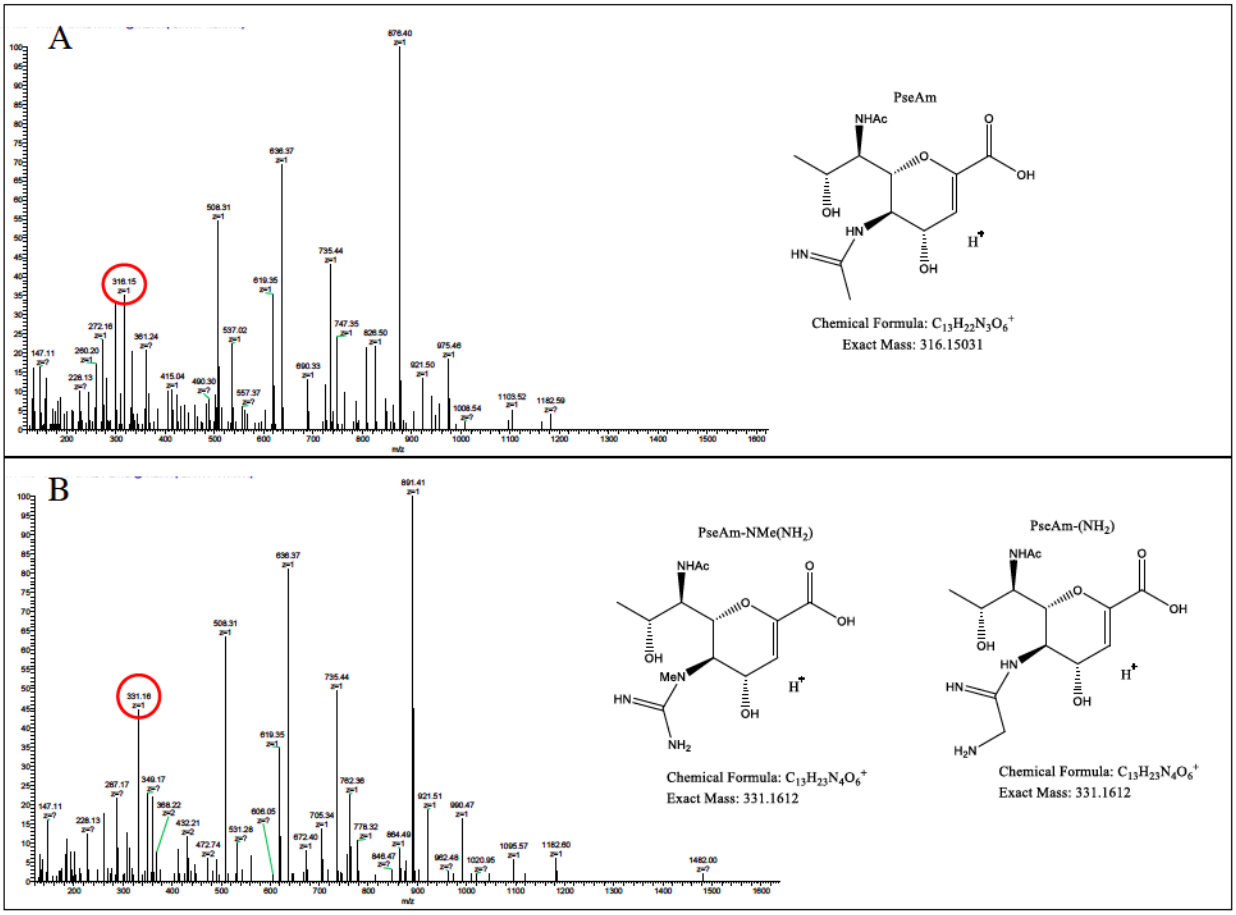

Figure 4-9. MS^2 fragmentation spectra of trypsin-digested *C. jejuni* 12664 flagellar glycopeptide ^{180}ISSSGEVQFTLK^{191}. A) MS^2 spectrum of ^{180}ISSSGEVQFTLK^{191} + a glycan of

oxonium ion m/z = 316.15031 ($C_{13}H_{22}O_6N_3^+$), B) MS^2 spectrum of ^{180}ISSSGEVQFTLK^{191} + a glycan of oxonium ion m/z = 331.1612 ($C_{13}H_{23}O_6N_4^+$). Oxonium ions are circled, and proposed structures of monosaccharides are shown.

4.3.10. Gp047 binding to *C. jejuni* 11168 flagellar glycans does not require di-*O*-methylglyceric acid (DMGA)

To rule out the possibility that the lack of DMGA-glycans was the reason for the lack of Gp047 binding in 12664 and 12661, we sought to determine whether Gp047 binding requires DMGA in addition to the 7-acetamidino group on Pse5Ac7Am in 11168. Importantly, this possibility had not been ruled out by our previous studies, since both DMGA- and DMGA-free versions of this glycan are lost when *pseA* is deleted to generate a Gp047 binding-negative strain. Furthermore, when we complemented this gene with a functional copy of *pseA* and restored binding, only the DMGA-containing versions of Pse5Ac7Ac and Pse5Ac7Am returned (Javed *et al.*, unpublished data). Hitchen *et al.* (2010) have shown that a *cj1295* mutant in *C. jejuni* 11168 is unable to synthesize DMGA-Pse5Ac7Ac or DMGA-Pse5Ac7Am [29]. We therefore generated a *cj1295* mutant in 11168 and used immunogold labeling/TEM to test whether Gp047 binding still occurred in this strain. We found no difference in Gp047 binding between the *cj1295* mutant and wild type cells (Figure 4-10), suggesting that DMGA is not required for Gp047 binding to *C. jejuni* flagella.

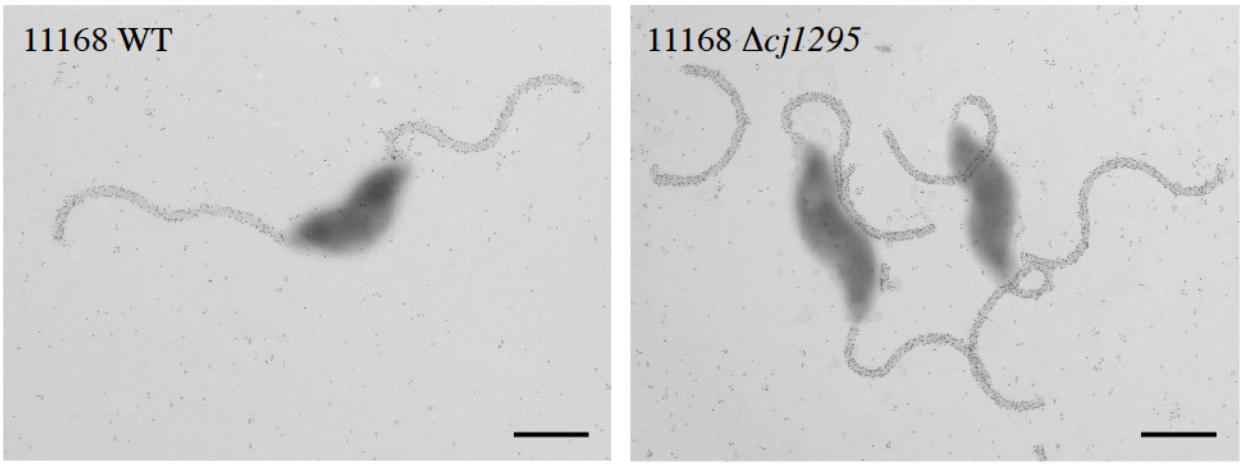

Figure 4-10. Transmission electron micrographs of Gp047-labeled *C. jejuni* 11168 and 11168Δ *cj1295*. Images are representative of experiments were done in duplicate. Scale bars represent 800 nm.

4.3.11. Differences in DUF2920-containing and *maf* genes may contribute to flagellar glycan differences between 11168, 12661 and 12664

To better understand the genetic basis for the observed differences in flagellar glycans detected on 11168, 12661 and 12664 flagella, we examined the differences in gene content in the flagellar glycosylation loci. We hypothesized that 12661 and 12664 would encode additional genes not encoded by 11168 that might explain their display of glycans of m/z = 332 and 331 glycans, respectively. Notably, both m/z values represent a gain of 15 Da relative to the other glycans present on flagella from each strain (m/z = 317 and 316, respectively). We thus hypothesized that an amine group (NH_2, 16 Da) might substitute for a hydrogen atom on the Pse/Leg glycans corresponding to these masses, and lead to the mass predicted for the uncharacterized glycan expressed by each strain. We therefore examined the genes that were

only present in 12661 and 12664 to see if any could encode an aminotransferase. However, none were found.

To identify candidate genes that might be involved in synthesis of the glycans of m/z = 332 and 331, we examined other differences in gene content between 12664, 12661 and 11168. In particular, we noted 12661- and 12664-specific differences in the number and location of genes containing a DUF2920 domain (DUF = domain of unknown function) (Figure 4-4, Regions C, D and I). In 12664, we noted the unique presence of a DUF2920-containing gene, *CJ12664_1248,* just downstream of the identically annotated *cj1310c* (Figure 4-4, Region D). In addition, we found that 12664 encodes another DUF2920-containing gene, *CJ12664_1277*, just upstream of *maf4* (*cj1340c*) (Figure 4-4, Region I), and we found that 12661 also encoded this second DUF2920-containing gene (*CJ12661_1263)*. However, strain 12661 is also missing the DUF2920-containing gene *cj1306* (Figure 4-4, Region C). Notably, whereas strains 11168 and 12664 encode a poly-G tract in *cj1305c*, another DUF2920-containing gene, a G to A transition disrupts the poly-G tract in strain 12661.

We also noted 12661- and 12664-specific differences in *maf* gene content, including differences in distribution of poly-G tracts among these genes. For instance, strain 12664 lacks the motility associated factor *maf5* (*cj1341c*), whereas *maf6* (*cj1342c*) is missing from both 12664 and 12661, relative to 11168 (Figure 4-4, Region I). As well, the poly-G tract in *maf2* present in strains 11168 and 12664 is absent in 12661. Other differences among the flagellar glycosylation loci included the fact that 12664 uniquely lacks the *fkbH* domain-containing gene *cj1302*

(Figure 4-4, Region B) (it is present as a pseudogene). In addition, 12661 uniquely lacks *cj1301,* which is annotated as an epimerase (Figure 4-4, Region B).

4.4. Discussion

C. jejuni flagellar glycosylation is essential for motility and virulence, but little is known about the mechanisms driving glycan diversity in this organism. Recent work involving experimental *C. jejuni* infection in humans has linked flagellar glycosylation gene variation to both the severity and persistence of *C. jejuni*-induced diarrheal disease [55]. In this study, a single *C. jejuni* strain was used to infect several volunteers, and whole genome sequencing of isolates from subjects who experienced severe and/or recurrent infections revealed an enrichment of *pseD* gene variants. Enrichment of variants in other flagellar glycosylation loci was also observed, suggesting that variation at this locus may be important in *C. jejuni* pathogenesis in humans.

Campylobacter infections are also associated with a number of post-diarrheal complications worldwide, including recurrent diarrhea, Guillain-Barré, irritable bowel syndrome and growth stunting [4,56–59]. *C. jejuni* is proposed to vary its glycans in response to host immune responses and to phages, but much remains to be understood about the mechanisms governing flagellar glycosylation variation in this organism. As well, whereas flagellar glycan structures have been well characterized for *C. jejuni* strains 11168 and 81-176 and *C. coli* VC167, the extent of strain-to-strain variation among these glycosylation pathways is poorly understood.

We previously described that Gp047, a protein encoded by all *C. jejuni* phages characterized to date, causes growth inhibition of *C. jejuni* 11168 by binding to its flagella [33]. We identified the receptor for Gp047 to be specifically Pse5Ac7Am [42]. We found that Gp047 bound to over 95% of tested *C. jejuni* strains and over 90% of tested *C. coli* strains, suggesting widespread prevalence of Pse5Ac7Am [35]. This glycan in particular has been shown to contribute to autoagglutination, microcolony formation, adherence, invasion, and virulence in a ferret model [26].

It is generally assumed that *C. jejuni,* like other bacteria, naturally coexists with phages in the environments it colonizes, such as the chicken gastrointestinal tract [60]. Therefore, based on the prevalence of *gp047* homologues in *Campylobacter* phages and the importance of both flagellar glycan variation and of Pse5Ac7Am expression in virulence, we hypothesized that Gp047 might represent a selective pressure that contributes to *C. jejuni* flagellar glycan variation. We therefore sought to characterize both the mechanism of Gp047-induced clearance of *C. jejuni* cells and the mechanism(s) by which *C. jejuni* is able to avoid this activity.

Other organisms, such as *Bacillus subtilis*, alter biofilm-related gene expression in response to flagellar binding, either by an antibody or by a surface [61,62]. *C. jejuni* has previously been shown to alter its protein expression during biofilm association, and thus it too may sense and respond to surface contact [63]. We hypothesized that *C. jejuni* might alter its gene expression in response to Gp047 binding. To test this, we analyzed cells treated with Gp047 by RNA-seq, and found that genes involved in the TCA cycle, oxidative phosphorylation, and carbon metabolism were down-regulated upon Gp047 treatment. We have yet to establish whether this

change in gene expression explains the reduction in growth upon Gp047 treatment that we have observed.

We next sought to examine the mechanism by which Gp047 might transmit a signal through the flagella that could lead to the observed gene expression changes. The *Campylobacter* flagellar motor is driven by the PMF, and *C. jejuni* cells are known to modulate their swimming speed according to viscosity by altering proton flow through the flagellar motor channel, which has been shown to increase flagellar torque in other flagellated bacteria [64,65]. We therefore hypothesized that the observed Gp047-induced growth effects might induce the flagellar motor complex to increase proton flow through the motor channel, perhaps as a way of compensating for increased drag or inhibition of flagellar rotation. This would presumably disrupt PMF homeostasis in the cell, which could explain the observed growth inhibition. Interestingly, we determined that Gp047 growth clearance activity does require flagellar motor function by showing that Gp047 is unable to clear growth of *motA* or *motB* mutants, which provides support for this hypothesis. However, further work is required to demonstrate that Gp047 binding to motile flagella indeed causes increased proton flow and PMF disruption, and to determine whether this disruption is responsible for the growth clearance effect observed. If this is found to be the case, further work will be required to determine why *Campylobacter* phages encode a protein with this activity. It is intriguing to speculate that *Campylobacter* phages may encode Gp047 in order to modify PMF in a way that favors phage DNA injection, as has been shown for T4 phage [66].

To better understand how *C. jejuni* might escape Gp047 binding that it might encounter in nature, we characterized a group of *C. jejuni* strains with varying susceptibility to Gp047-induced growth clearance. We hypothesized that cells might resist Gp047 activity by avoiding binding by the protein, either by not encoding Pse5Ac7Am at all, by encoding mechanisms of downregulating or off-switching their Pse5Ac7Am expression, or by expressing other glycans able to render Pse5Ac7Am unrecognizable to Gp047. We first used immunogold labeling and TEM to visualize Gp047 binding to five *C. jejuni* strains displaying reduced Gp047 clearing compared to strain 11168. Indeed, we found significant strain-to-strain variation in the level of Gp047 binding. Interestingly, we showed that Gp047 binding levels approximately correlated with levels of Gp047-induced clearing, supporting the hypothesis that these strains likely resist Gp047 clearing by expressing flagella reduced in Gp047 binding.

One possible explanation for the observed strain variation in Gp047 binding is that different strains express varying quantities of Pse5Ac7Am on their flagella, and that strains with reduced Gp047 binding simply express less Pse5Ac7Am. To evaluate this possibility, we first compared the flagellar glycosylation gene loci of each strain to that of 11168, which is robustly bound and cleared by Gp047. We found that the flagellar glycosylation loci of all strains were similar to that of 11168, with each strain encoding all genes required to synthesize Pse5Ac7Am. However, strains 12661 and 12664 clustered separately from the other strains according to their PseD sequence (Figure 4-S1). PseD is thought to be required for Pse5Ac7Am transfer onto flagellin, as this glycan was not detected on the flagella of a *pseD* mutant in *C. jejuni* strain 81-176, and yet Pse5Ac7Am was still found to accumulate in the cytosol of this mutant [13,26]. It is therefore plausible that sequence differences in PseD in strains 12661 and 12664 might lead to

changes in Pse5Ac7Am that could explain the reduced Gp047 binding to these two strains. For instance, PseD sequence differences could alter its efficiency or specificity, which could lead to the transfer of different sugars or of different amounts of Pse5Ac7Am. Interestingly, we found that 12661, which displays variability in its Gp047 binding, was uniquely found to encode a phase-variable poly-G tract in *pseD*. However, we have not yet identified conditions that select for phase variation at this poly-G tract. Interestingly, polymorphisms in *pseD* have been implicated in *C. jejuni* persistence in humans, and thus this additional insight into the regulation of its expression represents important new information that may inform future *C. jejuni* biocontrol strategies [55].

In addition to the possibility that PseD sequence differences may lead to differences in Gp047 binding observed for strains 12661 and 12664, strain differences in *maf* gene content and/or organization could explain the differences observed. Several paralogues of *pseD,* which include the *maf* genes (*maf1* through *maf6*)*,* and *pseE,* are encoded in the flagellar glycosylation locus of all strains examined here, and it is unknown to what extent these homologues might compensate for one another. For instance, others have shown that *maf1,* which is phase-variable, can compensate for a *maf5* mutant in *C. jejuni* strain 11168 [52]. Furthermore, the strains examined here display differences in *maf* gene content, in presence/absence of phase-variable tracts within encoded *maf* genes, and in the organization of the *maf* genes relative to other genes in the flagellar glycosylation locus. It is also unknown to what extent recombination at the flagellar glycosylation locus might influence *maf* gene expression, which may also contribute to the differences in Pse5Ac7Am display on flagella observed for the strains characterized here. In fact, we and others have previously reported evidence of *pseD* recombination following three

separate sequencing efforts of 12661 propagated in different labs over time [43]. Indeed, accurate assembly of sequencing reads spanning the *C. jejuni* flagellar glycosylation locus has proved challenging in the past due to repetitive regions (William Miller, personal communication). Overall, further work is required to understand the role of *pseD* and the other *maf* genes in Gp047 susceptibility, but the work of others supporting a role for *pseD* in Pse5Ac7Am transfer to flagella, the PseD sequence divergence observed here, and the different properties and combinations of the other *maf* paralogues in these strains points to this gene family as an attractive target for future study.

To determine whether strains exhibiting less Gp047 binding/clearing in fact expressed less Pse5Ac7Am, and/or expressed glycans that might interfere with Gp047 recognition of the Pse5Ac7Am epitope, we used MS to analyze the flagellar glycan structures of strains that showed reduced Gp047 binding (ie. 12661 [in its non-binding state] and 12664) compared to 11168. We found that 12661 expressed oxonium ions of m/z = 317 and 332, indicating that this strain likely expresses either Pse5Ac7Ac or Leg5Ac7Ac (which both have oxonium ions of m/z = 317). Oxonium ions of m/z = 332 have not previously been identified on *Campylobacter* flagella. As this mass is equal to 317 + 15, we propose that the m/z = 332 oxonium ion may correspond to Pse5Ac7Ac/Leg5Ac7Ac with the addition of an amine group (NH_2, 16 Da) in place of a hydrogen atom. Further work into understanding the nature, biological effect(s) and distribution of this novel glycan in *C. jejuni* may lead to interesting insights into the biology of the organism. Interestingly, the oxonium ion corresponding to Pse5Ac7Am (m/z = 316), the known receptor for Gp047, was not identified on 12661 flagella, providing a likely explanation for why 12661 does not bind Gp047 in this state. It is possible that as we suggested above, *pseD*

phase-variation may be responsible for this observation, but further work is required to fully evaluate this hypothesis.

Our analysis of 12664 flagellar glycans revealed oxonium ions of m/z = 316 and 331, indicating that this strain likely expresses either Pse5Ac7Am or Leg5Ac7Am (m/z = 316). Similar to the oxonium ion of 332 m/z described above for 12661, oxonium ions of m/z = 331 have not previously been identified on *Campylobacter* flagella. It is interesting that this m/z is equal to 316 + 15, which mirrors what we observed for 12661; in both cases, an oxonium ion corresponding to a commonly observed *Campylobacter* flagellar glycan was observed, as was a glycan with a m/z of this oxonium ion plus 15. This suggests that in both strains, the same chemical group may be added to either Pse5Ac7Ac/Pse5Ac7Am (or to the Leg equivalents of these sugars). We therefore propose that the m/z = 331 oxonium ion identified on 12664 flagellar glycopeptides may correspond to Pse5Ac7Am/Leg5Ac7Am with the addition of an amine group (NH_2). The identification of the oxonium ion corresponding to Pse5Ac7Am (m/z = 316), the known receptor for Gp047, on 12664 flagella was unexpected, given that Gp047 does not bind to this strain. It is possible that this oxonium ion corresponds not to Pse5Ac7Am, but instead to Leg5Am7Ac; we previously described that Leg5Am7Ac displayed on *C. coli* VC167 flagella was insufficient for Gp047 binding [32]. We are currently in the process of obtaining sufficient quantities of 12664 flagellar glycopeptides by NMR in order to conclusively show that the m/z = 316 glycan in this strain is indeed Leg5Am7Ac. Importantly, strain 12664 encodes the genes (*cj1321-1325/6*) previously shown by Howard *et al.* (2009) to be involved in Leg5Am7Ac synthesis [20]. In contrast, strain 12661 does not encode this locus, which would support why we did not detect ions of m/z = 316 on its flagella if in fact the ion of m/z = 316

indeed represents Leg5Am7Ac. However, if indeed Leg5Am7Ac replaces Pse5Ac7Am on 12664 flagella, which would explain its lack of Gp047 binding, it would call to question why Pse5Ac7Am is not also present. Strain 12664 encodes all genes required for Pse5Ac7Am synthesis and transfer, and 12664 does not encode a phase variable version of *pseD,* as we observed for 12661, negating *pseD* off-switching as an explanation for the absence of Pse5Ac7Am. It is possible that both Pse and Leg versions of the m/z = 316 ion might thus be present on 12664 flagella, perhaps indicating that instead, the glycan of m/z = 331 may shield flagella from Gp047 binding. Further work into understanding the mechanism behind the observed lack of Gp047 binding in this strain, in addition to the biology of the glycan of oxonium m/z = 331, is thus required.

It was notable that both 12661 and 12664 flagella lacked any oxonium ions corresponding to the DMGA-containing sugars found on 11168 flagella (m/z = 391 and 390). We thus mutagenized *cj1295*, which was shown to be responsible for DMGA-Pse5Ac7Ac and DMGA-Pse5Ac7Am synthesis in *C. jejuni* 11168 [29], and verified whether the mutant was still recognized by Gp047. As we observed no difference in Gp047 binding to 11168 compared to the *cj1295* mutant, we concluded that DMGA is not part of the Pse5Ac7Am binding epitope required for Gp047 binding to flagella. However, 12661 and 12664 both encode versions of *cj1295* (*cj12661_1226* and *cj12664_1233*), and therefore they would have both been expected to produce DMGA-linked Pse glycans. As *cj1295* encodes a phase-variable poly-G tract, we hypothesize that this gene may have been phased-off in 12661 and 12664 populations used for flagellar extraction in our experiments. Upon analysis of the Illumina sequence data upon whole-genome sequencing, we observed this gene to be predominantly on-switched in 12664

and approximately 50% on, 50% off in 12661. However, it is possible that this gene was switched off between the time of sequencing and the time of flagellar extraction. Alternatively, it is possible that other genes encoded by these strains play roles in DMGA display or regulation, and that expression of a *cj1295* homologue alone may not be sufficient to result in DMGA-glycan expression in these strains.

As strains 12661 and 12664 both encode glycans not previously observed on *Campylobacter* flagella, we sought to understand how these glycans might be synthesized. To identify candidate genes that might be involved in this process, we compared the flagellar glycosylation loci among 12661, 12664 and 11168. The main differences we observed were in number and location of *maf* and DUF2920-containing genes. Importantly, whether or not these genes displayed poly-G tracts varied among strains, as did the number of paralogues encoded of each gene family by each strain. We thus hypothesized that these gene families might be important in explaining the differing Gp047 susceptibilities among strains.

Based on their co-localization on the chromosome with other flagellar glycosylation genes, others have mutagenized certain *maf* genes and tested the effects of these mutations on flagellar properties [26,52,53,69]. Phenotypes have been identified for some of the *maf* genes, including *pseD* (previously *maf2*) and *pseE* (previously *maf5*) in *C. jejuni* 81-176 and 11168 (involved in Pse5Ac7Am and Pse5Ac7Ac transfer to flagellin, respectively) and *maf4* in *C. jejuni* 108 (involved in transfer of CO_2 or $C_2H_2O_2$ to Pse5Ac7Ac), but other *maf* genes have been mutagenized without discernable phenotype [13,26,52,69]. The fact that some *maf* genes likely

compensate for one another [52] could explain the lack of mutant phenotypes observed for some *maf* mutants.

As for DUF2920 genes, there has been some work into mutagenizing these in *C. jejuni* as well, including mutagenesis of the *cj1305c* homologue in *C. jejuni* 81-176, but similarly, no phenotypes were observed [26]. It is at this point unclear whether copy number of DUF2920 and *maf* genes plays a role in *C. jejuni* flagellar glycosylation, but the fact that the presence and sequence of genes from these two families constitute the main genetic differences at the flagellar glycosylation loci in 12661, 12664 and 11168, which we have shown display distinct flagellar glycan profiles, suggests that they do play an important role in flagellar glycosylation in *C. jejuni.* Alternatively, the genes important for the differences in Gp047 susceptibility among these strains could be located outside the flagellar glycosylation locus. Indeed, most genes involved in flagellar biogenesis, as well as some predicted to be involved in flagellar glycosylation, have been shown to be encoded outside this locus [52,55,70].

4.5. Conclusions

Overall, we have provided additional characterization of the previously observed growth clearance phenotype induced by the conserved *Campylobacter* phage-encoded protein, Gp047 [33]. We have shown that incubation with this protein induces changes in expression of energy metabolism genes in *C. jejuni* 11168, and that motile flagella are required for this phenotype. This suggests that upon Gp047 binding, the flagellar motor may transmit a signal to the cell to downshift its energy metabolism.

We also characterized *C. jejuni* strains naturally resistant to Gp047 clearing and found that strain heterogeneity in Gp047 binding likely explains this resistance. We found that different sequences and combinations of encoded *maf* and DUF2920-containing genes constitute the main differences between Gp047-resistant strains and 11168, highlighting these genes as important future targets for flagellar glycosylation studies. We also identified a transiently Gp047-resistant strain, 12661, and found that it in its Gp047-resistant state, this strain does not display Pse5Ac7Am, the receptor for Gp047, on its flagella. Interestingly, we found that this strain encodes a potentially phase-variable tract in *pseD,* the putative transferase for Pse5Ac7Am, which has not previously been reported to be phase-variable in *C. jejuni.* We also found that strains 12661 and another Gp047-resistant strain, 12664, each display a glycan not previously observed on *Campylobacter* flagella. The chemical structures of the unusual flagellar glycans produced by 12661 and 12664 strains, as well as the biological impacts of displaying these glycans, are interesting questions that remain to be pursued.

Together our results add to the current understanding of the interplay between *C. jejuni* and the phage-encoded flagellar glycan binding protein Gp047, and suggest that *C. jejuni* encodes as-yet uncharacterized mechanisms for flagellar glycosylation diversity. This study also highlights the utility of phage proteins as probes to rapidly and inexpensively identify subtle differences in bacterial glycans that lead to novel insights into bacterial glycobiology.

4.5. Supplementary data

A

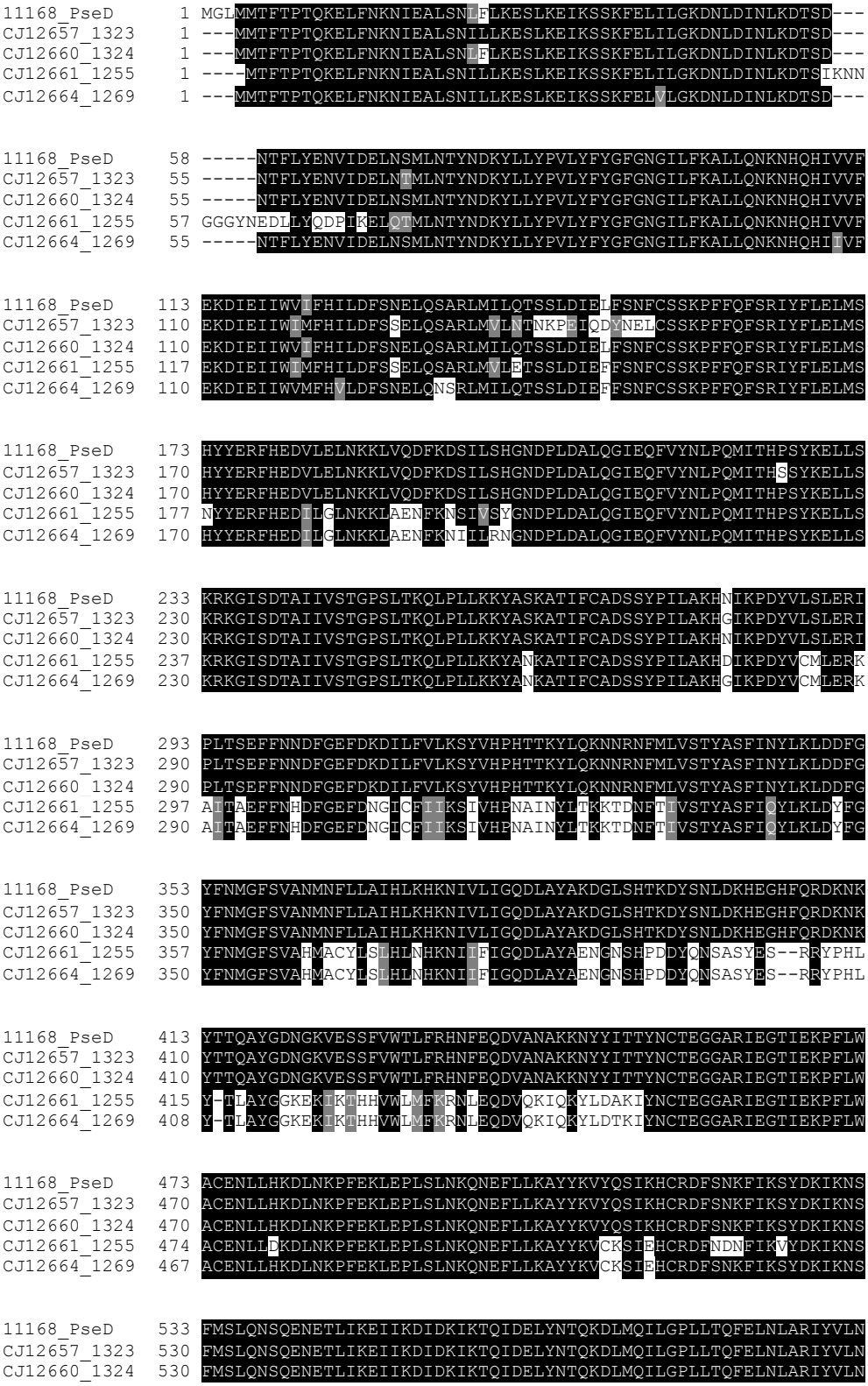

B

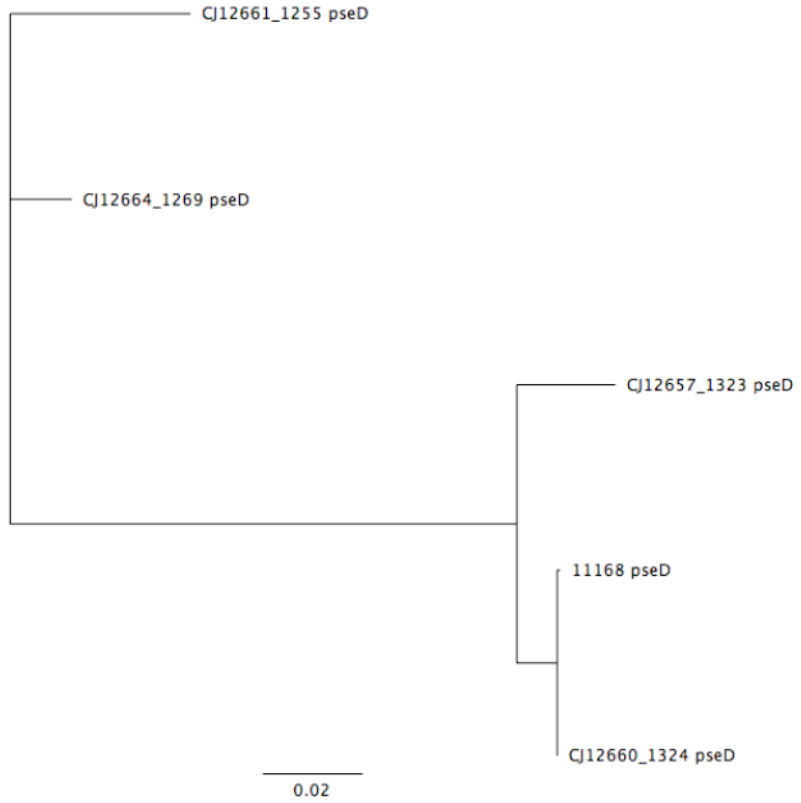

Figure 4-S1. PseD amino acid sequence alignment (**A**) and a phylogenetic tree (**B**) depicting the relationship between PseD between the five strains.

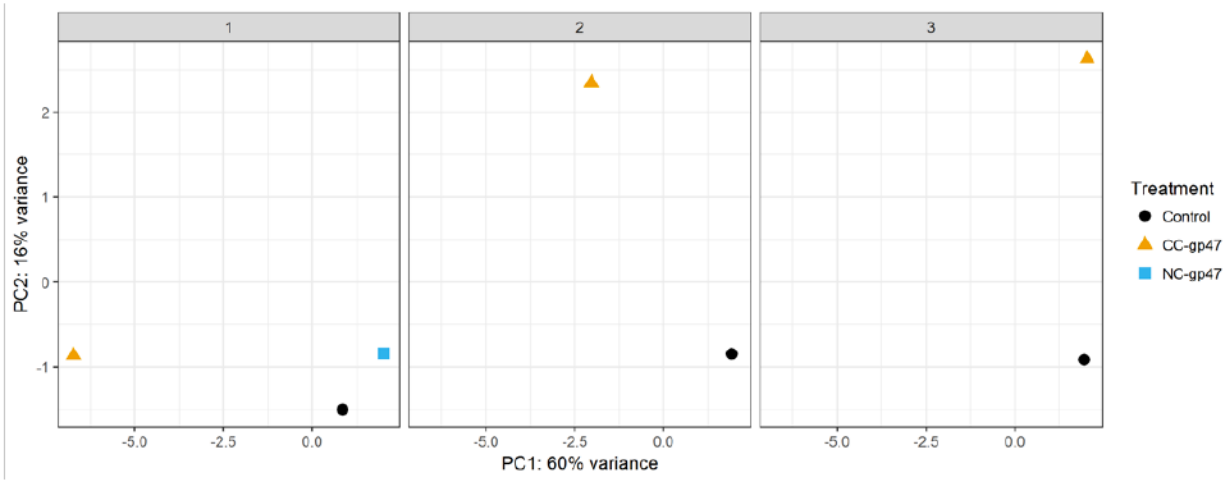

Figure 4-S2. Principal component analysis of differentially expressed *C. jejuni* 11168 genes 30 min following exposure to CC-Gp047, NC-Gp047 or a buffer control. Plots were generated using the data from the 500 genes with the greatest variation in expression across samples.

4.6. References

1. Heras, B.; Scanlon, M. J.; Martin, J. L. Targeting virulence not viability in the search for future antibacterials. *Br. J. Clin. Pharmacol.* **2015**, doi:10.1111/bcp.12356.
2. O'Neill, J. O. Antimicrobial Resistance: Tackling a crisis for the health and wealth of nations The Review on Antimicrobial Resistance Chaired. **2014**.
3. Bolton, D. J. *Campylobacter* virulence and survival factors. *Food Microbiol.* 2015, *48*, 99–108.
4. Amour, C.; Gratz, J.; Mduma, E.; Svensen, E.; Rogawski, E. T.; McGrath, M.; Seidman, J. C.; McCormick, B. J. J. J.; Shrestha, S.; Samie, A.; Mahfuz, M.; Qureshi, S.; Hotwani, A.; Babji, S.; Trigoso, D. R.; Lima, A. A. M. M.; Bodhidatta, L.; Bessong, P.; Ahmed, T.; Shakoor, S.; Kang, G.; Kosek, M.; Guerrant, R. L.; Lang, D.; Gottlieb, M.; Houpt, E. R.; Platts-Mills, J. A.; Etiology, Risk Factors, and Interactions of Enteric Infections and Malnutrition and the Consequences for Child Health and Development Project (MAL-ED) Network Investigators Epidemiology and Impact of *Campylobacter* Infection in Children in 8 Low-Resource Settings: Results from the MAL-ED Study. *Clin. Infect. Dis.* **2016**, *63*, 1171–1179, doi:10.1093/cid/ciw542.
5. Guerry, P. *Campylobacter* flagella: not just for motility. *Trends Microbiol.* 2007, *15*, 456–461.
6. Logan, S. M. Flagellar glycosylation - A new component of the motility repertoire?

Microbiology 2006, *152*, 1249–1262.

7. Guerry, P.; Szymanski, C. M. *Campylobacter* sugars sticking out. **2008**, doi:10.1016/j.tim.2008.07.002.
8. Schirm, M.; Arora, S. K.; Verma, A.; Vinogradov, E.; Thibault, P.; Ramphal, R.; Logan, S. M. Structural and Genetic Characterization of Glycosylation of Type a Flagellin in *Pseudomonas aeruginosa*. *J. Bacteriol.* **2004**, *186*, 2523–2531, doi:10.1128/JB.186.9.2523-2531.2004.
9. Goon, S.; Kelly, J. F.; Logan, S. M.; Ewing, C. P.; Guerry, P. Pseudaminic acid, the major modification on *Campylobacter* flagellin, is synthesized via the Cj1293 gene. *Mol. Microbiol.* **2003**, *50*, 659–671, doi:10.1046/j.1365-2958.2003.03725.x.
10. Logan, S. M.; Kelly, J. F.; Thibault, P.; Ewing, C. P.; Guerry, P. Structural heterogeneity of carbohydrate modifications affects serospecificity of *Campylobacter* flagellins. *Mol. Microbiol.* **2002**, *46*, 587–597, doi:10.1046/j.1365-2958.2002.03185.x.
11. Schirm, M.; Soo, E. C.; Aubry, A. J.; Austin, J.; Thibault, P.; Logan, S. M. Structural, genetic and functional characterization of the flagellin glycosylation process in *Helicobacter pylori*. *Mol. Microbiol.* **2003**, *48*, 1579–1592, doi:10.1046/j.1365-2958.2003.03527.x.
12. Schirm, M.; Schoenhofen, I. C.; Logan, S. M.; Waldron, K. C.; Thibault, P. Identification of unusual bacterial glycosylation by tandem mass spectrometry analyses of intact proteins. *Anal. Chem.* **2005**, *77*, 7774–7782, doi:10.1021/ac051316y.
13. McNally, D. J.; Hui, J. P. M.; Aubry, A. J.; Mui, K. K. K.; Guerry, P.; Brisson, J. R.; Logan, S. M.; Soo, E. C. Functional characterization of the flagellar glycosylation locus in *Campylobacter jejuni* 81-176 using a focused metabolomics approach. *J. Biol. Chem.*

2006, *281*, 18489–18498, doi:10.1074/jbc.M603777200.

14. McNally, D. J.; Aubry, A. J.; Hui, J. P.; Khieu, N. H.; Whitfield, D.; Ewing, C. P.; Guerry, P.; Brisson, J. R.; Logan, S. M.; Soo, E. C. Targeted metabolomics analysis of *Campylobacter coli* VC167 reveals legionaminic acid derivatives as novel flagellar glycans. *J. Biol. Chem.* **2007**, *282*, 14463–14475, doi:10.1074/jbc.M611027200.
15. Ewing, C. P.; Andreishcheva, E.; Guerry, P. Functional characterization of flagellin glycosylation in *Campylobacter jejuni* 81-176. *J. Bacteriol.* **2009**, *191*, 7086–7093, doi:10.1128/JB.00378-09.
16. Ulasi, G. N.; Creese, A. J.; Hui, S. X.; Penn, C. W.; Cooper, H. J. Comprehensive mapping of O-glycosylation in flagellin from *Campylobacter jejuni* 11168: A multienzyme differential ion mobility mass spectrometry approach. *Proteomics* **2015**, *15*, 2733–2745, doi:10.1002/pmic.201400533.
17. Zebian, N.; Merkx-Jacques, A.; Pittock, P. P.; Houle, S.; Dozois, C. M.; Lajoie, G. A.; Creuzenet, C. Comprehensive analysis of flagellin glycosylation in *Campylobacter jejuni* NCTC 11168 reveals incorporation of legionaminic acid and its importance for host colonization. *Glycobiology* **2016**, *26*, 386–397, doi:10.1093/glycob/cwv104.
18. Zampronio, C. G.; Blackwell, G.; Penn, C. W.; Cooper, H. J. Novel glycosylation sites localized in *Campylobacter jejuni* flagellin FlaA by liquid chromatography electron capture dissociation tandem mass spectrometry. *J. Proteome Res.* **2011**, *10*, 1238–1245, doi:10.1021/pr101021c.
19. Guerry, P.; Alm, R. A.; Power, M. E.; Logan, S. M.; Trust, T. J. Role of two flagellin genes in *Campylobacter* motility. *J. Bacteriol.* **1991**, *173*, 4757–4764.
20. Howard, S. L.; Jagannathan, A.; Soo, E. C.; Hui, J. P. M.; Aubry, A. J.; Ahmed, I.;

Karlyshev, A.; Kelly, J. F.; Jones, M. A.; Stevens, M. P.; Logan, S. M.; Wren, B. W. *Campylobacter jejuni* glycosylation island important in cell charge, legionaminic acid biosynthesis, and colonization of chickens. *Infect. Immun.* **2009**, *77*, 2544–2556, doi:10.1128/IAI.01425-08.

21. Szymanski, C. M.; Logan, S. M.; Linton, D.; Wren, B. W. *Campylobacter* - A tale of two protein glycosylation systems. *Trends Microbiol.* **2003**, *11*, 233–238.

22. Guerry, P.; Logan, S. M.; Thornton, S.; Trust, T. J. Genomic organization and expression of *Campylobacter* flagellin genes. *J. Bacteriol.* **1990**, *172*, 1853–1860.

23. Thibault, P.; Logan, S. M.; Kelly, J. F.; Brisson, J. R.; Ewing, C. P.; Trust, T. J.; Guerry, P. Identification of the Carbohydrate Moieties and Glycosylation Motifs in *Campylobacter jejuni* Flagellin. *J. Biol. Chem.* **2001**, *276*, 34862–34870, doi:10.1074/jbc.M104529200.

24. McNally, D. J.; Aubry, A. J.; Hui, J. P. M.; Khieu, N. H.; Whitfield, D.; Ewing, C. P.; Guerry, P.; Brisson, J. R.; Logan, S. M.; Soo, E. C. Targeted metabolomics analysis of *Campylobacter coli* VC167 reveals legionaminic acid derivatives as novel flagellar glycans. *J. Biol. Chem.* **2007**, *282*, 14463–14475, doi:10.1074/jbc.M611027200.

25. Schoenhofen, I. C.; McNally, D. J.; Vinogradov, E.; Whitfield, D.; Young, N. M.; Dick, S.; Wakarchuk, W. W.; Brisson, J. R.; Logan, S. M. Functional characterization of dehydratase/aminotransferase pairs from *Helicobacter* and *Campylobacter*: Enzymes distinguishing the pseudaminic acid and bacillosamine biosynthetic pathways. *J. Biol. Chem.* **2006**, *281*, 723–732, doi:10.1074/jbc.M511021200.

26. Guerry, P.; Ewing, C. P.; Schirm, M.; Lorenzo, M.; Kelly, J.; Pattarini, D.; Majam, G.; Thibault, P.; Logan, S. Changes in flagellin glycosylation affect *Campylobacter*

autoagglutination and virulence. *Mol. Microbiol.* **2006**, *60*, 299–311, doi:10.1111/j.1365-2958.2006.05100.x.

27. Lango-Scholey, L.; Aidley, J.; Woodacre, A.; Jones, M. A.; Bayliss, C. D. High throughput method for analysis of repeat number for 28 phase variable loci of *Campylobacter jejuni* strain NCTC11168. *PLoS One* **2016**, *11*, doi:10.1371/journal.pone.0159634.

28. Parkhill, J.; Wren, B. W.; Mungall, K.; Ketley, J. M.; Churcher, C.; Basham, D.; Chillingworth, T.; Davies, R. M.; Feltwell, T.; Holroyd, S.; Jagels, K.; Karlyshev, A. V.; Moule, S.; Pallen, M. J.; Penn, C. W.; Quail, M. A.; Rajandream, M. A.; Rutherford, K. M.; Van Vliet, A. H. M.; Whitehead, S.; Barrell, B. G. The genome sequence of the food-borne pathogen *Campylobacter jejuni* reveals hypervariable sequences. *Nature* **2000**, doi:10.1038/35001088.

29. Hitchen, P.; Brzostek, J.; Panico, M.; Butler, J. A.; Morris, H. R.; Dell, A.; Linton, D. Modification of the *Campylobacter jejuni* flagellin glycan by the product of the Cj1295 homopolymeric-tract-containing gene. *Microbiology* **2010**, *156*, 1953–1962, doi:10.1099/mic.0.038091-0.

30. Sørensen, M. C. H.; Gencay, Y. E.; Birk, T.; Baldvinsson, S. B.; Jäckel, C.; Hammerl, J. A.; Vegge, C. S.; Neve, H.; Brøndsted, L. Primary isolation strain determines both phage type and receptors recognised by *Campylobacter jejuni* bacteriophages. *PLoS One* **2015**, *10*, doi:10.1371/journal.pone.0116287.

31. Simpson, D. J.; Sacher, J. C.; Szymanski, C. M. Exploring the interactions between bacteriophage-encoded glycan binding proteins and carbohydrates. *Curr. Opin. Struct. Biol.* **2015**, *34*, 69–77, doi:10.1016/j.sbi.2015.07.006.

32. Javed, M. A.; van Alphen, L. B.; Sacher, J.; Ding, W.; Kelly, J.; Nargang, C.; Smith, D. F.; Cummings, R. D.; Szymanski, C. M. A receptor-binding protein of *Campylobacter jejuni* bacteriophage NCTC 12673 recognizes flagellin glycosylated with acetamidino-modified pseudaminic acid. *Mol. Microbiol.* **2015**, *95*, 101–115, doi:10.1111/mmi.12849.

33. Javed, M. A.; Sacher, J. C.; van Alphen, L. B.; Patry, R. T.; Szymanski, C. M. A flagellar glycan-specific protein encoded by *Campylobacter* phages inhibits host cell growth. *Viruses* **2015**, *7*, 6661–6674, doi:10.3390/v7122964.

34. Javed, M. A.; Ackermann, H. W.; Azeredo, J.; Carvalho, C. M.; Connerton, I.; Evoy, S.; Hammerl, J. A.; Hertwig, S.; Lavigne, R.; Singh, A.; Szymanski, C. M.; Timms, A.; Kropinski, A. M. A suggested classification for two groups of *Campylobacter* myoviruses. *Arch. Virol.* **2014**, *159*, 181–190, doi:10.1007/s00705-013-1788-2.

35. Javed, M. A.; Poshtiban, S.; Arutyunov, D.; Evoy, S.; Szymanski, C. M. Bacteriophage Receptor Binding Protein Based Assays for the Simultaneous Detection of *Campylobacter jejuni* and *Campylobacter coli*. *PLoS One* **2013**, *8*, doi:10.1371/journal.pone.0069770.

36. Kropinski, A. M.; Arutyunov, D.; Foss, M.; Cunningham, A.; Ding, W.; Singh, A.; Pavlov, A. R.; Henry, M.; Evoy, S.; Kelly, J.; Szymanski, C. M. Genome and proteome of *Campylobacter jejuni* bacteriophage NCTC 12673. *Appl. Environ. Microbiol.* **2011**, *77*, 8265–8271, doi:10.1128/AEM.05562-11.

37. Palyada, K.; Threadgill, D.; Stintzi, A. Iron acquisition and regulation in *Campylobacter jejuni*. *J. Bacteriol.* **2004**, *186*, 4714–4729, doi:10.1128/JB.186.14.4714-4729.2004.

38. Love, M. I.; Huber, W.; Anders, S. Moderated estimation of fold change and dispersion for RNA-seq data with DESeq2. *Genome Biol.* **2014**, *15*, doi:10.1186/s13059-014-0550-

8.

39. Dobin, A.; Davis, C. A.; Schlesinger, F.; Drenkow, J.; Zaleski, C.; Jha, S.; Batut, P.; Chaisson, M.; Gingeras, T. R. STAR: Ultrafast universal RNA-seq aligner. *Bioinformatics* **2013**, *29*, 15–21, doi:10.1093/bioinformatics/bts635.

40. Luo, W.; Friedman, M. S.; Shedden, K.; Hankenson, K. D.; Woolf, P. J. GAGE: Generally applicable gene set enrichment for pathway analysis. *BMC Bioinformatics* **2009**, *10*, doi:10.1186/1471-2105-10-161.

41. Beeby, M.; Ribardo, D. A.; Brennan, C. A.; Ruby, E. G.; Jensen, G. J.; Hendrixson, D. R. Diverse high-torque bacterial flagellar motors assemble wider stator rings using a conserved protein scaffold. *Proc. Natl. Acad. Sci. U. S. A.* **2016**, *113*, E1917-26, doi:10.1073/pnas.1518952113.

42. Javed, M. A.; van Alphen, L. B.; Sacher, J.; Ding, W.; Kelly, J.; Nargang, C.; Smith, D. F.; Cummings, R. D.; Szymanski, C. M. A receptor-binding protein of *Campylobacter jejuni* bacteriophage NCTC 12673 recognizes flagellin glycosylated with acetamidino-modified pseudaminic acid. *Mol. Microbiol.* **2015**, *95*, 101–115, doi:10.1111/mmi.12849.

43. Sacher, J. C., Yee, E., Szymanski, C. M., & Miller, W. G. Complete genome sequences of three *Campylobacter jejuni* phage-propagating strains. *Genome Announc.* **2018,** *6*, e00514-18.

44. Sacher, J. C., Yee, E., Szymanski, C. M., & Miller, W. G. Complete genome sequence of *Campylobacter jejuni* strain 12567, a livestock-associated clade representative. *Genome Announc.* **2018,** *6*, e00513-18.

45. Kearse, M.; Moir, R.; Wilson, A.; Stones-Havas, S.; Cheung, M.; Sturrock, S.; Buxton, S.; Cooper, A.; Markowitz, S.; Duran, C.; Thierer, T.; Ashton, B.; Meintjes, P.;

Drummond, A. Geneious Basic: An integrated and extendable desktop software platform for the organization and analysis of sequence data. *Bioinformatics* **2012**, *28*, 1647–1649, doi:10.1093/bioinformatics/bts199.

46. Di Tommaso, P.; Moretti, S.; Xenarios, I.; Orobitg, M.; Montanyola, A.; Chang, J.-M.; Taly, J.-F.; Notredame, C. T-Coffee: a web server for the multiple sequence alignment of protein and RNA sequences using structural information and homology extension. *Nucleic Acids Res.* **2011**, *39*, W13–W17, doi:10.1093/nar/gkr245.

47. Gundogdu, O.; Bentley, S. D.; Holden, M. T.; Parkhill, J.; Dorrell, N.; Wren, B. W. Re-annotation and re-analysis of the *Campylobacter jejuni* NCTC11168 genome sequence. *BMC Genomics* **2007**, *8*, 162, doi:1471-2164-8-162

48. Frost, J. A.; Kramer, J. M.; Gillanders, S. A. Phage typing of *Campylobacter jejuni* and *Campylobacter coli* and its use as an adjunct to serotyping. *Epidemiol. Infect.* **1999**, *123*, S095026889900254X, doi:10.1017/S095026889900254X.

49. Corcionivoschi, N.; Alvarez, L. A. J.; Sharp, T. H.; Strengert, M.; Alemka, A.; Mantell, J.; Verkade, P.; Knaus, U. G.; Bourke, B. Mucosal Reactive Oxygen Species Decrease Virulence by Disrupting *Campylobacter jejuni* Phosphotyrosine Signaling. *Cell Host Microbe* **2012**, *12*, 47–59, doi:10.1016/j.chom.2012.05.018.

50. Weingarten, R. A.; Taveirne, M. E.; Olson, J. W. The dual-functioning fumarate reductase is the sole succinate:quinone reductase in *Campylobacter jejuni* and is required for full host colonization. *J. Bacteriol.* **2009**, *191*, 5293–300, doi:10.1128/JB.00166-09.

51. Kassem, I. I.; Khatri, M.; Sanad, Y. M.; Wolboldt, M.; Saif, Y. M.; Olson, J. W.; Rajashekara, G. The impairment of methylmenaquinol:fumarate reductase affects hydrogen peroxide susceptibility and accumulation in *Campylobacter jejuni*.

Microbiology Open **2014**, *3*, 168–181, doi:10.1002/mbo3.158.

52. Karlyshev, A. V.; Linton, D.; Gregson, N. A.; Wren, B. W. A novel paralogous gene family involved in phase-variable flagella-mediated motility in *Campylobacter jejuni*. *Microbiology* **2002**, *148*, 473–480, doi:10.1099/00221287-148-2-473.

53. Karlyshev, A. V; Wren, B. W. Development and application of an insertional system for gene delivery and expression in *Campylobacter jejuni*. *Appl. Environ. Microbiol.* **2005**, *71*, 4004–13, doi:10.1128/AEM.71.7.4004-4013.2005.

54. Logan, S. M.; Hui, J. P. M.; Vinogradov, E.; Aubry, A. J.; Melanson, J. E.; Kelly, J. F.; Nothaft, H.; Soo, E. C. Identification of novel carbohydrate modifications on *Campylobacter jejuni* 11168 flagellin using metabolomics-based approaches. *FEBS J.* **2009**, *276*, 1014–1023, doi:10.1111/j.1742-4658.2008.06840.x.

55. Crofts, A. A.; Poly, F. M.; Ewing, C. P.; Kuroiwa, J. M.; Rimmer, J. E.; Harro, C.; Sack, D.; Talaat, K. R.; Porter, C. K.; Gutierrez, R. L.; DeNearing, B.; Brubaker, J.; Laird, R. M.; Maue, A. C.; Jaep, K.; Alcala, A.; Tribble, D. R.; Riddle, M. S.; Ramakrishnan, A.; McCoy, A. J.; Davies, B. W.; Guerry, P.; Trent, M. S. *Campylobacter jejuni* transcriptional and genetic adaptation during human infection. *Nat. Microbiol.* **2018**, *3*, 494, doi:10.1038/s41564-018-0133-7.

56. Miller, M.; Acosta, A. M.; Chavez, C. B.; Flores, J. T.; Olotegui, M. P.; Pinedo, S. R.; Trigoso, D. R.; Vasquez, A. O.; Ahmed, I.; Alam, D.; … and Shrestha, S. K. The MAL-ED study: A multinational and multidisciplinary approach to understand the relationship between enteric pathogens, malnutrition, gut physiology, physical growth, cognitive development, and immune responses in infants and children up to 2 years of . *Clin. Infect. Dis.* **2014**, *59*, S193–S206, doi:10.1093/cid/ciu653.

57. Poropatich, K. O.; Walker, C. L. F.; Black, R. E. Quantifying the association between *Campylobacter* infection and Guillain-Barre Syndrome: A systematic review. *J. Heal. Popul. Nutr.* **2010**, *28*, 545–552, doi:10.3329/jhpn.v28i6.6602.

58. Kaakoush, N. O., Castaño-Rodríguez, N., Mitchell, H. M., & Man, S. M. Global epidemiology of *Campylobacter* infection. *Clin. Microbiol. Rev.* **2015**, *28*, 3, 687-720.

59. Yuki, N.; Susuki, K.; Koga, M.; Nishimoto, Y.; Odaka, M.; Hirata, K.; Taguchi, K.; Miyatake, T.; Furukawa, K.; Kobata, T.; Yamada, M. Carbohydrate mimicry between human ganglioside GM1 and *Campylobacter jejuni* lipooligosaccharide causes Guillain-Barre syndrome. *Proc. Natl. Acad. Sci.* **2004**, *101*, 11404–11409, doi:10.1073/pnas.0402391101.

60. Connerton, P. L.; Timms, A. R.; Connerton, I. F. *Campylobacter* bacteriophages and bacteriophage therapy. *J. Appl. Microbiol.* 2011, *111*, 255–265.

61. Cairns, L. S.; Marlow, V. L.; Bissett, E.; Ostrowski, A.; Stanley-Wall, N. R. A mechanical signal transmitted by the flagellum controls signalling in *Bacillus subtilis*. *Mol. Microbiol.* **2013**, *90*, 6–21, doi:10.1111/mmi.12342.

62. Belas, R. Biofilms, flagella, and mechanosensing of surfaces by bacteria. *Trends Microbiol.* 2014, *22*, 517–527.

63. Kalmokoff, M.; Lanthier, P.; Tremblay, T.-L.; Foss, M.; Lau, P. C.; Sanders, G.; Austin, J.; Kelly, J.; Szymanski, C. M. Proteomic analysis of *Campylobacter jejuni* 11168 biofilms reveals a role for the motility complex in biofilm formation. *J. Bacteriol.* **2006**, *188*, 4312–20, doi:10.1128/JB.01975-05.

64. Szymanski, C. M.; King, M.; Haardt, M.; Armstrong, G. D. *Campylobacter jejuni* motility and invasion of Caco-2 cells. *Infect. Immun.* **1995**, *63*, 4295–4300.

65. Lele, P. P.; Hosu, B. G.; Berg, H. C. Dynamics of mechanosensing in the bacterial flagellar motor., doi:10.1073/pnas.1305885110.

66. Labedan, B.; Goldberg, E. B. Requirement for membrane potential in injection of phage T4 DNA. *Proc. Nat. Acad. Sci*. **1979,** *76*, 4669-4673.

67. Logan, S. M.; Schoenhofen, I. C.; Guerry, P. O-linked flagellar glycosylation in *Campylobacter*. In; Nachamkin, I., Szymanski, C. M., Blaser, M. J., Eds.; *Campylobacter*; ASM Press: Washington, D.C., 2008; pp. 471–481.

68. Gardner, S. P.; Kendall, K. J.; Taveirne, M. E.; Olson, J. W. Complete Genome Sequence of *Campylobacter jejuni* subsp. jejuni ATCC 35925. *Genome Announc.* **2017**, *5*, e00743-17, doi:10.1128/genomeA.00743-17.

69. van Alphen, L. B.; Wuhrer, M.; Bleumink-Pluym, N. M. C.; Hensbergen, P. J.; Deeldere, A. M.; Van Putten, J. P. M. A functional *Campylobacter jejuni maf4* gene results in novel glycoforms on flagellin and altered autoagglutination behaviour. *Microbiology* **2008**, *154*, 3385–3397, doi:10.1099/mic.0.2008/019919-0.

70. Hendrixson, D. R. Restoration of flagellar biosynthesis by varied mutational events in *Campylobacter jejuni. Mol. Microbiol.* **2008**, *70*, 519–536, doi:10.1111/j.1365-2958.2008.06428.x; 10.1111/j.1365-2958.2008.06428.x.

Chapter 5: *Campylobacter jejuni* phage NCTC 12673 dependence on flagellar glycosylation and flagellar motor genes is overcome by a single escape mutant

5.1. Introduction

Campylobacter jejuni is an important Gram-negative foodborne pathogen that causes worldwide diarrheal disease and severe post-infectious sequelae, such as Guillain-Barré syndrome, irritable bowel syndrome, growth stunting and arthritis [1–3]. Furthermore, antibiotic resistance is rising in *Campylobacter,* and thus alternative solutions are required to combat this pathogen [4,5]. Since *Campylobacter* species are commensals in chickens, many *Campylobacter* infections result from mishandling or consumption of contaminated poultry products [1]. As such, strategies aimed at preventing and/or at reducing its colonization of poultry flocks are predicted to have a large impact on reducing the number of human infections [5,6].

Bacteriophages (phages), the viruses that infect bacteria, are highly abundant in all environments harbouring bacteria. Because of their natural ability to specifically recognize and kill their hosts, along with their ability to evolve and adapt alongside their hosts, the exploitation of phages has been considered as a possible antimicrobial strategy [7]. As well, phage-host interaction studies can provide valuable insights into bacterial evolution [8]. Phages have been examined as a possible means to reduce *Campylobacter* colonization on farms, particularly as they can be added directly to chicken feed and water sources [5,9]. However, several challenges associated with broadness of strain coverage and efficiency of phage adsorption and infection must be surmounted before this strategy can be considered feasible in large-scale agricultural settings [9–11]. Improved understanding of *Campylobacter* phage-host interactions can directly contribute to the success of this strategy.

C. jejuni coats its surface with many glycoconjugate structures, both protein- and lipid-linked, and these structures largely contribute to strain-strain variability in this species [12,13]. We therefore sought to better understand how *Campylobacter* phages interact with *C. jejuni* glycans. Previous work has shown that *Campylobacter* phages tend to require either capsular polysaccharides (CPS) or flagellar motility for adsorption to host cells [14,15]. Taxonomic classification of *Campylobacter* phages has clustered most CPS-dependent phages into the Cp8virus genus, and most flagellar-dependent phages into the Cp220virus genus [16].

Phage NCTC 12673 is a *Campylobacter jejuni*-specific lytic phage of the *Myoviridae* family of tailed phages [17]. This phage was originally used as a *Campylobacter* typing phage and has been shown to require CPS for infection of *C. jejuni* [15]. It is a member of the Cp8virus (group III) family of the *Eucampyvirinae*, of which most members characterized to date have been shown to be CPS-dependent and flagella-independent [15]. However, NCTC 12673 phage was also shown not to plaque on the paralyzed flagella *cj0390* (*pflB*) [15]. As well, we recently found that this phage is unable to plaque on *motA* and *motB* mutants, which express paralyzed flagella due to a lack of a functional flagellar motor complex (Sacher *et al.,* in preparation) [18]. We thus sought to better understand the involvement of flagellar motility in *C. jejuni* infection by NCTC 12673.

Here we describe the observation that phage NCTC 12673 cannot plaque on mutants in at least four genes (*pseCFGH*) in the *C. jejuni* NCTC 11168 pseudaminic acid biosynthesis pathway for flagellar glycosylation, which is also required for motility [19]. We show that these genes are not required for phage adsorption, nor does their mutation induce anti-phage or stress response

gene expression. Interestingly, we found that a phage escape mutant able to plaque efficiently on *pse* mutant strains could also plaque efficiently on *motA* and *motB* mutant strains. Additionally, this escape mutant could plaque more efficiently on mutants in the oxidative stress defense (*katA* and *ahpC*) compared to the parent phage. This suggests that the reduced plaquing efficiency of phage NCTC 12673 on non-motile strains may be related to the previously documented increased oxidative stress sensitivity of non-motile mutants in *C. jejuni* [20]. Finally, we used whole-genome sequencing to determine that relative to the parent phage, the escape mutant phage is predicted to encode a truncated version of Gp047, a protein we have shown binds to acetamidino-modified pseudaminic acid on *C. jejuni* flagella [21].

5.2. Materials and Methods

5.2.1. Bacterial Growth Conditions

C. jejuni NCTC 11168 (MP21) [22] and its isogenic deletion mutants and complement strains were grown on 1.5% NZCYM agar plates, supplemented with 50 µg/mL kanamycin or 12-25 µg/mL chloramphenicol where needed, at 37°C under microaerobic conditions (85% N_2, 10% CO_2, 5% O_2). *Escherichia coli* strains were grown on LB agar, supplemented with 100 µg/mL ampicillin, 50 µg/mL kanamycin or 25 µg/mL chloramphenicol where needed. The list of bacterial strains and phages used in this study is given in Table 5-1.

5.2.2. Phage propagation and titration

Phage NCTC 12673 and its propagating strain *C. jejuni* 12661 [23] were obtained from the National Collection of Type Cultures (NCTC; Salisbury, United Kingdom). Phage MutC was also propagated on *C. jejuni* 12661 following initial isolation on *pseC* cells. Phage propagation and titration were performed following the methods described in [24], except that 4-h pre-growth of cultures was done with NZCYM broth instead of CBHI broth.

5.2.3. Growth assays

Cells were harvested from overnight NZCYM plate cultures, pelleted and washed once in NZCYM broth and set to an OD_{600} of 0.05 (approximately 10^8 colony forming units (CFU)/mL) in 20-40 mL NZCYM broth in 125-mL Erlenmeyer flasks, each containing a 1-inch sterile magnetic stir-bar. Cells were under microaerobic conditions and stirred at 200 rpm. Samples (1-mL) were taken just prior to incubation (t=0) and at regular intervals. OD_{600} was measured at each time point and colony counts were done by serially diluting 100-µL aliquots of cell suspension into NZCYM broth and plating dilutions onto pre-dried NZCYM plates. Plates were observed following 48-h incubation under microaerobic conditions, at which time single colonies were counted.

5.2.4. Efficiency of plating (EOP) assays

Efficiency of plating (EOP) assays were done by spotting serial dilutions of NCTC 12673 phage onto different strains and determining the proportion of plaque forming units formed on mutant strains compared to the corresponding wild type strain. Briefly, overnight bacterial cultures were harvested in NZCYM broth and set to an OD_{600} of 0.35. A 5-mL aliquot of this suspension was

transferred to a standard sized empty Petri dish and incubated at 37 °C without shaking for 4 h under microaerobic conditions. The suspension was then set to an OD_{600} of 0.5, and 200 μL of this was mixed with 5 mL sterile 0.6% molten NZCYM agar at 45 °C. This suspension was poured onto the surface of a pre-warmed NZCYM plate containing 1.5% agar. Plates were allowed to solidify for 15 min and then 10 μL of serial dilutions of a phage suspension (starting at 10^7 PFU/mL) was spotted onto the agar surface and allowed to completely soak into the agar (15 min) before inverting the plate and incubating at 37°C under microaerobic conditions. Plaques were counted after 18–24 h and converted to PFU/mL by multiplying countable numbers by the total dilution factor. This method is stored on Protocols.io (DOI: dx.doi.org/10.17504/protocols.io.mahc2b6).

5.2.5. Adsorption assays

Adsorption assays were done according to [25] with some modifications. Briefly, cells were harvested as detailed above for growth curves and after washing pellets three times in 1 mL NZCYM broth and set to an OD_{600} of 0.4 in 2 mL NZCYM broth in a small empty Petri plate. Then, 20 μL of 0.22-um-filtered phage lysate at 5.6 x 10^5PFU/mL was added and mixed by pipetting. The number of unadsorbed phages at t=0 was determined by removing 500 μL immediately after mixing phage and host and centrifuging at 15,000 rpm for 2 min at 4°C. Then, 100 μL from the supernatant was removed and kept on ice until all samples were ready for titration. After the t=0 sample was taken, phage-cell suspensions were incubated aerobically with 100 rpm shaking at 37°C for 90 min, at which point the sampling process was repeated. Samples from each time point were serially diluted in SM buffer and titered for plaque-forming

units to determine the number of unadsorbed phages over time, and the results of two biological replicates were averaged and graphed.

5.2.6. Total RNA extraction

C. jejuni 11168 wild type, *pseC* and *pseF* mutant cells were harvested from overnight NZCYM plate cultures, pelleted and washed once in NZCYM broth and set to an OD_{600} of 0.05 (2 x 10^8 CFU/mL) in 20 mL NZCYM broth in 125-mL Erlenmeyer flasks, each containing a 1-inch sterile magnetic stir-bar. Cells were grown under microaerobic conditions and magnetically stirred at 200 rpm. After 4.5 h incubation (mid-log phase, cells had achieved approximately 5 x 10^8 CFU/mL), the entire contents of each flask was transferred to a pre-prepared tube containing 2.6 mL (0.1 volume) ice cold 10% buffered phenol in 100% ethanol to stabilize RNA followed by immediate mixing and storage on ice until all samples were collected [26]. RNA was extracted from each sample using a hot phenol method [26]. RNA samples were sequentially DNAse-treated (37°C for 30 min) using RNAse-free DNAse I (Epicentre) and cleaned using the Zymo RNA Clean & Concentrator. PCR was used to confirm the absence of residual DNA. Total RNA quality was assessed using an Agilent Bioanalyzer and RNA was stored at -80°C until further use. Samples were extracted in biological triplicate.

5.2.7. RNA-sequencing

Total mRNA libraries from all replicates were generated. Samples were depleted of rRNA using the RiboZero Bacterial kit according to the manufacturer's instructions. Successful rRNA depletion was confirmed using the Agilent Bioanalyzer RNA 6000 Pico Kit. Strand-specific barcoded sequencing libraries were constructed using the Ion Total RNA-seq kit. Libraries were

quality-checked and quantified using the Bioanalyzer High Sensitivity DNA kit and pooled together in equimolar amounts. Template preparation from the pooled libraries was done using the Ion PI Hi-Q kit and sequenced on an Ion Torrent Proton using the Ion PI Hi-Q sequencing 200 kit on a single Proton V2 chip.

The raw sequencing reads were demultiplexed by the Ion Torrent suite software and mapped to the host (NCTC 11168) and phage (NCTC 12673) genomes using STAR [27]. Reads aligning to coding regions were counted using HT-seq [28]. The raw demultiplexed sequencing reads have been deposited at the NCBI SRA archive under accession number PRJNA454099. DESeq2 was used to identify differentially expressed transcripts over time and between different time points. Genes with a fold change +/- 1.5 and false discovery rate (FDR)-corrected *p*-value <0.05 were considered differentially expressed. Host and phage genes were analyzed separately. We also conducted gene set enrichment analysis (GSEA) on *C. jejuni* Kyoto Encyclopedia of Genes and Genomes (KEGG) pathways using the generally applicable gene set enrichment (GAGE) method [29] with a minimum FDR cutoff of <0.1 [27].

5.2.8. Isolation of MutC

MutC was isolated as a clear plaque following an efficiency of plating assay (as described above) whereby serial dilutions of phage NCTC 12673 were spotted onto a plate of *C. jejuni* NCTC 11168 *pseC* mutant cells. The plaque was isolated and purified according to the methods of [24] and propagated on *C. jejuni* 12661, the propagating strain for NCTC 12673.

5.2.9. Whole genome sequencing

Phage DNA (MutC and NCTC 12673) was prepared using hot phenol-chloroform extraction and submitted for Illumina library preparation and whole-genome sequencing to TAGC (Edmonton, Canada).

5.2.10. Genome variant frequency analysis

Variant calling was done using Geneious version 8.

Table 5-1. List of strains and phages used in this study.

Strain	Description/phenotype	Reference
C. jejuni NCTC 11168	Human enteropathy isolate, capsular, motile	[30]
C. jejuni NCTC 11168Δ*motA*	Non-motile (paralyzed flagella)	This work
C. jejuni NCTC 11168Δ*motB*	Non-motile (paralyzed flagella)	This work
C. jejuni NCTC 11168Δ*kpsM*	Acapsular	[31]
C. jejuni NCTC 11168Δ*pseC*	Non-motile (aflagellate)	This work
C. jejuni NCTC 11168Δ*pseH*	Non-motile (aflagellate)	[21]
C. jejuni NCTC 11168Δ*pseH/pseH*$^{+}$	Motile	This work
C. jejuni NCTC 11168Δ*pseG*	Non-motile (aflagellate)	[21]
C. jejuni NCTC 11168Δ*pseF*	Non-motile (aflagellate)	This work
C. jejuni NCTC 11168Δ*katA*	Hypersensitive to oxidative stress (lacks catalase)	[32]
C. jejuni NCTC 11168Δ*ahpC*	Hypersensitive to oxidative stress (lacks alkyl hydroxyperoxidase)	[32]
C. jejuni NCTC 11168Δ*sodB*	Hypersensitive to oxidative stress (lacks superoxide dismutase)	[32]
NCTC 12673	UK phage typing scheme phage 1	[17,33]
MutC	Spontaneous variant of NCTC 12673	This work

5.3. Results

5.3.1. Phage NCTC 12673 requires a functional pseudaminic acid biosynthetic pathway for infection

To determine whether flagellar glycosylation is important for NCTC 12673 infection, we examined phage infection of *pseC, pseF, pseG, pseH* mutants and found that compared to wild type *C. jejuni* NCTC 11168 infection (EOP = 1.00), infectivity was decreased on all mutants (Figure 5-1). Infectivity was undetectable upon mutation of *pseC* or *pseH*, and drastically reduced upon infection of *pseF* (EOP = 0.03) and *pseG* (EOP = 0.03). We complemented Δ*pseH* with a functional copy of the gene and found that infectivity was greatly improved (EOP = 0.27) compared to the *pseH* mutant.

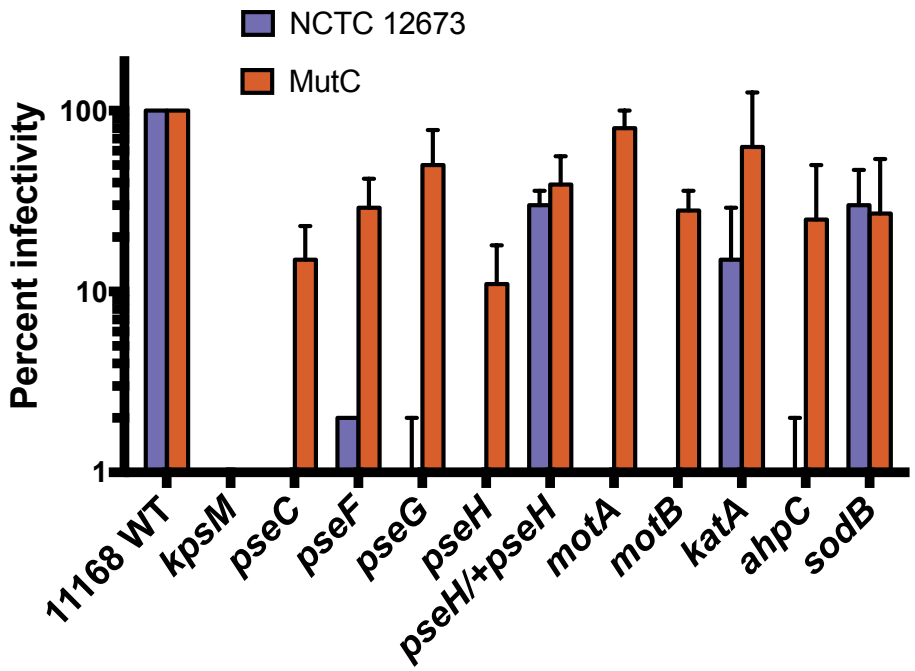

Figure 5-1. Percent efficiency of plating (EOP) of phages NCTC 12673, MutC on *C. jejuni* NCTC 11168 wild type and isogenic mutants in pseudaminic acid biosynthesis, flagellar motor and oxidative stress defense genes. Bars represent the mean of two to five biological replicates.

5.3.2. Phage NCTC 12673 adsorbs to pseudaminic acid pathway mutants at wild type levels

It has been well established that inactivation of *pseB, pseC, pseE, pseF, pseG, pseH* or *pseI*, which are all required for biosynthesis and flagellar transfer of pseudaminic acid in *C. jejuni*, prevents flagella biogenesis [19,34]. As other *Campylobacter* phages have been shown to depend on flagellar motility for infection, we first sought to determine whether NCTC 12673 phage adsorption was impaired on *pse* mutants. We titered the number of free phages remaining in the supernatant following incubation with *C. jejuni* NCTC 11168 wild type, *pseC, pseF, pseG* and *pseH* mutants, a *pseH/+pseH* complement strain and a *kpsM* mutant as a negative control, which lacks the capsule required for NCTC 12673 binding [15]. With the exception of *pseH*, which showed a slight, yet statistically significant decrease in adsorption compared to wild type cells ($P = 0.03$), we observed no differences in adsorption for most strains relative to wild type cells (Figure 5-2). In line with previous results, NCTC 12673 phage did not adsorb to *kpsM* mutant cells ($P = 0.0004$).

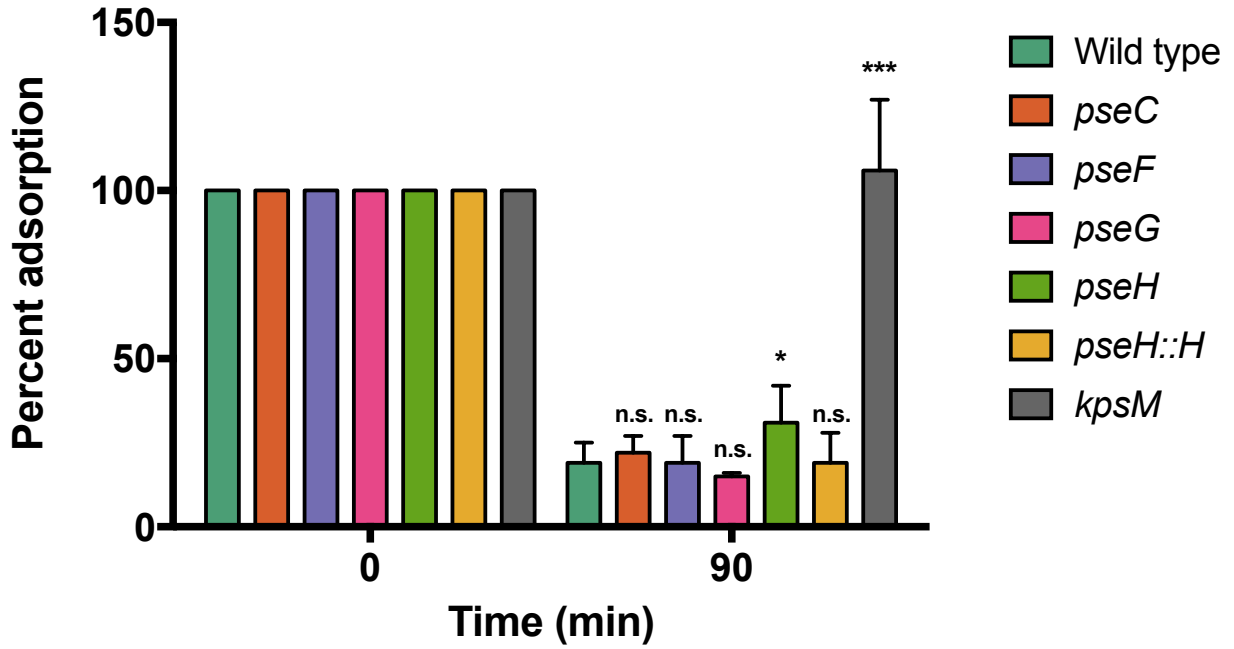

Figure 5-2. Phage NCTC 12673 adsorption to *C. jejuni* NCTC 11168 wild type and *pseC*, *pseF* *pseG, pseH, pseH/+pseH,* and *kpsM* strains. Bars represent an average of two biological replicates, and error bars represent standard deviations. Statistical significance as determined by unpaired t-test is indicated by asterisks as follows: $P < 0.05$ (*), $P < 0.01$ (**), $P < 0.001$ (***). n.s.: not significantly different from wild type adsorption.

5.3.3. *pseC* and *pseF* mutants display no evidence of stress response but down-regulate many flagellar genes

We next sought to determine whether downstream effects of *pse* mutation lead to stress responses or expression of anti-phage genes in the cell, which might help explain why the NCTC 12673 phage is unable to efficiently infect these strains. To test this, we used RNA-seq to compare total mRNA expression between *C. jejuni* NCTC 11168 wild type, *pseC* and *pseF* mutant cells during mid-log phase growth. We identified widespread downregulation of many

genes in both *pseC* and *pseF* cells compared to wild type cells (Figure 5-3). Most significantly down-regulated genes relative to wild type cells that were common to both mutant strains, and most were related to flagellar biogenesis, with several others related to amino acid biosynthesis. We did not observe substantial upregulation of many genes in either strain, with exceptions being the upregulation of *metA* and *metB* genes (encoding enzymes for methionine biosynthesis) and the upregulation of the CPS biosynthesis genes in *pseC* mutant cells compared to wild type cells. Apart from these *pseC*-specific up-regulated genes, direct comparison of *pseF* to *pseC* showed few other differences, but did highlight that more amino acid biosynthesis genes were down-regulated in *pseC* cells compared to *pseF* cells, and pointed to some differences in the flagella-related genes between the strains (Figure 5-3C).

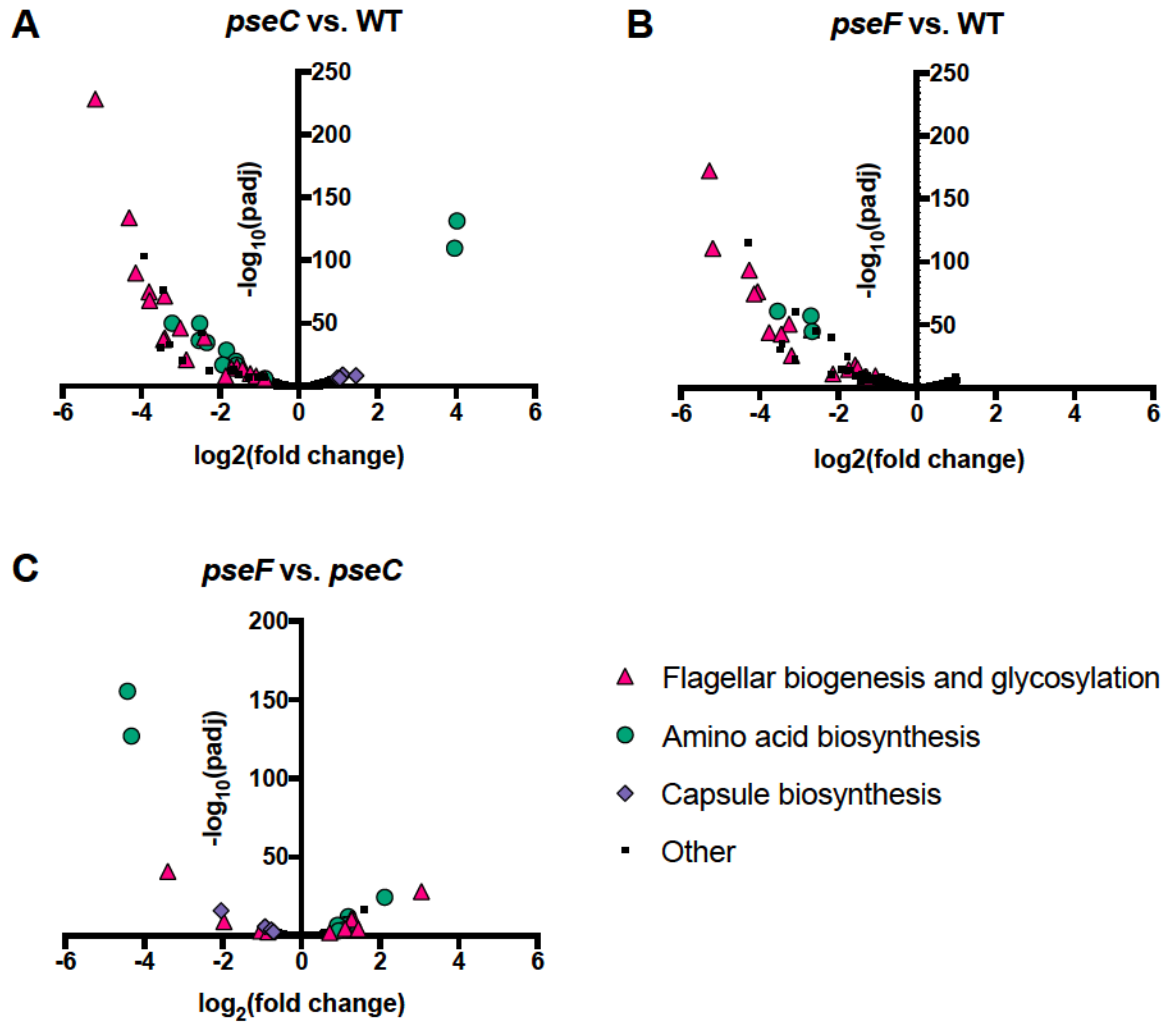

Figure 5-3. Volcano plots showing the most significantly differentially expressed genes between *C. jejuni* NCTC 11168 wild type, *pseC* and *pseF* cells. Significantly differentially expressed genes between *pseC* and wild type (A), between *pseF* and wild type (B) and between *pseF* and *pseC* (C) are shown.

5.3.4. Phage NCTC 12673 is unable to infect cells in the absence of flagellar motor proteins *motA* or *motB*

To better understand the possible NCTC 12673 dependence on flagellar motility, and to verify previous results that showed that this phage did not plaque on a "paralyzed" (full-length but non-motile) flagella (*pflB*) mutant, we tested NCTC 12673 phage plaquing efficiency on flagellar motor mutants *motA* and *motB* [35]. Interestingly, we found that NCTC 12673 phage infection was essentially abolished on both mutants (Figure 5-1).

5.3.5. Oxidative stress sensitivity of non-motile mutants may explain reduced NCTC 12673 plaquing efficiency

We recently showed that NCTC 12673 phage displays reduced plaquing on mutants of the oxidative stress defense genes *katA*, *ahpC* and *sodB* [46]. As well, Flint *et al*. have previously shown that many non-motile *C. jejuni* NCTC 11168 mutants are hypersensitive to oxidative stress, including *motAB, flgK, flgH, flgD, flgI, flgR,* and *pseB* mutants, though the reason for this is unknown [20]. With the exception of *motA* and *motB,* we observed that all of these genes were among the most significantly down-regulated in both *pseC* and *pseF* mutant strains (Figure 5-3). We therefore hypothesized that oxidative stress sensitivity might explain the observed dependence of NCTC 12673 on flagellar motility.

5.3.6. The NCTC 12673 escape mutant phage MutC efficiently plaques on non-motile and oxidative stress mutants

To better understand the mechanism for motility dependence by NCTC 12673, we sought to characterize an NCTC 12673 phage escape mutant, MutC, which we isolated as a clear plaque on *pseC* mutant cells. Interestingly, we found that MutC displayed a higher EOP on the *pse* and *mot* mutants compared to NCTC 12673 (Figure 5-1). However, like the parent phage, MutC did not infect *kpsM* cells, suggesting that it retained dependence on *C. jejuni* CPS.

To determine whether the apparent escape from dependence on motility also allowed MutC to escape dependence on oxidative stress defense genes, we next tested MutC infection of *katA, ahpC* and *sodB* mutants. We found that MutC infected *ahpC* mutant cells more efficiently than NCTC 12673 ($P = 0.02$). Whereas MutC did not show statistically significantly higher EOP on *katA* ($P = 0.17$), we did observe a trend toward increased EOP for MutC and a clear visual increase in MutC plaquing efficiency (MutC plaques were much larger and clearer) on *katA* cells (data not shown). Conversely, we did not observe a difference between MutC and NCTC 12673 infection of a *sodB* mutant ($P = 0.90$).

5.3.7. Genomic comparison between phages NCTC 12673 and MutC reveals differences in predicted length of Gp047, a flagellar glycan-binding protein

In order to understand the genetic reason(s) for the observed differences in NCTC 12673 and MutC plaquing on non-motile and *ahpC* mutants, we performed whole-genome sequencing of both phage genomes. Although the two phages displayed nucleotide changes at several locations across their 135-kbp genomes (Table 5-S1), we identified amino acid-level changes in only six

genes: *gp047,* a flagellar glycan-binding protein; *gp041,* a baseplate wedge protein homologue; *gp058* and *gp167,* both of which are annotated as homing endonucleases; and *gp114* and *gp116,* both of which are hypothetical protein-encoding genes (Table 5-2). We chose to focus on *gp047* as a likely candidate based on its known *C. jejuni* flagellar binding activity.

Table 5-2. Variant frequency table showing amino acid-level genetic differences between NCTC 12673 and MutC phages.

Gene	Predicted function	Phage	Nucleotide Change	Amino Acid Change	Variant Frequency
gp041	Gp6 baseplate wedge subunit	MutC	A → G	L → S	72.70%
		MutC	C → T	M → I	25.60%
gp047	Flagellar glycan binding protein	MutC	(A)7 → (A)6	Frame Shift	68.80%
		NCTC 12673	(A)7 → (A)6	Frame Shift	33.20%
		MutC	(A)7 → (A)6	Frame Shift	25.30%
gp058	Hef59 homing endonuclease	MutC	AA → GG	E → G	69.8%
gp114/ gp115	Hypothetical protein	MutC	(CC)4 → (CC)5	Frame Shift	37.00%
		NCTC 12673	(C)9 → (C)10	Frame Shift	31.20%
		MutC	(C)9 → (C)10	Frame Shift	43.70%
gp116	Hypothetical protein	NCTC 12673	(C)11 → (C)12	Frame Shift	28.90%
		NCTC 12673	(C)11 → (C)10	Frame Shift	27.10%
		MutC	(C)11 → (C)10	Frame Shift	62.80%
		MutC	G → A	T → M	68.70%
		NCTC 12673	G → T	T → N	73.80%
gp167	Hef168 homing endonuclease	MutC	C → T	D → N	64.00%

Gp047 is the flagellar glycan binding protein encoded by *Campylobacter* phages, but a role for this protein in the phage lifecycle has not yet been determined [36,37]. Upon analysis of Illumina sequencing data for MutC and NCTC 12673 phages, we identified the presence of two poly-T tracts within *gp047.* For each phage, we observed the presence of 6- and 7-T stretches at these locations at the frequencies given in Table 5-2. At one of these tracts, we observed both 6-T and 7-T variants for both phages. However, at the other tract, we observed that NCTC 12673 encoded only 7-T variants, whereas MutC encoded the 6-T variant at a frequency of 68.80%.

When both tracts contain 7 Ts, the predicted Gp047 protein is 1365 amino acids in length, whereas encoding 6 Ts at one or both tracts results in a predicted length of less than or equal to 83 amino acids. These data suggest that MutC may express a truncated version of Gp047 more frequently than NCTC 12673.

To verify the *gp047* variability observed upon whole-genome sequencing, we designed primers to PCR-amplify the poly-T tract regions of *gp047.* We then performed Sanger sequencing on the resultant amplicons using NCTC 12673 and MutC phage lysates of *C. jejuni* NCTC 12661 cells (the strain routinely used to propagate these phages) as templates. Indeed, we found variability in sequence data (represented by multiple chromatogram peaks) starting directly downstream of the *gp047* poly-T tracts for both phages.

5.3.8. Infection of a *motA* mutant may select for Gp047 truncation in NCTC 12673 phage

To test whether phage infection of non-motile mutants provides a selective pressure to encode 6-T variant-containing (and thus truncated) *gp047*, we sequenced *gp047* directly from NCTC 12673 and MutC phage plaques on *C. jejuni* NCTC 11168 *motA* mutant cells. Interestingly, we found that for both phages, *gp047* unambiguously displayed the 6-T variant in at least one of the poly-T tracts (n = 2 plaques each). Furthermore, the sequence variability described above was not observed.

5.4. Discussion

Phage NCTC 12673 is classified as a member of the Cp8virus family of *Campylobacter* phages, members of which tends to target CPS and not flagella [14,16,17]. As well, phage NCTC 12673 has been shown to infect several aflagellate mutants [15,17]. However, previous work showed that NCTC 12673 could not plaque on the paralyzed flagellar mutant *pflB*, and we recently found that phage NCTC 12673 is also unable to plaque on *motA* or *motB* mutants (Sacher *et al.*, in preparation). These results suggest that motile flagella do in fact play a role in phage NCTC 12673 infectivity of *C. jejuni* cells.

To elucidate the role of motility in NCTC 12673 infection, we analyzed whether the phage could plaque on mutants of the pseudaminic acid (*pse*) flagellar glycosylation pathway, which are unable to assemble flagella and are thus non-motile [19,38]. Interestingly, we found that mutagenesis of *pseC, pseF, pseH,* or *pseG* drastically reduced infection efficiency of *C. jejuni* NCTC 11168 cells, and that complementation of *pseH in trans* restored flagellar motility and significantly improved phage infection efficiency. Another flagella-requiring *Campylobacter* phage, F341, was shown to require flagellar motility for adsorption [25]. Conversely, here we show that NCTC 12673 phage can readily adsorb to aflagellate *pse* mutants, suggesting that it depends on flagella for another reason. We therefore hypothesized that defects in the *pse* pathway impact the phage lifecycle after the point of phage attachment to the cell surface.

Downstream effects on gene expression in response to mutagenesis of a gene are common. We therefore sought to understand the total effects of *pse* gene inactivation to identify possible explanations for the lack of phage infectivity of *pse* mutants. To test this, we performed RNA-

seq on *pseC* and *pseF* mutant cells. We did not observe signs of general stress response activation in the *pseC* and *pseF* mutants relative to wild type cells, but we did observe widespread downregulation of flagellar genes. This downregulation was not surprising, since *C. jejuni* is known to tightly regulate its flagellar expression, and *pse* genes are required for filament biogenesis [39–41]. It is therefore logical that the cell would encode mechanisms of preventing flagellar biogenesis in response to a lack of *pse* gene expression.

Interestingly, Flint *et al.* (2014) showed that several non-motile *C. jejuni* mutants, many of which lack genes we observed to be down-regulated in *pseC* and *pseF* mutants*,* are hypersensitive to oxidative stress [20]. Our recent transcriptomic analysis of NCTC 12673 phage during lytic infection of *C. jejuni* 11168 showed that upon infection, *C. jejuni* up-regulates the oxidative stress defense gene *katA* as well as genes required for KatA activity [46]. This led to the finding that *katA,* as well as *ahpC* and *sodB*, are important for efficient phage infection by NCTC 12673*,* suggesting that this phage cannot efficiently infect oxidatively-stressed cells. We therefore hypothesized that oxidative stress, rather than a lack of motility, might explain the inability of NCTC 12673 phage to plaque on non-motile mutants.

To better understand the mechanism by which NCTC 12673 phage depends on flagellar motility and/or oxidative stress sensitivity, we characterized a spontaneous NCTC 12673 phage mutant, MutC, which was isolated as a clear plaque following application of NCTC 12673 phage on *pseC* mutant cells. In addition to plaquing on *pseC* cells, we found that MutC could efficiently infect mutants in *motA*, *motB*, *pseC, pseF, pseG* and *pseH.* Interestingly, we found that MutC was also able to plaque more efficiently on *ahpC,* and to a lesser extent, *katA,* two of the three

oxidative stress defense mutants that resulted in reduced NCTC 12673 infectivity. Conversely, NCTC 12673 and MutC similarly infected a *sodB* mutant, suggesting that different antioxidant genes affect phage infection in different ways. The observation that MutC was able to simultaneously overcome dependence on non-motile and oxidative stress-hypersensitive mutants suggested that NCTC 12673 phage dependence on motility and its dependence on oxidative stress sensitivity are linked. It remains to be determined whether this correlation is causative, ie. whether defects in motility indeed reduce NCTC 12673 phage infectivity by causing cells to be hypersensitive to oxidative stress.

It is also noteworthy that *pseC* mutant cells up-regulated *metA* and *metB*, as methionine biosynthesis has been suggested to be a marker of oxidative stress in *C. jejuni* (David Kelly, personal communication). Of note, our results suggest that mutation of early pse pathway genes is more detrimental to phage infection compared to mutation of late pse pathway genes, but the reason for this remains unknown. It is possible that differences in *metA*, *metB*, CPS biosynthesis and/or amino acid biosynthesis may explain some of the difference between NCTC 12673 infectivity of these strains.

We sought to identify the genetic differences between NCTC 12673 and MutC to understand the molecular mechanism driving the observed differences in host requirements between the two phages. Interestingly, whole-genome sequence comparison showed phage-specific differences in the frequency of a poly-T tract-associated frameshift mutation in *gp047,* a conserved *Campylobacter* phage gene that we previously showed encodes a flagellar glycan-binding protein specific for acetamidino-modified pseudaminic acid [21]. The presence of two poly-T

tracts (6-7 Ts) in *gp047*, paired with the variant frequencies observed, suggests that full-length Gp047 is variably expressed by both NCTC 12673 and MutC phage populations. Homopolymeric nucleotide tracts of this length are not predicted to switch on and off as frequently as the 8-12G tracts present at nearly 30 loci across the *C. jejuni* genome [30,42]. This is supported by the fact that whereas clear-plaque variants of NCTC 12673 do arise on *mot* and *pse* mutants, they do not arise frequently. However, sequencing the *gp047* poly-T tracts from within phage lysates suggest that both NCTC 12673 and MutC express a mixed population of on- and off-switched *gp047*.

The differences in variant frequency at the poly-T tracts in *gp047* that we observed suggest that a much larger proportion of the MutC population expresses a severely truncated (or "off-switched") version of Gp047 compared to NCTC 12673. As well, one round of plaquing phage NCTC 12673 on *motA* mutant cells led to selection for *gp047* encoded in the "off" state. From these results, we speculate that full-length Gp047 expression may explain the reduced NCTC 12673 plaquing efficiency observed on non-motile mutants, and that MutC may have escaped this dependency by expressing a truncated form of Gp047.

The function of Gp047 in the phage lifecycle is unknown. Although we have previously described possible extracellular activities for Gp047, namely that binding of this protein to *C. jejuni* flagella leads to growth inhibition, it is possible that this protein also exhibits pre-lysis (ie. intracellular) effects on infected cells [37]. If full-length Gp047 does indeed prevent NCTC 12673 phage from infecting non-motile mutants, it is possible that this protein acts to conditionally repress the phage lifecycle in some way, and that its truncation promotes lysis

even in the presence of normally repressive conditions. It could be speculated that Gp047 de-repression may occur when it can bind to glycosylated flagellin subunits in the cytoplasm, which may exist in higher abundance in motile cells, thus providing a possible mechanism by which the phage might link its 'decision' to lyse cells to cell motility. It has previously been shown that 'carrier state' association between two NCTC 12673-related phages and *C. jejuni* leads to downregulation of flagellar motility, suggesting that motility and the phage life cycle may be linked for phages targeting this organism [43]. Further work into examining the function of Gp047 in the context of phage-infected cells, as well as the effect of inactivation of *gp047* on NCTC 12673 phage infection, is thus merited. Although we previously recombinantly expressed *gp047* in *C. jejuni* cells, we observed no difference in flagellar expression [37]. However, it is possible that Gp047 may play a role in phage infection without causing a visible effect on flagellar biogenesis. It is also possible that other phage factors, such as chaperones, are required for intracellular Gp047 activity, which could have led to an inactive protein when expressed recombinantly.

Together our data support a possible role for *gp047* in dictating NCTC 12673 phage interactions with non-motile and/or oxidatively stressed *C. jejuni* cells. However, the data do not rule out possible contributions of the other observed genetic changes between the two phages, and the effects of these changes should also be examined. Our preliminary work suggests the L to S change in MutC *gp041* is reproducible, suggesting that this change could also play a meaningful role in the phenotypic differences between the phages. In addition, analysis of *gp114* and *gp116* has shown that these genes exhibit phase-variability via poly-G tracts. However, we found these tracts to be highly variable following both *pseC* and wild type infection for both NCTC 12673

and MutC phages, thus reducing the likelihood that on/off switching in these genes is responsible for the stable difference in phenotypes observed between the two phages. To our knowledge, examples of phase variability in *Campylobacter* phages have not previously been reported. However, as *C. jejuni* expresses around 30 phase-variable genes, many of them governing surface structure expression [30,44], it would not be surprising to find that *Campylobacter* phages might have evolved such a mechanism to ensure evolutionary dominance over such a variable host. Therefore, the functions of *gp114* and *gp116* in the phage lifecycle should be pursued. Finally, our efforts to confirm the observed differences in the homing endonucleases *gp058* and *gp167* between NCTC 12673 and MutC phages showed that the nucleotide changes observed upon whole genome sequencing were not reproducible, suggesting against a role for these changes in explaining the phenotypic differences between NCTC 12673 and MutC.

To determine whether the observed dependence on *pse*, *mot* and oxidative stress pathways can be generalized beyond phage NCTC 12673, we tested the plaquing efficiency of *Campylobacter* phages F336, NCTC 12678 and NCTC 12669 on *pseC, pseF, motA,* and *motB* mutants. Preliminary data has shown that phages F336 and NCTC 12669 exhibit the same trends in infectivity on these mutants as NCTC 12673, whereas NCTC 12678 was able to infect these *pse* and *mot* mutants, similar to MutC. These phages have not yet been genome-sequenced, but *gp047* homologues in all three phages have been identified, and the C-terminal quarters (previously shown to be responsible for flagellar binding in the NCTC 12673 version) were recombinantly expressed and found to be active [16]. Future work into understanding how

NCTC 12678 is able to infect non-motile strains, and whether this phenotype is linked to oxidative stress, should provide interesting insights.

Overall, this work provides novel insights into NCTC 12673 phage interactions with *C. jejuni* 11168. We have shown that the apparent dependence of phage NCTC 12673 on *C. jejuni* motility is not related to adsorption, but instead may be linked to its reduced infection efficiency of strains hypersensitive to oxidative stress. Furthermore, we have shown evidence that Gp047 is variably expressed in a NCTC 12673 phage population, and have shown a correlation between Gp047 off-switching and improved infection of non-motile strains. Further work into establishing a role for Gp047 in phage infection, as well as the conditions required for this activity, is merited.

5.5. Supplementary data

Table 5-S1. Complete list of genetic polymorphisms and variant frequencies between NCTC 12673 phage (parent) and MutC, a spontaneous mutant phage isolated on *C. jejuni* 11168 *pseC* mutant cells.

Gene	Predicted function	Phage	Min	Max	Amino Acid Change	Change	Codon Change	Polymorphism Type	Variant Frequency
gp047	Flagellar glycan binding protein	MutC	40,821	40,821	Frame Shift	(A)7 -> (A)6	Frame Shift	Deletion (tandem repeat)	68.80%
gp114/gp115	Hypothetical protein	MutC	100,737	100,736	Frame Shift	(CC)4 -> (CC)5	Frame Shift	Insertion (tandem repeat)	37.00%
gp116	Hypothetical protein	Parent	101,692	101,691	Frame Shift	(C)11 -> (C)12	Frame Shift	Insertion (tandem repeat)	28.90%

gp116	Hypothetical protein	Parent	101,691	101,691	Frame Shift	(C)11 -> (C)10	Frame Shift	Deletion (tandem repeat)	27.10%
gp116	Hypothetical protein	MutC	101,691	101,691	Frame Shift	(C)11 -> (C)10	Frame Shift	Deletion (tandem repeat)	62.80%
gp041	gp6 baseplate wedge	MutC	31,844	31,844	L -> S	A -> G	TTA -> TCA	SNP (transition)	72.70%
gp058	Hef59	MutC	50,606	50,607	E -> G	AA -> GG	GAA -> GGG	Substitution	69.8% -> 69.9%
gp167	Hef168	MutC	132,316	132,316	D -> N	C -> T	GAT -> AAT	SNP (transition)	64.00%
gp116	Hypothetical protein	MutC	101,202	101,202	T -> M	G -> A	ACG -> ATG	SNP (transition)	68.70%
gp116	Hypothetical protein	Parent	101,112	101,112	T -> N	G -> T	ACT -> AAT	SNP (transversion)	73.80%
gp041	gp6 baseplate wedge	MutC	31,885	31,885	M -> I	C -> T	ATG -> ATA	SNP (transition)	25.60%
gp114/gp115	Hypothetical protein	Parent	100,737	100,736	Frame Shift	(C)9 -> (C)10	Frame Shift	Insertion (tandem repeat)	31.20%
gp114/gp115	Hypothetical protein	MutC	100,737	100,736	Frame Shift	(C)9 -> (C)10	Frame Shift	Insertion (tandem repeat)	43.70%
upstream of *gp113*	Intergenic region	Parent	99,920	99,921	N/A (not within a CDS)	AC -> GT	N/A (not within a CDS)	Substitution	73.9% -> 77.1%
upstream of *gp113*	Intergenic region	MutC	99,920	99,921	N/A (not within a CDS)	AC -> GT	N/A (not within a CDS)	Substitution	98.5% -> 98.6%
gp047	putative tail fibre	Parent	40,935	40,935	Frame Shift	(A)7 -> (A)6	Frame Shift	Deletion (tandem repeat)	33.20%
gp047	putative tail fibre	MutC	40,935	40,935	Frame Shift	(A)7 -> (A)6	Frame Shift	Deletion (tandem repeat)	25.30%

5.6. References

1. Kaakoush, N. O., Castaño-Rodríguez, N., Mitchell, H. M., & Man, S. M. Global epidemiology of *Campylobacter* infection. *Clin. Microbiol. Rev.* **2015**, *28*, 3, 687-720.

2. Yuki, N.; Susuki, K.; Koga, M.; Nishimoto, Y.; Odaka, M.; Hirata, K.; Taguchi, K.;

Miyatake, T.; Furukawa, K.; Kobata, T.; Yamada, M. Carbohydrate mimicry between human ganglioside GM1 and *Campylobacter jejuni* lipooligosaccharide causes Guillain-Barre syndrome. *Proc. Natl. Acad. Sci.* **2004**, *101*, 11404–11409, doi:10.1073/pnas.0402391101.

3. Amour, C.; Gratz, J.; Mduma, E.; Svensen, E.; Rogawski, E. T.; McGrath, M.; Seidman, J. C.; McCormick, B. J. J. J.; Shrestha, S.; Samie, A.; Mahfuz, M.; Qureshi, S.; Hotwani, A.; Babji, S.; Trigoso, D. R.; Lima, A. A. M. M.; Bodhidatta, L.; Bessong, P.; Ahmed, T.; Shakoor, S.; Kang, G.; Kosek, M.; Guerrant, R. L.; Lang, D.; Gottlieb, M.; Houpt, E. R.; Platts-Mills, J. A.; Etiology, Risk Factors, and Interactions of Enteric Infections and Malnutrition and the Consequences for Child Health and Development Project (MAL-ED) Network Investigators Epidemiology and Impact of *Campylobacter* Infection in Children in 8 Low-Resource Settings: Results from the MAL-ED Study. *Clin. Infect. Dis.* **2016**, *63*, 1171–1179, doi:10.1093/cid/ciw542.
4. Hampton, T. Report Reveals Scope of US Antibiotic Resistance Threat. *JAMA* **2013**, *310*, 1661, doi:10.1001/jama.2013.280695.
5. Johnson, T. J.; Shank, J. M.; Johnson, J. G. Current and Potential Treatments for Reducing *Campylobacter* Colonization in Animal Hosts and Disease in Humans. *Front. Microbiol.* **2017**, *8*, 487, doi:10.3389/fmicb.2017.00487.
6. Wassenaar, T. M. Following an imaginary *Campylobacter* population from farm to fork and beyond: A bacterial perspective. *Lett. Appl. Microbiol.* 2011, *53*, 253–263.
7. Abedon, S.; Kuhl, S. J.; Blasdel, B. G.; Kutter, E. M. Phage treatment of human infections. *Bacteriophage* **2011**, doi:10.4161/bact.1.2.15845.
8. De Smet, J.; Hendrix, H.; Blasdel, B. G.; Danis-Wlodarczyk, K.; Lavigne, R.

Pseudomonas predators: Understanding and exploiting phage-host interactions. *Nat. Rev. Microbiol.* **2017**.

9. Connerton, P. L.; Timms, A. R.; Connerton, I. F. *Campylobacter* bacteriophages and bacteriophage therapy. *J. Appl. Microbiol.* **2011**, *111*, 255–265.

10. El-Shibiny, A.; Connerton, P. L.; Connerton, I. F. *Campylobacter* succession in broiler chickens. *Vet. Microbiol.* **2007**, *125*, 323–332, doi:10.1016/j.vetmic.2007.05.023.

11. El-Shibiny, A.; Scott, A.; Timms, A.; Metawea, Y.; Connerton, P.; Connerton, I. Application of a group II *Campylobacter* bacteriophage to reduce strains of *Campylobacter jejuni* and *Campylobacter coli* colonizing broiler chickens. *J. Food Prot.* **2009**, *72*, 733–740.

12. Karlyshev, A. V.; Ketley, J. M.; Wren, B. W. The *Campylobacter jejuni* glycome. *FEMS Microbiol. Rev.* **2005**, *29*, 377–390.

13. Nothaft, H.; Szymanski, C. M. Protein glycosylation in bacteria: sweeter than ever. *Nat. Rev. Microbiol.* **2010**, *8*, 765–778, doi:10.1038/nrmicro2383.

14. Sørensen, M. C. H.; Gencay, Y. E.; Birk, T.; Baldvinsson, S. B.; Jäckel, C.; Hammerl, J. A.; Vegge, C. S.; Neve, H.; Brøndsted, L. Primary isolation strain determines both phage type and receptors recognised by *Campylobacter jejuni* bacteriophages. *PLoS One* **2015**, *10*, doi:10.1371/journal.pone.0116287.

15. Coward, C.; Grant, A. J.; Swift, C.; Philp, J.; Towler, R.; Heydarian, M.; Frost, J. A.; Maskell, D. J. Phase-variable surface structures are required for infection of *Campylobacter jejuni* by bacteriophages. *Appl. Environ. Microbiol.* **2006**, *72*, 4638–4647, doi:10.1128/AEM.00184-06.

16. Javed, M. A.; Ackermann, H. W.; Azeredo, J.; Carvalho, C. M.; Connerton, I.; Evoy, S.;

Hammerl, J. A.; Hertwig, S.; Lavigne, R.; Singh, A.; Szymanski, C. M.; Timms, A.; Kropinski, A. M. A suggested classification for two groups of *Campylobacter* myoviruses. *Arch. Virol.* **2014**, *159*, 181–190, doi:10.1007/s00705-013-1788-2.

17. Kropinski, A. M.; Arutyunov, D.; Foss, M.; Cunningham, A.; Ding, W.; Singh, A.; Pavlov, A. R.; Henry, M.; Evoy, S.; Kelly, J.; Szymanski, C. M. Genome and proteome of *Campylobacter jejuni* bacteriophage NCTC 12673. *Appl. Environ. Microbiol.* **2011**, *77*, 8265–8271, doi:10.1128/AEM.05562-11.

18. Beeby, M.; Ribardo, D. A.; Brennan, C. A.; Ruby, E. G.; Jensen, G. J.; Hendrixson, D. R. Diverse high-torque bacterial flagellar motors assemble wider stator rings using a conserved protein scaffold. *Proc. Natl. Acad. Sci. U. S. A.* **2016**, *113*, E1917-26, doi:10.1073/pnas.1518952113.

19. Goon, S.; Kelly, J. F.; Logan, S. M.; Ewing, C. P.; Guerry, P. Pseudaminic acid, the major modification on *Campylobacter* flagellin, is synthesized via the Cj1293 gene. *Mol. Microbiol.* **2003**, *50*, 659–671, doi:10.1046/j.1365-2958.2003.03725.x.

20. Flint, A.; Sun, Y.-Q. Q.; Butcher, J.; Stahl, M.; Huang, H.; Stintzi, A. Phenotypic screening of a targeted mutant library reveals *Campylobacter jejuni* defenses against oxidative stress. *Infect. Immun.* **2014**, *82*, 2266–2275, doi:10.1128/IAI.01528-13.

21. Javed, M. A.; van Alphen, L. B.; Sacher, J.; Ding, W.; Kelly, J.; Nargang, C.; Smith, D. F.; Cummings, R. D.; Szymanski, C. M. A receptor-binding protein of *Campylobacter jejuni* bacteriophage NCTC 12673 recognizes flagellin glycosylated with acetamidino-modified pseudaminic acid. *Mol. Microbiol.* **2015**, *95*, 101–115, doi:10.1111/mmi.12849.

22. Sørensen, M. C. H.; van Alphen, L. B.; Harboe, A.; Li, J.; Christensen, B. B.; Szymanski, C. M.; Brøndsted, L. Bacteriophage F336 recognizes the capsular phosphoramidate

modification of *Campylobacter jejuni* NCTC11168. *J. Bacteriol.* **2011**, *193*, 6742–6749, doi:10.1128/JB.05276-11.

23. Frost, J. A.; Kramer, J. M.; Gillanders, S. A. Phage typing of *Campylobacter jejuni* and *Campylobacter coli* and its use as an adjunct to serotyping. *Epidemiol. Infect.* **1999**, *123*, S095026889900254X, doi:10.1017/S095026889900254X.

24. Sørensen, M. C. H.; Gencay, Y. E.; Brøndsted, L. Methods for initial characterization of *Campylobacter jejuni* bacteriophages. In *Methods in Molecular Biology*; 2017; Vol. 1512, pp. 91–105 ISBN 978-1-4939-6536-6.

25. Baldvinsson, S. B.; Holst Sørensen, M. C.; Vegge, C. S.; Clokie, M. R. J.; Brøndsted, L. *Campylobacter jejuni* motility is required for infection of the flagellotropic bacteriophage F341. *Appl. Environ. Microbiol.* **2014**, *80*, 7096–7106, doi:10.1128/AEM.02057-14.

26. Palyada, K.; Threadgill, D.; Stintzi, A. Iron acquisition and regulation in *Campylobacter jejuni*. *J. Bacteriol.* **2004**, *186*, 4714–4729, doi:10.1128/JB.186.14.4714-4729.2004.

27. Love, M. I.; Huber, W.; Anders, S. Moderated estimation of fold change and dispersion for RNA-seq data with DESeq2. *Genome Biol.* **2014**, *15*, doi:10.1186/s13059-014-0550-8.

28. Dobin, A.; Davis, C. A.; Schlesinger, F.; Drenkow, J.; Zaleski, C.; Jha, S.; Batut, P.; Chaisson, M.; Gingeras, T. R. STAR: Ultrafast universal RNA-seq aligner. *Bioinformatics* **2013**, *29*, 15–21, doi:10.1093/bioinformatics/bts635.

29. Luo, W.; Friedman, M. S.; Shedden, K.; Hankenson, K. D.; Woolf, P. J. GAGE: Generally applicable gene set enrichment for pathway analysis. *BMC Bioinformatics* **2009**, *10*, doi:10.1186/1471-2105-10-161.

30. Parkhill, J.; Wren, B. W.; Mungall, K.; Ketley, J. M.; Churcher, C.; Basham, D.;

Chillingworth, T.; Davies, R. M.; Feltwell, T.; Holroyd, S.; Jagels, K.; Karlyshev, A. V.; Moule, S.; Pallen, M. J.; Penn, C. W.; Quail, M. A.; Rajandream, M. A.; Rutherford, K. M.; Van Vliet, A. H. M.; Whitehead, S.; Barrell, B. G. The genome sequence of the food-borne pathogen *Campylobacter jejuni* reveals hypervariable sequences. *Nature* **2000**, doi:10.1038/35001088.

31. St. Michael, F.; Szymanski, C. M.; Li, J.; Chan, K. H.; Khieu, N. H.; Larocque, S.; Wakarchuk, W. W.; Brisson, J. R.; Monteiro, M. A. The structures of the lipooligosaccharide and capsule polysaccharide of *Campylobacter jejuni* genome sequenced strain NCTC 11168. *Eur. J. Biochem.* **2002**, *269*, 5119–5136, doi:10.1046/j.1432-1033.2002.03201.x.

32. Palyada, K.; Sun, Y. Q.; Flint, A.; Butcher, J.; Naikare, H.; Stintzi, A. Characterization of the oxidative stress stimulon and PerR regulon of *Campylobacter jejuni*. *BMC Genomics* **2009**, *10*, 481, doi:10.1186/1471-2164-10-481.

33. Grajewski, B. A.; Kusek, J. W.; Gelfand, H. M. Development of bacteriophage typing system for *Campylobacter jejuni* and *Campylobacter coli*. *J. Clin. Microbiol.* **1985**, *22*, 13–18.

34. Szymanski, C. M.; Logan, S. M.; Linton, D.; Wren, B. W. *Campylobacter* - A tale of two protein glycosylation systems. *Trends Microbiol.* 2003, *11*, 233–238.

35. Beeby, M.; Ribardo, D. A.; Brennan, C. A.; Ruby, E. G.; Jensen, G. J. Diverse high-torque bacterial flagellar motors assemble wider stator rings using a conserved protein scaffold. **2016**, 1–10, doi:10.1073/pnas.1518952113.

36. Javed, M. A. M. A.; van Alphen, L. B. L. B.; Sacher, J.; Ding, W.; Kelly, J.; Nargang, C.; Smith, D. F. D. F.; Cummings, R. D. R. D.; Szymanski, C. M. C. M. A receptor-binding

protein of *Campylobacter jejuni* bacteriophage NCTC 12673 recognizes flagellin glycosylated with acetamidino-modified pseudaminic acid. *Mol. Microbiol.* **2015**, *95*, 101–115, doi:10.1111/mmi.12849.

37. Javed, M. A. M. A.; Sacher, J. C. J. C.; van Alphen, L. B. L. B.; Patry, R. T. R. T.; Szymanski, C. M. C. M. A flagellar glycan-specific protein encoded by *Campylobacter* phages inhibits host cell growth. *Viruses* **2015**, *7*, 6661–6674, doi:10.3390/v7122964.

38. Logan, S. M. Flagellar glycosylation - A new component of the motility repertoire? *Microbiology* **2006**, *152*, 1249–1262.

39. Boll, J. M.; Hendrixson, D. R. A regulatory checkpoint during flagellar biogenesis in *Campylobacter jejuni* initiates signal transduction to activate transcription of flagellar genes. *MBio* **2013**, *4*, e00432-13, doi:10.1128/mBio.00432-13; 10.1128/mBio.00432-13.

40. Gilbreath, J. J.; Cody, W. L.; Merrell, D. S.; Hendrixson, D. R. Change is good: variations in common biological mechanisms in the epsilonproteobacterial genera *Campylobacter* and *Helicobacter*. *Microbiol. Mol. Biol. Rev.* **2011**, *75*, 84–132, doi:10.1128/MMBR.00035-10.

41. Guerry, P. Campylobacter flagella: not just for motility. *Trends Microbiol.* ***2007***, *15*, 456–461.

42. Lango-Scholey, L.; Aidley, J.; Woodacre, A.; Jones, M. A.; Bayliss, C. D. High throughput method for analysis of repeat number for 28 phase variable loci of *Campylobacter jejuni* strain NCTC11168. *PLoS One* **2016**, *11*, doi:10.1371/journal.pone.0159634.

43. Siringan, P.; Connerton, P. L.; Cummings, N. J.; Connerton, I. F. Alternative bacteriophage life cycles: the carrier state of *Campylobacter jejuni*. *Open Biol.* **2014**, 4,

130200, doi:10.1098/rsob.130200.

44. Aidley, J.; Holst Sørensen, M. C.; Bayliss, C. D.; Brøndsted, L. Phage exposure causes dynamic shifts in the expression states of specific phase-variable genes of *Campylobacter* jejuni. *Microbiol. (United Kingdom)* **2017**, *163*, 911–919, doi:10.1099/mic.0.000470.

45. Sacher, J. C.; Flint, A.; Butcher, J.; Blasdel, B.; Reynolds, H. M.; Lavigne, R.; Stintzi, A.; Szymanski, C. M. Transcriptomic analysis of the *Campylobacter jejuni* response to T4-like phage NCTC 12673 infection. *Viruses* **2018,** *10*, 332.

Chapter 6: Conclusions

6.1. Overview

In addition to encoding capsular polysaccharides and lipooligosaccharides, *C. jejuni* encodes both N- and O-linked glycosylation systems [1–3]. As glycosylated structures are essential to the biology and virulence of this organism and others, and since much is already known about *C. jejuni* glycobiology, *C. jejuni* has become a model organism for bacterial glycobiology studies [4].

Phages are predicted to be a main driver of bacterial evolution, and have likely been interacting with bacterial glycans since their beginnings [5]. However, little is known about how phages and *Campylobacter* interact, or how glycans influence these interactions. The goal of my doctoral work has been to study *C. jejuni*-phage interactions in the context of glycobiology. Specifically, I have sought to characterize how a conserved glycan-binding protein encoded by *Campylobacter* phages influences *C. jejuni* biology, and why phages of *Campylobacter* would encode such a protein. The conserved nature of this protein paired with the observation that flagellar glycosylation mutants can resist infection by certain phages led us to hypothesize that flagellar glycosylation and phage infection are intertwined in *C. jejuni*. My work has uncovered new insights into this phage-glycan interplay that create an exciting foundation for future studies.

6.2. Model organisms and reasons for their selection

I have studied the interactions between NCTC 12673 phage and *C. jejuni* 11168, the first sequenced strain of the species [6]. NCTC 12673 phage encodes Gp047, a 1365-amino acid protein specific for certain *C. jejuni* flagellar glycans [7,8]. We found that NCTC 12673 could

not infect mutants of the pathway that generates these glycans in *C. jejuni* 11168, and thus chose this phage-host system as a model for studying phage-glycan interactions.

6.3. Main findings

6.3.1. Part I: Understanding the interactions between Gp047 and *C. jejuni* cells

6.3.1.1. Gp047 inhibits growth of *C. jejuni* expressing flagellar acetamidino-modified pseudaminic acid glycans

Originally, it was thought that Gp047 was the NCTC 12673 tail fiber protein responsible for host recognition. This was hypothesized based on its location on the phage genome relative to other genes associated with building the virion structure, and its large size (4.1 kb), hallmarks of tail fiber status in related T4-like phages [8]. Early work was aimed at determining the receptor specificity of this protein, and it was assumed that it would target CPS since it was known that the phage required CPS to infect cells [8,9]. However, our group later determined that Gp047 binds instead to *C. jejuni* flagellin [7]. I joined the lab at this point, and helped determine that Gp047 binds specifically to flagellar Pse5Ac7Am sugars, reducing their motility upon binding [7]. Despite multiple attempts, I was not able to localize Gp047 expression on the virion surface, nor could I show NCTC 12673 binding to flagella. This was in accordance with the apparent absence of Gp047 in the NCTC 12673 phage proteome [8]. These results suggested that in addition to not being CPS-specific, Gp047 was also not likely to be a tail fiber protein. Instead, we hypothesized that like other viruses that express specific effector proteins [10], Gp047 might have an extracellular effector function related to flagellar glycan-binding.

To better understand the function, role and activity of Gp047, I next set out to characterize the unexpected growth clearance activity that others in our group had observed when Gp047 was spotted on *C. jejuni* growing on agar plates. I helped show that Gp047 binding clears growth of *C. jejuni* cells only in the presence of Pse5Ac7Am-decorated flagella, and that this activity occurs in liquid culture as well [11]. I also determined that this protein does not appear to lyse cells or alter their morphology, but instead appears to inhibit their growth [11].

From these results, we sought to determine why *Campylobacter* phages would make such a protein, and also how and why *Campylobacter* could be growth-inhibited as a result of its flagella being bound by a protein. As it was, and still is, largely unknown why *Campylobacter* generates such diversity in its flagellar sugars, particularly when it has such little room in its small genome [6,12], we hypothesized that phage pressures might have driven the evolution of some of this diversity. Our group in collaboration with others have shown that *C. jejuni* displays phase-variable chemical modifications on its capsular sugars, and that the combination of these modifications paired with the combination of sugars making up the capsule alter the infectivity of several phages [13–15]. Therefore, we hypothesized that *C. jejuni* flagellar glycans might serve a similar purpose in protecting cells from phages. I thus sought to identify the mechanism of Gp047 clearing of *C. jejuni* in order to better understand how this protein might constitute a selective pressure against the organism and identify ways *C. jejuni* might be able to escape this pressure.

6.3.1.2. Probing with Gp047 reveals previously unexplored diversity in *C. jejuni* flagellar glycans

To identify the mechanism of Gp047 clearing of *C. jejuni,* I sought to identify strains resistant to clearing but still susceptible to binding. Essentially, I sought to decouple binding from clearing. I hypothesized that a molecular switch existed in *C. jejuni* that would convert a binding signal into a growth-inhibitory signal, and surmised that decoupling these processes would lead to understanding that signal, should it exist.

I identified a subset of strains displaying reduced clearing by Gp047, and yet were all agglutinated by the protein, suggesting that they might exhibit the binding-positive, clearing-negative phenotype we were seeking [16]. However, upon further analysis of Gp047 binding to these strains using electron microscopy, I found that compared to *C. jejuni* 11168, these strains in fact exhibited reduced binding as well. This suggested that these strains were not in fact binding/clearing-decoupled, but instead either partially or completely avoided Gp047 binding in the first place.

As one of our research questions had been to understand how *C. jejuni* might avoid Gp047 binding in nature, however, I continued to characterize these strains. I sought to test the hypothesis that these strains displayed reduced Gp047 binding as a result of varying their flagellar glycans, so I submitted flagella from these strains for MS analysis. Interestingly, this led to the finding that these *C. jejuni* strains, which were relatively poorly characterized, displayed glycans different from those observed for better-characterized strains such as 11168 (Chapter 4). As well, one strain exhibited on and off-switching of its Gp047 binding ability,

suggesting a phase variable Pse5Ac7Am expression in this strain. Phase variability had not previously been observed for the genes encoding this sugar. Alongside our MS analysis of these strains, we genome-sequenced the strains and compared their flagellar glycosylation loci to learn more about possible mechanisms for their flagellar glycosylation differences (genome announcements for these strains were accepted for publication in *Genome Announcements* in May 2018). In fact, we found that the strain exhibiting Gp047 binding variability encodes a phase-variable poly-G tract in its *pseD* gene. Overall, this study illuminated new insights into the capacity of *C. jejuni* to express and vary its flagellar glycans. Furthermore, our study highlights the use of a phage glycan-binding protein as a useful reagent in bacterial glycobiology, as no reagent has previously been observed to be able to distinguish between such small differences in flagellar glycans, particularly pseudaminic acid sugars like those studied here [5].

6.3.1.3. Gp047 binding induces downregulation of pathways for cellular energy metabolism, and does not occur when flagella are paralyzed

Alongside the above-described studies, I continued to pursue the question of how Gp047 clears growth after it binds *C. jejuni* flagella. Excitingly, I determined that Gp047 binding/clearing decoupling occurred in *motA* and *motB* mutants of *C. jejuni* 11168. These mutants cannot make functional flagellar motor complexes, and make full-length yet paralyzed flagella [17]. I found that Gp047 clearing was essentially abolished on these mutants, and yet that flagellar binding was still robust (Chapter 4). This suggested that the mechanism of Gp047 clearing may be linked to proton motive force changes in the cell upon flagellar binding. We came to this hypothesis because *motA* and *motB* proteins are known to allow protons to flow from the

periplasm through a channel in the inner membrane and into the cytoplasm, and this allows the flagellar motor to turn [17,18]. As well, flagellar motors in bacteria such as *C. jejuni* are known to sense changes in viscosity and to alter the torque they generate in response [19,20]. We presumed that Gp047 binding might induce overcompensation by the *C. jejuni* flagellar motor, resulting in an increase in protons allowed to flow through the channel. If this increase was substantial, it might lead to stress in the cell due to a disruption of PMF homeostasis. Further work into establishing this model as the mechanism by which Gp047 causes growth clearance is ongoing.

Concurrently with work aimed at decoupling Gp047 binding from clearing, we used another strategy, RNA-sequencing, to understand the effect of Gp047 on cells. We sought to identify genes up-regulated or down-regulated in response to Gp047 treatment that might hint at the downstream pathways induced upon binding. This study showed that several pathways involved with energy metabolism were down-regulated in response to Gp047 compared to untreated cells, such as TCA cycle genes and short chain fatty acid metabolism pathways (Chapter 4). It remains to be determined whether this represents cells actively downshifting their metabolism in response to Gp047, perhaps representing an evolved response to protect against an incoming phage attack, or whether these metabolic changes are downstream consequences of the above-hypothesized disruption in PMF balance.

6.3.2. Part II: Understanding why NCTC 12673 phage requires a functional flagellar glycosylation pathway for infection

6.3.2.1. *C. jejuni* pseudaminic acid biosynthesis genes are required for bacteriophage NCTC 12673 infection

In addition to making a protein that binds to host flagellar glycans, work done by others in our group prior to my starting on this project showed that NCTC 12673 phage could not efficiently propagate on cells unable to make these same glycans. It was noteworthy that NCTC 12673 phage was classified as a CPS-dependent phage, and not a flagella-dependent phage, based on its ability to infect some non-motile mutants and its inability to infect acapsular mutants [9]. I thus sought to characterize this apparent dependence on flagellar glycosylation. I found that this phage could still adsorb to the cell surface of flagellar glycosylation mutants, suggesting that disruption of this pathway impacts a downstream part of the phage infection process, such as DNA injection, replication or assembly. We first hypothesized that the phage uses the glycans in some way, perhaps to glycosylate its DNA, as T4 does with glucose residues [21]. To test this, we examined phage DNA by MS for the presence of glycan intermediates of the pseudaminic acid pathway. We did not find any glycans present on the DNA, however, this led to the unexpected discovery that *Campylobacter* phages across two phylogenetic groups completely substitute deoxyguanosine in their DNA for non-canonical bases. This work is currently in preparation for submission to *Nature Microbiology*.

6.3.2.2. Motility defects likely explain phage NCTC 12673 dependence on *C. jejuni* pseudaminic acid biosynthesis genes

We next tested the hypothesis that the phage was susceptible to some side-effect of the pseudaminic acid biosynthesis pathway being interrupted. To test whether cell stress-related side effects of flagellar glycosylation mutations could explain the observed lack of phage propagation on these mutants, I examined the transcriptomes of two mutants in the flagellar glycan pathway. Whereas I did not detect signs of global cell stress response, I did observe widespread downregulation of many flagellar filament biogenesis- and flagellar glycosylation-related genes (Chapter 5). As motility was the main perturbation in these mutants, this suggested that the lack of motility of the flagellar glycosylation mutants might explain the apparent dependence on the flagellar glycosylation pathway by the phage. I therefore tested NCTC 12673 phage plaquing on *motA* and *motB,* the non-motile paralyzed flagellar mutants described above, and observed no plaquing on these mutants, supporting this hypothesis. As well, I showed that a phage escape mutant that could plaque on *pseC* could also readily plaque on *motA* and *motB* mutants, further supporting the notion that a lack of motility, and not of flagellar glycans, may have led to the reduced infectivity of NCTC 12673 phage infection of *pse* mutants.

6.3.2.3. Oxidative stress sensitivity may explain the reduced ability of phage NCTC 12673 to plaque on non-motile *C. jejuni* mutants

In light of these results, it was still unclear why this phage would depend on motility, especially since it could adsorb equally to cells with or without flagellar filaments. Interestingly, work by Flint *et al.* (2014) has shown that non-motile mutants of *C. jejuni* are hypersensitive to oxidative stress, and this is speculated to result from issues with PMF homeostasis [22]. Concurrent to this

work, and primarily to learn more about the host factors important for this phage during infection, I had also examined NCTC 12673 infection of *C. jejuni* cells using RNA-seq. Interestingly, this work led to the finding that genes that aid in oxidative stress defense are up-regulated during phage infection, and that interruption of antioxidant genes reduces NCTC 12673 phage infectivity (this study will be submitted for publication to *Viruses* in May 2018). This apparent sensitivity of NCTC 12673 phage to oxidative stress, paired with the observation by Flint *et al.* that non-motile *C. jejuni* mutants are hypersensitive to oxidative stress [22], led me to hypothesize that oxidative stress hypersensitivity might explain the inability of this phage to plaque on mutants in the *C. jejuni* flagellar glycosylation pathway. To test this, we plaqued the above-mentioned *pseC* escape mutant phage on *C. jejuni* antioxidant mutants, and interestingly, the mutant phage was able to plaque better than NCTC 12673 on two of the three antioxidant mutants tested. The fact that one phage escape mutant simultaneously gained the ability to plaque on mutants in both antioxidant and motility genes suggests that the two types of defects are linked from a phage perspective. This finding supported the hypothesis that oxidative stress sensitivity may explain the inability of NCTC 12673 to plaque on non-motile mutants.

6.3.2.4. Changes in Gp047 expression may impact NCTC 12673 phage ability to infect non-motile *C. jejuni* cells

Excitingly, genome sequence comparison between NCTC 12673 and this escape mutant phage that could efficiently infect *pse, mot* and antioxidant mutants showed that the main difference between the two phages mapped to a nonsense mutation in *gp047* encoded by the escape mutant phage. In contrast, NCTC 12673 phage encodes the full-length version. This suggests that the flagellar glycan binding protein Gp047 may play a role in allowing phage infection to proceed

on non-motile and/or oxidatively stressed mutants. Further work is required to establish a role for this protein in regulating phage infection, but it is exciting to speculate that Gp047 might have multiple roles in the phage lifecycle: one being to bind to surface-exposed glycosylated flagella, perhaps as an effector protein released upon phage lysis as described above, and another being to mediate whether or not phage lysis proceeds based on sensing the flagellation state or oxidative stress state of the cell.

6.4. Final remarks

Overall, this work has identified several new insights into the complex interplay between phages and *C. jejuni* flagellar glycosylation. Our findings suggest that phages may encode proteins with very specific glycan-binding functions with roles that may extend beyond host recognition and adsorption. Further work in this area should provide exciting new insights into how phages may have impacted flagellar glycan evolution in *Campylobacter*, as well as new insights into the function of flagellar glycans in this organism.

6.5. References

1. Nothaft, H.; Szymanski, C. M. Bacterial protein N-glycosylation: New perspectives and applications. *J. Biol. Chem.* **2013**, *288*, 6912–6920.
2. Logan, S. M.; Schoenhofen, I. C.; Guerry, P. O-linked flagellar glycosylation in *Campylobacter*. In; Nachamkin, I., Szymanski, C. M., Blaser, M. J., Eds.; *Campylobacter*; ASM Press: Washington, D.C., 2008; pp. 471–481.
3. Karlyshev, A. V.; Ketley, J. M.; Wren, B. W. The *Campylobacter jejuni* glycome. *FEMS*

Microbiol. Rev. ***2005***, *29*, 377–390.

4. Szymanski, C. M.; Logan, S. M.; Linton, D.; Wren, B. W. *Campylobacter* - A tale of two protein glycosylation systems. *Trends Microbiol.* ***2003***, *11*, 233–238.
5. Simpson, D. J.; Sacher, J. C.; Szymanski, C. M. Exploring the interactions between bacteriophage-encoded glycan binding proteins and carbohydrates. *Curr. Opin. Struct. Biol.* **2015**, *34*, 69–77, doi:10.1016/j.sbi.2015.07.006.
6. Parkhill, J.; Wren, B. W.; Mungall, K.; Ketley, J. M.; Churcher, C.; Basham, D.; Chillingworth, T.; Davies, R. M.; Feltwell, T.; Holroyd, S.; Jagels, K.; Karlyshev, A. V.; Moule, S.; Pallen, M. J.; Penn, C. W.; Quail, M. A.; Rajandream, M. A.; Rutherford, K. M.; Van Vliet, A. H. M.; Whitehead, S.; Barrell, B. G. The genome sequence of the food-borne pathogen *Campylobacter jejuni* reveals hypervariable sequences. *Nature* **2000**, doi:10.1038/35001088.
7. Javed, M. A.; van Alphen, L. B.; Sacher, J.; Ding, W.; Kelly, J.; Nargang, C.; Smith, D. F.; Cummings, R. D.; Szymanski, C. M. A receptor-binding protein of *Campylobacter jejuni* bacteriophage NCTC 12673 recognizes flagellin glycosylated with acetamidino-modified pseudaminic acid. *Mol. Microbiol.* **2015**, *95*, 101–115, doi:10.1111/mmi.12849.
8. Kropinski, A. M.; Arutyunov, D.; Foss, M.; Cunningham, A.; Ding, W.; Singh, A.; Pavlov, A. R.; Henry, M.; Evoy, S.; Kelly, J.; Szymanski, C. M. Genome and proteome of *Campylobacter jejuni* bacteriophage NCTC 12673. *Appl. Environ. Microbiol.* **2011**, *77*, 8265–8271, doi:10.1128/AEM.05562-11.
9. Coward, C.; Grant, A. J.; Swift, C.; Philp, J.; Towler, R.; Heydarian, M.; Frost, J. A.; Maskell, D. J. Phase-variable surface structures are required for infection of *Campylobacter jejuni* by bacteriophages. *Appl. Environ. Microbiol.* **2006**, *72*, 4638–4647,

doi:10.1128/AEM.00184-06.

10. Faruque, S. M.; Mekalanos, J. J. Phage-bacterial interactions in the evolution of toxigenic Vibrio cholerae. *Virulence* **2012**, *3*.

11. Javed, M. A.; Sacher, J. C.; van Alphen, L. B.; Patry, R. T.; Szymanski, C. M. A flagellar glycan-specific protein encoded by *Campylobacter* phages inhibits host cell growth. *Viruses* **2015**, *7*, 6661–6674, doi:10.3390/v7122964.

12. Guerry, P. *Campylobacter* flagella: not just for motility. *Trends Microbiol.* **2007**, *15*, 456–461.

13. Gencay, Y. E.; Sørensen, M. C. H.; Wenzel, C. Q.; Szymanski, C. M.; Brøndsted, L. Phase Variable Expression of a Single Phage Receptor in *Campylobacter jejuni* NCTC12662 Influences Sensitivity Toward Several Diverse CPS-Dependent Phages. *Front. Microbiol.* **2018**, *9*, 82, doi:10.3389/fmicb.2018.00082.

14. Aidley, J.; Holst Sørensen, M. C.; Bayliss, C. D.; Brøndsted, L. Phage exposure causes dynamic shifts in the expression states of specific phase-variable genes of *Campylobacter jejuni*. *Microbiol. (United Kingdom)* **2017**, *163*, 911–919, doi:10.1099/mic.0.000470.

15. Sørensen, M. C. H.; van Alphen, L. B.; Fodor, C.; Crowley, S. M.; Christensen, B. B.; Szymanski, C. M.; Brøndsted, L. Phase Variable Expression of Capsular Polysaccharide Modifications Allows *Campylobacter jejuni* to Avoid Bacteriophage Infection in Chickens. *Front. Cell. Infect. Microbiol.* **2012**, *2*, doi:10.3389/fcimb.2012.00011.

16. Javed, M. A.; Poshtiban, S.; Arutyunov, D.; Evoy, S.; Szymanski, C. M. Bacteriophage Receptor Binding Protein Based Assays for the Simultaneous Detection of *Campylobacter jejuni* and *Campylobacter coli*. *PLoS One* **2013**, *8*, doi:10.1371/journal.pone.0069770.

17. Beeby, M.; Ribardo, D. A.; Brennan, C. A.; Ruby, E. G.; Jensen, G. J. Diverse high-torque bacterial flagellar motors assemble wider stator rings using a conserved protein scaffold. **2016**, 1–10, doi:10.1073/pnas.1518952113.

18. Mohawk, K. L.; Poly, F.; Sahl, J. W.; Rasko, D. A.; Guerry, P. High frequency, spontaneous *motA* mutations in *Campylobacter jejuni* strain 81-176. *PLoS One* **2014**, *9*, doi:10.1371/journal.pone.0088043.

19. Lele, P. P.; Hosu, B. G.; Berg, H. C. Dynamics of mechanosensing in the bacterial flagellar motor. *Proc. Nat. Acad. Sci.* **2013**, *110*, 29, 11839-11844, doi:10.1073/pnas.1305885110.

20. Chaban, B.; Coleman, I.; Beeby, M. Evolution of higher torque in *Campylobacter*-type bacterial flagellar motors. *Sci. Rep.* **2018**, *8*, 97, doi:10.1038/s41598-017-18115-1.

21. Miller, E. S.; Kutter, E.; Mosig, G.; Arisaka, F.; Kunisawa, T.; Rüger, W. Bacteriophage T4 genome. *Microbiol. Mol. Biol. Rev.* **2003**, *67*, 86–156, doi:10.1128/MMBR.67.1.86-156.2003.

22. Flint, A.; Sun, Y.-Q. Q.; Butcher, J.; Stahl, M.; Huang, H.; Stintzi, A. Phenotypic screening of a targeted mutant library reveals *Campylobacter jejuni* defenses against oxidative stress. *Infect. Immun.* **2014**, *82*, 2266–2275, doi:10.1128/IAI.01528-13.

Bibliography

1. Abedon, S. T. Commentary: Communication between Viruses Guides Lysis-Lysogeny Decisions. *Front. Microbiol.* **2017**, *8*, 983, doi:10.3389/fmicb.2017.00983.

2. Abedon, S.; Kuhl, S. J.; Blasdel, B. G.; Kutter, E. M. Phage treatment of human infections. *Bacteriophage* **2011**, doi:10.4161/bact.1.2.15845.

3. Abedon, S.T. Bacteriophage Ecology: Population Growth, Evolution, and Impact of Bacterial Viruses; Cambridge University Press: Cambridge, UK, **2008**; Volume 15.

4. Abu-Qarn, M.; Eichler, J.; Sharon, N. Not just for Eukarya anymore: protein glycosylation in Bacteria and Archaea. *Curr. Opin. Struct. Biol*. **2008**, *18*, 544–550.

5. Aidley, J.; Holst Sørensen, M. C.; Bayliss, C. D.; Brøndsted, L. Phage exposure causes dynamic shifts in the expression states of specific phase-variable genes of *Campylobacter jejuni*. *Microbiol. (United Kingdom)* **2017**, *163*, 911–919, doi:10.1099/mic.0.000470.

6. Akiba, M.; Lin, J.; Barton, Y.-W.; Zhang, Q. Interaction of CmeABC and CmeDEF in conferring antimicrobial resistance and maintaining cell viability in *Campylobacter jejuni*. *J. Antimicrob. Chemother.* **2006**, *57*, 52–60, doi:10.1093/jac/dki419.

7. Alanis, A. J. Resistance to Antibiotics: Are We in the Post-Antibiotic Era? *Arch. Med. Res.* **2005**, *36*, 697–705, doi:DOI: 10.1016/j.arcmed.2005.06.009.

8. Alemka, A.; Nothaft, H.; Zheng, J.; Szymanski, C. M. N-glycosylation of *Campylobacter jejuni* surface proteins promotes bacterial fitness. *Infect. Immun.* **2013**, doi:10.1128/IAI.01370-12.

9. Amour, C.; Gratz, J.; Mduma, E.; Svensen, E.; Rogawski, E. T.; McGrath, M.; Seidman, J. C.; McCormick, B. J. J. J.; Shrestha, S.; Samie, A.; Mahfuz, M.; Qureshi, S.; Hotwani, A.; Babji, S.; Trigoso, D. R.; Lima, A. A. M. M.; Bodhidatta, L.; Bessong, P.; Ahmed, T.; Shakoor, S.; Kang, G.; Kosek, M.; Guerrant, R. L.; Lang, D.; Gottlieb, M.; Houpt, E. R.; Platts-Mills, J. A.; Etiology, Risk Factors, and Interactions of Enteric Infections and

Malnutrition and the Consequences for Child Health and Development Project (MAL-ED) Network Investigators Epidemiology and Impact of *Campylobacter* Infection in Children in 8 Low-Resource Settings: Results from the MAL-ED Study. Clin. Infect. Dis. **2016**, *63*, 1171–1179, doi:10.1093/cid/ciw542.

10. Anjum, A.; Brathwaite, K. J.; Aidley, J.; Connerton, P. L.; Cummings, N. J.; Parkhill, J.; Connerton, I.; Bayliss, C. D. Phase variation of a Type IIG restriction-modification enzyme alters site-specific methylation patterns and gene expression in *Campylobacter jejuni* strain NCTC11168. Nucleic Acids Res. **2016**, *44*, 4581–4594, doi:10.1093/nar/gkw019.
11. Ankrah, N. Y. D.; May, A. L.; Middleton, J. L.; Jones, D. R.; Hadden, M. K.; Gooding, J. R.; LeCleir, G. R.; Wilhelm, S. W.; Campagna, S. R.; Buchan, A. Phage infection of an environmentally relevant marine bacterium alters host metabolism and lysate composition. *ISME J.* **2014**, *8*, 1089–100, doi:10.1038/ismej.2013.216.
12. Arutyunov, D.; Szymanski, C. M. A novel DNA-binding protein from *Campylobacter jejuni* bacteriophage NCTC12673. *FEMS Microbiol. Lett.* **2015**, 362, doi:10.1093/femsle/fnv160.
13. Atterbury, R. J.; Dillon, E.; Swift, C.; Connerton, P. L.; Frost, J. A.; Dodd, C. E. R.; Rees, C. E. D.; Connerton, I. F. Correlation of *Campylobacter* bacteriophage with reduced presence of hosts in broiler chicken ceca. *Appl. Environ. Microbiol*. **2005**, *71*, 4885–4887, doi:10.1128/AEM.71.8.4885-4887.2005.
14. Backert, S.; Hofreuter, D. Molecular methods to investigate adhesion, transmigration, invasion and intracellular survival of the foodborne pathogen *Campylobacter jejuni. J. Microbiol. Methods* **2013**.

15. Bacon, D. J.; Szymanski, C. M.; Burr, D. H.; Silver, R. P.; Alm, R. A.; Guerry, P. A phase-variable capsule is involved in virulence of *Campylobacter jejuni* 81-176. *Mol. Microbiol*. **2001**, *40*, 769–777, doi:10.1046/j.1365-2958.2001.02431.x.

16. Balaban, M.; Hendrixson, D.R. Polar flagellar biosynthesis and a regulator of flagellar number influence spatial parameters of cell division in *Campylobacter jejuni. PLoS Pathog.* **2011**, *7*, e1002420.

17. Baldvinsson, S. B.; Holst Sørensen, M. C.; Vegge, C. S.; Clokie, M. R. J.; Brøndsted, L. *Campylobacter jejuni* motility is required for infection of the flagellotropic bacteriophage F341. *Appl. Environ. Microbiol*. ***2014***, *80*, 7096–7106, doi:10.1128/AEM.02057-14.

18. Bartual, S. G.; Otero, J. M.; Garcia-Doval, C.; Llamas-Saiz, A. L.; Kahn, R.; Fox, G. C.; van Raaij, M. J. Structure of the bacteriophage T4 long tail fiber receptor-binding tip. *Proc. Nat. Acad. Sci.* **2010,** *107*, 20287-20292.

19. Baxa, U.; Steinbacher, S.; Miller, S.; Weintraub, A.; Huber, R.; Seckler, R. Interactions of phage P22 tails with their cellular receptor, *Salmonella* O-antigen polysaccharide. *Biophys. J.* **1996**, *71*, 2040–2048.

20. Bayliss, C. D.; Bidmos, F. A.; Anjum, A.; Manchev, V. T.; Richards, R. L.; Grossier, J. P.; Wooldridge, K. G.; Ketley, J. M.; Barrow, P. A.; Jones, M. A.; Tretyakov, M. V. Phase variable genes of *Campylobacter jejuni* exhibit high mutation rates and specific mutational patterns but mutability is not the major determinant of population structure during host colonization. *Nucleic Acids Res*. **2012**, *40*, 5876–5889, doi:10.1093/nar/gks246.

21. Beauchamp, J. M.; Leveque, R. M.; Dawid, S.; DiRita, V. J. Methylation-dependent DNA discrimination in natural transformation of *Campylobacter jejuni. Proc. Natl. Acad. Sci*. **2017**, 201703331, doi:10.1073/pnas.1703331114.

22. Beeby, M.; Ribardo, D. A.; Brennan, C. A.; Ruby, E. G.; Jensen, G. J. Diverse high-torque bacterial flagellar motors assemble wider stator rings using a conserved protein scaffold. 2016, 1–10, doi:10.1073/pnas.1518952113.

23. Beeby, M.; Ribardo, D. A.; Brennan, C. A.; Ruby, E. G.; Jensen, G. J.; Hendrixson, D. R. Diverse high-torque bacterial flagellar motors assemble wider stator rings using a conserved protein scaffold. *Proc. Natl. Acad. Sci. U. S. A*. **2016**, *113*, E1917-26, doi:10.1073/pnas.1518952113.

24. Belas, R. Biofilms, flagella, and mechanosensing of surfaces by bacteria. *Trends Microbiol.* **2014**, *22*, 517–527.

25. Black, R.E.; Levine, M.M.; Clements, M.L.; Hughes, T.P.; Blaser, M.J. Experimental *Campylobacter jejuni* infection in humans. J. Infect. Dis. **1988**, *157*, 472–479.

26. Blasdel, B. G.; Ceyssens, P.-J.; Chevallereau, A.; Debarbieux, L.; Lavigne, R. Comparative transcriptomics reveals a conserved Bacterial Adaptive Phage Response (BAPR) to viral predation. bioRxiv **2018**, doi:10.1101/248849.

27. Blasdel, B. G.; Chevallereau, A.; Monot, M.; Lavigne, R.; Debarbieux, L. Comparative transcriptomics analyses reveal the conservation of an ancestral infectious strategy in two bacteriophage genera. *ISME J. **2017***, doi:10.1038/ismej.2017.63.

28. Blasdel, B.; Ceyssens, P.-J.; Lavigne, R. Preparing cDNA Libraries from Lytic Phage-Infected Cells for Whole Transcriptome Analysis by RNA-Seq. In; 2018; pp. 185–194.

29. Boll, J. M.; Hendrixson, D. R. A regulatory checkpoint during flagellar biogenesis in *Campylobacter jejuni* initiates signal transduction to activate transcription of flagellar genes. *MBio* **2013**, *4*, e00432-13, doi:10.1128/mBio.00432-13; 10.1128/mBio.00432-13.

30. Bolton, D. J. *Campylobacter* virulence and survival factors. Food Microbiol. 2015, 48, 99–108.

31. Boyd, E. F. Bacteriophage-encoded bacterial virulence factors and phage-pathogenicity island interactions. *Adv. Virus Res*. **2012**, *82*, 91–118, doi:10.1016/B978-0-12-394621-8.00014-5; 10.1016/B978-0-12-394621-8.00014-5.

32. Bozzola, J.J.; Russell, L.D. Electron Microscopy: Principles and Techniques for Biologists; Jones and Bartlett Publishers: Sudbury, USA, **1992**; pp. 40–62.

33. Brathwaite, K. J.; Siringan, P.; Connerton, P. L.; Connerton, I. F. Host adaption to the bacteriophage carrier state of *Campylobacter jejuni*. *Res. Microbiol*. **2015**, *166*, 504–515, doi:10.1016/j.resmic.2015.05.003.

34. Briers, Y.; Walmagh, M.; van Puyenbroeck, V.; Cornelissen, A.; Cenens, W.; Aertsen, A.; Oliveira, H.; Azeredo, J.; Verween, G.; Pirnay, J.P.; et al. Engineered endolysin-based "Artilysins" to combat multidrug-resistant gram-negative pathogens. *mBio* **2014**, *5*, e01379-14.

35. Brovko, L. Y.; Anany, H.; Griffiths, M. W. Bacteriophages for detection and control of bacterial pathogens in food and food-processing environment. *Adv. Food Nutr. Res.* **2012**, *67*, 241–288, doi:10.1016/B978-0-12-394598-3.00006-X; 10.1016/B978-0-12-394598-3.00006-X.

36. Bryan, D.; El-Shibiny, A.; Hobbs, Z.; Porter, J.; Kutter, E. M. Bacteriophage T4 infection of stationary phase *E. coli*: Life after log from a phage perspective. *Front. Microbiol*. **2016**, 7, doi:10.3389/fmicb.2016.01391.

37. Bryson, A. L.; Hwang, Y.; Sherrill-Mix, S.; Wu, G. D.; Lewis, J. D.; Black, L.; Clark, T. A.; Bushman, F. D. Covalent Modification of Bacteriophage T4 DNA Inhibits CRISPR-Cas9. *MBio* **2015**, *6*, e00648-15, doi:10.1128/mBio.00648-15.

38. Butcher, J.; Stintzi, A. The Transcriptional Landscape of *Campylobacter jejuni* under Iron Replete and Iron Limited Growth Conditions. *PLoS One* **2013**, *8*, e79475, doi:10.1371/journal.pone.0079475.

39. Cairns, L. S.; Marlow, V. L.; Bissett, E.; Ostrowski, A.; Stanley-Wall, N. R. A mechanical signal transmitted by the flagellum controls signalling in *Bacillus subtilis*. *Mol. Microbiol*. **2013**, *90*, 6–21, doi:10.1111/mmi.12342.

40. Campbell, A. The future of bacteriophage biology. *Nat. Rev. Genet*. **2003**, *4*, 471–477, doi:10.1038/nrg1089.

41. Carvalho, C. M.; Gannon, B. W.; Halfhide, D. E.; Santos, S. B.; Hayes, C. M.; Roe, J. M.; Azeredo, J. The in vivo efficacy of two administration routes of a phage cocktail to reduce numbers of *Campylobacter coli* and *Campylobacter jejuni* in chickens. BMC Microbiol. **2010**, *10*, 232, doi:10.1186/1471-2180-10-232.

42. Casjens, S. R. Comparative genomics and evolution of the tailed-bacteriophages. *Curr. Opin. Microbiol.* **2005**, *8*, 451–458, doi:10.1016/j.mib.2005.06.014.

43. Casjens, S. R.; Molineux, I. J. Short noncontractile tail machines: adsorption and DNA delivery by podoviruses. *Adv. Exp. Med. Biol.* **2012**, *726*, 143–179, doi:10.1007/978-1-4614-0980-9_7; 10.1007/978-1-4614-0980-9_7.

44. Cenens, W.; Makumi, A.; Govers, S. K.; Lavigne, R.; Aertsen, A. Viral Transmission Dynamics at Single-Cell Resolution Reveal Transiently Immune Subpopulations Caused by a Carrier State Association. *PLoS Genet*. **2015**, 1–19, doi:10.1371/journal.pgen.1005770.

45. Cenens, W.; Makumi, A.; Mebrhatu, M. T.; Lavigne, R.; Aertsen, A. Phage-host interactions during pseudolysogeny: Lessons from the Pid/dgo interaction. *Bacteriophage* **2013**, *3*, e25029, doi:10.4161/bact.25029.

46. Ceyssens, P.-J.; Minakhin, L.; Van den Bossche, A.; Yakunina, M.; Klimuk, E.; Blasdel, B.; De Smet, J.; Noben, J.-P.; Bläsi, U.; Severinov, K.; Lavigne, R. Development of giant bacteriophage ϕKZ is independent of the host transcription apparatus. *J. Virol.* **2014**, *88*, 10501–10, doi:10.1128/JVI.01347-14.

47. Chaban, B.; Coleman, I.; Beeby, M. Evolution of higher torque in *Campylobacter*-type bacterial flagellar motors. *Sci. Rep.* **2018**, *8*, 97, doi:10.1038/s41598-017-18115-1.

48. Champion, O. L.; Gaunt, M. W.; Gundogdu, O.; Elmi, A.; Witney, A. A.; Hinds, J.; Dorrell, N.; Wren, B. W. Comparative phylogenomics of the food-borne pathogen *Campylobacter jejuni* reveals genetic markers predictive of infection source. *Proc. Natl. Acad. Sci.* **2005**, *102*, 16043–16048, doi:10.1073/pnas.0503252102.

49. Chan, B. K.; Sistrom, M.; Wertz, J. E.; Kortright, K. E.; Narayan, D.; Turner, P. E. Phage selection restores antibiotic sensitivity in MDR *Pseudomonas aeruginosa*. *Sci. Rep*. **2016**, *6*, doi:10.1038/srep26717.

50. Cheng, J.; Yu, H.; Lau, K.; Huang, S.; Chokhawala, H. A.; Li, Y.; Tiwari, V. K.; Chen, X. Multifunctionality of *Campylobacter jejuni* sialyltransferase CstII: Characterization

of GD3/GT3 oligosaccharide synthase, GD3 oligosaccharide sialidase, and trans-sialidase activities. *Glycobiology* **2008**, doi:10.1093/glycob/cwn047.

51. Chevallereau, A.; Blasdel, B. G.; De Smet, J.; Monot, M.; Zimmermann, M.; Kogadeeva, M.; Sauer, U.; Jorth, P.; Whiteley, M.; Debarbieux, L.; Lavigne, R. Next-Generation "-omics" Approaches Reveal a Massive Alteration of Host RNA Metabolism during Bacteriophage Infection of *Pseudomonas aeruginosa*. *PLoS Genet.* **2016**, doi:10.1371/journal.pgen.1006134.

52. Clark, C. G.; Ng, L.-K. Sequence variability of *Campylobacter* temperate bacteriophages. *BMC Microbiol*. **2008**, *8*, 49, doi:10.1186/1471-2180-8-49.

53. Clark, C. G.; Price, L.; Ahmed, R.; Woodward, D. L.; Melito, P. L.; Rodgers, F. G.; Jamieson, F.; Ciebin, B.; Li, A.; Ellis, A. Characterization of waterborne outbreak-associated *Campylobacter jejuni*, Walkerton, Ontario. Emerg. Infect. Dis. **2003**, *9*, 1232–1241, doi:10.3201/eid0910.020584.

54. Connerton, P. L.; Timms, A. R.; Connerton, I. F. *Campylobacter* bacteriophages and bacteriophage therapy. *J. Appl. Microbiol*. **2011**, *111*, 255–265.

55. Corcionivoschi, N.; Alvarez, L. A. J.; Sharp, T. H.; Strengert, M.; Alemka, A.; Mantell, J.; Verkade, P.; Knaus, U. G.; Bourke, B. Mucosal Reactive Oxygen Species Decrease Virulence by Disrupting *Campylobacter jejuni* Phosphotyrosine Signaling. *Cell Host Microbe* **2012**, *12*, 47–59, doi:10.1016/j.chom.2012.05.018.

56. Cordero, R.J.; Pontes, B.; Frases, S.; Nakouzi, A.S.; Nimrichter, L.; Rodrigues, M.L.; Viana, N.B.; Casadevall, A. Antibody binding to *Cryptococcus neoformans* impairs budding by altering capsular mechanical properties. *J. Immunol.* **2013**, *190*, 317–323.

57. Cornelissen, A.; Ceyssens, P.J.; Krylov, V.N.; Noben, J.P.; Volckaert, G.; Lavigne, R. Identification of EPS-degrading activity within the tail spikes of the novel *Pseudomonas putida* phage AF. *Virology* **2012**, *434*, 251–256.

58. Coward, C.; Grant, A. J.; Swift, C.; Philp, J.; Towler, R.; Heydarian, M.; Frost, J. A.; Maskell, D. J. Phase-variable surface structures are required for infection of *Campylobacter jejuni* by bacteriophages. *Appl. Environ. Microbiol*. **2006**, *72*, 4638–4647, doi:10.1128/AEM.00184-06.

59. Coward, C.; Grant, A.J.; Swift, C.; Philp, J.; Towler, R.; Heydarian, M.; Frost, J.A.; Maskell, D.J. Phase-variable surface structures are required for infection of *Campylobacter jejuni* by bacteriophages. *Appl. Environ. Microbiol*. **2006**, *72*, 4638–4647.

60. Crofts, A. A.; Poly, F. M.; Ewing, C. P.; Kuroiwa, J. M.; Rimmer, J. E.; Harro, C.; Sack, D.; Talaat, K. R.; Porter, C. K.; Gutierrez, R. L.; DeNearing, B.; Brubaker, J.; Laird, R. M.; Maue, A. C.; Jaep, K.; Alcala, A.; Tribble, D. R.; Riddle, M. S.; Ramakrishnan, A.; McCoy, A. J.; Davies, B. W.; Guerry, P.; Trent, M. S. *Campylobacter jejuni* transcriptional and genetic adaptation during human infection. *Nat. Microbiol*. **2018**, 3, 494, doi:10.1038/s41564-018-0133-7.

61. Das, B.; Bischerour, J.; Barre, F. X. Molecular mechanism of acquisition of the cholera toxin genes. *Indian J. Med. Res.* **2011**, *133*, 195–200.

62. Davidson, A. R.; Cardarelli, L.; Pell, L. G.; Radford, D. R.; Maxwell, K. L. Long noncontractile tail machines of bacteriophages. Adv. Exp. Med. Biol. **2012**, *726*, 115–142, doi:10.1007/978-1-4614-0980-9_6; 10.1007/978-1-4614-0980-9_6.

63. Day, W. A.; Sajecki, J. L.; Pitts, T. M.; Joens, L. A.; Joens, L. A. Role of catalase in *Campylobacter jejuni* intracellular survival. *Infect. Immun.* **2000**, *68*, 6337–45.

64. De Smet, J.; Hendrix, H.; Blasdel, B. G.; Danis-Wlodarczyk, K.; Lavigne, R. *Pseudomonas* predators: Understanding and exploiting phage-host interactions. *Nat. Rev. Microbiol.* **2017**.

65. De Smet, J.; Zimmermann, M.; Kogadeeva, M.; Ceyssens, P. J.; Vermaelen, W.; Blasdel, B.; Bin Jang, H.; Sauer, U.; Lavigne, R. High coverage metabolomics analysis reveals phage-specific alterations to *Pseudomonas aeruginosa* physiology during infection. *ISME J.* **2016**, doi:10.1038/ismej.2016.3.

66. Di Tommaso, P.; Moretti, S.; Xenarios, I.; Orobitg, M.; Montanyola, A.; Chang, J.-M.; Taly, J.-F.; Notredame, C. T-Coffee: a web server for the multiple sequence alignment of protein and RNA sequences using structural information and homology extension. *Nucleic Acids Res*. **2011**, *39*, W13–W17, doi:10.1093/nar/gkr245.

67. Dobin, A.; Davis, C. A.; Schlesinger, F.; Drenkow, J.; Zaleski, C.; Jha, S.; Batut, P.; Chaisson, M.; Gingeras, T. R. STAR: Ultrafast universal RNA-seq aligner. Bioinformatics **2013**, *29*, 15–21, doi:10.1093/bioinformatics/bts635.

68. Doron, S.; Fedida, A.; Hernández-Prieto, M. A.; Sabehi, G.; Karunker, I.; Stazic, D.; Feingersch, R.; Steglich, C.; Futschik, M.; Lindell, D.; Sorek, R. Transcriptome dynamics of a broad host-range cyanophage and its hosts. *ISME J.* **2016**, *10*, 1437–55, doi:10.1038/ismej.2015.210.

69. Drulis-Kawa, Z.; Majkowska-Skrobek, G.; Maciejewska, B. Bacteriophages and Phage-Derived Proteins – Application Approaches. *Curr. Med. Chem.* **2015**, *22*, 1757–1773, doi:10.2174/0929867322666150209152851.

70. Drulis-Kawa, Z.; Majkowska-Skrobek, G.; Maciejewska, B.; Delattre, A.-S.; Lavigne, R. Learning from Bacteriophages - Advantages and Limitations of Phage and Phage-Encoded Protein Applications. *Curr. Protein Pept. Sci.* **2012**, doi:10.2174/138920312804871193.

71. Dugar, G.; Herbig, A.; Förstner, K. U.; Heidrich, N.; Reinhardt, R.; Nieselt, K.; Sharma, C. M. High-Resolution Transcriptome Maps Reveal Strain-Specific Regulatory Features of Multiple *Campylobacter jejuni* Isolates. *PLoS Genet*. **2013**, *9*, e1003495, doi:10.1371/journal.pgen.1003495.

72. Dugar, G.; Leenay, R. T.; Eisenbart, S. K.; Bischler, T.; Aul, B. U.; Beisel, C. L.; Sharma, C. M. CRISPR RNA-Dependent Binding and Cleavage of Endogenous RNAs by the *Campylobacter jejuni* Cas9. *Mol. Cell,* **2018**, *69*, 893–905.e7, doi:10.1016/j.molcel.2018.01.032.

73. Eichler, J.; Koomey, M. Sweet New Roles for Protein Glycosylation in Prokaryotes. *Trends Microbiol*. **2017**, doi:10.1016/j.tim.2017.03.001.

74. El-Shibiny, A.; Connerton, P. L.; Connerton, I. F. *Campylobacter* succession in broiler chickens. *Vet. Microbiol.* **2007**, *125*, 323–332, doi:10.1016/j.vetmic.2007.05.023.

75. El-Shibiny, A.; Scott, A.; Timms, A.; Metawea, Y.; Connerton, P.; Connerton, I. Application of a group II *Campylobacter* bacteriophage to reduce strains of *Campylobacter jejuni* and *Campylobacter coli* colonizing broiler chickens. *J. Food Prot*. **2009**, *72*, 733–740.

76. Erez, Z.; Steinberger-Levy, I.; Shamir, M.; Doron, S.; Stokar-Avihail, A.; Peleg, Y.; Melamed, S.; Leavitt, A.; Savidor, A.; Albeck, S.; Amitai, G.; Sorek, R. Communication

between viruses guides lysis-lysogeny decisions. *Nature* **2017**, *541*, 488–493, doi:10.1038/nature21049.

77. Ewing, C. P.; Andreishcheva, E.; Guerry, P. Functional characterization of flagellin glycosylation in *Campylobacter jejuni* 81-176. *J. Bacteriol.* **2009**, *191*, 7086–7093, doi:10.1128/JB.00378-09.

78. Faruque, S. M.; Mekalanos, J. J. Phage-bacterial interactions in the evolution of toxigenic *Vibrio cholerae*. *Virulence* **2012**, *3*.

79. Fernández, L.; González, S.; Campelo, A. B.; Martínez, B.; Rodríguez, A.; García, P. Low-level predation by lytic phage phiIPLA-RODI promotes biofilm formation and triggers the stringent response in *Staphylococcus aureus*. *Sci. Rep.* **2017***, 7*, 40965, doi:10.1038/srep40965.

80. Fernández, L.; Rodríguez, A.; García, P. Phage or foe: an insight into the impact of viral predation on microbial communities. *ISME J.* **2018**, doi:10.1038/s41396-018-0049-5.

81. Fineran, P. C.; Blower, T. R.; Foulds, I. J.; Humphreys, D. P.; Lilley, K. S.; Salmond, G. P. C. The phage abortive infection system, ToxIN, functions as a protein-RNA toxin-antitoxin pair. Proc. Natl. Acad. Sci. U. S. A. **2009**, 106, 894–9, doi:10.1073/pnas.0808832106.

82. Fischer, S.; Kittler, S.; Klein, G.; Glünder, G. Impact of a Single Phage and a Phage Cocktail Application in Broilers on Reduction of *Campylobacter jejuni* and Development of Resistance. *PLoS One* **2013**, *8*, doi:10.1371/journal.pone.0078543.

83. Flint, A.; Sun, Y. Q.; Stintzi, A. Cj1386 is an ankyrin-containing protein involved in heme trafficking to catalase in *Campylobacter jejuni*. *J. Bacteriol.* **2012**, *194*, 334–345, doi:10.1128/JB.05740-11.

84. Flint, A.; Sun, Y.-Q. Q.; Butcher, J.; Stahl, M.; Huang, H.; Stintzi, A. Phenotypic screening of a targeted mutant library reveals *Campylobacter jejuni* defenses against oxidative stress. *Infect. Immun.* **2014**, *82*, 2266–2275, doi:10.1128/IAI.01528-13.

85. FROST, J. A.; KRAMER, J. M.; Gillanders, S. A. Phage typing of *Campylobacter jejuni* and *Campylobacter coli* and its use as an adjunct to serotyping. *Epidemiol. Infect*. **1999**, *123*, S095026889900254X, doi:10.1017/S095026889900254X.

86. Gadagkar, R.; Gopinathan, K.P. Bacteriophage burst size during multiple infections. *J. Biosci.* **1980**, *2*, 253–259.

87. Galkin, V. E.; Yu, X.; Bielnicki, J.; Heuser, J.; Ewing, C. P.; Guerry, P.; Egelman, E. H. Divergence of quaternary structures among bacterial flagellar filaments. *Science* **2008**, *320*, 382–385, doi:10.1126/science.1155307.

88. Gallet, R.; Shao, Y.; Wang, I.N. High adsorption rate is detrimental to bacteriophage fitness in a biofilm-like environment. *BMC Evolut. Biol.* **2009**, *9*, 241.

89. Gao, B.; Lara-Tejero, M.; Lefebre, M.; Goodman, A. L.; Galán, J. E. Novel components of the flagellar system in epsilonproteobacteria. *MBio* **2014**, *5*, doi:10.1128/mBio.01349-14.

90. Gardner, S. P.; Kendall, K. J.; Taveirne, M. E.; Olson, J. W. Complete Genome Sequence of *Campylobacter jejuni* subsp. jejuni ATCC 35925. *Genome Announc.* **2017**, *5*, e00743-17, doi:10.1128/genomeA.00743-17.

91. Gardner, S. P.; Olson, J. W. Barriers to Horizontal Gene Transfer in *Campylobacter jejuni*. *Adv. Appl. Microbiol.* **2012**, *79*, 19–42, doi:10.1016/B978-0-12-394318-7.00002-4.

92. Gaynor, E. C.; Cawthraw, S.; Manning, G.; MacKichan, J. K.; Falkow, S.; Newell, D. G. The genome-sequenced variant of *Campylobacter jejuni* NCTC 11168 and the original clonal clinical isolate differ markedly in colonization, gene expression, and virulence-associated phenotypes. *J. Bacteriol*. **2004**, *186*, 503–17, doi:10.1128/JB.186.2.503-517.2004.

93. Gebhart, D.; Lok, S.; Clare, S.; Tomas, M.; Stares, M.; Scholl, D.; Donskey, C.J.; Lawley, T.D.; Govoni, G.R. A modified R-type bacteriocin specifically targeting *Clostridium difficile* prevents colonization of mice without affecting gut microbiota diversity. *mBio* **2015**, *6,* doi:10.1128/mBio.02368-14.

94. Gencay, Y. E.; Sørensen, M. C. H.; Wenzel, C. Q.; Szymanski, C. M.; Brøndsted, L. Phase Variable Expression of a Single Phage Receptor in *Campylobacter jejuni* NCTC12662 Influences Sensitivity Toward Several Diverse CPS-Dependent Phages. *Front. Microbiol.* **2018**, 9, *82*, doi:10.3389/fmicb.2018.00082.

95. Gilbreath, J. J.; Cody, W. L.; Merrell, D. S.; Hendrixson, D. R. Change is good: variations in common biological mechanisms in the epsilonproteobacterial genera *Campylobacter* and *Helicobacter*. *Microbiol. Mol. Biol. Rev*. **2011**, *75*, 84–132, doi:10.1128/MMBR.00035-10.

96. Goon, S.; Kelly, J. F.; Logan, S. M.; Ewing, C. P.; Guerry, P. Pseudaminic acid, the major modification on *Campylobacter* flagellin, is synthesized via the Cj1293 gene. *Mol. Microbiol.* **2003**, *50*, 659–671, doi:10.1046/j.1365-2958.2003.03725.x.

97. Gots, J. S.; Hunt, G. R. Amino acid requirements for the maturation of bacteriophage in lysogenic *Escherichia coli*. *J. Bacteriol.* **1953**, *66*, 3, 353-361.

98. Grajewski, B. A.; Kusek, J. W.; Gelfand, H. M. Development of bacteriophage typing system for *Campylobacter jejuni* and *Campylobacter coli*. *J. Clin. Microbiol*. **1985**, *22*, 13–18.

99. Grant, K. A.; Park, S. F. Molecular characterization of *katA* from *Campylobacter jejuni* and generation of a catalase-deficient mutant of *Campylobacter coli* by interspecific allelic exchange. *Microbiology* **1995**, *141*, 1369–1376, doi:10.1099/13500872-141-6-1369.

100. Guccione, E.; del Rocio Leon-Kempis, M.; Pearson, B. M.; Hitchin, E.; Mulholland, F.; van Diemen, P. M.; Stevens, M. P.; Kelly, D. J. Amino acid-dependent growth of *Campylobacter jejuni* : key roles for aspartase (AspA) under microaerobic and oxygen-limited conditions and identification of AspB (Cj0762), essential for growth on glutamate. *Mol. Microbiol.* **2008**, *69*, 77–93, doi:10.1111/j.1365-2958.2008.06263.x.

101. Guerry, P. *Campylobacter* flagella: not just for motility. *Trends Microbiol.* **2007**, 15, 456–461.

102. Guerry, P. N-linked glycosylation in Archaea: Two paths to the same glycan. *Mol. Microbiol.* **2011**, 81, 1133–1135.

103. Guerry, P.; Alm, R. A.; Power, M. E.; Logan, S. M.; Trust, T. J. Role of two flagellin genes in *Campylobacter* motility. J. Bacteriol. **1991**, 173, 4757–4764.

104. Guerry, P.; Ewing, C. P.; Hickey, T. E.; Prendergast, M. M.; Moran, A. P. Sialylation of lipooligosaccharide cores affects immunogenicity and serum resistance of *Campylobacter jejuni*. *Infect. Immun.* **2000**, doi:10.1128/IAI.68.12.6656-6662.2000.

105. Guerry, P.; Ewing, C. P.; Schirm, M.; Lorenzo, M.; Kelly, J.; Pattarini, D.; Majam, G.; Thibault, P.; Logan, S. Changes in flagellin glycosylation affect *Campylobacter*

autoagglutination and virulence. *Mol. Microbiol.* **2006**, 60, 299–311, doi:10.1111/j.1365-2958.2006.05100.x.

106. Guerry, P.; Ewing, C.P.; Schirm, M.; Lorenzo, M.; Kelly, J.; Pattarini, D.; Majam, G.; Thibault, P.; Logan, S. Changes in flagellin glycosylation affect *Campylobacter* autoagglutination and virulence. *Mol. Microbiol.* **2006**, 60, 299–311.

107. Guerry, P.; Logan, S. M.; Thornton, S.; Trust, T. J. Genomic organization and expression of *Campylobacter* flagellin genes. *J. Bacteriol.* **1990**, 172, 1853–1860.

108. Guerry, P.; Szymanski, C. M. *Campylobacter* sugars sticking out. *Trends Microbiol.* **2008**, 16, 428-435, doi:10.1016/j.tim.2008.07.002.

109. Guerry, P.; Szymanski, C. M.; Prendergast, M. M.; Hickey, T. E.; Ewing, C. P.; Pattarini, D. L.; Moran, A. P. Phase variation of *Campylobacter jejuni* 81-176 lipooligosaccharide affects ganglioside mimicry and invasiveness in vitro. *Infect. Immun.* 2002, doi:10.1128/IAI.70.2.787-793.2002.

110. Gundogdu, O.; Bentley, S. D.; Holden, M. T.; Parkhill, J.; Dorrell, N.; Wren, B. W. Re-annotation and re-analysis of the *Campylobacter jejuni* NCTC11168 genome sequence. *BMC Genomics* **2007**, 8, 162, doi:1471-2164-8-162.

111. Gundogdu, O.; Bentley, S. D.; Holden, M. T.; Parkhill, J.; Dorrell, N.; Wren, B. W. Re-annotation and re-analysis of the *Campylobacter jejuni* NCTC11168 genome sequence. *BMC Genomics* **2007**, 8, doi:10.1186/1471-2164-8-162.

112. Hagens, S.; Loessner, M. J. Application of bacteriophages for detection and control of foodborne pathogens. *Appl. Microbiol. Biotechnol.* **2007**, *76*, 513-519.

113. Hammerl, J. A.; Jackel, C.; Reetz, J.; Beck, S.; Alter, T.; Lurz, R.; Barretto, C.; Brussow, H.; Hertwig, S. *Campylobacter jejuni* Group III Phage CP81 Contains Many T4-Like

Genes without Belonging to the T4-Type Phage Group: Implications for the Evolution of T4 Phages. *J. Virol.* **2011**, 85, 8597–8605, doi:10.1128/JVI.00395-11.

114. Hampton, T. Report Reveals Scope of US Antibiotic Resistance Threat. *JAMA* **2013**, 310, 1661, doi:10.1001/jama.2013.280695.

115. Hatfull, G. F.; Hendrix, R. W. Bacteriophages and their genomes. *Curr. Opin. Virol.* **2011**, 1, 298–303, doi:10.1016/j.coviro.2011.06.009; 10.1016/j.coviro.2011.06.009.

116. Hendrixson, D. R. Regulation of flagellar gene expression and assembly. In; Nachamkin, I., Szymanski, C. M., Blaser, M. J., Eds.; *Campylobacter*; American Society for Microbiology: Washington, D.C., **2008**; pp. 545–558.

117. Hendrixson, D. R. Restoration of flagellar biosynthesis by varied mutational events in *Campylobacter jejuni. Mol. Microbiol.* **2008**, *70*, 519–536, doi:10.1111/j.1365-2958.2008.06428.x; 10.1111/j.1365-2958.2008.06428.x.

118. Heras, B.; Scanlon, M. J.; Martin, J. L. Targeting virulence not viability in the search for future antibacterials. *Br. J. Clin. Pharmacol.* **2015**, doi:10.1111/bcp.12356.

119. Hitchen, P.; Brzostek, J.; Panico, M.; Butler, J. A.; Morris, H. R.; Dell, A.; Linton, D. Modification of the *Campylobacter jejuni* flagellin glycan by the product of the Cj1295 homopolymeric-tract-containing gene. *Microbiology* **2010**, 156, 1953–1962, doi:10.1099/mic.0.038091-0.

120. Holberger, L. E.; Garza-Sánchez, F.; Lamoureux, J.; Low, D. A.; Hayes, C. S. A novel family of toxin/antitoxin proteins in *Bacillus* species. *FEBS Lett.* **2012**, 586, 132–6, doi:10.1016/j.febslet.2011.12.020.

121. Hooton, S. P. T.; Brathwaite, K. J.; Connerton, I. F. The bacteriophage carrier state of *Campylobacter jejuni* features changes in host non-coding RNAs and the acquisition of new host-derived CRISPR spacer sequences. *Front. Microbiol.* **2016**, 7.

122. Hooton, S. P. T.; Connerton, I. F. *Campylobacter jejuni* acquire new host-derived CRISPR spacers when in association with bacteriophages harboring a CRISPR-like Cas4 protein. *Front. Microbiol*. **2015**, 6, 1–9, doi:10.3389/fmicb.2014.00744.

123. Howard-Varona, C.; Roux, S.; Dore, H.; Solonenko, N. E.; Holmfeldt, K.; Markillie, L. M.; Orr, G.; Sullivan, M. B. Regulation of infection efficiency in a globally abundant marine *Bacteriodetes* virus. *ISME J.* **2017**, 11, 284–295, doi:10.1038/ismej.2016.81.

124. Howard, S. L.; Jagannathan, A.; Soo, E. C.; Hui, J. P. M.; Aubry, A. J.; Ahmed, I.; Karlyshev, A.; Kelly, J. F.; Jones, M. A.; Stevens, M. P.; Logan, S. M.; Wren, B. W. *Campylobacter jejuni* glycosylation island important in cell charge, legionaminic acid biosynthesis, and colonization of chickens. *Infect. Immun*. **2009**, 77, 2544–2556, doi:10.1128/IAI.01425-08.

125. Hutinet, G.; Swarjo, M. A.; de Crécy-Lagard, V. Deazaguanine derivatives, examples of crosstalk between RNA and DNA modification pathways. *RNA Biol.* **2017**, 14, 1175-1184.

126. Huys, I.; Pirnay, J. P.; Lavigne, R.; Jennes, S.; De Vos, D.; Casteels, M.; Verbeken, G. Paving a regulatory pathway for phage therapy. Europe should muster the resources to financially, technically and legally support the introduction of phage therapy. *EMBO Rep.* **2013**, doi:10.1038/embor.2013.163.

127. Hyman, P.; Abedon, S. T. Bacteriophage host range and bacterial resistance. *Adv. Appl. Microbiol.* **2010**, 70, 217–248.

128. Hyman, P.; Abedon, S. T. Bacteriophage host range and bacterial resistance. *Adv. Appl. Microbiol.* **2010**.

129. Iwashita, S.; Kanegasaki, S. Enzymic and molecular properties of base-plate parts of bacteriophage P22. *FEBS J.* **1976,** 1, 87-94.

130. Iwashkiw, J. A.; Vozza, N. F.; Kinsella, R. L.; Feldman, M. F. Pour some sugar on it: The expanding world of bacterial protein O-linked glycosylation. *Mol. Microbiol.* **2013**, 89, 14–28.

131. Janež, N.; Kokošin, A.; Zaletel, E.; Vranac, T.; Kovač, J.; Vučković, D.; Možina, S. S.; Serbec, V. C.; Zhang, Q.; Accetto, T.; Podgornik, A.; Peterka, M. Identification and characterisation of new *Campylobacter* group III phages of animal origin. *FEMS Microbiol. Lett.* **2014**, 359, 64–71.

132. Janež, N.; Kokošin, A.; Zaletel, E.; Vranac, T.; Kovač, J.; Vučković, D.; Smole Možina, S.; Čurin Šerbec, V.; Zhang, Q.; Accetto, T.; et al. Identification and Characterisation of new *Campylobacter* group III phages of animal origin. *FEMS Microbiol. Lett*. **2014**, 359, 64–71.

133. Janež, N.; Loc-Carrillo, C. Use of phages to control *Campylobacter* spp. *J. Microbiol. Methods* **2013**, 95, 68–75, doi:10.1016/j.mimet.2013.06.024.

134. Javed, M. A.; Sacher, J. C.; van Alphen, L. B.; Patry, R. T.; Szymanski, C. M. A flagellar glycan-specific protein encoded by *Campylobacter* phages inhibits host cell growth. *Viruses* **2015**, 7, 6661–6674, doi:10.3390/v7122964.

135. Javed, M. A.; van Alphen, L. B.; Sacher, J.; Ding, W.; Kelly, J.; Nargang, C.; Smith, D. F.; Cummings, R. D.; Szymanski, C. M. A receptor-binding protein of *Campylobacter jejuni* bacteriophage NCTC 12673 recognizes flagellin glycosylated with acetamidino-

modified pseudaminic acid. *Mol. Microbiol.* **2015**, 95, 101–115, doi:10.1111/mmi.12849.

136. Javed, M. A.; Ackermann, H. W.; Azeredo, J.; Carvalho, C. M.; Connerton, I.; Evoy, S.; Hammerl, J. A.; Hertwig, S.; Lavigne, R.; Singh, A.; Szymanski, C. M.; Timms, A.; Kropinski, A. M. A suggested classification for two groups of *Campylobacter* myoviruses. *Arch. Virol.* **2014**, 159, 181–190, doi:10.1007/s00705-013-1788-2.

137. Javed, M. A.; Poshtiban, S.; Arutyunov, D.; Evoy, S.; Szymanski, C. M. Bacteriophage Receptor Binding Protein Based Assays for the Simultaneous Detection of *Campylobacter jejuni* and *Campylobacter coli*. *PLoS One* **2013**, 8, doi:10.1371/journal.pone.0069770.

138. Javed, M. A.; van Alphen, L. B.; Sacher, J.; Ding, W.; Kelly, J.; Nargang, C.; Smith, D. F.; Cummings, R. D.; Szymanski, C. M. A receptor-binding protein of *Campylobacter* jejuni bacteriophage NCTC 12673 recognizes flagellin glycosylated with acetamidino-modified pseudaminic acid. *Mol. Microbiol.* **2015**, 95, 101–115, doi:10.1111/mmi.12849.

139. Javed, M.A.; Ackermann, H.-W.; Azeredo, J.; Carvalho, C.M.; Connerton, I.F.; Evoy, S.; Hammerl, J.A.; Hertwig, S.; Lavigne, R.; Singh, A.; *et al.* A suggested classification for two groups of *Campylobacter* Myoviruses. *Arch. Virol*. **2014**, 159, 181–190.

140. Javed, M.A.; Poshtiban, S.; Arutyunov, D.; Evoy, S.; Szymanski, C.M. Bacteriophage receptor binding protein based assays for the simultaneous detection of *Campylobacter jejuni* and *Campylobacter coli. PLoS ONE* **2013**, 8, e69770.

141. Javed, M.A.; van Alphen, L.B.; Sacher, J.; Ding, W.; Kelly, J.; Nargang, C.; Smith, D.F.; Cummings, R.D.; Szymanski, C.M. A receptor-binding protein of *Campylobacter* jejuni

bacteriophage NCTC 12673 recognizes flagellin glycosylated with acetamidino-modified pseudaminic acid. *Mol. Microbiol.* **2015**, 95, 101–115.

142. Johnson, T. J.; Shank, J. M.; Johnson, J. G. Current and Potential Treatments for Reducing *Campylobacter* Colonization in Animal Hosts and Disease in Humans. *Front. Microbiol.* **2017**, 8, 487, doi:10.3389/fmicb.2017.00487.

143. Johnson, T. J.; Shank, J. M.; Patel, K. M.; Paredes, M. D.; Lee, E. D.; Mitchell, M. K.; Denes, T. G.; Johnson, J. G. Moderate-Throughput Identification and Comparison of *Campylobacter*-Infecting Bacteriophages. *bioRxiv* **2017**, 201822, doi:10.1101/201822.

144. Kaakoush, N. O., Castaño-Rodríguez, N., Mitchell, H. M., & Man, S. M. Global epidemiology of *Campylobacter* infection. *Clin. Microbiol. Rev.* **2015**, *28*, 3, 687-720.

145. Kaakoush, N. O.; Miller, W. G.; De Reuse, H.; Mendz, G. L. Oxygen requirement and tolerance of *Campylobacter jejuni*. *Res. Microbiol.* **2007**, 158, 644–650, doi:10.1016/J.RESMIC.2007.07.009.

146. Kaakoush, N. O.; Mitchell, H. M.; Man, S. M. *Campylobacter*. In Molecular Medical Microbiology; **2015**; pp. 1187–1236 ISBN 978-0-12-397169-2.

147. Kalmokoff, M.; Lanthier, P.; Tremblay, T.-L.; Foss, M.; Lau, P. C.; Sanders, G.; Austin, J.; Kelly, J.; Szymanski, C. M. Proteomic analysis of *Campylobacter jejuni* 11168 biofilms reveals a role for the motility complex in biofilm formation. *J. Bacteriol.* **2006**, 188, 4312–20, doi:10.1128/JB.01975-05.

148. Kandiba, L.; Aitio, O.; Helin, J.; Guan, Z.; Permi, P.; Bamford, D. H.; Eichler, J.; Roine, E. Diversity in prokaryotic glycosylation: An archaeal-derived N-linked glycan contains legionaminic acid. *Mol. Microbiol.* **2012**, 84, 578–593, doi:10.1111/j.1365-2958.2012.08045.x.

149. Karlyshev, A. V; Linton, D.; Gregson, N. A.; Lastovica, A. J.; Wren, B. W. Genetic and biochemical evidence of a *Campylobacter jejuni* capsular polysaccharide that accounts for Penner serotype specificity. *Mol. Microbiol.* **2000**, 35, 529–541.

150. Karlyshev, A. V; Wren, B. W. Development and application of an insertional system for gene delivery and expression in *Campylobacter jejuni*. *Appl. Environ. Microbiol.* **2005**, 71, 4004–13, doi:10.1128/AEM.71.7.4004-4013.2005.

151. Karlyshev, A. V.; Champion, O. L.; Churcher, C.; Brisson, J. R.; Jarrell, H. C.; Gilbert, M.; Brochu, D.; St Michael, F.; Li, J.; Wakarchuk, W. W.; Goodhead, I.; Sanders, M.; Stevens, K.; White, B.; Parkhill, J.; Wren, B. W.; Szymanski, C. M. Analysis of *Campylobacter jejuni* capsular loci reveals multiple mechanisms for the generation of structural diversity and the ability to form complex heptoses. *Mol. Microbiol.* **2005**, doi:10.1111/j.1365-2958.2004.04374.x.

152. Karlyshev, A. V.; Champion, O. L.; Churcher, C.; Brisson, J. R.; Jarrell, H. C.; Gilbert, M.; Brochu, D.; St Michael, F.; Li, J.; Wakarchuk, W. W.; Goodhead, I.; Sanders, M.; Stevens, K.; White, B.; Parkhill, J.; Wren, B. W.; Szymanski, C. M. Analysis of *Campylobacter jejuni* capsular loci reveals multiple mechanisms for the generation of structural diversity and the ability to form complex heptoses. *Mol. Microbiol.* **2005**, 55, 90–103, doi:10.1111/j.1365-2958.2004.04374.x.

153. Karlyshev, A. V.; Ketley, J. M.; Wren, B. W. The *Campylobacter jejuni* glycome. *FEMS Microbiol. Rev.* **2005**, 29, 377–390.

154. Karlyshev, A. V.; Linton, D.; Gregson, N. A.; Wren, B. W. A novel paralogous gene family involved in phase-variable flagella-mediated motility in *Campylobacter jejuni*. *Microbiology* **2002**, 148, 473–480, doi:10.1099/00221287-148-2-473.

155. Kassem, I. I.; Khatri, M.; Sanad, Y. M.; Wolboldt, M.; Saif, Y. M.; Olson, J. W.; Rajashekara, G. The impairment of methylmenaquinol:fumarate reductase affects hydrogen peroxide susceptibility and accumulation in *Campylobacter jejuni*. *Microbiology Open* **2014**, *3*, 168–181, doi:10.1002/mbo3.158.

156. Kazmierczak, B. I.; Hendrixson, D. R. Spatial and numerical regulation of flagellar biosynthesis in polarly flagellated bacteria. *Mol. Microbiol.* **2013**, 88, 655–663, doi:10.1111/mmi.12221; 10.1111/mmi.12221.

157. Kearse, M.; Moir, R.; Wilson, A.; Stones-Havas, S.; Cheung, M.; Sturrock, S.; Buxton, S.; Cooper, A.; Markowitz, S.; Duran, C.; Thierer, T.; Ashton, B.; Meintjes, P.; Drummond, A. Geneious Basic: An integrated and extendable desktop software platform for the organization and analysis of sequence data. *Bioinformatics* **2012**, 28, 1647–1649, doi:10.1093/bioinformatics/bts199.

158. Kittler, S.; Fischer, S.; Abdulmawjood, A.; Glunder, G.; Klein, G. Effect of bacteriophage application on *Campylobacter jejuni* loads in commercial broiler flocks. *Appl. Environ. Microbiol.* **2013**, 79, 7525–7533.

159. Kittler, S.; Fischer, S.; Abdulmawjood, A.; Glünder, G.; Kleina, G. Effect of bacteriophage application on *Campylobacter jejuni* loads in commercial broiler flocks. *Appl. Environ. Microbiol.* **2013**, 79, 7525–7533, doi:10.1128/AEM.02703-13.

160. Klumpp, J.; Fouts, D. E.; Sozhamannan, S. Next generation sequencing technologies and the changing landscape of phage genomics. *Bacteriophage* **2012**, 1–10.

161. Kropinski, A. M.; Arutyunov, D.; Foss, M.; Cunningham, A.; Ding, W.; Singh, A.; Pavlov, A. R.; Henry, M.; Evoy, S.; Kelly, J.; Szymanski, C. M. Genome and proteome

of *Campylobacter jejuni* bacteriophage NCTC 12673. *Appl. Environ. Microbiol*. **2011**, 77, 8265–8271, doi:10.1128/AEM.05562-11.

162. Kropinski, A. M.; Turner, D.; E Nash, J. H.; - Wolfgang Ackermann, H.; Lingohr, E. J.; Warren, R. A.; Ehrlich, K. C.; Ehrlich, M.; Lingohr, E.; The Sequence of Two Bacteriophages with Hypermodified Bases Reveals Novel Phage - Host Interactions. *Viruses.* **2018**, doi:10.3390/v10050217.

163. Kropinski, A.M.; Arutyunov, D.; Foss, M.; Cunningham, A.; Ding, W.; Singh, A.; Pavlov, A.R.; Henry, M.; Evoy, S.; Kelly, J.; Szymanski, C.M. Genome and proteome of *Campylobacter jejuni* bacteriophage NCTC 12673. *Appl. Environ. Microbiol*. **2011**, 77, 8265–8271.

164. Krylov, V. N. Role of horizontal gene transfer by bacteriophages in the origin of pathogenic bacteria. *Genetika* **2003**, 39, 595–620.

165. Kumar, A.; Drozd, M.; Pina-Mimbela, R.; Xu, X.; Helmy, Y. A.; Antwi, J.; Fuchs, J. R.; Nislow, C.; Templeton, J.; Blackall, P. J.; Rajashekara, G. Novel anti-*Campylobacter* compounds identified using high throughput screening of a pre-selected enriched small molecules library. *Front. Microbiol*. **2016**, doi:10.3389/fmicb.2016.00405.

166. Labedan, B.; Goldberg, E. B. Requirement for membrane potential in injection of phage T4 DNA. *Proc. Nat. Acad. Sci*. **1979,** *76*, 4669-4673.

167. Lango-Scholey, L.; Aidley, J.; Woodacre, A.; Jones, M. A.; Bayliss, C. D. High throughput method for analysis of repeat number for 28 phase variable loci of *Campylobacter jejuni* strain NCTC11168. *PLoS One* **2016**, 11, doi:10.1371/journal.pone.0159634.

168. Larsen, J.C.; Szymanski, C.; Guerry, P. N-linked protein glycosylation is required for full competence in *Campylobacter jejuni* 81–176. *J. Bacteriol.* **2004**, 186, 6508–6514.

169. Lee, Y.-J.; Dai, N.; Walsh, S. E.; Müller, S.; Fraser, M. E.; Kauffman, K. M.; Guan, C.; Corrêa, I. R.; Weigele, P. R. Identification and biosynthesis of thymidine hypermodifications in the genomic DNA of widespread bacterial viruses. *Proc. Natl. Acad. Sci.* **2018**, doi:10.1073/pnas.1714812115.

170. Leiman, P. G.; Shneider, M. M. Contractile tail machines of bacteriophages. *Adv. Exp. Med. Biol.* **2012**, 726, 93–114, doi:10.1007/978-1-4614-0980-9_5; 10.1007/978-1-4614-0980-9_5.

171. Lele, P. P.; Hosu, B. G.; Berg, H. C. Dynamics of mechanosensing in the bacterial flagellar motor. *Proc. Natl. Acad. Sci.* **2013**, *110*, 29, 11839-11844, doi:10.1073/pnas.1305885110.

172. Leskinen, K.; Blasdel, B. G.; Lavigne, R.; Skurnik, M. RNA-sequencing reveals the progression of Phage-Host interactions between φR1-37 and *Yersinia enterocolitica*. *Viruses* **2016**, 8, doi:10.3390/v8040111.

173. Leverentz, B.; Conway, W. S.; Camp, M. J.; Janisiewicz, W. J.; Abuladze, T.; Yang, M.; Saftner, R.; Sulakvelidze, A. Biocontrol of *Listeria monocytogenes* on fresh-cut produce by treatment with lytic bacteriophages and a bacteriocin. *Appl. Environ. Microbiol.* **2003**, 69, 4519–4526.

174. Li, R.; Fang, L.; Tan, S.; Yu, M.; Li, X.; He, S.; Wei, Y.; Li, G.; Jiang, J.; Wu, M. Type I CRISPR-Cas targets endogenous genes and regulates virulence to evade mammalian host immunity. *Cell Res.* **2016**, 26, 1273–1287, doi:10.1038/cr.2016.135.

175. Lin, J.; Michel, L. O.; Zhang, Q. CmeABC functions as a multidrug efflux system in *Campylobacter jejuni*. *Antimicrob. Agents Chemother.* **2002**, 46, 2124–31, doi:10.1128/AAC.46.7.2124-2131.2002.

176. Lin, X.; Ding, H.; Zeng, Q. Transcriptomic response during phage infection of a marine cyanobacterium under phosphorus-limited conditions. *Environ. Microbiol*. **2016**, 18, 450–460, doi:10.1111/1462-2920.13104.

177. Lis, L.; Connerton, I. F. The minor flagellin of *Campylobacter jejuni* (FlaB) confers defensive properties against bacteriophage infection. *Front. Microbiol.* **2016**, 7, doi:10.3389/fmicb.2016.01908.

178. Loc Carrillo, C.; Atterbury, R. J.; El-Shibiny, A.; Connerton, P. L.; Dillon, E.; Scott, A.; Connerton, I. F. Bacteriophage therapy to reduce *Campylobacter jejuni* colonization of broiler chickens. *Appl. Environ. Microbiol.* **2005**, 71, 6554–6563, doi:71/11/6554 [pii] 10.1128/AEM.71.11.6554-6563.2005.

179. Loc Carrillo, C.; Atterbury, R.J.; El-Shibiny, A.; Connerton, P.L.; Dillon, E.; Scott, A.; Connerton, I.F. Bacteriophage therapy to reduce *Campylobacter jejuni* colonization of broiler chickens. *Appl. Environ. Microbiol.* **2005**, 71, 6554–6563.

180. Logan, S. M. Flagellar glycosylation - A new component of the motility repertoire? *Microbiology* **2006**, 152, 1249–1262.

181. Logan, S. M.; Hui, J. P. M.; Vinogradov, E.; Aubry, A. J.; Melanson, J. E.; Kelly, J. F.; Nothaft, H.; Soo, E. C. Identification of novel carbohydrate modifications on *Campylobacter jejuni* 11168 flagellin using metabolomics-based approaches. *FEBS J.* **2009**, 276, 1014–1023, doi:10.1111/j.1742-4658.2008.06840.x.

182. Logan, S. M.; Kelly, J. F.; Thibault, P.; Ewing, C. P.; Guerry, P. Structural heterogeneity of carbohydrate modifications affects serospecificity of *Campylobacter* flagellins. *Mol. Microbiol.* **2002**, 46, 587–597, doi:10.1046/j.1365-2958.2002.03185.x.

183. Logan, S. M.; Schoenhofen, I. C.; Guerry, P. O-linked flagellar glycosylation in *Campylobacter*. In; Nachamkin, I., Szymanski, C. M., Blaser, M. J., Eds.; *Campylobacter*; ASM Press: Washington, D.C., **2008**; pp. 471–481.

184. Louwen, R.; Horst-Kreft, D.; De Boer, A. G.; Van Der Graaf, L.; De Knegt, G.; Hamersma, M.; Heikema, A. P.; Timms, A. R.; Jacobs, B. C.; Wagenaar, J. A.; Endtz, H. P.; Van Der Oost, J.; Wells, J. M.; Nieuwenhuis, E. E. S.; Van Vliet, A. H. M.; Willemsen, P. T. J.; Van Baarlen, P.; Van Belkum, A. A novel link between *Campylobacter jejuni* bacteriophage defence, virulence and Guillain-Barre syndrome. *Eur. J. Clin. Microbiol.* Infect. Dis. **2013**, 32, 207–226, doi:10.1007/s10096-012-1733-4.

185. Louwen, R.; van Baarlen, P. Are bacteriophage defence and virulence two sides of the same coin in *Campylobacter jejuni*? *Biochem. Soc. Trans.* **2013**, 41, 1475–81, doi:10.1042/BST20130127.

186. Love, M. I.; Huber, W.; Anders, S. Moderated estimation of fold change and dispersion for RNA-seq data with DESeq2. Genome Biol. **2014**, 15, doi:10.1186/s13059-014-0550-8.

187. Lu, M. J.; Henning, U. The immunity (imm) gene of *Escherichia coli* bacteriophage T4. *J. Virol.* **1989**, 63, 3472–8.

188. Luo, W.; Friedman, M. S.; Shedden, K.; Hankenson, K. D.; Woolf, P. J. GAGE: Generally applicable gene set enrichment for pathway analysis. *BMC Bioinformatics* **2009**, 10, doi:10.1186/1471-2105-10-161.

189. McClelland, E.E.; Nicola, A.M.; Prados-Rosales, R.; Casadevall, A. Ab binding alters gene expression in *Cryptococcus neoformans* and directly modulates fungal metabolism. *J. Clin. Invest.* **2010**, 120, 1355–1361.

190. McNally, D. J.; Aubry, A. J.; Hui, J. P. M.; Khieu, N. H.; Whitfield, D.; Ewing, C. P.; Guerry, P.; Brisson, J. R.; Logan, S. M.; Soo, E. C. Targeted metabolomics analysis of *Campylobacter coli* VC167 reveals legionaminic acid derivatives as novel flagellar glycans. *J. Biol. Chem.* **2007**, 282, 14463–14475, doi:10.1074/jbc.M611027200.

191. McNally, D. J.; Hui, J. P. M.; Aubry, A. J.; Mui, K. K. K.; Guerry, P.; Brisson, J. R.; Logan, S. M.; Soo, E. C. Functional characterization of the flagellar glycosylation locus in *Campylobacter jejuni* 81-176 using a focused metabolomics approach. *J. Biol. Chem.* **2006**, 281, 18489–18498, doi:10.1074/jbc.M603777200.

192. McNally, D. J.; Lamoureux, M. P.; Karlyshev, A. V.; Fiori, L. M.; Li, J.; Thacker, G.; Coleman, R. A.; Khieu, N. H.; Wren, B. W.; Brisson, J. R.; Jarrell, H. C.; Szymanski, C. M. Commonality and biosynthesis of the O-methyl phosphoramidate capsule modification in *Campylobacter jejuni. J. Biol. Chem.* **2007**, 282, 28566–28576, doi:10.1074/jbc.M704413200.

193. Ménard, R.; Schoenhofen, I. C.; Tao, L.; Aubry, A.; Bouchard, P.; Reid, C. W.; Lachance, P.; Twine, S. M.; Fulton, K. M.; Cui, Q.; Hogues, H.; Purisima, E. O.; Sulea, T.; Logan, S. M. Small-molecule inhibitors of the pseudaminic acid biosynthetic pathway: Targeting motility as a key bacterial virulence factor. *Antimicrob. Agents Chemother.* **2014**, 58, 7430–7440, doi:10.1128/AAC.03858-14.

194. Merino, S.; Tomás, J. M. Gram-negative flagella glycosylation. *Int. J. Mol. Sci*. **2014**, 15, 2840–2857.

195. Mescher, M. F.; Strominger, J. L. Purification and characterization of a prokaryotic glucoprotein from the cell envelope of *Halobacterium salinarium*. *J. Biol. Chem*. **1976**, 251, 2005–2014.

196. Meunier, M.; Guyard-Nicodème, M.; Dory, D.; Chemaly, M. Control strategies against *Campylobacter* at the poultry production level: Biosecurity measures, feed additives and vaccination. *J. Appl. Microbiol.* **2016**.

197. Miller, E. S.; Kutter, E.; Mosig, G.; Arisaka, F.; Kunisawa, T.; Rüger, W. Bacteriophage T4 genome. *Microbiol. Mol. Biol. Rev*. **2003**, 67, 86–156, table of contents, doi:10.1128/MMBR.67.1.86-156.2003.

198. Miller, M.; Acosta, A. M.; Chavez, C. B.; Flores, J. T.; Olotegui, M. P.; Pinedo, S. R.; Trigoso, D. R.; Vasquez, A. O.; Ahmed, I.; Alam, D.; … and Shrestha, S. K. The MAL-ED study: A multinational and multidisciplinary approach to understand the relationship between enteric pathogens, malnutrition, gut physiology, physical growth, cognitive development, and immune responses in infants and children up to 2 years of age. *J Clin. Infect. Dis.* **2014**, 59, S193–S206, doi:10.1093/cid/ciu653.

199. Mohawk, K. L.; Poly, F.; Sahl, J. W.; Rasko, D. A.; Guerry, P. High frequency, spontaneous *motA* mutations in *Campylobacter jejuni* strain 81-176. *PLoS One* **2014**, 9, doi:10.1371/journal.pone.0088043.

200. Mojardín, L.; Salas, M. Global transcriptional analysis of virus-host interactions between phage φ29 and *Bacillus subtilis*. *J. Virol.* **2016**, 90, JVI.01245-16, doi:10.1128/JVI.01245-16.

201. Moore, J. E.; Barton, M. D.; Blair, I. S.; Corcoran, D.; Dooley, J. S. G.; Fanning, S.; Kempf, I.; Lastovica, A. J.; Lowery, C. J.; Matsuda, M.; McDowell, D. A.; McMahon,

A.; Millar, B. C.; Rao, J. R.; Rooney, P. J.; Seal, B. S.; Snelling, W. J.; Tolba, O. The epidemiology of antibiotic resistance in *Campylobacter*. *Microbes Infect*. **2006**.

202. Moreau, P.; Diggle, S. P.; Friman, V.-P. Bacterial cell-to-cell signaling promotes the evolution of resistance to parasitic bacteriophages. *Ecol. Evol.* **2017**, 7, 1936–1941, doi:10.1002/ece3.2818.

203. Morimoto, D.; Kimura, S.; Sako, Y.; Yoshida, T. Transcriptome Analysis of a Bloom-Forming Cyanobacterium Microcystis aeruginosa during Ma-LMM01 Phage Infection. *Front. Microbiol.* **2018**, 9, 2, doi:10.3389/fmicb.2018.00002.

204. Kaakoush, N. O., Castaño-Rodríguez, N., Mitchell, H. M., & Man, S. M. Global epidemiology of *Campylobacter* infection. *Clin. Microbiol. Rev.* **2015**, *28*, 3, 687-720.

205. Neuberger, A. Carbohydrates in protein: The carbohydrate component of crystalline egg albumin. *Biochem. J.* **1938**, 32, 1435–1451.

206. Nieva, J.; Wentworth, P., Jr. The antibody-catalyzed water oxidation pathway—A new chemical arm to immune defense? *Trends Biochem. Sci.* **2004**, 29, 274–278.

207. Nothaft, H.; Davis, B.; Lock, Y. Y.; Perez-Munoz, M. E.; Vinogradov, E.; Walter, J.; Coros, C.; Szymanski, C. M. Engineering the *Campylobacter* jejuni N-glycan to create an effective chicken vaccine. *Sci. Rep.* **2016**, doi:10.1038/srep26511.

208. Nothaft, H.; Szymanski, C. M. Bacterial protein N-glycosylation: New perspectives and applications. *J. Biol. Chem.* **2013**, 288, 6912–6920.

209. Nothaft, H.; Szymanski, C. M. Protein glycosylation in bacteria: sweeter than ever. Nat. Rev. Microbiol. **2010**, 8, 765–778, doi:10.1038/nrmicro2383.

210. O'Neill, J. Antimicrobial Resistance: Tackling a crisis for the health and wealth of nations The Review on Antimicrobial Resistance Chaired. **2014**.

211. O'Sullivan, L.; Lucid, A.; Neve, H.; Franz, C. M. A. P.; Bolton, D.; McAuliffe, O.; Paul Ross, R.; Coffey, A. Comparative genomics of Cp8viruses with special reference to *Campylobacter* phage vB_CjeM_los1, isolated from a slaughterhouse in Ireland. *Arch. Virol.* **2018**, 1–16, doi:10.1007/s00705-018-3845-3.

212. Ofir, G.; Melamed, S.; Sberro, H.; Mukamel, Z.; Silverman, S.; Yaakov, G.; Doron, S.; Sorek, R. DISARM is a widespread bacterial defence system with broad anti-phage activities. *Nat. Microbiol.* **2018**, 3, 90–98, doi:10.1038/s41564-017-0051-0.

213. Palyada, K.; Sun, Y. Q.; Flint, A.; Butcher, J.; Naikare, H.; Stintzi, A. Characterization of the oxidative stress stimulon and PerR regulon of *Campylobacter jejuni. BMC Genomics* **2009**, 10, 481, doi:10.1186/1471-2164-10-481.

214. Palyada, K.; Threadgill, D.; Stintzi, A. Iron acquisition and regulation in *Campylobacter jejuni. J. Bacteriol.* **2004**, 186, 4714–4729, doi:10.1128/JB.186.14.4714-4729.2004.

215. Parkhill, J.; Wren, B. W.; Mungall, K.; Ketley, J. M.; Churcher, C.; Basham, D.; Chillingworth, T.; Davies, R. M.; Feltwell, T.; Holroyd, S.; Jagels, K.; Karlyshev, A. V.; Moule, S.; Pallen, M. J.; Penn, C. W.; Quail, M. A.; Rajandream, M. A.; Rutherford, K. M.; Van Vliet, A. H. M.; Whitehead, S.; Barrell, B. G. The genome sequence of the food-borne pathogen *Campylobacter jejuni* reveals hypervariable sequences. *Nature* **2000**, doi:10.1038/35001088.

216. Parkhill, J.; Wren, B.W.; Mungall, K.; Ketley, J.M.; Churcher, C.; Basham, D.; Chillingworth, T.; Davies, R.M.; Feltwell, T.; Holroyd, S.; et al. The genome sequence of the food-borne pathogen *Campylobacter jejuni* reveals hypervariable sequences. *Nature* **2000**, 403, 665–668.

217. Patry, R. T.; Stahl, M.; Perez-Munoz, M. E.; Wenzel, C. Q.; Sacher, J. C.; Coros, C.; Walter, J.; Vallance, B. A.; Szymanski, C. M. Bacterial warfare: growth inhibition of ganglioside-mimicking gut bacteria by AB5 toxins. Submitted to *Nature Microbiol*.

218. Penner, J. L.; Hennessy, J. N.; Congi, R. V. Serotyping of *Campylobacter jejuni* and *Campylobacter coli* on the basis of thermostable antigens. *Eur. J. Clin. Microbiol*. **1983**, doi:10.1007/BF02019474.

219. Pirnay, J. P.; Verbeken, G.; Ceyssens, P. J.; Huys, I.; de Vos, D.; Ameloot, C.; Fauconnier, A. The magistral phage. *Viruses* **2018**, 10, doi:10.3390/v10020064.

220. Poropatich, K. O.; Walker, C. L. F.; Black, R. E. Quantifying the association between *Campylobacter* infection and Guillain-Barre Syndrome: A systematic review. *J. Heal. Popul. Nutr.* **2010**, *28*, 545–552, doi:10.3329/jhpn.v28i6.6602.

221. Poshtiban, S.; Javed, M.A.; Arutyunov, D.; Singh, A.; Banting, G.; Szymanski, C.M.; Evoy, S. Phage receptor binding protein-based magnetic enrichment method as an aid for real time PCR detection of foodborne bacteria. *Analyst* **2013**, 138, 5619–5626.

222. Pumbwe, L.; Piddock, L. J. V. Identification and molecular characterisation of *CmeB*, a *Campylobacter jejuni* multidrug efflux pump. *FEMS Microbiol. Lett.* **2002**, 206, 185–189, doi:10.1111/j.1574-6968.2002.tb11007.x.

223. Ridley, K. A.; Rock, J. D.; Li, Y.; Ketley, J. M. Heme utilization in *Campylobacter jejuni*. *J. Bacteriol.* **2006**, 188, 7862–75, doi:10.1128/JB.00994-06.

224. Roach, D. R.; Debarbieux, L. Phage therapy: awakening a sleeping giant. *Emerg. Top. Life Sci.* **2017**, 1, 93–103, doi:10.1042/ETLS20170002.

225. Rosenquist, H.; Nielsen, N. L.; Sommer, H. M.; Nørrung, B.; Christensen, B. B. Quantitative risk assessment of human campylobacteriosis associated with thermophilic

Campylobacter species in chickens. *Int. J. Food Microbiol*. **2003**, doi:10.1016/S0168-1605(02)00317-3.

226. Sails, A. D.; Wareing, D. R. A.; Bolton, F. J.; Fox, A. J.; Curry, A. Characterisation of 16 *Campylobacter jejuni* and *C. coli* typing bacteriophages. *J. Med. Microbiol*. **1998**, 47, 123–128, doi:10.1099/00222615-47-2-123.

227. Sacher, J. C., Yee, E., Szymanski, C. M., & Miller, W. G. Complete genome sequence of *Campylobacter jejuni* strain 12567, a livestock-associated clade representative. *Genome Announc.* **2018,** *6*, e00513-18.

228. Sacher, J. C., Yee, E., Szymanski, C. M., & Miller, W. G. Complete genome sequences of three *Campylobacter jejuni* phage-propagating strains. *Genome Announc.* **2018,** *6*, e00514-18.

229. Sacher, J. C.; Flint, A.; Butcher, J.; Blasdel, B.; Reynolds, H. M.; Lavigne, R.; Stintzi, A.; Szymanski, C. M. Transcriptomic analysis of the *Campylobacter jejuni* response to T4-like phage NCTC 12673 infection. *Viruses* **2018,** *10*, 332.

230. Schirm, M.; Arora, S. K.; Verma, A.; Vinogradov, E.; Thibault, P.; Ramphal, R.; Logan, S. M. Structural and Genetic Characterization of Glycosylation of Type a Flagellin in *Pseudomonas aeruginosa. J. Bacteriol*. **2004**, 186, 2523–2531, doi:10.1128/JB.186.9.2523-2531.2004.

231. Schirm, M.; Schoenhofen, I. C.; Logan, S. M.; Waldron, K. C.; Thibault, P. Identification of unusual bacterial glycosylation by tandem mass spectrometry analyses of intact proteins. *Anal. Chem*. **2005**, 77, 7774–7782, doi:10.1021/ac051316y.

232. Schirm, M.; Soo, E. C.; Aubry, A. J.; Austin, J.; Thibault, P.; Logan, S. M. Structural, genetic and functional characterization of the flagellin glycosylation process in

Helicobacter pylori. Mol. Microbiol. **2003**, 48, 1579–1592, doi:10.1046/j.1365-2958.2003.03527.x.

233. Schmelcher, M.; Donovan, D.M.; Loessner, M.J. Bacteriophage endolysins as novel antimicrobials. *Future Microbiol*. **2012**, 7, 1147–1171.

234. Schoenhofen, I. C.; McNally, D. J.; Vinogradov, E.; Whitfield, D.; Young, N. M.; Dick, S.; Wakarchuk, W. W.; Brisson, J. R.; Logan, S. M. Functional characterization of dehydratase/aminotransferase pairs from *Helicobacter* and *Campylobacter*: Enzymes distinguishing the pseudaminic acid and bacillosamine biosynthetic pathways. *J. Biol. Chem*. **2006**, 281, 723–732, doi:10.1074/jbc.M511021200.

235. Scholl, D.; Cooley, M.; Williams, S. R.; Gebhart, D.; Martin, D.; Bates, A.; Mandrell, R. An engineered R-type pyocin is a highly specific and sensitive bactericidal agent for the food-borne pathogen *Escherichia coli* O157:H7. *Antimicrob. Agents Chemother*. **2009**, 53, 3074–3080, doi:10.1128/AAC.01660-08; 10.1128/AAC.01660-08.

236. Scholl, D.; Cooley, M.; Williams, S.R.; Gebhart, D.; Martin, D.; Bates, A.; Mandrell, R. An engineered R-type pyocin is a highly specific and sensitive bactericidal agent for the food-borne pathogen *Escherichia coli* O157:H7. *Antimicrob. Agents Chemother*. **2009**, 53, 3074–3080.

237. Schuch, R.; Fischetti, V. A. Detailed genomic analysis of the Wbeta and gamma phages infecting *Bacillus anthracis*: implications for evolution of environmental fitness and antibiotic resistance. *J. Bacteriol.* **2006**, doi:10.1128/JB.188.8.3037-3051.2006.

238. Seed, K. D.; Yen, M.; Shapiro, B. J.; Hilaire, I. J.; Charles, R. C.; Teng, J. E.; Ivers, L. C.; Boncy, J.; Harris, J. B.; Camilli, A. Evolutionary consequences of intra-patient phage predation on microbial populations. *Elife* **2014,** *3*, e03497.

239. Simpson, D.J.; Sacher, J.C.; Szymanski, C.M. Exploring the interactions between bacteriophage-encoded glycan binding proteins and carbohydrates. *Curr. Opin. Struct.* Biol. **2015**, 34, 69–77.

240. Singh, A.; Arutyunov, D.; McDermott, M.T.; Szymanski, C.M.; Evoy, S. Specific detection of *Campylobacter jejuni* using the bacteriophage NCTC 12673 receptor binding protein as a probe. *Analyst* **2011**, 136, 4780–4786.

241. Singh, A.; Arutyunov, D.; Szymanski, C.M.; Evoy, S. Bacteriophage based probes for pathogen detection. *Analyst* **2012**, 137, 3405–3421.

242. Singh, A.; Arya, S. K.; Glass, N.; Hanifi-Moghaddam, P.; Naidoo, R.; Szymanski, C. M.; Tanha, J.; Evoy, S. Bacteriophage tailspike proteins as molecular probes for sensitive and selective bacterial detection. *Biosens. Bioelectron*. **2010**, 26, 131–138, doi:DOI: 10.1016/j.bios.2010.05.024.

243. Singh, A.; Glass, N.; Tolba, M.; Brovko, L.; Griffiths, M.; Evoy, S. Immobilization of bacteriophages on gold surfaces for the specific capture of pathogens. *Biosens. Bioelectron.* **2009,** *24*, 3645-3651.

244. Singh, A.; Poshtiban, S.; Evoy, S. Recent advances in bacteriophage based biosensors for food-borne pathogen detection. *Sensors (Basel)*. **2013**, 13, 1763–1786, doi:10.3390/s130201763; 10.3390/s130201763.

245. Siringan, P.; Connerton, P. L.; Cummings, N. J.; Connerton, I. F. Alternative bacteriophage life cycles: the carrier state of *Campylobacter jejuni*. *Open Biol.* **2014**, 4, 130200, doi:10.1098/rsob.130200.

246. Sleytr, U. B. Heterologous reattachment of regular arrays of glycoproteins on bacterial surfaces. *Nature* **1975**, 257, 400–402.

247. Soo, E. C.; Hui, J. P. Metabolomics in glycomics. *Methods Mol. Biol*. **2010**, 600, 175–186, doi:10.1007/978-1-60761-454-8_12; 10.1007/978-1-60761-454-8_12.

248. Sørensen, M. C. H.; Gencay, Y. E.; Birk, T.; Baldvinsson, S. B.; Jäckel, C.; Hammerl, J. A.; Vegge, C. S.; Neve, H.; Brøndsted, L. Primary isolation strain determines both phage type and receptors recognised by *Campylobacter jejuni* bacteriophages. *PLoS One* **2015**, 10, doi:10.1371/journal.pone.0116287.

249. Sørensen, M. C. H.; Gencay, Y. E.; Brøndsted, L. Methods for initial characterization of Cam*pylobacter jejuni* bacteriophages. In *Methods in Molecular Biology*; **2017**; Vol. 1512, pp. 91–105 ISBN 978-1-4939-6536-6.

250. Sørensen, M. C. H.; van Alphen, L. B.; Fodor, C.; Crowley, S. M.; Christensen, B. B.; Szymanski, C. M.; Brøndsted, L. Phase Variable Expression of Capsular Polysaccharide Modifications Allows *Campylobacter jejuni* to Avoid Bacteriophage Infection in Chickens. *Front. Cell. Infect. Microbiol.* **2012**, 2, doi:10.3389/fcimb.2012.00011.

251. Sørensen, M. C. H.; van Alphen, L. B.; Harboe, A.; Li, J.; Christensen, B. B.; Szymanski, C. M.; Brøndsted, L. Bacteriophage F336 recognizes the capsular phosphoramidate modification of *Campylobacter jejuni* NCTC11168. *J. Bacteriol.* **2011**, 193, 6742–6749, doi:10.1128/JB.05276-11.

252. Sorensen, M.C.; Gencay, Y.E.; Birk, T.; Baldvinsson, S.B.; Jackel, C.; Hammerl, J.A.; Vegge, C.S.; Neve, H.; Brondsted, L. Primary isolation strain determines both phage type and receptors recognised by *Campylobacter jejuni* bacteriophages. *PLoS ONE* **2015**, 10, e0116287.

253. St. Michael, F.; Szymanski, C.M.; Li, J.; Chan, K.H.; Khieu, N.H.; Larocque, S.; Wakarchuk, W.W.; Brisson, J.R.; Monteiro, M.A. The structures of the

lipooligosaccharide and capsule polysaccharide of *Campylobacter jejuni* genome sequenced strain NCTC 11168. *Eur. J. Biochem.* **2002**, 269, 5119–5136.

254. St. Michael, F.; Szymanski, C. M.; Li, J.; Chan, K. H.; Khieu, N. H.; Larocque, S.; Wakarchuk, W. W.; Brisson, J. R.; Monteiro, M. A. The structures of the lipooligosaccharide and capsule polysaccharide of *Campylobacter jejuni* genome sequenced strain NCTC 11168. *Eur. J. Biochem.* 2002, 269, 5119–5136, doi:10.1046/j.1432-1033.2002.03201.x.

255. Stahl, M.; Butcher, J.; Stintzi, A. Nutrient acquisition and metabolism by *Campylobacter jejuni*. *Front. Cell. Infect. Microbiol.* **2012**, 2, 5, doi:10.3389/fcimb.2012.00005.

256. Steinbacher, S.; Seckler, R.; Miller, S.; Steipe, B.; Huber, R.; Reinemer, P. Crystal structure of P22 tailspike protein: Interdigitated subunits in a thermostable trimer. *Science* **1994**, 265, 383–386.

257. Stern, A.; Sorek, R. The phage-host arms race: shaping the evolution of microbes. *Bioessays* **2011**, *33*, 43-51.

258. Strutt, S. C.; Torrez, R. M.; Kaya, E.; Negrete, O. A.; Doudna, J. A. RNA-dependent RNA targeting by CRISPR-Cas9. *Elife* **2018**, 7, doi:10.7554/eLife.32724.

259. Suttle, C. A. Viruses in the sea. *Nature* **2005**, 437, 356–361, doi:10.1038/nature04160.

260. Svensson, S. L.; Pryjma, M.; Gaynor, E. C. Flagella-mediated adhesion and extracellular DNA release contribute to biofilm formation and stress tolerance of *Campylobacter jejuni. PLoS One* **2014**, 9, e106063, doi:10.1371/journal.pone.0106063; 10.1371/journal.pone.0106063.

261. Szymanski, C. M.; King, M.; Haardt, M.; Armstrong, G. D. *Campylobacter jejuni* motility and invasion of Caco-2 cells. *Infect. Immun.* **1995**, 63, 4295–4300.

262. Szymanski, C. M.; Logan, S. M.; Linton, D.; Wren, B. W. *Campylobacter* - A tale of two protein glycosylation systems. *Trends Microbiol.* **2003**, 11, 233–238.

263. Szymanski, C. M.; Yao, R.; Ewing, C. P.; Trust, T. J.; Guerry, P. Evidence for a system of general protein glycosylation in *Campylobacter jejuni*. *Mol. Microbiol.* **1999**, 32, 1022–1030, doi:10.1046/j.1365-2958.1999.01415.x.

264. Ternhag, A.; Asikainen, T.; Giesecke, J.; Ekdahl, K. A meta-analysis on the effects of antibiotic treatment on duration of symptoms caused by infection with *Campylobacter* species. *Clin. Infect. Dis.* **2007**, doi:10.1086/509924.

265. Thiaville, J. J.; Kellner, S. M.; Yuan, Y.; Hutinet, G.; Thiaville, P. C.; Jumpathong, W.; Mohapatra, S.; Brochier-Armanet, C.; Letarov, A. V.; Hillebrand, R.; Malik, C. K.; Rizzo, C. J.; Dedon, P. C.; de Crécy-Lagard, V. Novel genomic island modifies DNA with 7-deazaguanine derivatives. *Proc. Natl. Acad. Sci.* **2016**, doi:10.1073/pnas.1518570113.

266. Thibault, P.; Logan, S. M.; Kelly, J. F.; Brisson, J. R.; Ewing, C. P.; Trust, T. J.; Guerry, P. Identification of the Carbohydrate Moieties and Glycosylation Motifs in *Campylobacter jejuni* Flagellin. *J. Biol. Chem.* **2001**, 276, 34862–34870, doi:10.1074/jbc.M104529200.

267. Thibault, P.; Logan, S.M.; Kelly, J.F.; Brisson, J.R.; Ewing, C.P.; Trust, T.J.; Guerry, P. Identification of the carbohydrate moieties and glycosylation motifs in *Campylobacter jejuni* flagellin. *J. Biol. Chem.* **2001**, 276, 34862–34870.

268. Timms, A. R.; Cambray-Young, J.; Scott, A. E.; Petty, N. K.; Connerton, P. L.; Clarke, L.; Seeger, K.; Quail, M.; Cummings, N.; Maskell, D. J.; Thomson, N. R.; Connerton, I.

F. Evidence for a lineage of virulent bacteriophages that target *Campylobacter*. *BMC Genomics* **2010**, 11, 214, doi:10.1186/1471-2164-11-214.

269. Trigo, G.; Martins, T.G.; Fraga, A.G.; Longatto-Filho, A.; Castro, A.G.; Azeredo, J.; Pedrosa, J. Phage therapy is effective against infection by *Mycobacterium ulcerans* in a murine footpad model. *PLoS Negl. Trop. Dis.* **2013**, 7, e2183.

270. Ulasi, G. N.; Creese, A. J.; Hui, S. X.; Penn, C. W.; Cooper, H. J. Comprehensive mapping of O-glycosylation in flagellin from *Campylobacter jejuni* 11168: A multienzyme differential ion mobility mass spectrometry approach. *Proteomics* **2015**, 15, 2733–2745, doi:10.1002/pmic.201400533.

271. Umaraw, P.; Prajapati, A.; Verma, A. K.; Pathak, V.; Singh, V. P. Control of *Campylobacter* in poultry industry from farm to poultry processing unit: A review. *Crit. Rev. Food Sci. Nutr.* **2017**, 57, 659–665, doi:10.1080/10408398.2014.935847.

272. van Alphen, L. B.; Wuhrer, M.; Bleumink-Pluym, N. M. C.; Hensbergen, P. J.; Deeldere, A. M.; Van Putten, J. P. M. A functional *Campylobacter jejuni maf4* gene results in novel glycoforms on flagellin and altered autoagglutination behaviour. *Microbiology* **2008**, 154, 3385–3397, doi:10.1099/mic.0.2008/019919-0.

273. Wagenaar, J. A.; Bergen, M. A. P. V; Mueller, M. A.; Wassenaar, T. M.; Carlton, R. M. Phage therapy reduces *Campylobacter jejuni* colonization in broilers. *Vet. Microbiol.* **2005**, 109, 275–283, doi:10.1016/j.vetmic.2005.06.002.

274. Wang, P.X.; Sanders, P.W. Immunoglobulin light chains generate hydrogen peroxide. *J. Am. Soc. Nephrol.* **2007**, 18, 1239–1245.

275. Wang, X.; Kim, Y.; Ma, Q.; Hong, S. H.; Pokusaeva, K.; Sturino, J. M.; Wood, T. K. Cryptic prophages help bacteria cope with adverse environments. *Nat. Commun.* **2010**, 1, 147, doi:10.1038/ncomms1146.

276. Waseh, S.; Hanifi-Moghaddam, P.; Coleman, R.; Masotti, M.; Ryan, S.; Foss, M.; MacKenzie, R.; Henry, M.; Szymanski, C. M.; Tanha, J. Orally administered P22 phage tailspike protein reduces *Salmonella* colonization in chickens: prospects of a novel therapy against bacterial infections. *PLoS One* **2010**, 5, e13904, doi:10.1371/journal.pone.0013904; 10.1371/journal.pone.0013904.

277. Wassenaar, T. M. Following an imaginary *Campylobacter* population from farm to fork and beyond: A bacterial perspective. *Lett. Appl. Microbiol*. **2011**, 53, 253–263.

278. Weigele, P.; Raleigh, E. A. Biosynthesis and Function of Modified Bases in Bacteria and Their Viruses. *Chem. Rev.* **2016**, 116, 12655–12687, doi:10.1021/acs.chemrev.6b00114.

279. Weingarten, R. A.; Taveirne, M. E.; Olson, J. W. The dual-functioning fumarate reductase is the sole succinate:quinone reductase in *Campylobacter jejuni* and is required for full host colonization. *J. Bacteriol.* **2009**, *191*, 5293–300, doi:10.1128/JB.00166-09.

280. Williams, S. R.; Gebhart, D.; Martin, D. W.; Scholl, D. Retargeting R-type pyocins to generate novel bactericidal protein complexes. *Appl. Environ. Microbiol*. **2008**, 74, 3868–3876, doi:10.1128/AEM.00141-08.

281. Woodall, C. A.; Jones, M. A.; Barrow, P. A.; Hinds, J.; Marsden, G. L.; Kelly, D. J.; Dorrell, N.; Wren, B. W.; Maskell, D. J. *Campylobacter jejuni* gene expression in the chick cecum: evidence for adaptation to a low-oxygen environment. Infect. Immun. **2005**, 73, 5278–85, doi:10.1128/IAI.73.8.5278-5285.2005.

282. Yano, M.; Gohil, S.; Coleman, J.R.; Manix, C.; Pirofski, L.A. Antibodies to *Streptococcus pneumoniae* capsular polysaccharide enhance pneumococcal quorum sensing. *mBio* **2011**, 2, doi:10.1128/mBio.00176-11.

283. Yuki, N. Carbohydrate mimicry: a new paradigm of autoimmune diseases. *Curr. Opin. Immunol*. **2005**, 17, 577–582, doi:10.1016/j.coi.2005.09.004.

284. Yuki, N.; Susuki, K.; Koga, M.; Nishimoto, Y.; Odaka, M.; Hirata, K.; Taguchi, K.; Miyatake, T.; Furukawa, K.; Kobata, T.; Yamada, M. Carbohydrate mimicry between human ganglioside GM1 and *Campylobacter jejuni* lipooligosaccharide causes Guillain-Barre syndrome. *Proc. Natl. Acad. Sci.* **2004**, 101, 11404–11409, doi:10.1073/pnas.0402391101.

285. Zampara, A.; Sørensen, M. C. H.; Elsser-Gravesen, A.; Brøndsted, L. Significance of phage-host interactions for biocontrol of *Campylobacter jejuni* in food. Food Control **2017**, 73, 1169–1175, doi:10.1016/j.foodcont.2016.10.033.

286. Zampronio, C. G.; Blackwell, G.; Penn, C. W.; Cooper, H. J. Novel glycosylation sites localized in *Campylobacter jejuni* flagellin FlaA by liquid chromatography electron capture dissociation tandem mass spectrometry. *J. Proteome Res*. **2011**, 10, 1238–1245, doi:10.1021/pr101021c.

287. Zebian, N.; Merkx-Jacques, A.; Pittock, P. P.; Houle, S.; Dozois, C. M.; Lajoie, G. A.; Creuzenet, C. Comprehensive analysis of flagellin glycosylation in *Campylobacter jejuni* NCTC 11168 reveals incorporation of legionaminic acid and its importance for host colonization. *Glycobiology* **2016**, 26, 386–397, doi:10.1093/glycob/cwv104.

288. Zunk, M.; Kiefel, M. J. The occurrence and biological significance of the α-keto-sugars pseudaminic acid and legionaminic acid within pathogenic bacteria. *RSC Adv.* **2014**, 4, 3413–3421, doi:10.1039/C3RA44924F.

Appendix I: Complete genome sequences of three *Campylobacter jejuni* phage-propagating strains

A version of this appendix was published as:

Sacher, J. C.; Yee, E.; Szymanski, C. M.; Miller, W. G. Complete genome sequences of Three *Campylobacter jejuni* Phage-Propagating Strains. *Genome Announc.* **2018,** *6,* e00514-18.

Abstract

Bacteriophage therapy can potentially reduce *Campylobacter jejuni* numbers in livestock, but requires a detailed understanding of phage-host interactions. *C. jejuni* strains readily infected by certain phages are designated as phage-propagating strains. Here we report the complete genome sequences of three such strains, NCTC 12660, NCTC 12661, and NCTC 12664.

A1.1. Genome Announcement

Campylobacter jejuni causes diarrheal disease worldwide and *C. jejuni* infections arise from consuming and mishandling contaminated poultry (1–3). Phages are being explored as antibiotic alternatives to reduce *C. jejuni* burden (4–6). Phages are highly strain-specific so understanding the factors that contribute to this specificity, including capsular polysaccharides (CPS), flagella (7), and restriction/modification systems (8, 9) can maximize the strain range targeted (10).

C. jejuni strains were historically tracked based on phage susceptibility (11, 12). For these typing schemes, each phage was designated a readily-infected 'phage-propagating' strain. To identify factors governing phage susceptibility in *C. jejuni*, we sequenced the genomes of three *C. jejuni* phage-propagating strains isolated from chickens (12): NCTC 12660, NCTC 12661 and NCTC 12664.

Whole-genome sequencing was performed using the PacBio RS and Illumina MiSeq sequencing platforms. PacBio sequence data were assembled to construct a single, closed chromosomal contig for each strain. MiSeq reads were used to validate base calls and to determine the variability at each poly-G tract. Protein-, rRNA- and tRNA-encoding genes were identified as

described (13). The genome sizes ranged from 1.61-1.68 Mbp with an average GC content of 30.6%. The three genomes show high similarity to strain NCTC 11168, although 12660 has at least one small inversion compared to 11168. These four genomes encode a similar number of genes and pseudogenes, with the genome of 12660 slightly larger due to the presence of a genomic island. Many of the pseudogenes identified were conserved across all or most of the three strains and 11168.

We identified several differences in restriction/modification (R/M) and CRISPR/Cas systems between these strains. Relative to the others, 12661 lacks a type I R/M system, 12661 and 12664 lack the type IIG RE *cj1051,* 12661 uniquely encodes a type III R/M system and the type IIG RE CJ12661_0039, and the type IV R/M system subunit *mcrB* is a pseudogene in 12660. Interestingly, all but 12664 encode a full type II-C CRISPR/Cas system, with *cas9* a pseudogene in 12664.

CPS variability influences *C. jejuni* phage susceptibility (7, 14), but flagellar glycans play an unknown role (15). Strains 12661 and 12664 cluster separately from 12660 and 11168 in CPS and flagellar glycosylation gene content, which could lead to differences in phage-host interactions (Sacher *et al.,* unpublished observations). In addition to *C. jejuni* strain-strain variation, within-strain genome variation has been observed (16, 17). We compared our 12661 sequence to two prior genomes sequenced for this strain: GenBank accession numbers CP010906 (18) and CP020045 (17). Gardner *et al.* observed two alleles for *pseD,* encoding the flagellar acetamidino-substituted pseudaminic acid transferase (17, 19). Our 12661 *pseD* was 100% and 86% identical to these alleles. The *pseD* sequence from the earliest 12661 genome

(18) has regions of similarity to each of the *pseD* genes from the subsequently-sequenced genomes. This suggests possible recombination, although sequencing or assembly issues could be responsible. Either scenario could be explained by the many *pseD* homologues encoded by most *C. jejuni* strains (20). This example highlights the plasticity of *C. jejuni* genomes.

A1.2. Accession number(s)

The complete genome sequences of *C. jejuni* strains NCTC 12660, NCTC 12661 and NCTC 12664 have been deposited in GenBank under the accession numbers CP028910, CP028911 and CP028912, respectively.

A1.3. References

1. Fitzgerald C. 2015. *Campylobacter*. Clin Lab Med 2:289-98.
2. Wassenaar TM. 2011. Following an imaginary *Campylobacter* population from farm to fork and beyond: A bacterial perspective. Lett Appl Microbiol 53:253-263.
3. Kaakoush NO, Mitchell HM, Man SM. 2015. *Campylobacter*, p. 1187–1236. In Molecular Medical Microbiology, 2nd ed. Academic Press, London, UK.
4. Zampara A, Sørensen MCH, Elsser-Gravesen A, Brøndsted L. 2017. Significance of phage-host interactions for biocontrol of *Campylobacter jejuni* in food. Food Control 73:1169–1175.
5. Hammerl JA, Jäckel C, Alter T, Janzcyk P, Stingl K, Knüver MT, Hertwig S. 2014. Reduction of *Campylobacter jejuni* in broiler chicken by successive application of group II and group III phages. PLoS One 9: e114785.

6. Kittler S, Fischer S, Abdulmawjood A, Glünder G, Kleina G. 2013. Effect of bacteriophage application on *Campylobacter jejuni* loads in commercial broiler flocks. Appl Environ Microbiol 79:7525–7533.
7. Sørensen MCH, Gencay YE, Birk T, Baldvinsson SB, Jäckel C, Hammerl JA, Vegge CS, Neve H, Brøndsted L. 2015. Primary isolation strain determines both phage type and receptors recognised by *Campylobacter jejuni* bacteriophages. PLoS One 10: e0116287.
8. Dupuis M-È, Villion M, Magadán AH, Moineau S. 2013. CRISPR-Cas and restriction–modification systems are compatible and increase phage resistance. Nat Commun 4:2087.
9. Gardner SP, Olson JW. 2012. Barriers to Horizontal Gene Transfer in *Campylobacter jejuni*. Adv Appl Microbiol 79:19–42.
10. Fischer S, Kittler S, Klein G, Glünder G. 2013. Impact of a Single Phage and a Phage Cocktail Application in Broilers on Reduction of Campylobacter jejuni and Development of Resistance. PLoS One 8: e78543.
11. Grajewski BA, Kusek JW, Gelfand HM. 1985. Development of a bacteriophage typing system for *Campylobacter jejuni* and *Campylobacter coli*. J Clin Microbiol 22:13–18.
12. Frost JA, Kramer JM, Gillanders SA. 1999. Phage typing of *Campylobacter jejuni* and *Campylobacter coli* and its use as an adjunct to serotyping. Epidemiol Infect 123: 47-55.
13. Miller WG, Yee E, Chapman MH, Smith TPL, Bono JL, Huynh S, Parker CT, Vandamme P, Luong K, Korlach J. 2014. Comparative Genomics of the *Campylobacter lari* Group. Genome Biol Evol 6:3252–3266.
14. Sørensen MCH, van Alphen LB, Harboe A, Li J, Christensen BB, Szymanski CM, Brøndsted L. 2011. Bacteriophage F336 recognizes the capsular phosphoramidate modification of *Campylobacter jejuni* NCTC11168. J Bacteriol 193:6742–6749.

15. Baldvinsson SB, Holst Sørensen MC, Vegge CS, Clokie MRJ, Brøndsted L. 2014. *Campylobacter jejuni* motility is required for infection of the flagellotropic bacteriophage F341. Appl Environ Microbiol 80:7096–7106.
16. Wassenaar TM, Geilhausen B, Newell DG. 1998. Evidence of genomic instability in *Campylobacter jejuni* isolated from poultry. Appl Environ Microbiol 64:1816–21.
17. Gardner SP, Kendall KJ, Taveirne ME, Olson JW. 2017. Complete Genome Sequence of *Campylobacter jejuni* subsp. *jejuni* ATCC 35925. Genome Announc 5:e00743-17.
18. Ghaffar NM, Connerton PL, Connerton IF. 2015. Filamentation of *Campylobacter* in broth cultures. Front Microbiol 6:657.
19. Guerry P, Ewing CP, Schirm M, Lorenzo M, Kelly J, Pattarini D, Majam G, Thibault P, Logan S. 2006. Changes in flagellin glycosylation affect *Campylobacter* autoagglutination and virulence. Mol Microbiol 60:299–311.
20. Karlyshev A V., Linton D, Gregson NA, Wren BW. 2002. A novel paralogous gene family involved in phase-variable flagella-mediated motility in *Campylobacter jejuni*. Microbiology 148:473–480.

Appendix II: Complete genome sequence of *Campylobacter jejuni* strain 12567, a livestock-associated clade representative

A version of this appendix has been accepted for publication in *Genome Announcements* as:

Sacher, J. C., Yee, E., Szymanski, C. M., & Miller, W. G. Complete genome sequence of *Campylobacter jejuni* strain 12567, a livestock-associated clade representative. *Genome Announc.* **2018,** *6*, e00513-18.

Abstract

We report the complete genome sequence of *Campylobacter jejuni* strain 12567, a member of a *C. jejuni* livestock-associated clade that expresses glycoconjugates associated with improved gastrointestinal tract persistence.

A2.1. Genome Announcement

Campylobacter jejuni, a human gastrointestinal pathogen causing diarrheal disease (1), naturally colonizes chickens, so human infections commonly arise from the consumption and mishandling of contaminated poultry products (2). Expression of highly-variable, glycosylated surface structures is important for *C. jejuni* poultry persistence, and further understanding of the mechanisms behind their presentation can inform strategies to reduce bacterial burden (3, 4).

C. jejuni strain 12567 is a poultry-derived, livestock-associated clade representative (3), a poorly-studied isolate whose glycoconjugates have been disproportionately well-characterized (5, 6). The capsular polysaccharide (CPS) modification *O*-methyl phosphoramidate (MeOPN), which mediates *C. jejuni*-phage interactions (7), was found on 12567 CPS (6). Strain 12567 also expresses precursors for the flagellar legionaminic acid modifications Leg5Am7Ac and Leg5AmNMe7Ac, which are thought to assist in chicken colonization (3). Binding of 12567 by a phage protein specific for the flagellar pseudaminic acid derivative Pse5Ac7Am suggests that 12567 also synthesizes this glycan (3, 8, 9). The 12567 genome sequence therefore provides a resource for studying different *C. jejuni* glycoconjugate expression mechanisms.

We present the complete genome sequence of *C. jejuni* strain 12567. The Illumina MiSeq and PacBio RS next-generation sequencing platforms were used to complete the genome. Assembly of the MiSeq reads generated a draft genome of 427 contigs; closure of the genome, especially across the flagellar modification, lipooligosaccharide and CPS loci, required PacBio sequencing. Illumina MiSeq reads (920-fold coverage) were used to validate all base calls and determine the variability of each poly-G tract. The final coverage across the genome was 1,318-fold. Strain 12567 has a circular genome of 1,931 kbp with an average GC content of 30.4%. Protein-, rRNA- and tRNA-encoding genes were identified as described (10). The genome contains 1,628 putative protein-coding genes and 49 pseudogenes.

Examination of the 12567 CPS locus showed almost identical gene content to the reference strain *C. jejuni* NCTC 11168, with the only difference being three MeOPN transferase genes (CJ12567_1407, CJ12567_1408, CJ12567_1409) in strain 12567 compared to two (*cj1421c* and *cj1422c*) in strain 11168. The flagellar glycosylation loci of strains 12567 and 11168 are also similar, though only 12567 encodes functional copies of an aminoglycoside N3'-acetyltransferase and the methyltransferase *ptmH*, both of which are pseudogenes in 11168. The presence of *ptmH* in 12567 provides a possible explanation for why this strain makes Leg5AmNMe7Ac (3), which has been shown to require *ptmH* in *Campylobacter coli* VC167 (11). Strain 12567 also exhibits differences in *maf* (motility-associated factor) gene content compared to 11168. Although 12567 encodes the same number of poly-G tract-containing *maf* genes as 11168, the position of the *maf* genes *maf1*, *maf3*, *maf5* and *maf6* within the flagellar locus and the presence/absence of phase-variable poly-G tracts within these genes differs between the two strains.

The genome sequence of strain 12567 provides genetic information to complement the phenotypic characterization of its CPS and flagellar glycans. Whereas this strain exhibits many similarities to 11168, also a livestock-associated strain, the differences in gene content at two biologically-relevant glycoconjugate biosynthesis loci provide new understanding of *C. jejuni* glycobiology.

A2.2. Accession number(s)

The complete genome sequence of *C. jejuni* strain 12567 has been deposited in GenBank under the accession number CP028909.

A2.3. References

1. Kaakoush NO, Mitchell HM, Man SM. 2015. *Campylobacter*, p. 1187–1236. In Molecular Medical Microbiology, 2nd ed. Academic Press, London, UK.
2. Fitzgerald C. 2015. *Campylobacter*. Clin Lab Med 2:289-98.
3. Howard SL, Jagannathan A, Soo EC, Hui JPM, Aubry AJ, Ahmed I, Karlyshev A, Kelly JF, Jones MA, Stevens MP, Logan SM, Wren BW. 2009. *Campylobacter jejun*i glycosylation island important in cell charge, legionaminic acid biosynthesis, and colonization of chickens. Infect Immun 77:2544–2556.
4. Wassenaar TM. 2011. Following an imaginary *Campylobacter* population from farm to fork and beyond: A bacterial perspective. Lett Appl Microbiol 53:253-263.

5. Champion OL, Gaunt MW, Gundogdu O, Elmi A, Witney AA, Hinds J, Dorrell N, Wren BW. 2005. Comparative phylogenomics of the food-borne pathogen *Campylobacter jejuni* reveals genetic markers predictive of infection source. Proc Natl Acad Sci 102:16043–16048.
6. McNally DJ, Lamoureux MP, Karlyshev A V., Fiori LM, Li J, Thacker G, Coleman RA, Khieu NH, Wren BW, Brisson JR, Jarrell HC, Szymanski CM. 2007. Commonality and biosynthesis of the O-methyl phosphoramidate capsule modification in *Campylobacter jejuni*. J Biol Chem 282:28566–28576.
7. Sørensen MCH, van Alphen LB, Fodor C, Crowley SM, Christensen BB, Szymanski CM, Brøndsted L. 2012. Phase Variable Expression of Capsular Polysaccharide Modifications Allows *Campylobacter jejuni* to Avoid Bacteriophage Infection in Chickens. Front Cell Infect Microbiol 2:11.
8. Javed MA, Poshtiban S, Arutyunov D, Evoy S, Szymanski CM. 2013. Bacteriophage Receptor Binding Protein Based Assays for the Simultaneous Detection of *Campylobacter jejuni* and *Campylobacter coli*. PLoS One 8: e69770.
9. Javed MA, van Alphen LB, Sacher J, Ding W, Kelly J, Nargang C, Smith DF, Cummings RD, Szymanski CM. 2015. A receptor-binding protein of *Campylobacter jejuni* bacteriophage NCTC 12673 recognizes flagellin glycosylated with acetamidino-modified pseudaminic acid. Mol Microbiol 95:101–115.
10. Miller WG, Yee E, Chapman MH, Smith TPL, Bono JL, Huynh S, Parker CT, Vandamme P, Luong K, Korlach J. 2014. Comparative Genomics of the *Campylobacter lari* Group. Genome Biol Evol 6:3252–3266.

11. McNally DJ, Aubry AJ, Hui JPM, Khieu NH, Whitfield D, Ewing CP, Guerry P, Brisson JR, Logan SM, Soo EC. 2007. Targeted metabolomics analysis of *Campylobacter coli* VC167 reveals legionaminic acid derivatives as novel flagellar glycans. J Biol Chem 282:14463–14475.